DISSERTATION


OPTIMIZATION OF A CENTRIFUGAL ELECTROSPINNING PROCESS USING

RESPONSE SURFACE METHODS AND ARTIFICIAL NEURAL NETWORKS


Submitted by

Frank E. Greenawalt

Department of Mechanical Engineering


In partial fulfillment of the requirements

For the Degree of Doctor of Philosophy

Colorado State University

Fort Collins, Colorado

Spring 2014


Doctoral Committee:

    Advisor: William S. Duff

    Thomas H. Bradley
    John W. Labadie
    Ketul C. Popat

ABSTRACT


OPTIMIZATION OF A CENTRIFUGAL ELECTROSPINNING PROCESS USING

RESPONSE SURFACE METHODS AND ARTIFICIAL NEURAL NETWORKS

For complex system designs involving a large number of process variables, models are typically created for evaluating the system behavior for various operating conditions. These models are useful in understanding the effect that various process variables have on the process responses. Design of Experiments (DOE) and Response Surface Methodologies (RSM) are often used together as an effective approach to optimize a process. RSM and DOE commonly employ first and second order algebraic models. Artificial Neural Networks (ANN) is a more recently developed modeling approach. An evaluation of these three approaches is made in conjunction with experimentation on a newly developed centrifugal electrospinning prototype. The centrifugal electrospinning process is taken from the exploratory design phase through the pre-production phase to determine optimized manufacturing operating conditions.

Centrifugal Electrospinning is a sub platform technology to electrospinning for producing nanofibrous materials with a high surface to volume ratio, significant fiber interconnectivity and microscale interstitial spaces. [131] Centrifugal electrospinning is a potentially more cost effective advanced technology which evolved from traditional electrospinning. Despite there being a substantial amount of research in centrifugal electrospinning, there are still many aspects of this complex process that are not well understood.

This study started with researching and developing a functional centrifugal electrospinning prototype test apparatus which, through patent searches, was found to be innovative in nature.   Once a functional test apparatus was designed, an exploration of the process parameter settings was conducted to locate an experimental setup condition where the process was able to produce acceptable sub-micron polymeric fibers.  At this point, an RSM/DOE approach was used to find a setting point that produced a media efficiency value that was close to optimal.

An Artificial Neural Network architecture was then developed with the goal of building a model that accurately predicts response surface values.  The ANN model was then used to predict responses in place of experimentation on the prototype in the RSM/DOE optimization process.  Different levels of use of the ANN were then formulated using RSM/DOE and ANN to investigate its potential advantages in terms of time, and cost effectiveness to the overall optimization approach.

The development of an innovative centrifugal electrospinning process was successful.   A new electrospinning design was developed from the research.  A patent application is currently pending on the centrifugal electrospinning applicator developed from this research.  Near optimum operating settings for the prototype were found.

Typically there is a substantial expense associated with evolving a well-designed prototype and experimentally investigating a new process.  The use of ANN with RSM/DOE in the research was seen to reduce this expense while identifying settings close to those found when using RSM/DOE with experimentation alone.  This research also provides insights into the effectiveness of the RSM/DOE approach in the context of

prototype development and provides insights into how different combinations of

RSM/DOE and ANN may be applied to complex processes.

# ACKNOWLEDGEMENTS

TABLE OF CONTENTS

LIST OF TABLES

# LIST OF FIGURES

CHAPTER 1 INTRODUCTION


Investigating the behavior of complex systems often requires the use of

mathematical models.  These models are approximations used to characterize the

responses of the system and allow a researcher to make accurate predictions about a

process within a given design space.   Models used in the Design of Experiments (DOE)

(Box, et al., 1978, Montgomery, 1991) and the Artificial Neural Network (ANN) (Smith,

1993) models are two common techniques for approximating a process or system.

The DOE (Montgomery, 1991) method uses a collection of formal techniques to

efficiently design, analyze and often optimize using experiments.  The DOE method can

generate a response surface model using mathematical techniques to represent

relationships between independent and dependent process variables.  In DOE

statistically significant design factors and interdependencies are studied through

statistical analysis. (Montgomery, 1991)  In the traditional DOE approach, first and

second order algebraic models are used to approximate a response within a localized

region of the design space.

Response Surface Methodology (RSM) (Box and Draper, 1987) is a classical

optimizing approach which utilizes a collection of formal techniques to locate an

optimum response of a system.  The RSM method was introduced by G. E. P. Box and

K. B. Wilson in 1951.   The RSM approach sequentially steps through the design space

using local first order mathematical models to ultimately find an optimum response that

is verified via second order mathematical models.

Artificial Neural Network (ANN) (Smith, 1993) models have the ability to more globally approximate the experimentation region. The ANN technique was inspired by the cognitive and data processing capabilities that are characteristic of biological neural networks. The ANN method is known to be able to approximate nearly any functional form and works well even when the system behavior to be modeled is nonlinear.

The Centrifugal Electrospinning prototype development process is the research application context used for this research. The Centrifugal Electrospinning process has been studied over the last decade. In Electrospinning, sub-micron sized polymeric fibers can be obtained as a non-woven mat. In this process, the polymer solution is sufficiently charged such that the polymeric molecules overcome the surface tension by the viscous and centrifugal forces thereby forming and projecting elongated fibers to a grounded surface or collector. Despite the ongoing research in centrifugal electrospinning, there are still many aspects of this complex process that are not understood.

A primary accomplishment of the research was the incorporating of ANN model into the optimization process in order to reduce experimentation expenses while still identifying settings close to those found when using RSM/DOE with experimentation alone. This research also provides insights into the effectiveness of the RSM/DOE approach in the context of prototype development and provides insights into how different combinations of RSM/DOE and ANN may be applied to complex processes.

Once a functional test apparatus was designed, an exploration of the process parameter settings was conducted to locate an experimental setup condition where the

process was able to produce acceptable sub-micron polymeric fibers.  The research was conducted via the following steps:

1.  Review and compare the known centrifugal electrospinning designs and select the most promising design concepts for producing a functional centrifugal electrospinning test apparatus.

2. Develop a physical centrifugal electrospinning test apparatus

A working centrifugal electrospinning test apparatus was constructed from a centrifugal electrospinning emitter design selected in step 1.  The centrifugal electrospinning emitter was constructed based on available drawings and illustrations found in research publications.  Drive motors, pumps and other needed features were incorporated into the test apparatus in order to build a functional centrifugal electrospinning test apparatus.  The centrifugal electrospinning test apparatus was integrated into an existing electrospinning machine and test enclosure.

When experimentation on the test apparatus was started, the process variables were adjusted until the polymer fibers measured less than one micron in diameter.  When these experimental settings were confirmed, process variables were documented and used as an experimentation starting point.

3. Develop an experimental test plan

An experimental test plan was established which identified the fixed process settings, the independent and dependent process variables and the test equipment setup.

3

Selection of the primary process variables that affected efficiency and fiber diameter size for a centrifugal electrospinning process and their feasible ranges was based on 6 years of engineering experience with a commercialized electrospinning process, patent literature and the variable ranges found in the centrifugal electrospinning research.   Boundary constraints of the independent process variables were not initially known and thus, some adjustments to the initial independent variable ranges were required as experiments were conducted.

4.  Execute RSM/DOE analysis

The RSM/DOE approaches along with the algebraic models were used to locate an optimum response using the starting point determined in step 2.  This method examines a design in a small sub-region of the available design space and models the data with a first order algebraic expression which includes interactions.  The method then proceeds to climb up toward the desired optimum response surface using steepest ascent. The process typically stops when the response shows no further improvement. During the process, various features of the response surface are evaluated at each experimental design.   If the existence of an optimum in the experimental region is suspected, a second-degree polynomial is fit to further evaluate the response surface. The second-order equation is used to discover a possible maximum point.  To accomplish this, a Quadratic Program is formulated and solved.  A local interior maximum point or a maximizing boundary point of the region is determined from the Quadratic Program.  Further experimental trials are then conducted in an experimental region around the found point.

5.  Train ANN Architecture

The intent of this step is to build an ANN that accurately predicts response surface values on a more global scale.  The Feed Forward (FF) neural network was selected for doing this.  A database for building the ANN is constructed by identifying a set of points on the response surface that both span the feasible region and adequately cover its interior.  The extent of success in predicting response surface values using the ANN are then evaluated.

6.  Exploratory Alternative Steps in the ANN Model

The intent of this step is to evaluate the effectiveness of the ANN model as a replacement for experimentation on the prototype in the RSM/DOE optimization process. Steps in the RSM/DOE optimization process are followed substituting the ANN model for the experimentation and the predictions at various RSM/DOE procedure termination points are validated by experimentation on the prototype.

7.  Evaluate the Alternative Approach

Potential advantages and disadvantages of the traditional RSM/DOE and the incorporation of the ANN model are considered and discussed.

# CHAPTER 2 INTRODUCTION OF RSM/DOE

## 2.1 Introduction

The typical DOE method is a technique used to analyze a localized region within a larger design space.  In the DOE, algebraic models are used to characterize the local region and are often used to help locate an optimum in the localized region, if such is present.  The RSM method utilizes these same algebraic models in a sequential procedure for finding an optimum within a typically larger design space.  Both RSM and DOE, as they are used in this research, use first and second-order linear models with interaction terms.

Montgomery (2001) defines RSM as "a collection of mathematical and statistical techniques useful for the modeling and analysis of problems in which a response of interest is influenced by several variables and the objective is to optimize this response."  The origin of RSM is usually attributed to the research by Box and Wilson (1951), which changed dramatically the way engineers, scientists, and statisticians approached industrial experimentation.  The response surface method is based on the assumption that

$$y = f\left(x_1, x_2, \ldots, x_{k)}\right) + \varepsilon \tag{2-1}$$

where

$y$ - Response

$f$ – Response function (unknown)

$x_1, x_2, \ldots, x_k$ - Controllable input variables

$\varepsilon$ - Statistical error or noise (assumed to be independent, identically and normally distributed)

2.2 First Order RSM/DOE Models

In the practical application areas, such as manufacturing systems, it is likely that the relationship between the response and the independent variables is incompletely known. In order to approximate the functional relationship, a low-order polynomial is used to locally fit a set of data. Typically in DOE, a linear model with interactions between design variables $x$ is initially used:

$$\gamma = \beta_0 + \sum_{i=1}^{k} \beta_i x_i + \sum \sum_{i<j} \beta_{ij} x_i x_j + \varepsilon \qquad (2\text{-}2)$$

where

$y$ - Response

$x_1, x_2, \dots, x_k$ - Controllable input variables

$\varepsilon$ - Statistical error or noise (assumed to be independent, identically and normally distributed)

2.3 Two-Level Factorial Designs and Normalization

A common DOE experimental design is one with all input factors set at just two levels. These levels are called `high' and `low' and are normalized to a range of `+1' and `-1'. This normalization is referred to as a coded factor representation. A design with all possible high/low combinations of all the input factors is called a full factorial design in two levels. As the number of factors in a two level factorial design increases, the number of experimental runs for even a single replicate can become very large. For

example, a single replicate of an eight factor two level experiment would require $2^8 =$ 256 trials.

The number of trials required can be reduced by the use of fractional-factorial designs. For example, a single replicate of a $2_{IV}^{8-3}$ fractional-factorial two level experiment would require $2^{(8-3)}$ = 64 trials. The justification for using fractional factorial rather than full factorial designs is the sparsity of effects principle. (Montgomery, 2001) The principle states that, most of the time, responses are affected by a small number of main effects and lower order interactions, while higher order interactions are usually relatively unimportant. Fractional factorial designs are often used when experimental trials are costly or time consuming. Fractional factorial designs are sometimes used in screening experiments during the initial stages of experimentation.

A fractional factorial design is generated from a full factorial design by choosing an alias structure. Aliasing (confounding) refers to not being able to statistically discern which of the aliased two-way, three-way, etc. interactions are influencing the model determination. The alias structure defines which effects are confounded with each other. There was a dollar and time investment cost associated with each experimental trial for this research, so a fractional factorial design was selected to reduce the number of runs required. A $2_{IV}^{8-3}$ fractional factorial with design generators F=ABC, G=ABD, H=BCDE, where A, B, C, D, E designate the different factors, was selected for the first-order models in all the DOE experiments. In this two-level resolution IV design, none of the main effects are aliased with each other or two-way interactions. However, some two-way interactions are aliased with each other. The following alias structure describes the confounding that occurs in a $2_{IV}^{8-3}$ fractional factorial design.

8

Design Generators: F = ABC, G = ABD, H = BCDE
Alias Structure (up to order 4)

I + ABCF + ABDG + CDFG
A + BCF + BDG + CEGH + DEFH
B + ACF + ADG + CDEH + EFGH
C + ABF + DFG + AEGH + BDEH
D + ABG + CFG + AEFH + BCEH
E + ACGH + ADFH + BCDH + BFGH
F + ABC + CDG + ADEH + BEGH
G + ABD + CDF + ACEH + BEFH
H + ACEG + ADEF + BCDE + BEFG
AB + CF + DG
AC + BF + EGH + ADFG + BCDG
AD + BG + EFH + ACFG + BCDF
AE + CGH + DFH + BCEF + BDEG
AF + BC + DEH + ACDG + BDFG
AG + BD + CEH + ACDF + BCFG
AH + CEG + DEF + BCFH + BDGH
BE + CDH + FGH + ACEF + ADEG
BH + CDE + EFG + ACFH + ADGH
CD + FG + BEH + ABCG + ABDF
CE + AGH + BDH + ABEF + DEFG
CG + DF + AEH + ABCD + ABFG
CH + AEG + BDE + ABFH + DFGH
DE + AFH + BCH + ABEG + CEFG
DH + AEF + BCE + ABGH + CFGH
EF + ADH + BGH + ABCE + CDEG
EG + ACH + BFH + ABDE + CDEF
EH + ACG + ADF + BCD + BFG
FH + ADE + BEG + ABCH + CDGH
GH + ACE + BEF + ABDH + CDFH
ABE + CEF + DEG + ACDH + AFGH + BCGH + BDFH
ABH + CFH + DGH + ACDE + AEFG + BCEG + BDEF
ACD + AFG + BCG + BDF + ABEH + CEFH + DEGH

For the DOE effects models, the hierarchy principle can identify which of a combination of aliased (confounded) two-way interactions is likely to be significant. The hierarchy principle states that when two or more two-way interactions are confounded with one another, the interaction that is the most likely to be significant is the one containing factors whose main effects are themselves significant. (Montgomery, 2001)

9

In many practical applications, the main effects generally dominate the interaction effects. (Louviere, Hensher and Swait, 2000)  The main effects typically account for 70-90 percent of explained variance two-way interactions typically account for 5-15 percent of explained variance and higher-order interactions account for the remaining explained variance.

Though the hierarchy principle and the typically observed dominance of main and two-way interaction effects provide useful guidance in the DOE/RSM analysis of a system, the validity of both assumptions need some verification in a specific experimental system investigation.

Except for two-way interactions, higher order interactions are difficult to interpret meaningfully and typically higher-order interactions are often ignored. (Louviere, Hensher and Swait, 2000)  If statistically significant, three-way interactions were identified and considered in the analysis.  However, no attempt was made to interpret the three-way interactions and interactions higher than three-way were ignored.

2.4 Center Points and Curvature

A potential concern in the use of two-level fractional factorial designs is the assumption of linearity in the factor effects.[2]  Center points are used in a DOE/RSM to evaluate the possibility of quadratic curvature within the experimental design region.  If the response surface is found to have quadratic curvature, then an optimum may be suspected to exist in the experimental design region.  In this case, a second-order response surface model may be used to further evaluate the response surface.

However, quadratic curvature may also occur when an optimum is not present in the model design space.

In the RSM approach, especially when quadratic curvature is detected, the size of the experimental region is appropriately reduced to improve the estimate of the gradient. [Montgomery 2001]

2.5 Method of Steepest Ascent (RSM)

When the DOE is analyzed, it may be suspected that an optimum is not contained in the experimental region.  A steepest ascent path search based on the gradient direction may be conducted originating from the center point of the experimental region.   If the factors are normalized to their coded values, so that the center point factor values are equal to zero, interaction terms do not appear in the gradient expression.

In the method of steepest ascent, replicated experimental runs are conducted along the steepest ascent path until progressive steps result in statistically significant decreased response values.  If the statistically significant decreased response is outside the experimental region, the point is considered a candidate for a center point for a subsequent experimental design.  An ANOVA analysis of the difference in means is conducted for the steepest ascent runs to determine the point or points where this happens.

2.6 Higher-Order RSM/DOE Model

The true functional relationship between independent variables may not be linear over the experimental space.  If this is the case, a higher order polynomial, usually a quadratic model is needed to better estimate the functional relationship and to determine if the region in the design space is likely to contain an optimum.  A second-order (quadratic) model is:

$$\gamma = \beta_0 + \sum_{i=1}^{k} \beta_i x_i + \sum_{i=1}^{k} \beta_i x_i^2 + \sum\sum_{i<j} \beta_{ij} x_i x_j + \varepsilon \qquad (2\text{-}3)$$

where

$y$ - Response

$x_1, x_2, \dots, x_k$ - Controllable input variables

$\varepsilon$ - Statistical error or noise (assumed to be independent, identically and normally distributed)

The degree of success when trying to fit experimental data to a higher-order response surface is often dependent on the choice of experimental design.  There are many methods of response surface designs associated with determining a second order model.  Some of the more common response surface designs used are:

- Orthogonal
- Central Composite Design (CCD)
- Spherical Central Composite Design (SCCD)
- Box-Behnken
- Faced-Centered Central Composite Design (FCCD)
- Small Composite
- Mixed Resolution Design (MRD)

A frequent choice, the Face-Centered Central Composite Design (FCCD) using

star points was selected as the second-order model for this research.  The FCCD

contains an imbedded two-level factorial or fractional factorial design with center points

that is augmented with a group of points centered on the faces of the cuboidal

experimental region.  If these points are placed a distance from the cube face, they are

called "star points."   The FCCD experiment provides the estimate of the coefficients of

the second-order model.  If the distance from the center of the design space to a

factorial point is ±1 unit for each factor, that is the factor values are coded, the distance

from the center of the design space to a star point is typically chosen as $\pm\alpha$ with $|\alpha| > 1$.

The precise value of $\alpha$ depends on the number of unaliased factors involved.

(Montgomery 2001) In this research $\alpha$ turned out to be either ± 2.8284 or ± 3.3636.


2.7 DOE Experimental Influences

There were several effects which could impact the accuracy of the experimental

results.  Some of these are:

1.  Resolution of equipment gauges and displays

2.  Accuracy of the efficiency response test equipment

3.  SEM fiber analysis accuracy

4.  Ability to account for all potential blocking factors

5.  Equipment precision in setting the values of the factors


As the experimental trials were conducted, special care was taken to minimize

these potential influences by following a consistent test apparatus setup and sample

13

testing method.  Blocking is a design technique to minimize variability of the factors and

the response which could be influenced by nuisance factors during the experimental

trial.    If a potential nuisance factor is known to exist, blocking can be included in the

analysis to eliminate bias and gain a more accurate estimate of the actual error term.

# CHAPTER 3 INTRODUCTION OF ARTIFICIAL NEURAL NETWORKS

## 3.1 Introduction

The field of Neural Networks has arisen from diverse sources. The pursuit of this technology is evident for researchers in many fields of science and engineering. Neural networks consist of layers of interconnected nodes and each node produces a non-linear function of its input. The input to a node comes from other nodes. The complete neural network represents a very complex set of interdependencies which may incorporate a high degree of nonlinearity, allowing very general system behavior to be modeled. In the simplest networks, the output from one node is fed into another node in such a way as to connect layers of interconnecting nodes.

## 3.2 Artificial Neural Network Modeling

Neural networks are composed of simple elements, inspired by biological nervous systems, operating in parallel. The connections between elements determine the network model. A neural network can be trained using different values of the connections (weights) between elements. Bias neurons are added to neural networks to assist with learning patterns. A bias neuron is a neuron that has a constant output and is not connected to a previous layer. The Bias neuron value is typically set to a value of one, but it can be any value.

Neural networks are typically trained, so that a particular input leads to a specific target output. Figure 1 below shows a typical neural network.

$$I_j = \sum_{i=1}^{n} w_{ij} x_i \quad \textit{Sum of Weighted Inputs}$$

$$y_j = \Phi(I_j) \quad \textit{Activation Function}$$
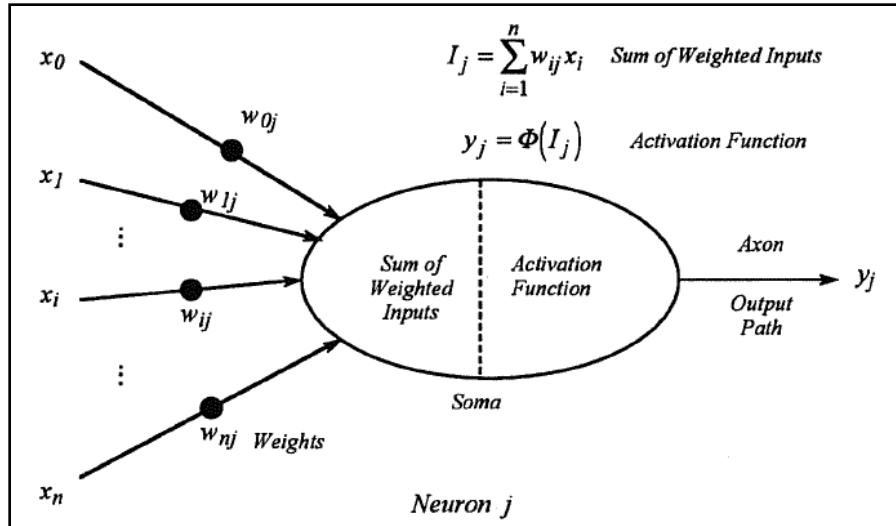
Figure 1: Neuron Model

Neural networks have been trained to perform complex functions in various fields, including pattern recognition, identification, speech, and control systems. Neural networks can also be trained to solve problems that are difficult for computers or human beings to solve.

3.2.1 Supervised Learning Networks

Supervised learning networks encompass the set of problems that have output values which are dependent on the input data. A supervised learning network can generate a model that predicts the dependent output values based on the independent input values. The model is learned by observing input and output values from a training dataset. Supervised learning is mostly accomplished using statistically-based methods. Some supervised learning methods include, but are not limited to:

- Linear regression

- Linear classification

- Decision tree methods

- Neural Networks

Supervised neural networks are trained to produce desired outputs in response to sample inputs, making them well-suited to modeling and controlling dynamic systems, and predicting future events. The four most common types of supervised neural networks are:

1. Feed Forward networks
   o These are most commonly used for prediction, pattern recognition, and nonlinear function fitting. Supported Feed Forward networks include Feed Forward backpropagation, cascade-forward backpropagation, Feed Forward input-delay backpropagation, linear, and perceptron networks.

2. Radial Basis networks
   o These provide an alternative, fast method for designing nonlinear Feed Forward networks. The Radial Basis function neural network (RBF) is similar to other neural net algorithms. RBF uses a cross-validation technique to handle the noise. As the algorithm trains it continually tests on a small set called the "cross-validation set."

3. Dynamic networks

   o   These use memory and recurrent feedback connections to recognize
       spatial and temporal patterns in data. They are commonly used for time-
       series prediction, nonlinear dynamic system modeling, and control
       systems applications.

4. Learning vector quantization (LVQ)

   o   This is a powerful method for classifying patterns that are not linearly
       separable. LVQ allows class boundaries to be specified.


3.2.2 Unsupervised Learning Networks

Unsupervised learning networks are trained by letting the network continually
adjust itself to new inputs. Unlike the supervised learning, there is not a prior set of
categories into which the patterns are to be classified; rather the system must develop
its own representation of the inputs.  The following are two types of unsupervised
networks:

1. Competitive layers recognize and group similar input vectors, enabling them to
   automatically sort inputs. Competitive layers are commonly used for
   classification and pattern recognition.

2. Self-organizing maps learn to classify input vectors according to similarity. Like
   competitive layers, they are used for classification and pattern recognition tasks.

3.2.3 Designing and Training Neural Networks

Training a neural network is a process using mathematical procedures to automatically adjust the network's weights and biases. The training process dictates an algorithm that affects all the weights and biases of a given network. The network training can be applied to individual weights and biases within a network. The coefficient of determination is computed to determine model fit. The coefficient of determination denoted $R^2$ or R squared indicates how well data points fit a line or curve. $R$ squared is computed as:

$$R^2 = 1 - \left( \frac{\text{SSE}}{\text{TSS}} \right)$$

The SSE is the sum of squared error between the model predictions and the target input values. The TSS is the sum of the squared differences of each input from the overall mean of the inputs. Consequently, a perfect fit exists when R squared = 1 and no fit when R squared = 0. However, as the model is forced to go through all the data points and the data contains random inaccuracies, a perfect fit is undesirable in regard to the usefulness of the ANN for prediction purposes. A perfect fit model creates a neural network generalization issue called overfitting. In this case the error on the training set is driven to a very small value, but when new data is presented to the network the error is large.[137] The work flow for developing a neural network has seven primary steps.

1. Collect data
2. Create the network
3. Configure the network
4. Initialize the weights and biases

5. Train the network

6. Validate the network

7. Use the network

3.3 Research Journal Articles

There were no known comparisons of using RSM/DOE and ANN methods found in the research using a centrifugal electrospinning process. The following literature reviews were the noteworthy journal articles used as a reference for this research.

1. Comparison of Empirical and Neural Network Hot-Rolling Process Models [21]

The research article was a comparison of an empirical model compared to an ANN model. The empirical model was composed of an exponential smoothing technique using three different approximation functions developed from authors in the hot-rolling process field. An online or fixed weight multi-layer feedforward neural network was used to represent the ANN model. The data set consisted of 640 points. A comparison of both models was made by using performance criteria VAF (variance accounted for) and the MSE (mean squared error). The conclusion was that the ANN model could predict the responses more accurately than the empirical model based on both the performance criteria VAF and the MSE. The VAF analysis results improved thirteen to twenty-four percent and the MSE results improved eighty-five to ninety-six percent.

2. Applying Linear Regression and Neural Network Meta-Models for Evolutionary Algorithm Based Simulation Optimization[9]


This thesis combines the use of evolution algorithms, simulation models and meta-models to produce a more efficient simulation optimization technique. The goal is to determine the best settings when using a RSM/DOE and Neural Networks as the meta-models to assist in the determination of the optimum value in a simulation. RSM/DOE and Neural Networks are tested to determine the effectiveness of the meta-modeling technique and the overall effectiveness of finding the best solution.  The research shows that the tested function did allow the search algorithm to find the region near the optimal solution.  The linear regression meta-modeling technique was said to provide a broad picture of the solution landscape.  The neural-network provided a better local area modeling technique with the true function providing the best for pin-point evaluation.  In the conclusion, the thesis recommended that a progressive combination of the three could provide the benefits of all of them. This approach would also reduce the computational cost of the optimization.


3. Advantages of Artificial Neural Networks (ANN) as Alternative Modeling Technique for Data Sets Showing Nonlinear Relationships Using Data from a Galenical Study on a Solid Dosage Form[3]


Artificial Neural Networks (ANN) methodology was used to assess experimental data showing highly non-linear relationships from a tablet compression study and this

was compared to classical modeling technique (i.e. Response Surface Methodology, RSM). The RSM modeling used 102 trials. A full quadratic DOE model was used and the alpha level of 0.05 was used to eliminate the main effects and interactions having a lack of significance. The comparison intended to quantitatively describe the degree of data fitting and predicting abilities of the developed models. The coefficient of determination was used to compare the model fit. The ANN model coefficient of determination was much closer to one than the RSM modeling in this study. Experimental trials were used to compare the ANN model predictions to the actual experimental response. Important relationships could be recognized from the ANN model only, whereas the RSM model ignored them. This was based on the injector forces which were detectable by the ANN model and not by the RSM modeling. It was concluded that the ANN methodology represented a useful alternative to classical modeling techniques when applied to data sets representing non-linear relationships based on the results and comparisons used in the study.

4. Comparison of Artificial Neural Networks (ANN) with Classical Modeling Techniques Using Different Experimental Designs and Data from a Galenical study on a solid dosage form[20]

In this paper, the ANN methodology is compared to the classical statistical method (RSM methodology) by evaluating the model fit. The ANN model used a Feed Forward multilayer network. Twenty-four samples were used to train the ANN model and four samples were used to test the ANN model. The network was trained ten times

using a new random data set each time.  The training was stopped when the MSE no longer decreased.  This was an indication that model overfitting was beginning.  The RSM models were quadratic and computed by multi-linear regression.  Factors with a p-value under 0.05 were considered significant.  The p-value is the probability of obtaining a test statistic at least as extreme as the one you actually calculated from your sample.  The same twenty-eight samples from the ANN model were used for the RSM models.  176 experimental trials were kept to validate the two models.  Two sets of data were taken from the experimental trial data.  One was random and the other was from the original experimental design.  Both ANN and RSM had similar results using the original experimental trials.  The results were different using the randomized experimental trial data.  The variables for the ANN methodology were determined to show a greater robustness than the RSM methodology when using random data samples.  Based on the results of this study, it appeared the ANN methodology was less sensitive to the way the experimental trial data was organized.

5.  Integration of Design of Experiments and Artificial Neural Networks for Achieving Affordable Concurrent Design [153]

In this journal article, the DOE and ANN approaches are compared using a high speed civil transport aircraft design.  The design is believed to have a typical nonlinear response behavior.  The intent of the study was to determine if a strategy using both DOE and ANN could be used to reduce product development time and cost.  Advantages and disadvantages of these two methods are discussed.  For the DOE, a central composite design (CCD) using nine factors and three responses was created

23

using RSM approach.  The RSM approach required 531 experiments.  A second DOE was also created using eighty-five nonstandard experiments based on the heuristic rules.  NORMAN was the program used to generate the DOE models.  The R squared value was used for measuring the accuracy of the curve fitting.   For the ANN modeling, three different sets of data were used to create three ANN models.  The RSM data (531 trials), the nonstandard data (eighty-five trials), and eighty-five random experiments were used to create the three ANN models.  The exact ANN architecture used is not mentioned.  Only the number of hidden layers and hidden nodes are given.  All the networks were trained on a trial and error basis with the best results being illustrated. The major observations that were noted in the study were as follows:

- • The DOE technique is efficient for modeling typical engineering behaviors, but falls short in modeling behaviors that are highly nonlinear with values varying within a large variable range.
- • The ANN in general needs a large set of sample data to be trained properly.
- • The ANN model trained by the experiments designed using the DOE techniques is better than the model trained by random experiments.
- • When using either the DOE or the ANN models in the optimization, the solutions converged quicker in comparison to using the computer intensive analysis program.

The journal article study concluded that the ANN technique is very beneficial in efficiently analyzing highly nonlinear behaviors, provided that a large and

24

comprehensive set of data are used to train the network. The DOE technique was

shown to be not as accurate in approximating highly nonlinear behaviors.    An

integration strategy was proposed, employing DOE techniques in the initial stage to

create smooth low-order nonlinear functions and utilizing ANN techniques in the later

stage to model highly nonlinear behaviors based on the experiments selected by the

DOE approach.

CHAPTER 4 PROCESS APPLICATION BACKGROUND

4.1 Characteristics of Nanofibers in Air Filtration Theory

Filtration theories generally rely on the assumption of continuous flow around the fibers with a non-slip flow condition.[113]  A non-slip flow condition is where the air velocity is zero at the fiber surface.   When the fiber diameter is less than 0.5 microns, the air slips at the fiber surface so there is less pressure drop.[113]  Figure 2 below shows a non-slip flow and slip flow condition.
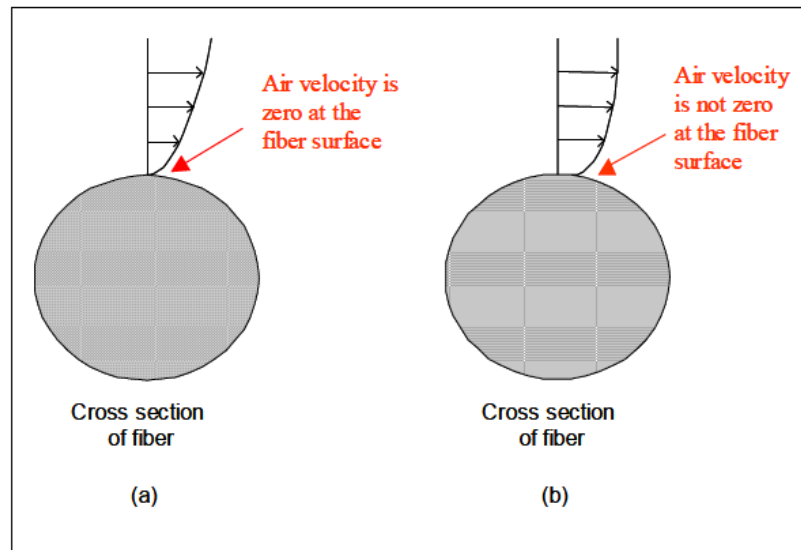


Figure 2: Velocity profiles at the fiber surface for (a) non-slip flow; and (b) slip flow *[113]*

Nanofibers are applied to a media substrate.  Substrates are used to provide added mechanical properties of the media.  Figure 3 shows an SEM image of a substrate media layer and a fiber layer.
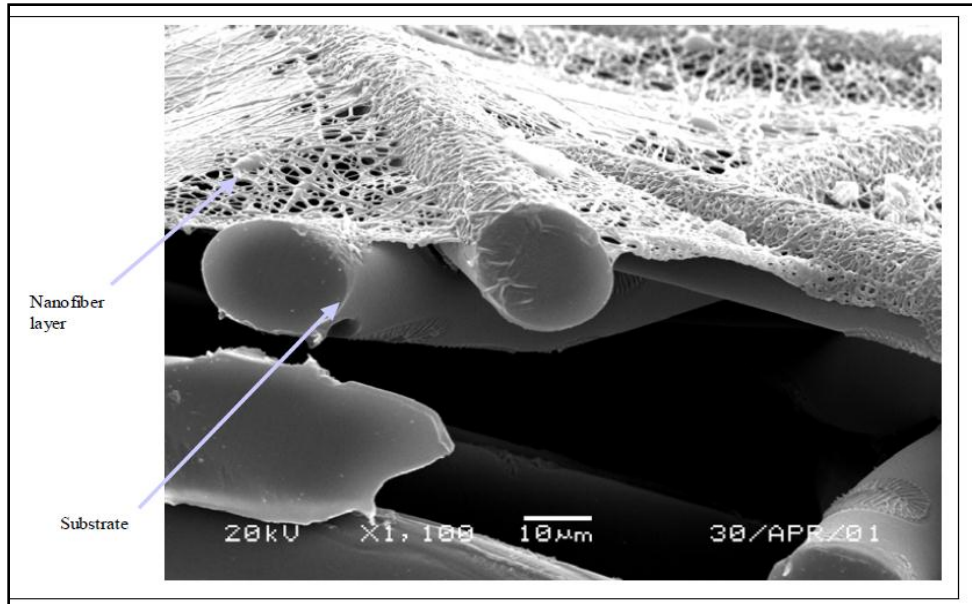
Figure 3: Electrospun fibers on media substrate [113]

As for filtration theories, the ability to produce high efficiency media without greatly increasing pressure drop adds to the complexity of using the centrifugal electrospinning process. The fibers attached to the media substrate must be less than 0.5 micron in order to minimize negative pressure drop.  The density of the fibers is used to increase the media efficiency.   As the density of fibers is increased, the fibers become so pronounced that the fiber diameters blend together which increases the fiber diameter and the pressure drop.  For this reason, it is important to minimize fiber diameter while increasing media efficiency which will minimize pressure drop.  Figure 4 shows SEM images of low and high efficiency media with fibers applied by a centrifugal electrospinning process.
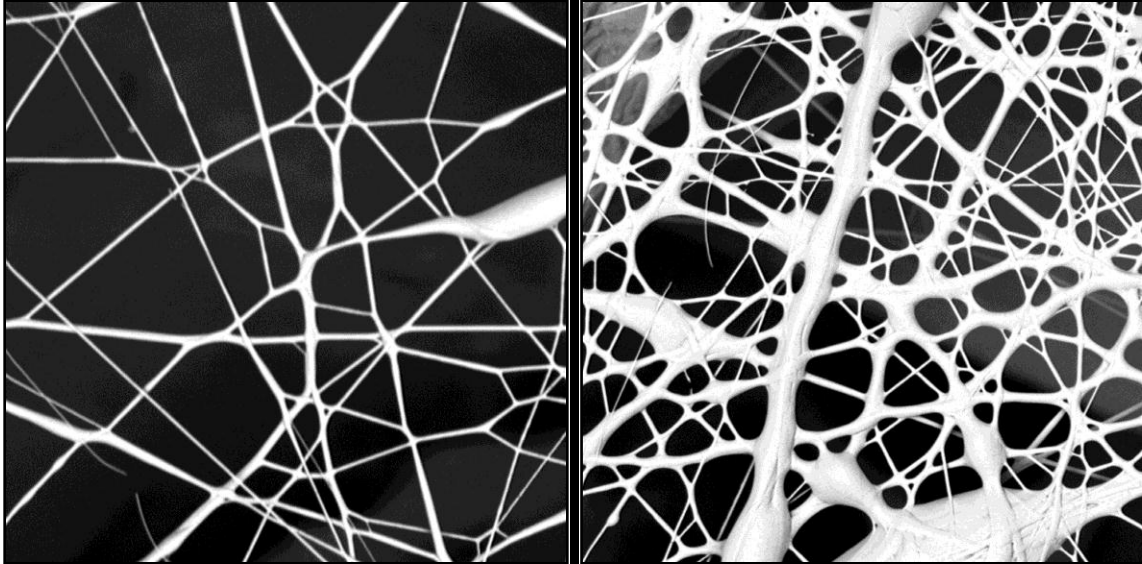
Figure 4: Fiber Morphology of Low and High Efficiency

4.2 Centrifugal Electrospinning Evolution

Nanofiber technology has been used for over 30 years in the filtration industry. The main type of process used for generating nanofibers has changed over the years. The first process developed was called Electrohydrodynamics, followed by an enhanced process called Electrospraying with the latest process developed called Electrospinning. Figure 5 shows the number of journal articles related to these processes over the years.
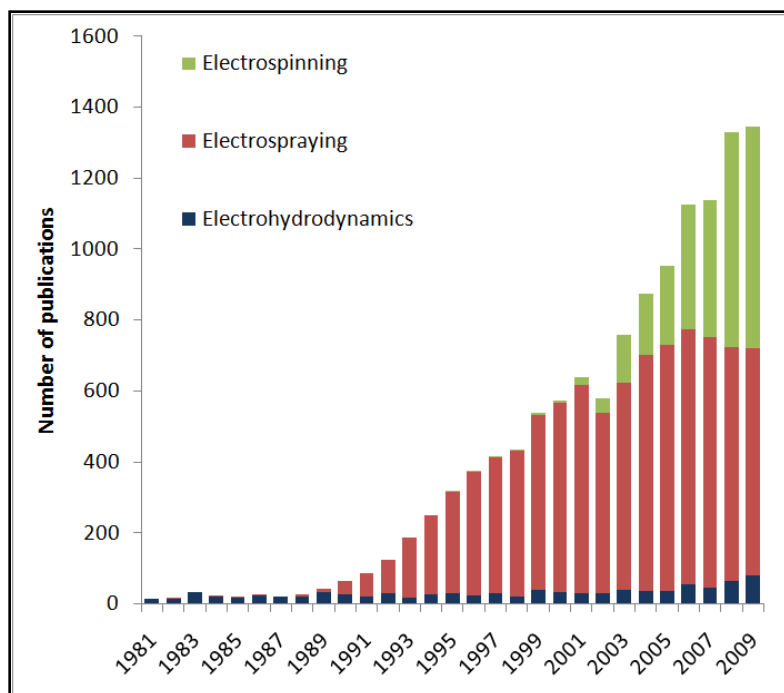
Figure 5: Electrohydrodynamic publications based on a search of publication titles In ISI Web of Knowledge in October 2010

The electrospinning process started with the use of nozzles to inject the polymer solution into an electrostatic field.  A new method of electrospinning was then developed called Free Surface or Nozzle-less electrospinning, which was developed in order to improve production output in applications where a large amount of fibers were needed. There are only a few companies in the world that offer commercialized free surface electrospinning equipment.

The more recent attempts to increase the production output of fibers use a process called Centrifugal Electrospinning, which uses a combination of centrifugal and electrostatic forces.  The centrifugal force applies a shear force on the polymer solution to generate the initial fibers with the electrostatic force then drawing the fibers to an even smaller diameter.  The electrostatic force also directs the flight of the fibers to the collector.  At the moment, this type of process is able to generate the fiber output higher

29

than traditional electrospinning.  The different types of centrifugal electrospinning

emitters found in the research are discussed in Chapter 5.

# CHAPTER 5 CENTRIFUGAL ELECTROSPINNING DESIGNS

5.1 Bell Style by Swerea IVF

A bell style centrifugal electrospinning emitter was developed by a company called Swerea IVF. [16] The process was developed to produce a large scale production of fibers. This style of centrifugal electrospinning emitter is frequently referenced in centrifugal electrospinning literature. The bell style emitter is capable of producing a nonwoven layer of fibers on a media substrate.  In this design, a polymer solution is pumped into the center of the bell style emitter while the bell is rotating at a high speed. The electrostatic field guides the fibers to the target collector while additionally elongating the fibers in the process.  The following figure shows the application and emitter shape.
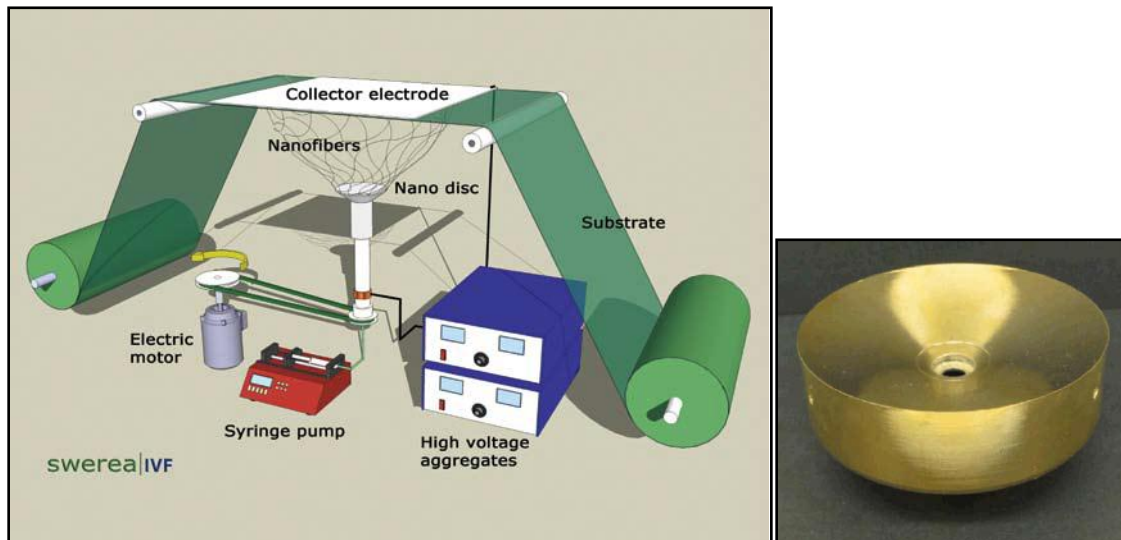


Figure 6: Bell Style - Rotating spinning bell [16]

The bell style emitter is known to leave a heavy concentration of fibers in the shape of an outer ring. This style of centrifugal electrospinning emitter also produces

holes and beads in the fiber morphology which negatively impact the overall media efficiency.

## 5.2 Spinneret Style by Fiberio Technology Corporation

Fiberio Technology Corporation developed a spinneret style centrifugal spinning design. "This new method is called Force spinning TM which uses centrifugal forces, rather than electrical forces as in electrospinning. The technological challenge of bringing the fibers down to the nanometer scale was resolved by a set of designed spinnerets that when combined with the developed thermal systems, speed, and collection systems allow for a novel production system." [4]
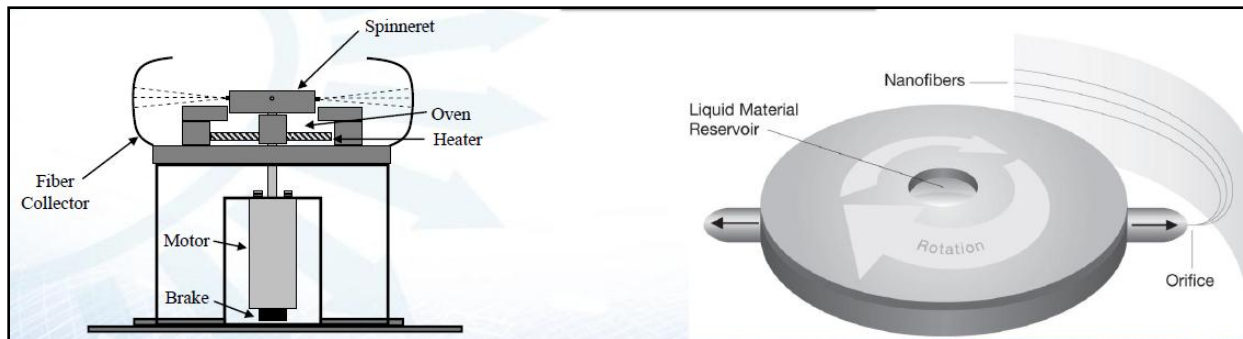


Figure 7: Sketch (a), Actual Prototype (b) and Spinneret sample [53]

This style of centrifugal emitter was designed around the concept of the cotton candy machine. Using this style of fiber emitter produces a uniform fiber layer on media substrate offering additional design considerations.

## 5.3 Spraying Atomizer Style by DuPont

This style of centrifugal electrospinning is designed around a rotary spray head. Both US patent publication US 2010/0032872 A1 and European patent EP 1 999 304 B1 relate to this design. The design generates fiber output with a uniform nonwoven fiber layer. In addition to centrifugal and electrostatic forces, this design uses air to control solvent evaporation rate and the aerodynamic flight of the fibers. Below is a cross-sectional view of the patented design.[135, 137]
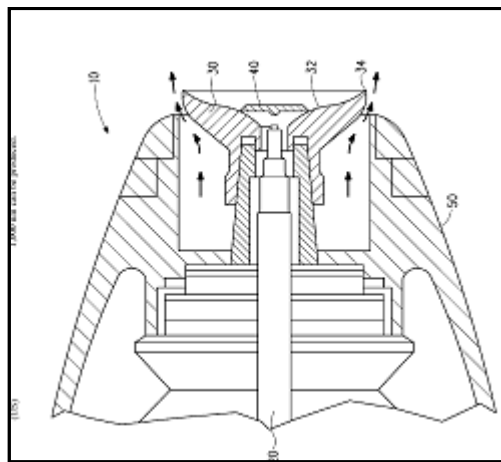


Figure 8: Paint Spraying Atomizer [135, 137]

## 5.4 Spraying Atomizer Style by Dienes/Reiter

The company Reiter OFT has developed together with the German research institute ITV Denkendorf this centrifuge fiber spinning design.[74]   This style of centrifugal electrospinning design uses an atomizing technique.  Figure 9 shows a cross-sectional view of the patented design along with an illustration of fibers being generated from the atomizer.
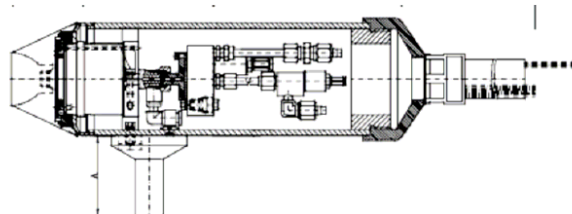
Figure 9: Atomizer Style [74]

## 5.5 Rotary Spinneret by Kurokawa

This style of centrifugal electrospinning is designed around a rotary spinneret.

Publication US patent US 2011/0156319 A1 relate to this design.  This design uses a

mechanical gear drive system to rotate the spinneret. The patent illustrations show the

fibers being projected horizontally onto a media substrate. Below is a cross-sectional

view of the design.[79]
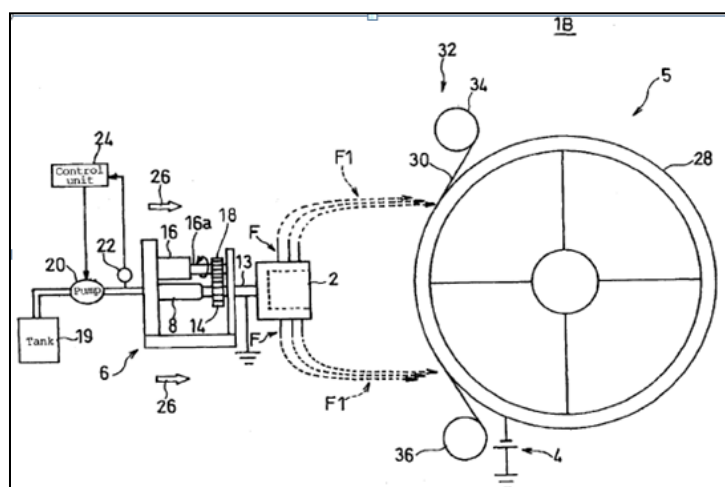


Figure 10: Rotary Spinneret Style [79]

# CHAPTER 6 EXPERIMENT OVERVIEW

6.1 Introduction

The specific pre-experiment information is discussed in this chapter. The test apparatus, process variables, materials, and other details are reviewed. Different factors and assumptions are also outlined in order to define the scope of the experimental conditions.

6.2 Test Apparatus

After review of the various known centrifugal electrospinning designs, the DuPont design and the Bell Style by Swerea IVF design were selected to assist in fabricating a working centrifugal electrospinning test apparatus. These two design concepts were chosen because of the following:

- Added feature of using air to control fiber trajectory

- Amount of design information

- Ease at which to integrate centrifugal electrospinning emitter design into test bench

- Ability to develop a functional centrifugal electrospinning emitter using the given design concepts

Due to limitations in the design disclosures, only a small portion of the design concepts were actually used to create the functional centrifugal electrospinning test apparatus.

Two test emitters were built to provide one backup in case of catastrophic failure during experimental trials.  Both emitters were mounted on a fiberglass structure to support the emitter under the collector.  The following figure below shows the orientation of the test emitter with respect to the collector. The test apparatus orientation was based on Figure 6 from the bell style design by Swerea IVF.
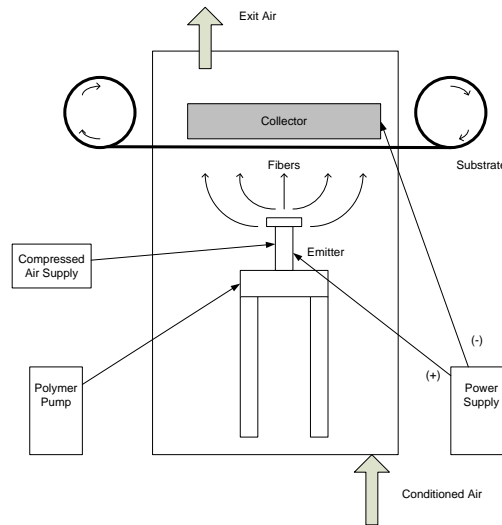


Figure 11: Test Emitter Orientation Layout

6.3 Test Equipment

Fiber Measurement Equipment

Phenom G2 Pro SEM with Cressington 108 gold sputter coater
- Magnification range 20 - 45,000x
- Images up to 2048 x 2048 pixels, 2.9 nm
- Sample loading in less than 30 seconds

Figure 12: Phenom G2 Pro SEM with Cressington 108 gold sputter coater

It should be noted that the actual diameter recorded will be somewhat lower since the fibers are sputtered with gold in order to avoid electrostatic charging by the electron beam in the SEM. The thickness of the gold layer can be estimated to be in the range 10- 50 nm (20-100 nm on the diameter).

Method of Fiber Diameter Measurement

1. 4" diameter sample size
2. Number of samples per experimental trial (1-5)
3. Cressington gold sputter time - 30 seconds
4. SEM Magnification 9200X to 9,500X
5. Number of images per sample (5)
6. Fiber Sizing Software - Phenom Pro Suite Fibermetric
7. Number of fiber selections per sample – Minimum of 40 data points
8. Fiber selections omitted
    a. Fiber Intersections
    b. Non-fiber selections
    c. Adjacent selections
    d. Poor focus selections with high standard deviation
    e. Morphology anomalies

The following figure shows a sample SEM image of the Fibermetric fiber software analysis.
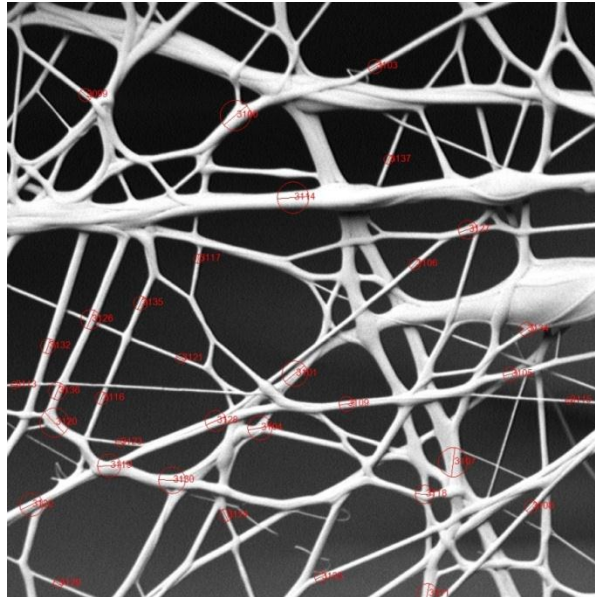

Figure 13: Fiber Analysis Example

Method of Media Efficiency Measurement

A custom media efficiency test bench was used to evaluate the media efficiency. The test process injected 0.8 micron particles into a non-static air stream that pass through a 4" diameter media sample.  Upstream and downstream particle counters are used to compute the ratio of upstream and downstream which result in a percent efficiency.  All the efficiency test samples were taken from the center of the emitter path.

6.4 Media Substrate and Polymer Solution

There are many choices of polymer solutions and media grades that could be used in this research.  Material properties were held constant in order to focus the research on the process variables.

Media Substrate

- Cellulose Grade Air Filtration - Flat
- Substrate Efficiency - 20.997
- Thickness (in) - 0.0115
- Media Width - 24 inches
- Basis Weight ($g/m^2$) - 51.0

Polymer Solution

- Type of Solvent - Alcohol and Nylon

6.5 Factors and Response

Response Variable (Primary):

- $y_0$ - Media Efficiency (%)

Response Variable (Secondary):

- $y_1$ - Minimum fiber diameter (nm)

Response Variable (Alternate):

- $y_2$ - Mean fiber diameter (nm)
- $y_3$ - Maximum fiber diameter (nm)
- $y_4$ - Range of fiber diameter (nm)
- $y_5$ - Percent of fiber diameters less than 500 nm

Fixed Independent Variables

- Type of geometry of emitter - conical
- Collector configuration - flat
- Velocity of substrate - 10 fpm

During each set of experimental trials, potential blocking factors were considered as needed in the modeling evaluations. The two primary blocking factors considered were the day of the experimental trial and the batch number of the polymer.

# CHAPTER 7 APPLICATION OF TRADITIONAL METHODS

## 7.1 Overview

This chapter describes research on the application of the traditional RSM/DOE approach with experiments on the prototype for the purpose of finding operational settings for the prototype that produce media efficiency responses close to optimum.

Part of this research was funded by a company not associated with Colorado State University, which for copyright purposes restricted the disclosure of the definition and numerical values of the factors. The eight factors are labeled as A, B, C, D, E, F, G, and the value of the factors was disguised to range from zero to one hundred.

## 7.2 Initial Startup Experiment

A Scanning Electron Microscope (SEM) was used to evaluate the fiber diameters. The initial variable settings selected were based on prior experience and technical findings. Minor adjustments were made in the process settings until the polymer fibers generated from the test apparatus measured less than one micron in diameter. Table 1 shows the first five successful trial settings.

Table 1: Test Startup Variable Settings - Coded

| Run Order | Basic Design | | | | | | | |
|-----------|--------------|--------------|--------------|--------------|--------------|-----------------|-----------------|-------------------|
| | Factor A | Factor B | Factor C | Factor D | Factor E | Factor F=ABC | Factor G=ABD | Factor H=BCDE |
| P1 | 97.62 | 37.50 | 4.76 | 33.33 | 90.00 | 80.00 | 60.00 | 80.00 |
| P2 | 97.62 | 37.50 | 4.76 | 20.00 | 40.00 | 80.00 | 60.00 | 80.00 |
| P3 | 97.62 | 6.25 | 4.76 | 20.00 | 40.00 | 60.00 | 65.00 | 80.00 |
| P4 | 97.62 | 6.25 | 28.57 | 20.00 | 40.00 | 60.00 | 65.00 | 80.00 |
| P5 | 97.62 | 6.25 | 28.57 | 33.33 | 40.00 | 53.33 | 60.00 | 80.00 |

Table 2 shows the different response information collected from the initial experimental trials shown in Table 1.

Table 2: Initial Test Startup Response Results

| Media Efficiency % | Fiber Diameter | | | | |
| | Mean | Min | Max | Range | %>500nm |
|---|---|---|---|---|---|
| 49.476 | 430.38 | 149.84 | 932.62 | 782.78 | 22.2 |
| 31.310 | 435.07 | 173.08 | 997.34 | 824.26 | 22.8 |
| 27.600 | 468.87 | 185.90 | 809.18 | 623.28 | 24.9 |
| 30.440 | 460.79 | 154.03 | 912.01 | 757.98 | 29.0 |
| 29.130 | 446.05 | 187.84 | 997.27 | 809.43 | 20.6 |

The initial experimental trial results were able to produce fiber diameters less than one micron which met the primary startup objective.  On the average seventy-five percent of the fibers were less than 500 nanometers in diameter.   There were safety related process issues with trials P1 and P2 so these specific experimental trials had to be eliminated.  The media efficiency was selected as the primary response, but a composite objective function was evaluated during one of the steepest ascent trials. The information related to this evaluation can be found in Appendix 1.13.

Based on the successful experimental trial information, the following eight factor settings were established as the starting point or center point for the first design of experiment (DOE1a).  That is,

 A = 73.8   B = 53.1   C = 28.6   D = 33.3   E = 67.0   F = 66.7   G = 60.0   H = 40.0

## 7.3 RSM/DOE Experimentation Context

The notations used throughout this study to reference the eight factors are shown in Table 3.

Table 3: Factor Notations

| 1 | $x_1$ | A |
|---|-------|---|
| 2 | $x_2$ | B |
| 3 | $x_3$ | C |
| 4 | $x_4$ | D |
| 5 | $x_5$ | E |
| 6 | $x_6$ | F |
| 7 | $x_7$ | G |
| 8 | $x_8$ | H |

The variable values established in section 7.2 were used as the center point for the first design of experiment.

To perform the DOE analysis, the uncoded (natural) variables were converted to coded variables (variables scaled to the range -1 to +1). Coding a variable in this manner eliminates any undue influence in the modeling due to different magnitudes of scales of the factors and, as will be seen, greatly simplifies the algebra of the RSM procedure.

Potential nuisance factors associated with the experimental trials, such as trial runs on different days, were avoided to prevent a need for blocking. As discussed in Chapter 2, blocking could be included in the analysis to eliminate bias and gain a more accurate estimate of the actual error term. However, this would be undesirable because it would increase the number of trials required for the DOE.

Two replicates were used in each set of experiments to achieve a better estimate of the error term. The experimental trials were conducted in a random order to remove any bias due to the order in which experimental trials were conducted.

42

The two-level fractional factorial design with a resolution IV was selected. This factorial design was discussed in section 2.4. A total of sixty-four experimental trials were required for this fractional factorial design not including center points. The following table shows the coded $2^{8-3}_{IV}$ fractional factorial design along with the basic design. In the table, + is represents +1 and – represents -1.

Table 4: Coded Fractional Factorial Design

| Std Order | Basic Design | | | | | Factor F=ABC | Factor G=ABD | Factor H=BCDE |
|---|---|---|---|---|---|---|---|---|
| | Factor A | Factor B | Factor C | Factor D | Factor E | | | |
| 1 | - | - | - | - | - | - | - | + |
| 2 | + | - | - | - | - | + | + | + |
| 3 | - | + | - | - | - | + | + | - |
| 4 | + | + | - | - | - | - | - | - |
| 5 | - | - | + | - | - | + | - | - |
| 6 | + | - | + | - | - | - | + | - |
| 7 | - | + | + | - | - | - | + | + |
| 8 | + | + | + | - | - | + | - | + |
| 9 | - | - | - | + | - | - | + | - |
| 10 | + | - | - | + | - | + | - | - |
| 11 | - | + | - | + | - | + | - | + |
| 12 | + | + | - | + | - | - | + | + |
| 13 | - | - | + | + | - | + | + | + |
| 14 | + | - | + | + | - | + | + | + |
| 15 | - | + | + | + | - | + | + | - |
| 16 | + | + | + | + | - | + | + | - |
| 17 | - | - | - | - | + | - | - | - |
| 18 | + | - | - | - | + | - | - | - |
| 19 | - | + | - | - | + | - | - | + |
| 20 | + | + | - | - | + | - | - | + |
| 21 | - | - | + | - | + | + | - | + |
| 22 | + | - | + | - | + | + | - | + |
| 23 | - | + | + | - | + | + | - | - |
| 24 | + | + | + | - | + | + | - | - |
| 25 | - | - | - | + | + | - | + | + |
| 26 | + | - | - | + | + | - | + | + |
| 27 | - | + | - | + | + | - | + | - |
| 28 | + | + | - | + | + | - | + | - |
| 29 | - | - | + | + | + | + | + | - |
| 30 | + | - | + | + | + | + | + | - |
| 31 | - | + | + | + | + | + | + | + |
| 32 | + | + | + | + | + | + | + | + |

Based on the background research, the five factors anticipated to be the most dominant were assigned to the basic design and the three remaining factors were aliased to three way and four way interactions.

The generators for the aliasing in the fractional factorial design are shown in Table 4.  Factor F is aliased with the ABC interaction, the factor G is aliased with the ABD interaction and the factor H is aliased with the BCDE interaction.   As explained in Chapter 2, additional confounding in the main effects and interactions are produced by this aliasing.

A first-order model was generated from the coded $2^{8-3}_{IV}$ fractional factorial design experiment.    An analysis of the residual errors from the squared error model was used to reveal any departure from the modeling assumptions and to check the adequacy of the model.  Four different residual plots were generated and evaluated to test for the following:

1. Normality of the model error term
2. Skewness and outliners or outliers
3. Constant variance and outliers
4. Systematic effects in the data due to time or data collection order

The inclusion of center points was used to better the estimate of experimental error and to check for pure quadratic curvature.  If there is no evidence of pure quadratic curvature, the response at the center will approximately equal the average of the responses of the factorial runs at the corner points of the DOE cube.  Evidence of

pure quadratic curvature would suggest that a saddle point or a point of maximum response is near the boundary of the cube.

Contour plots were used to visualize the nature of the response surface.   The contour plots could provide evidence of a localized minimum or maximum response if closed circular contour lines are present.  A second-order model was generated if there was evidence of pure quadratic curvature.

A list of the nomenclature and terminology used in this RSM/DOE approach are shown in Table 5.

Table 5: RSM/DOE Terminology Reference

| DOE | Design of Experiments |
|---|---|
| DOEna | Two level factorial experimental design for the $n^{th}$ iteration of the analysis used for building $1^{st}$ order models |
| DOEnb | Experimental design with addition of FCCD points to DOEna used for building 2nd order models |
| SA | Steepest Ascent |
| RSM | Response Surface Method |
| SAn | SA optimization search from the DOEna center point in the gradient direction |
| Quadratic Programming | Optimization of a quadratic equation subject to a linear set of inequalities |
| Validation | Testing of a point found by the various investigative processes by experimentation on the prototype |

A flow diagram was developed to display the logic steps taken in the RSM/DOE approach.  This flow diagram is shown in Figure 14.
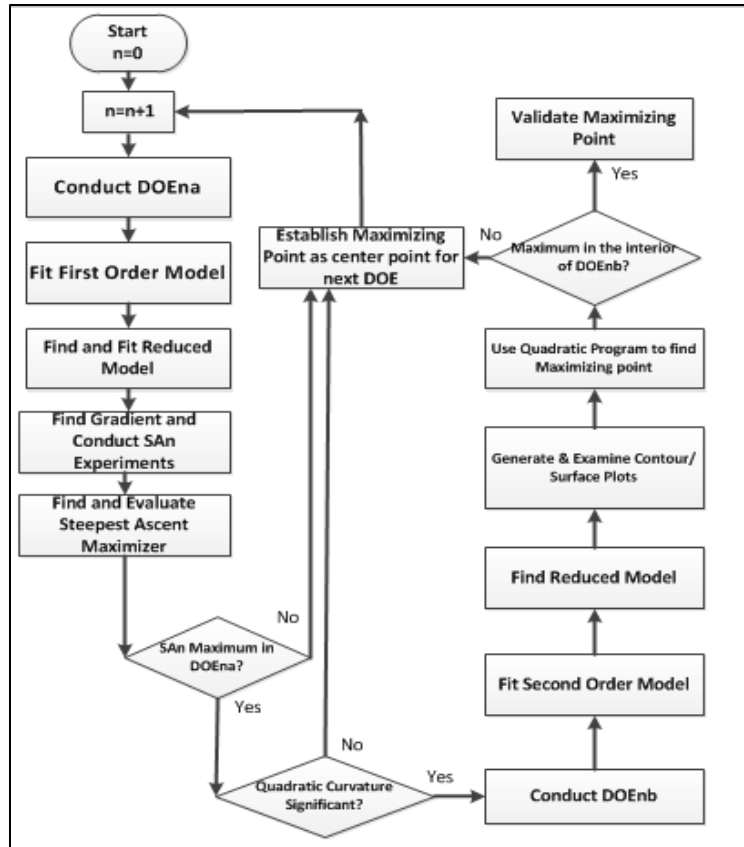
Figure 14: RSM/DOE Flow Diagram

The flow diagram in Figure 14 was created to summarize the steps of RSM approach which were discussed in Chapter 2. The flow diagram shows the decision point where if there is significant quadratic curvature that a second order model would be used better estimate the response surface in this experimental region.

7.4 Detailed RSM/DOE Steps Utilized in Finding a Maximum Response

7.4.1 DOE1a Analysis

Using the starting point shown in section 7.3 for the initial experiments as the center point, the following variable setting values (DOE1a) were used as the high, low and center point settings for fitting the initial first-order effects model.

Table 6: DOE1a - High, Low, and Center Point Values

|  | Factor A | Factor B | Factor C | Factor D | Factor E | Factor F | Factor G | Factor H |
|---|---|---|---|---|---|---|---|---|
| Low | 70.95 | 45.31 | 23.81 | 30.00 | 66.00 | 40.00 | 61.00 | 32.00 |
| Center | 73.81 | 53.13 | 28.57 | 33.33 | 67.00 | 46.67 | 60.00 | 40.00 |
| High | 76.79 | 60.94 | 33.33 | 36.67 | 68.00 | 53.33 | 59.00 | 48.00 |

The range between the high and low values for each factor was selected to adequately model the overall properties of the response surface in the immediate vicinity of the center point and to accurately estimate the gradient at the center point. The following table shows the coverage of the feasible ranges provided by the initial high and low point values.

Table 7: DOE1a - Feasibility Variable Range

|  | Factor A | Factor B | Factor C | Factor D | Factor E | Factor F | Factor G | Factor H |
|---|---|---|---|---|---|---|---|---|
| % of Range | 6% | 13% | 10% | 7% | 2% | 20% | 2% | 5% |
| % to Min (Center pt.) | 75% | 63% | 5% | 33% | 74% | 20% | 60% | 85% |
| % to Max (Center pt.) | 25% | 38% | 95% | 67% | 26% | 80% | 40% | 15% |

Using the eight factors, a sixty-nine experiment $2_{IV}^{8-3}$ fractional factorial design was developed. This experimental design is shown in Table 4. Five center points were included in the experimental design.

The alias structure of this experimental design can be found in section 2.4. The possible blocking factors, the day of the trial, the polymer batch and the substrate roll number were all identical for the DOE1a experimental trials, so no blocking was needed.

An effects analysis was conducted based on the experimental trials using the experimental design. The results of the coded estimated effects and coefficients analysis for effects and interactions up to a level of three-way interactions are shown in

Table 8. Also shown in Table 8 are those two-way interactions that were confounded. The confounding involving three-way and higher order interactions are not shown. (For the confounding involving three-way and higher order interactions, see the confounding structure provided in Chapter 2.)

Table 8: Estimated Effects and Coefficients for DOE1a (coded units)

| Term | | | Effect | Coef | P | S |
|---|---|---|---|---|---|---|
| Alias | Alias | Alias | | | | |
| Constant | | | | 32.384 | 0.000 | |
| A | | | 0.805 | 0.402 | 0.000 | |
| B | | | 1.243 | 0.622 | 0.000 | |
| C | | | -0.368 | -0.184 | 0.080 | S1 |
| D | | | 0.449 | 0.225 | 0.034 | |
| E | | | -1.162 | -0.581 | 0.000 | |
| F | | | 0.014 | 0.007 | 0.944 | S1 |
| G | | | -0.542 | -0.271 | 0.062 | S1 |
| H | | | -0.435 | -0.218 | 0.040 | |
| AB | CF | DG | -0.567 | -0.283 | 0.009 | |
| AC | BF | | 0.208 | 0.104 | 0.314 | S2 |
| AD | BG | | -0.318 | -0.159 | 0.127 | S2 |
| AE | | | 0.575 | 0.287 | 0.008 | |
| AF | BC | | 1.106 | 0.553 | 0.000 | |
| AG | BD | | 0.669 | 0.335 | 0.002 | |
| AH | | | -0.223 | -0.111 | 0.281 | S2 |
| BE | | | -0.448 | -0.224 | 0.035 | |
| BH | | | 0.013 | 0.007 | 0.948 | S2 |
| CD | FG | | 0.049 | 0.025 | 0.811 | S2 |
| CE | | | -2.003 | -1.002 | 0.000 | |
| CG | DF | | 0.277 | 0.139 | 0.182 | S2 |
| CH | | | -0.710 | -0.355 | 0.001 | |
| DE | | | 0.557 | 0.279 | 0.010 | |
| DH | | | 0.867 | 0.433 | 0.000 | |
| EF | | | 0.294 | 0.144 | 0.158 | S2 |
| EG | | | 0.361 | 0.181 | 0.085 | S2 |
| EH | | | 0.241 | 0.121 | 0.244 | S2 |
| FH | | | 0.860 | 0.430 | 0.000 | |
| GH | | | 0.467 | 0.234 | 0.028 | |
| ABE | | | -0.201 | -0.101 | 0.330 | S2 |
| ABH | | | 0.675 | 0.338 | 0.002 | S3 |
| ACH | | | -0.060 | -0.030 | 0.770 | S2 |
| Ct Pt | | | | 0.150 | 0.694 | |

R-Sq. = 90.64%   R-Sq. (adj.) = 82.33%

Notes:
S1 Red Shading - Main effects retained to preserve hierarchy
S2 Blue Shading - Effects eliminated due to lack of statistical significance
S3 Green Shading – Statistically significant three-way interactions

A level of significance of $\alpha > 0.05$ was used to compare to the p-values in Table 8 to select which of the effects in the model were to be considered statistically significant. The main effects having a lack of significance are C, F, and G which are shaded and labeled "S1" in Table 8. The two-way and three-way interactions having a lack of significance which can be eliminated from the DOE1a effects model are shaded and labeled "S2" in Table 8. The experimental results of DOE1a and the four residual plots are shown in Appendix 1.1.

The contour plots in Figure 15 and Figure 16 show the properties of the response surface as depicted by the first-order model. The contour plots did not provide evidence of a localized minimum or maximum response since there were no closed circular contour lines present.
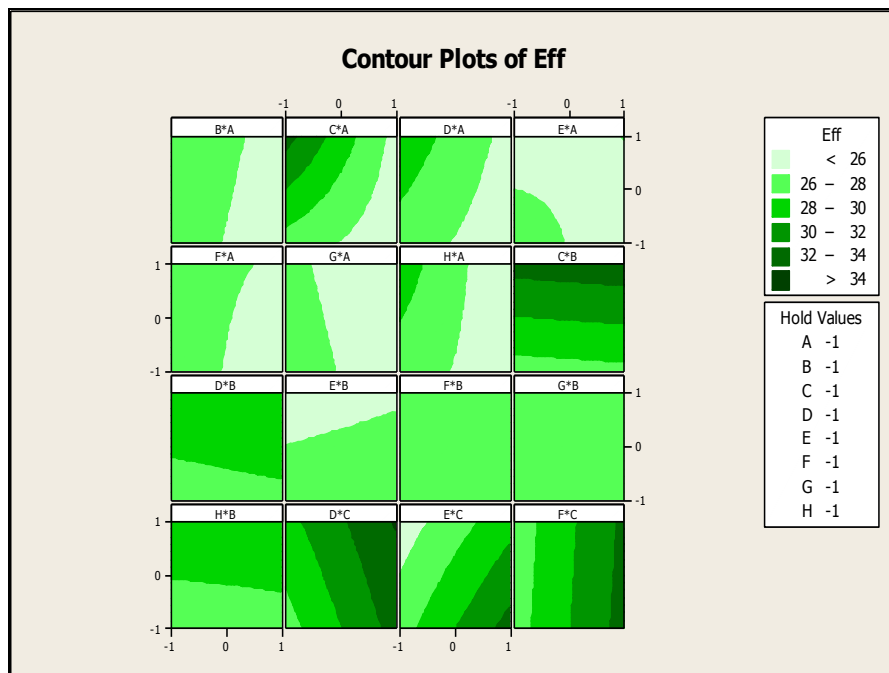


Figure 15: DOE1a Contour Plot 1 of 2
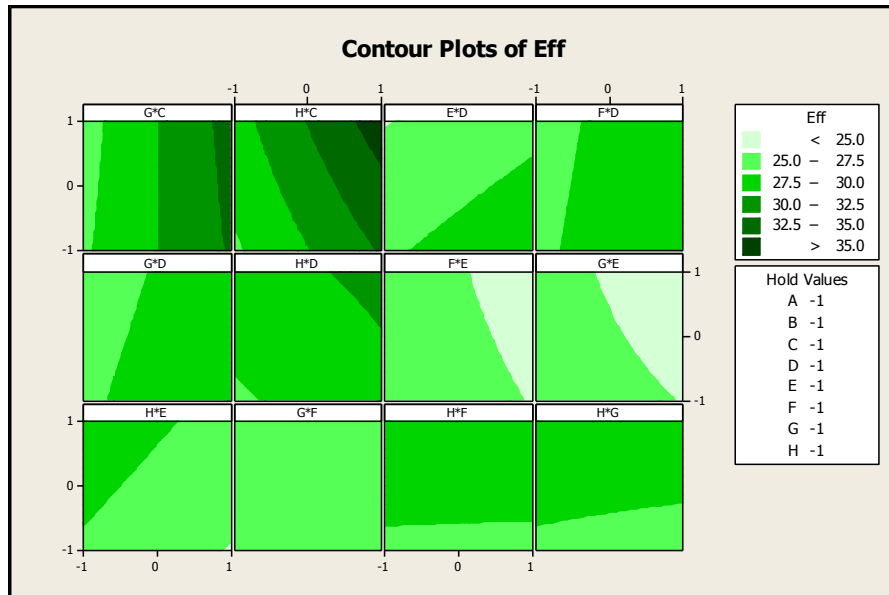
Figure 16: DOE1a Contour Plot 2 of 2

There are thirty-seven degrees of freedom (DOF) available in this experiment for estimating of the Mean Squared Error (MSE) in the DOE analysis. In order to further improve the estimate of the MSE and the accuracy of the model, a reduced analysis was conducted that removed model terms that were not statistically significant.

7.4.2 Reduced DOE1a Analysis

A reduced effects model was generated based on eliminating the effects showing a lack of significance as discussed in section 7.4.1. The main effects showing a lack of significance were kept to preserve hierarchy. The reduced DOE1a effects analysis results are presented in Table 9.

Table 9: Estimated Effects Analysis for DOE1a reduced model (coded units)

| Term | | | Effect | Coef | P | S |
|---|---|---|---|---|---|---|
| Alias | Alias | Alias | | | | |
| Constant | | | | 32.494 | 0.000 | |
| A | | | 0.815 | 0.402 | 0.001 | |
| B | | | 1.243 | 0.623 | 0.000 | |
| C | | | -0.348 | -0.185 | 0.087 | S1 |
| D | | | 0.439 | 0.225 | 0.038 | |
| E | | | -1.152 | -0.584 | 0.000 | |
| F | | | 0.012 | 0.007 | 0.947 | S1 |
| G | | | -0.542 | -0.273 | 0.013 | |
| H | | | -0.435 | -0.218 | 0.045 | |
| AB | | DG | -0.557 | -0.285 | 0.010 | S4 |
| AE | | | 0.565 | 0.287 | 0.009 | |
| AF | BC | | 1.107 | 0.555 | 0.000 | S4 |
| AG | BD | | 0.669 | 0.338 | 0.003 | S4 |
| BE | | | -0.446 | -0.226 | 0.039 | |
| CE | | | -2.001 | -1.008 | 0.000 | |
| CH | | | -0.710 | -0.354 | 0.002 | |
| DE | | | 0.567 | 0.278 | 0.011 | |
| DH | | | 0.877 | 0.435 | 0.000 | |
| FH | | | 0.861 | 0.430 | 0.000 | |
| GH | | | 0.457 | 0.236 | 0.031 | |
| ABH | | | 0.675 | 0.338 | 0.002 | S4 |
| Ct Pt | | | | 0.152 | 0.731 | |

R-Sq. = 84.08%   R-Sq. (adj.) = 77.45%

Notes:

S1 Red Shading - Main effects retained to preserve hierarchy

S4 Yellow Shading – Statistically significant aliased (confounded) interactions

The two main effects which have a lack of significance are labeled "S1" in Table 9. The statistically significant aliased two-way interactions are shaded and labeled "S4" in Table 9. Only one two-way aliased (confounded) interaction CF contained main effects which had a lack of significance. Based on this, only one of the aliased (confounded) two-way interactions CF could be eliminated by the hierarchy principle. Table 10 shows the estimated effects analysis with the further reduced confounding of the AB interaction via the hierarchy principle and the elimination of the three-way interaction.

Table 10: Estimated Effects Analysis for DOE1a Reduced

| Term | | | Effect | Coef | P | S |
|---|---|---|---|---|---|---|
| Alias | Alias | Alias | | | | |
| Constant | | | | 32.384 | 0.000 | |
| A | | | 0.805 | 0.402 | 0.001 | |
| B | | | 1.243 | 0.622 | 0.000 | |
| C | | | -0.368 | -0.184 | 0.088 | S1 |
| D | | | 0.449 | 0.225 | 0.038 | |
| E | | | -1.162 | -0.581 | 0.000 | |
| F | | | 0.014 | 0.007 | 0.946 | S1 |
| G | | | -0.542 | -0.271 | 0.013 | |
| H | | | -0.435 | -0.218 | 0.045 | |
| AB | | DG | -0.567 | -0.283 | 0.010 | S4 |
| AE | | | 0.575 | 0.287 | 0.009 | |
| AF | BC | | 1.106 | 0.553 | 0.000 | S4 |
| AG | BD | | 0.669 | 0.335 | 0.003 | S4 |
| BE | | | -0.448 | -0.224 | 0.039 | |
| CE | | | -2.003 | -1.002 | 0.000 | |
| CH | | | -0.710 | -0.355 | 0.002 | |
| DE | | | 0.557 | 0.279 | 0.011 | |
| DH | | | 0.867 | 0.433 | 0.000 | |
| FH | | | 0.860 | 0.430 | 0.000 | |
| GH | | | 0.467 | 0.234 | 0.032 | |
| Ct Pt | | | | 0.150 | 0.703 | |

R-Sq. = 83.78%   R-Sq. (adj.) = 78.27%

Notes:
S1 Red Shading - Main effects retained to preserve hierarchy
S4 Yellow Shading – Statistically significant aliased (confounded) interactions

There are now forty-nine degrees of freedom (DOF) available in this experiment for estimating the Mean Squared Error (MSE).  The adjusted R squared measure accounts for the fact that the model fit is being evaluated with fewer terms.  The adjusted R squared measure changed very little, actually increasing from 77.45 percent to 78.27 percent, when eliminating the significant three-way interaction.   Therefore, there has been no real increase in the predictive accuracy of the reduced model caused by the elimination of this statistically significant three-way interaction.

Often, a folding experiment and additional experimental trials would be required to determine which of the confounded two-way interactions show significance, or if both show significance. However, in this case, folding of the effects experiments were

avoided because, as will be seen later, it was determined that the DOE1a experimental region did not contain an optimum.

The p-value for the center point in Table 10 was examined to detect the presence of quadratic curvature (lack of fit). A p-value greater than the selected alpha value of 0.05 for the test indicates there is no significant lack of fit in the first-order model. Since the p-value for the center point was equal to 0.703, no quadratic curvature is suggested in the response surface region. This, combined with the lack of an apparent localized minimum or maximum in the contour plots, supports the conclusion that the optimum will lie outside the experimental region.

The following equation is the coded fitted linear regression model where the aliased confounded terms for DOE1a are indicated.

$$y = 32.384 + 0.402A + 0.622B - 0.184C + 0.225D - 0.581E + 0.007F - 0.271G$$
$$- 0.218H - 0.283(AB, DG) + 0.287AE + 0.553(AF, BC)$$
$$+ 0.335(AG, BD) - 0.224BE - 1.002CE - 0.355CH + 0.279DE$$
$$+ 0.433DH + 0.430FH + 0.234GH$$

Where A stands for coded factor $x_A$ , (AB, BG) stands for coded factors $x_A * x_B$ or $x_B * x_D$ and so forth.

Folding was not needed for this experimental region because DOE1a was determined to not contain an optimum and the steepest ascent coded gradient path equation will have no interaction terms when the starting point (0, 0, 0, 0, 0, 0, 0, 0) is substituted into the expressions for the partial coded variable equation. This may be

seen by taking the partial derivative of the first order model with respect to each variable

and substituting (0, 0, 0, 0, 0, 0, 0, 0).

$$\frac{\partial y}{\partial A} = 0.402$$

$$\frac{\partial y}{\partial B} = 0.622$$

$$\frac{\partial y}{\partial C} = -0.184$$

$$\frac{\partial y}{\partial D} = 0.225$$

$$\frac{\partial y}{\partial E} = -0.581$$

$$\frac{\partial y}{\partial F} = 0.007$$

$$\frac{\partial y}{\partial G} = -0.271$$

$$\frac{\partial y}{\partial H} = -0.218$$

The experimental results for DOE1a and the four main residual plots are shown

in Appendix 1.1.

7.4.3 SA1 Steepest Ascent

The method of steepest ascent (SA1), based on following a path through the

feasible region in the gradient direction, was used to move toward a better response.

Replicated experimental runs were conducted along the path until consecutive steps

resulted in a decreased response. The $x_A$ variable was chosen as the base and the

step size was selected as 0.5 for a balance between too large of a step and too small of a step. The steepest ascent setup along with the coded coefficients are given below.

Path of Steepest Ascent Overview

Total # of Runs              7
Total # of Factors           8
Base Factor Name             Factor A
Step Size Base Factor by     0.50

The coded steepest ascent path is:

$$x\ \mathbf{i_1}, -0.11x\mathbf{i_2}, -x\mathbf{i_3}, -0.212x\mathbf{i_4},\ \ 0.766x\mathbf{i_5}, -0.42x\mathbf{i_6}, 0.103x\mathbf{i_7}, -0.66x\mathbf{i_8}$$

Where:  x = coded factor A

Table 11 shows the coded steepest ascent path and the factor values.

Table 11: SA1 Steepest Ascent (coded)

|        | Factor A or (x) | Factor B | Factor C | Factor D | Factor E | Factor F | Factor G | Factor H |
|--------|-----------------|----------|----------|----------|----------|----------|----------|----------|
| Step 0 | 0.00            | 0.00     | 0.00     | 0.00     | 0.00     | 0.00     | 0.00     | 0.00     |
| Step 1 | -0.50           | 0.06     | 0.50     | 0.11     | -0.38    | 0.12     | -0.05    | 0.33     |
| Step 2 | -1.00           | 0.11     | 1.00     | 0.21     | -0.77    | 0.24     | -0.10    | 0.66     |
| Step 3 | -1.50           | 0.17     | 1.50     | 0.32     | -1.15    | 0.36     | -0.15    | 0.99     |
| Step 4 | -2.00           | 0.22     | 2.00     | 0.42     | -1.53    | 0.48     | -0.21    | 1.32     |
| Step 5 | -2.50           | 0.28     | 2.50     | 0.53     | -1.92    | 0.60     | -0.26    | 1.65     |
| Step 6 | -3.00           | 0.34     | 3.0      | 0.63     | -2.30    | 0.72     | -0.31    | 1.98     |

At step 3 of the steepest ascent the H factor reached its upper limit of one and were held there for subsequent steps. Three replications of each step were conducted in the experimental trials to get a better estimate of an average. Table 12 also shows the experimental results and Figure 17 shows a plot of the average response at each step of the steepest ascent.

Table 12: SA1 Steepest Ascent

| Steepest Ascent | Efficiency Prediction | Efficiency Average | Std Dev | Trial 1 | Trial 2 | Trial 3 | Trial 4 | Trial 5 | MSE |
|---|---|---|---|---|---|---|---|---|---|
| Step 0 | 28.340 | 23.857 | 0.520 | 23.916 | 23.276 | 24.690 | 23.680 | 23.721 | 20.3 |
| Step 1 | 31.824 | 30.892 | 0.590 | 30.211 | 31.201 | 31.263 | | | 1.1 |
| Step 2 | 36.461 | 36.225 | 0.494 | 36.214 | 35.736 | 36.724 | | | 0.2 |
| Step 3 | 42.286 | 40.518 | 1.268 | 41.819 | 39.285 | 40.449 | | | 4.2 |
| Step 4 | 48.666 | 42.336 | 0.401 | 42.759 | 42.287 | 41.961 | | | 40.2 |
| Step 5 | 55.534 | 44.573 | 0.276 | 44.846 | 44.295 | 44.577 | | | 82.2 |
| Step 6 | 63.353 | 37.465 | 1.578 | 36.100 | 37.101 | 39.193 | | | 84.6 |
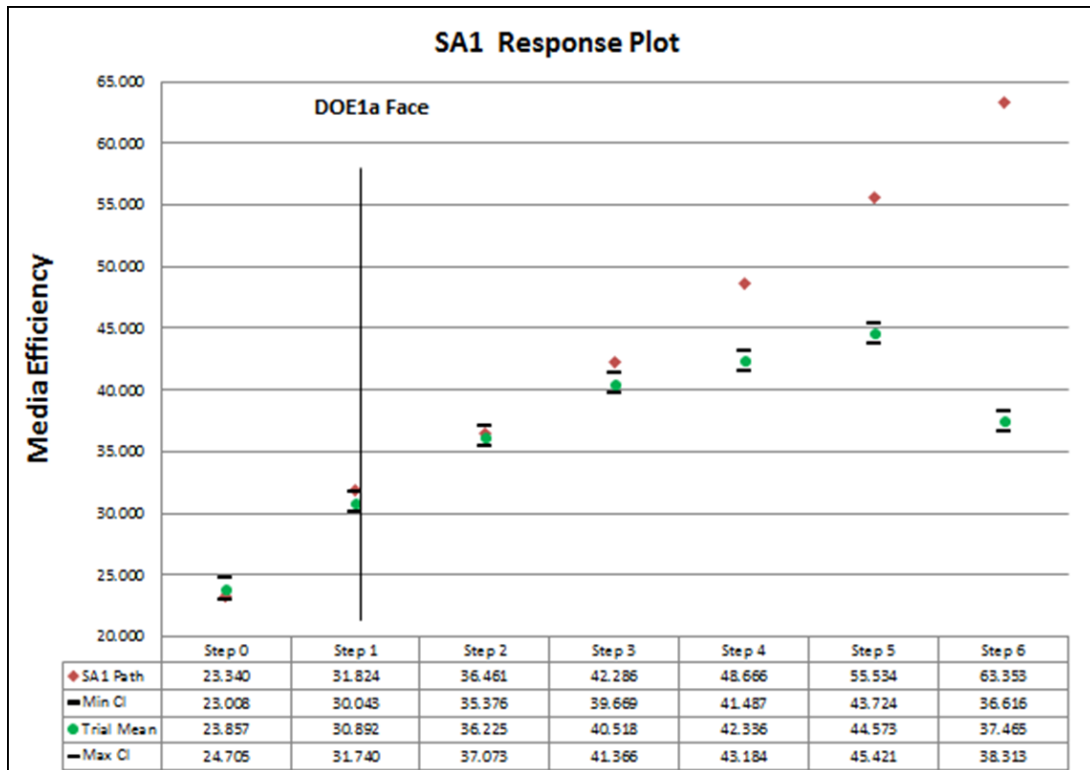


Figure 17: SA1 Response Plot

The vertical line shown in Figure 17 represents the DOE1a boundary to visualize when the Steepest Ascent path crosses the DOE1a boundary. A total of eighteen experimental trials were conducted for SA1 steepest ascent. At step 5 of the steepest ascent, the efficiency response stopped increasing. The steepest ascent results plotted in Figure 17 show that the response continues to increase well outside the experimental region of the DOE1a model. The linear points in Figure 17 represent the predicted

responses along the SA1 path.  Confidence Intervals were plotted based on using the pooled standard deviation of 0.9446 calculated in Appendix 1.12.

The secondary and alternate responses discussed in section 6.5 were also measured in this experimental trial.  The results are shown in the following table.

Table 13: SA1 Steepest Ascent - Alternate Responses

| Steepest Ascent | Mean | Min Diameter | Max Diameter | Diameter Range |
|---|---|---|---|---|
| Step 0 | 444.53 | 161.14 | 1058.37 | 897.23 |
| Step 1 | 419.29 | 119.12 | 1052.34 | 933.22 |
| Step 2 | 400.90 | 128.40 | 1136.18 | 1007.79 |
| Step 3 | 390.13 | 127.82 | 1023.92 | 896.09 |
| Step 4 | 491.74 | 143.01 | 1368.33 | 1225.32 |
| Step 5 | 431.70 | 108.07 | 1227.23 | 1119.16 |

An SEM image of the fiber morphology of each step of the steepest ascent is shown in Figure 18.   The density of fibers is clearly shown to increase at each step of the steepest ascent.  The range and size of fibers observed appears to be consistent with the analytical fiber analysis conducted using the Phenom Fibermetric software.
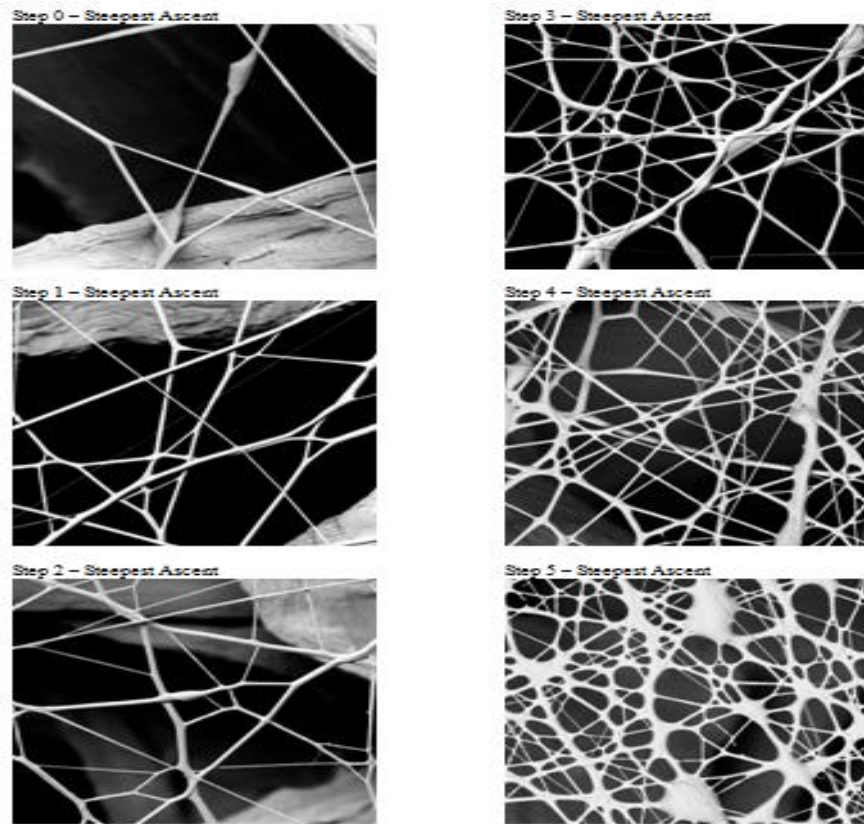
Figure 18: Fiber Images of Steepest Ascent for SA1 - (9300x)

### 7.4.4 DOE2a Analysis

Based on the steepest ascent SA1, a second first-order effects model (DOE2a) was developed. The independent variables used for the center point of the DOE2a were to be set to the same as step 5 of steepest ascent SA1. The following table shows the initial high, low and center point settings for fitting the second first-order model.

Table 14: DOE2a - High, Low, and Center Point Values

| | Basic Design | | | | | Factor F=ABC | Factor G=ABD | Factor H=BCDE |
|---|---|---|---|---|---|---|---|---|
| | Factor A | Factor B | Factor C | Factor D | Factor E | | | |
| Low | 11.43 | 53.13 | 82.14 | 39.33 | 11.00 | 69.33 | 53.50 | 60.00 |
| Center | 14.29 | 60.94 | 86.90 | 42.67 | 14.00 | 72.67 | 56.00 | 68.00 |
| High | 17.38 | 68.75 | 91.67 | 46.00 | 16.00 | 76.00 | 58.50 | 80.00 |

The range between the high and low values for each factor were selected to adequately model the overall properties of the response surface in the immediate vicinity of the center point and to accurately estimate the gradient at the center point.

Since the H factor reached the upper limit, the center point was changed to 68.0 to allow for a high and low condition for this variable.  The high and low setting of factor B was set to smallest increment around the center point.  The following table shows the coverage of the feasible ranges provided by the initial high and low point values.

Table 15: DOE2a - Feasibility Variable Range

|  | Factor A | Factor B | Factor C | Factor D | Factor E | Factor F | Factor G | Factor H |
|---|---|---|---|---|---|---|---|---|
| % of Range | 3% | 6% | 4% | 1% | 3% | 5% | 7% | 6% |
| % to Min (Center pt.) | 6% | 69% | 61% | 14% | 33% | 55% | 75% | 94% |
| % to Max (Center Pt) | 94% | 31% | 39% | 86% | 67% | 45% | 25% | 6% |

Using the eight factors, a sixty-seven experiment $2_{IV}^{8-3}$ fractional factorial design was developed.  This experimental design is represented in Table 4.  Three center points are included in the experimental design.

The alias structure of this experimental design can be found in section 2.4. The possible blocking factors, the day of the trial, the polymer batch and the substrate roll number were all identical for the DOE2a experimental trials, so no blocking was needed.

An effects analysis was conducted based on the experimental trials using the experimental design.   The results of the coded estimated effects and coefficients analysis are shown in Table 16 along with those two-way interactions that were confounded.  The confounding structure involving three-way and higher order

interactions are not shown.  (For the confounding involving three-way and higher order

interactions, see the confounding structure provided in Chapter 2.)

Table 16: Estimated Effects and Coefficients for DOE2a (coded units)

| Term | Alias | Alias | Effect | Coef | P | S |
|---|---|---|---|---|---|---|
| Alias | Alias | Alias | | | | |
| Constant | | | | 39.7005 | 0.000 | |
| A | | | 6.9615 | 3.4808 | 0.000 | |
| B | | | -0.9501 | -0.4751 | 0.000 | |
| C | | | -1.2904 | -0.6452 | 0.000 | |
| D | | | 0.5711 | 0.2855 | 0.000 | |
| E | | | 0.0443 | 0.0222 | 0.759 | S1 |
| F | | | 0.7669 | 0.3834 | 0.000 | |
| G | | | -0.7230 | -0.3615 | 0.000 | |
| H | | | -0.5136 | -0.2568 | 0.001 | |
| AB | CF | DG | 1.2741 | 0.6371 | 0.000 | |
| AC | BF | | 0.7304 | 0.3652 | 0.000 | |
| AD | BG | | 2.0121 | 1.0061 | 0.000 | |
| AE | | | -0.6339 | -0.3169 | 0.000 | |
| AF | BC | | -0.0077 | -0.0039 | 0.957 | S2 |
| AG | BD | | 0.4708 | 0.2354 | 0.002 | |
| AH | | | -0.3261 | -0.1630 | 0.029 | |
| BE | | | -0.0812 | -0.0406 | 0.574 | S2 |
| BH | | | -0.1999 | -0.1000 | 0.171 | S2 |
| CD | FG | | 0.1211 | 0.0606 | 0.403 | S2 |
| CE | | | 0.0343 | 0.0172 | 0.812 | S2 |
| CG | DF | | -0.2159 | -0.1079 | 0.140 | S2 |
| CH | | | -0.1532 | -0.0766 | 0.292 | S2 |
| DE | | | -0.3156 | -0.1578 | 0.034 | |
| DH | | | 0.1055 | 0.0527 | 0.466 | S2 |
| EF | | | 0.3376 | 0.1688 | 0.024 | |
| EG | | | -0.1002 | -0.0501 | 0.489 | S2 |
| EH | | | -1.9794 | -0.9897 | 0.000 | |
| FH | | | 0.4955 | 0.2478 | 0.001 | |
| GH | | | 0.1912 | 0.0956 | 0.190 | S2 |
| ABE | | | -0.0761 | -0.0380 | 0.598 | S2 |
| ABH | | | -0.0180 | -0.0090 | 0.901 | S2 |
| ACD | | | -0.3500 | -0.1750 | 0.020 | S3 |
| Ct Pt | | | | 4.8722 | 0.000 | |

R-Sq. = 99.00%    R-Sq. (adj.) = 98.05

Notes:

S1 Red Shading - Main effects retained to preserve hierarchy

S2 Blue Shading - Effects eliminated due to lack of statistical significance

S3 Green Shading – Statistically significant three-way interactions

A level of significance of   $\alpha > 0.05$ was used to compare to the p-values in

Table 16 to determine which of the effects in the model were statistically significant. The

main effect having a lack of significance was factor E.  This main effect is shaded and

labeled "S1" in Table 16.  The effects having a lack of significance which can be

60

eliminated from the DOE2a effects model are shaded and labeled "S2" in Table 16. The experimental results of DOE2a and the four main residual plots are shown in Appendix 1.2.

The contour plots in Figure 19 and Figure 20 show the properties of the response surface as depicted by the first-order model. The contour plots did not provide evidence of a localized minimum or maximum response since there were no closed circular contour lines present.
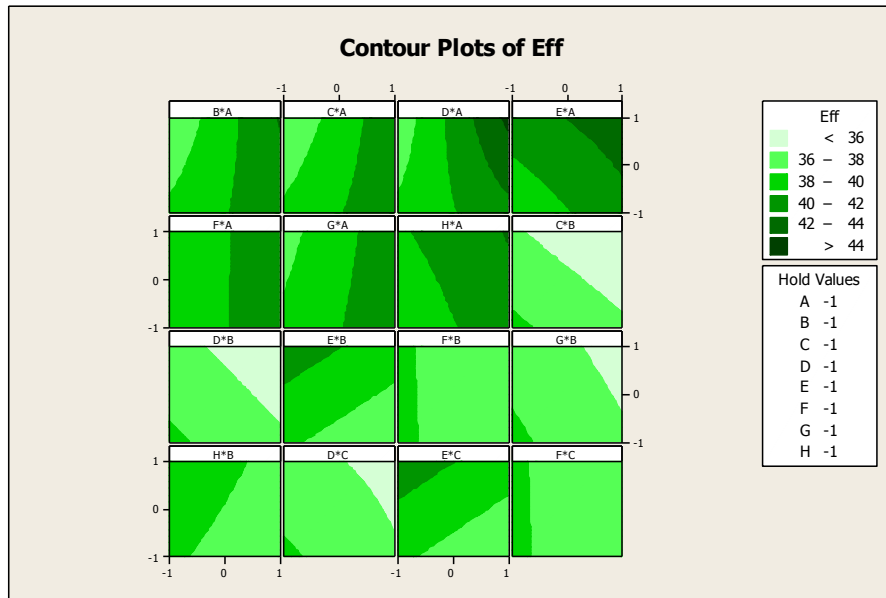


Figure 19: DOE2a Contour Plot 1 of 2
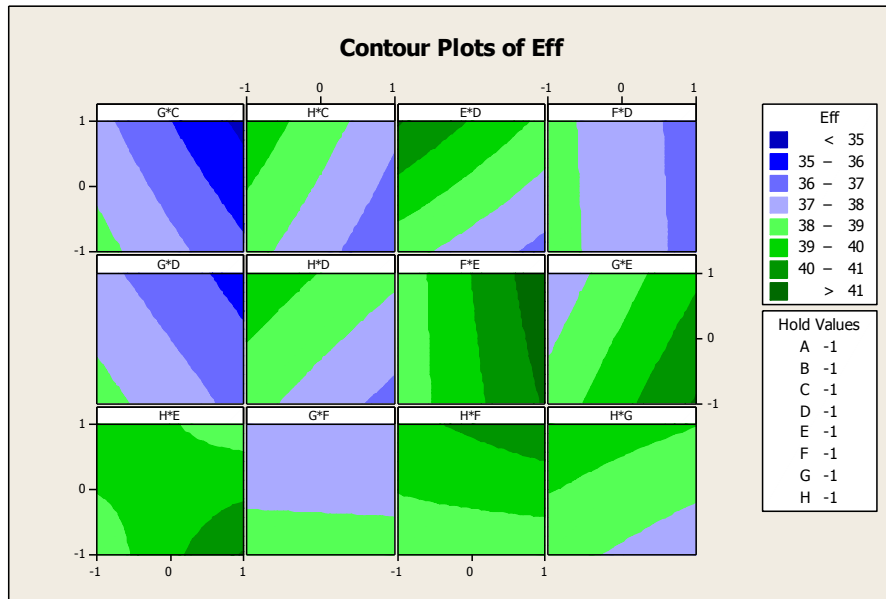
Figure 20: DOE2a Contour Plot 2 of 2

There are thirty-five degrees of freedom (DOF) available for estimating of the Mean Squared Error (MSE) in the DOE analysis.  In order to further improve the estimate of the MSE and the accuracy of the model, a reduced analysis was conducted that removed model terms that were not statistically significant.

7.4.5 Reduced DOE2a Analysis

A reduced effects model was generated based on eliminating the effects having a lack of significance discussed in section 7.4.4.  The main effects having a lack of significance were kept to preserve the hierarchy principle.  The reduced DOE2a effects analysis results are presented in Table 17.

Table 17: Estimated Effects and Coefficients for DOE2a reduced model (coded units)

| Term | Alias | Alias | Effect | Coef | P | S |
|---|---|---|---|---|---|---|
| Alias | Alias | Alias | | | | |
| Constant | | | | 39.7025 | 0.000 | |
| A | | | 6.9615 | 3.4808 | 0.000 | |
| B | | | -0.9501 | -0.4751 | 0.000 | |
| C | | | -1.2904 | -0.6452 | 0.000 | |
| D | | | 0.5711 | 0.2855 | 0.000 | |
| E | | | 0.0443 | 0.0222 | 0.755 | S1 |
| F | | | 0.7669 | 0.3834 | 0.000 | |
| G | | | -0.7230 | -0.3615 | 0.000 | |
| H | | | -0.5136 | -0.2568 | 0.001 | |
| AB | CF | DG | 1.2741 | 0.6371 | 0.000 | S4 |
| AC | BF | | 0.7304 | 0.3652 | 0.000 | S4 |
| AD | BG | | 2.0121 | 1.0061 | 0.000 | S4 |
| AE | | | -0.6339 | -0.3169 | 0.000 | |
| AG | BD | | 0.4708 | 0.2354 | 0.001 | S4 |
| AH | | | -0.3261 | -0.1630 | 0.024 | |
| DE | | | -0.3156 | -0.1578 | 0.028 | |
| EF | | | 0.3376 | 0.1688 | 0.019 | |
| EH | | | -1.9794 | -0.9897 | 0.000 | |
| FH | | | 0.4955 | 0.2478 | 0.001 | |
| ACD | | | -0.3500 | -0.1750 | 0.016 | |
| Ct Pt | | | | 4.8722 | 0.773 | |

R-Sq. = 98.71%   R-Sq. (adj.) = 98.15%

Notes:
S1 Red Shading - Main effects retained to preserve hierarchy
S4 Yellow Shading – Statistically significant aliased (confounded) interactions

There are forty-seven degrees of freedom (DOF) available for estimating the Mean Squared Error (MSE). The main effect which lacks significance is shaded and labeled "S1" in Table 17.  The statistically significant aliased two-way interactions are shaded and labeled "S4" in Table 17.  Based on the results shown in Table 17, none the aliased (confounded) two-way interactions could be eliminated by the hierarchy principle.  Table 18 shows the estimated effects analysis with the further reduced confounded and three-way interactions.

Table 18: Estimated Effects Analysis for DOE2a reduced model (coded units)

| Term | | | Effect | Coef | P | S |
|---|---|---|---|---|---|---|
| Alias | Alias | Alias | | | | |
| Constant | | | | 39.7005 | 0.000 | |
| A | | | 6.9615 | 3.4808 | 0.000 | |
| B | | | -0.9501 | -0.4751 | 0.000 | |
| C | | | -1.2904 | -0.6452 | 0.000 | |
| D | | | 0.5711 | 0.2855 | 0.000 | |
| E | | | 0.0443 | 0.0222 | 0.752 | S1 |
| F | | | 0.7669 | 0.3834 | 0.000 | |
| G | | | -0.7230 | -0.3615 | 0.000 | |
| H | | | -0.5136 | -0.2568 | 0.001 | |
| AB | CF | DG | 1.2741 | 0.6371 | 0.000 | S4 |
| AC | BF | | 0.7304 | 0.3652 | 0.000 | S4 |
| AD | BG | | 2.0121 | 1.0061 | 0.000 | S4 |
| AE | | | -0.6339 | -0.3169 | 0.000 | |
| AG | BD | | 0.4708 | 0.2354 | 0.001 | S4 |
| AH | | | -0.3261 | -0.1630 | 0.024 | |
| DE | | | -0.3156 | -0.1578 | 0.028 | |
| EF | | | 0.3376 | 0.1688 | 0.019 | |
| EH | | | -1.9794 | -0.9897 | 0.000 | |
| FH | | | 0.4955 | 0.2478 | 0.001 | |
| Ct Pt | | | | 4.8722 | 0.773 | |

R-Sq. = 98.23%   R-Sq. (adj.) = 97.35%

Notes:
S1 Red Shading - Main effects retained to preserve hierarchy
S4 Yellow Shading – Statistically significant aliased (confounded) interactions

The adjusted R squared measure reflects the fact that the model fit is being evaluated with fewer terms.  In this case, the adjusted R squared measure essentially did not change, going from 98.15 percent to 97.35 percent, when eliminating the significant three-way interaction.   Therefore there has been no increase in the lack of fit of the reduced model caused by the elimination of this statistically significant three-way interaction.

Often, a folding experiment and additional experimental trials would be required to determine which of the confounded two-way interactions show significance, or if both show significance.  However, in this case, folding of the effects experiments was avoided because, as it will be seen later, it was determined that the DOE2a

experimental region did not contain an optimum and a steepest ascent analysis would be conducted.

The p-value for the center point in Table 18 was examined as a test for quadratic curvature.  A p-value less than the selected alpha value of 0.05 for the test indicates there is quadratic curvature.  Since the p-value for the center point was equal to 0.773, no quadratic curvature is suggested in the response surface region.  This, combined with the monotonic response increase apparent in the contour plots, supports the conclusion that the optimum will lie outside the experimental region.

The following equation would be the coded fitted linear regression model which includes the aliased confounded terms for DOE2a.

$$y = 39.700 + 3.481A - 0.475B - 0.645C + 0.285D + 0.022E + 0.383F - 0.362G$$
$$- 0.257H + 0.637(AB, CF, DG) + 0.365(AC, BF) + 1.006(AD, BG)$$
$$- 0.317AE + 0.235(AG, BD) - 0.163AH - 0.158DE + 0.169EF$$
$$- 0.989EH + 0.248FH$$

Where A stands for coded factor $x_A$ , (AB, BG) stands for coded factors $x_A * x_B$ or $x_B * x_D$ and so forth.


Folding was not needed for this experimental region because DOE1a was determined to not contain an optimum and the steepest ascent coded gradient path equation will have no interaction terms when the starting point (0, 0, 0, 0, 0, 0, 0, 0) is substituted into the expressions for the partial coded variable equation.  This may be seen by taking the partial derivative of the first order model with respect to each variable and substituting (0, 0, 0, 0, 0, 0, 0, 0).

$$\frac{\partial y}{\partial A} = 3.481$$

$$\frac{\partial y}{\partial B} = -0.475$$

$$\frac{\partial y}{\partial C} = -0.645$$

$$\frac{\partial f}{\partial D} = 0.285$$

$$\frac{\partial y}{\partial E} = 0.022$$

$$\frac{\partial y}{\partial F} = 0.383$$

$$\frac{\partial y}{\partial G} = -0.362$$

$$\frac{\partial y}{\partial H} = -0.257$$

The experimental results for DOE2a and the four main residual plots are shown in Appendix 1.2.

7.4.6 Steepest Ascent - SA2

The method of steepest ascent (SA2) based on following a path in the gradient direction was used to move toward a better response. The method of steepest ascent (SA2) was based on the DOE2a model gradient.

Replicated experimental runs were conducted along the path until consecutive steps resulted in a decreased response. The step size was selected to be 0.5 which

was the smallest possible for incrementing the independent variables at a measureable difference based on the resolution of the equipment controls.   The steepest ascent setup along with the coded coefficients are given below.


Path of Steepest Ascent Overview

Total # of Runs                8
Total # of Factors             8
Base Factor Name                    Factor A
Step Size Base Factor by           0.0650
Coded Coefficient of Base Factor     3.4737

The coded steepest ascent path is:

$$x\,\mathbf{i_1},\, -0.140x\mathbf{i_2},\, -0.095x\mathbf{i_3},\, 0.228x\mathbf{i_4},\, -0.035x\mathbf{i_5},\, -0.082x\mathbf{i_6},\, -0.204x\mathbf{i_7},\, -0.073x\mathbf{i_8}$$

where:  x = coded factor A

Table 19 shows the coded steepest ascent experiment including the factor values for each step.

Table 19: SA2 Steepest Ascent Design - Coded

|        | Factor A (x) | Factor B | Factor C | Factor D | Factor E | Factor F | Factor G | Factor H |
|--------|--------------|----------|----------|----------|----------|----------|----------|----------|
| Step 0 | 0.000        | 0.000    | 0.000    | 0.000    | 0.000    | 0.000    | 0.000    | 0.000    |
| Step 1 | 0.460        | -0.068   | -0.045   | 0.120    | -0.009   | -0.042   | -0.100   | -0.050   |
| Step 2 | 1.020        | -0.137   | -0.095   | 0.220    | -0.025   | -0.082   | -0.200   | -0.050   |
| Step 3 | 1.500        | -0.205   | -0.140   | 0.340    | -0.056   | -0.122   | -0.300   | -0.100   |
| Step 4 | 1.980        | -0.274   | -0.185   | 0.440    | -0.072   | -0.162   | -0.400   | -0.150   |
| Step 5 | 2.460        | -0.342   | -0.230   | 0.560    | -0.088   | -0.201   | -0.500   | -0.150   |
| Step 6 | 2.940        | -0.410   | -0.280   | 0.660    | -0.103   | -0.241   | -0.600   | -0.200   |
| Step 7 | 3.420        | -0.479   | -0.325   | 0.780    | -0.119   | -0.281   | -0.700   | -0.250   |

The calculated factor B values were not within the incremental limits so B was held constant.  The factor F and the factor G were also held constant, since the factor increments were beyond the equipment capabilities.   Two replications were conducted at each step in the experimental trials to get a better estimate of an average.     Table

20 shows the experimental trial results for each step of the steepest ascent and Figure

21 shows a graphical representation of the experimental trial results.

Table 20: SA2 Steepest Ascent for Efficiency Response

| Step | Std Dev | Mean Eff Response | Trial 1 | Trial 2 | Trial 3 | Trial 4 | DOE2a Prediction | MSE |
|------|---------|-------------------|---------|---------|---------|---------|------------------|------|
| Step 0 | 0.276 | 44.573 | 44.846 | 44.295 | 44.577 |  | 43.169 | 32.3 |
| Step 1 | 1.164 | 45.926 | 47.113 | 45.879 | 44.787 |  | 44.315 | 22.3 |
| Step 2 | 2.281 | 46.575 | 49.379 | 47.463 | 44.996 | 44.462 | 45.606 | 10.0 |
| Step 3 | 1.895 | 47.886 | 49.645 | 49.358 | 46.654 | 45.887 | 46.650 | 4.5 |
| Step 4 | 1.739 | 49.197 | 49.910 | 51.252 | 48.312 | 47.312 | 47.652 | 2.3 |
| Step 5 | 0.921 | 48.780 | 48.117 | 50.101 | 48.719 | 48.184 | 48.212 | 7.2 |
| Step 6 | 1.362 | 48.363 | 46.323 | 48.950 | 49.125 | 49.055 | 49.316 | 35.0 |
| Step 7 | 2.458 | 47.947 | 44.530 | 47.799 | 49.532 | 49.927 | 50.103 | 86.3 |
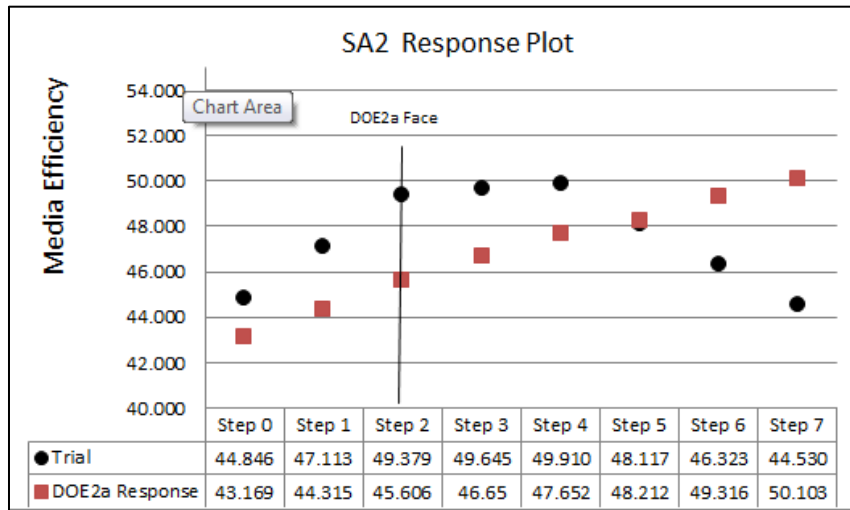


Figure 21: SA2 Response Plot

A total of twenty-one experimental trials were conducted for SA2 steepest

ascent.  At step 4 of the steepest ascent, the efficiency response stopped increasing.

The steepest ascent results plotted in Figure 21 show that the response continues to

increase well outside the experimental region of the DOE2a model.

Figure 23 presents an Analysis of Variance (ANOVA) for the means of the SA2

results along with the pooled standard deviation.

```
                         Individual 95% CIs For Mean Based on Pooled StDev
Level    N    Mean   StDev    +---------+---------+---------+---------
Step 0   3   44.573  0.276    (-------*-------)
Step 1   3   45.926  1.164        (-------*-------)
Step 2   4   46.575  2.281         (------*------)
Step 3   4   47.886  1.895             (-------*------)
Step 4   4   49.197  1.739                  (------*------)
Step 5   4   48.780  0.921                (------*------)
Step 6   4   48.363  1.362               (------*-------)
Step 7   4   47.947  2.458              (------*------)
                                +---------+---------+---------+---------
                              42.5      45.0      47.5      50.0

Pooled StDev = 1.713
```
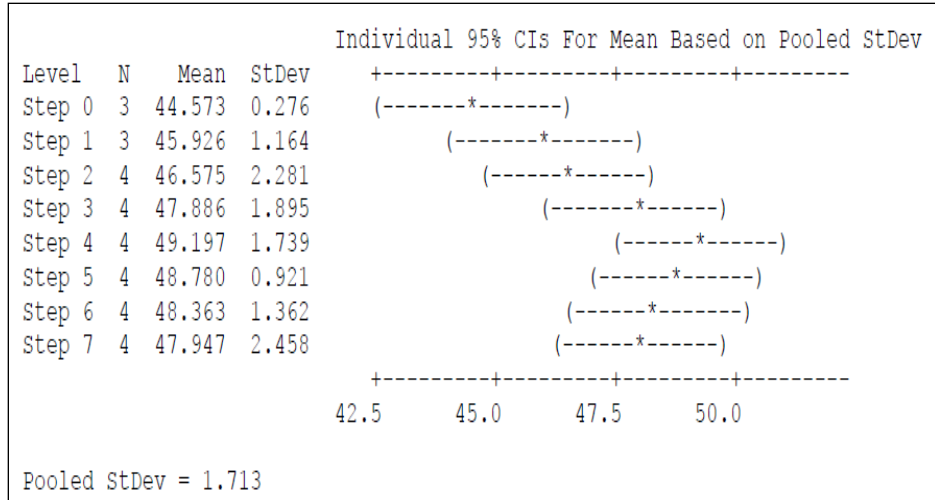
Figure 22: SA2 ANOVA Analysis

### 7.4.7 DOE3a Analysis

Based on the steepest ascent SA2 results, a third first-order effects model was developed.  The center point of the DOE3a was the same point as step 4 of steepest ascent SA2.   The ranges of the high and low points are set similar to DOE2a. The following factor settings in Table 21 were used as the initial high, low and center point values.

Table 21: DOE3a - High, Low, and Center Point Values

|         | Factor A | Factor B | Factor C | Factor D | Factor E | Factor F | Factor G | Factor H |
|---------|----------|----------|----------|----------|----------|----------|----------|----------|
| Low     | 16.67    | 53.13    | 81.67    | 38.27    | 12.05    | 59.33    | 46.00    | 56.00    |
| Center  | 20.24    | 60.94    | 85.24    | 43.27    | 15.80    | 72.67    | 56.00    | 64.00    |
| High    | 23.81    | 68.75    | 88.81    | 48.27    | 19.55    | 86.00    | 66.00    | 72.00    |

The following table shows the coverage of the feasible ranges provided by the initial high and low point values.

Table 22: DOE3a - Feasibility Variable Range

|                    | Factor A | Factor B | Factor C | Factor D | Factor E | Factor F | Factor G | Factor H |
|--------------------|----------|----------|----------|----------|----------|----------|----------|----------|
| % of Range         | 11%      | 19%      | 10%      | 14%      | 12%      | 29%      | 28%      | 6%       |
| % to Min(Center Pt)| 23%      | 75%      | 65%      | 48%      | 22%      | 65%      | 66%      | 95%      |
| % to Max(Center Pt)| 78%      | 25%      | 35%      | 52%      | 78%      | 36%      | 34%      | 5%       |

A sixty-seven trial experiment was conducted based on the fractional factorial design. The alias structure which describes the confounding in the $2_{IV}^{8-3}$ fractional factorial design can be found in section 2.4. The possible blocking factors considered for the experimental trial were the day of the trial, the polymer batch and the substrate roll number. For the DOE3a experimental trials, no blocking was needed.

The center point of the DOE3a was the same point as step 4 of steepest ascent SA2; however, there was a noticeable difference in the two different trial results. Step 4 of the steepest ascent experimental trials had an average response of 49.197 and the DOE3a center point had an average trial response of 54.143. The significant difference between these two experimental trials is likely caused by a bias produced by the use of a different polymer batch for SA2 versus DOE3 on each of the different days.

The results of the DOE analysis of the coded main effects, interactions and coefficients of the model are shown in Table 23 along with those two-way interactions that were confounded. The confounded structure involving three-way and higher order interactions is not shown. (For the confounding involving three-way and higher order interactions, see the confounding structure provided in Chapter 2.)

Table 23: Estimated Effects and Coefficients for DOE3a (coded units)

| Term | | | Effect | Coef | P | S |
|---|---|---|---|---|---|---|
| Alias | Alias | Alias | | | | |
| Constant | | | | 46.835 | 0.000 | |
| A | | | 1.902 | 0.951 | 0.000 | |
| B | | | 0.531 | 0.265 | 0.156 | S1 |
| C | | | 2.447 | 1.224 | 0.000 | |
| D | | | -2.379 | -1.190 | 0.000 | |
| E | | | -1.144 | -0.572 | 0.003 | |
| F | | | 0.065 | 0.032 | 0.862 | S1 |
| G | | | -0.063 | -0.031 | 0.866 | S1 |
| H | | | 1.992 | 0.996 | 0.000 | |
| AB | CF | DG | -0.027 | -0.014 | 0.941 | S2 |
| AC | BF | | -0.118 | -0.059 | 0.750 | S2 |
| AD | BG | | 0.015 | 0.008 | 0.967 | S2 |
| AE | | | 0.023 | 0.011 | 0.951 | S2 |
| AF | BC | | -0.214 | -0.107 | 0.565 | S2 |
| AG | BD | | -0.057 | -0.028 | 0.878 | S2 |
| AH | | | -0.050 | -0.025 | 0.892 | S2 |
| BE | | | -0.240 | -0.120 | 0.517 | S2 |
| BH | | | -0.963 | -0.482 | 0.012 | |
| CD | FG | | 1.859 | 0.929 | 0.000 | |
| CE | | | 0.846 | 0.423 | 0.026 | |
| CG | DF | | 0.083 | 0.042 | 0.822 | S2 |
| CH | | | 0.134 | 0.067 | 0.718 | S2 |
| DE | | | 0.484 | 0.242 | 0.195 | S2 |
| DH | | | 0.780 | 0.390 | 0.039 | |
| EF | | | 0.025 | 0.012 | 0.947 | S2 |
| EG | | | -0.203 | -0.101 | 0.585 | S2 |
| EH | | | 0.404 | 0.202 | 0.277 | S2 |
| FH | | | 0.064 | 0.032 | 0.863 | S2 |
| GH | | | -0.008 | -0.004 | 0.983 | S2 |
| ABE | | | 0.138 | 0.069 | 0.710 | S3 |
| ABH | | | 0.179 | 0.090 | 0.628 | S3 |
| ACD | | | 0.002 | 0.001 | 0.996 | S3 |
| Ct Pt | | | | 4.736 | 0.000 | |

R-Sq. = 87.43%   R-Sq. (adj.) = 80.68%

Notes:
S1 Red Shading - Main effects retained to preserve hierarchy
S2 Blue Shading - Effects eliminated due to lack of statistical significance
S3 Green Shading – Three-way interactions eliminated due to lack of statistical significance.

A level of significance of $\alpha > 0.05$ was used to compare to the p-values in

Table 23 to determine which of the main effects and interactions in the model were

statistically significant.    The main effects having a lack of significance are B, F, and G

which are shaded and labeled "S1" in Table 23.  The two-way and three-way

interactions having a lack of significance which can be eliminated from the DOE3a

effects model are shaded and labeled "S2" in Table 23.   The experimental results of

DOE3a and the four main residual plots are shown in Appendix 1.3.

The contour plots in Figure 23 and Figure 24 show the properties of the response

surface as depicted by the first-order model.  The contour plots did not provide evidence

of a localized minimum or maximum response since there were no closed circular

contour lines present.
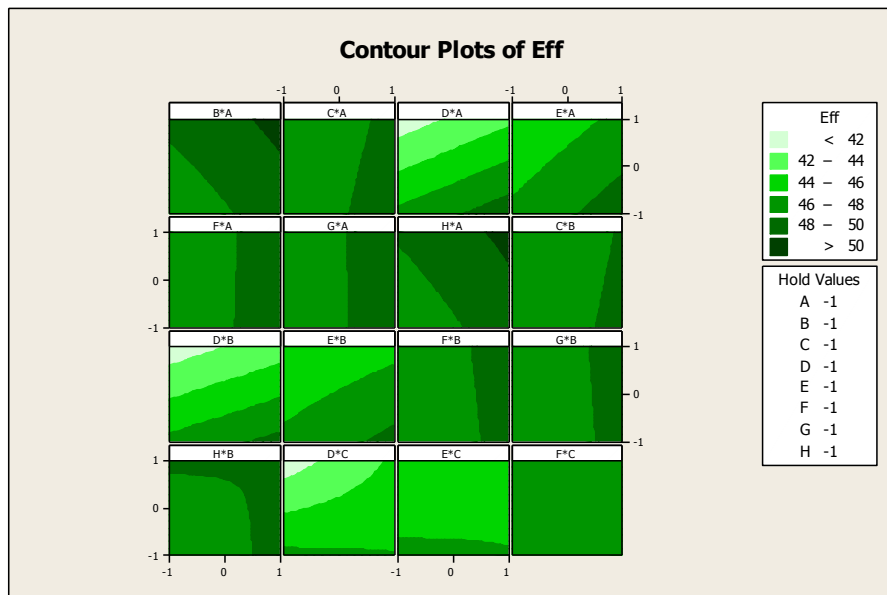


Figure 23: DOE3a Contour Plot 1 of 2
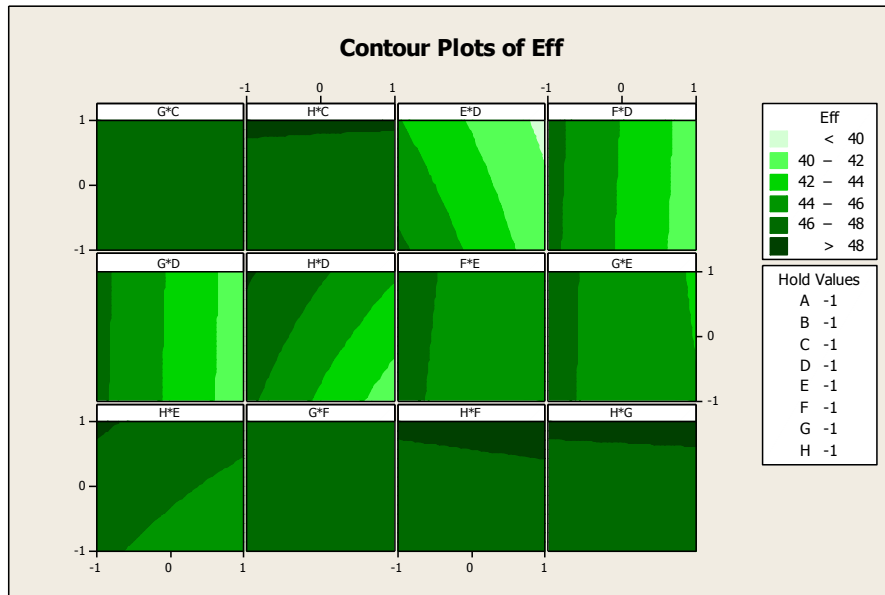
Figure 24: DOE3a Contour Plot 2 of 2

There are thirty-five degrees of freedom (DOF) available for estimating of the Mean Squared Error (MSE) in the DOE analysis.  In order to improve the estimate of the MSE and the accuracy of the model, a reduced analysis was conducted that removed model terms that were not statistically significant.

7.4.8 Reduced DOE3a Analysis

A reduced effects model was generated based on eliminating the effects having a lack of statistical significance as discussed in section 7.3.7.   The main effects having a lack of significance from the full DOE3a were kept to preserve hierarchy if they were involved in any for the significant aliased (confounded) two-way interactions. The reduced DOE3a effects analysis results are presented in Table 24.

Table 24: Estimated Effects and Coefficients for DOE3a reduced model (coded units)

| Term | | | Effect | Coef | P | S |
|---|---|---|---|---|---|---|
| Alias | Alias | Alias | | | | |
| Constant | | | | 46.835 | 0.000 | |
| A | | | 1.902 | 0.951 | 0.000 | |
| B | | | 0.531 | 0.265 | 0.111 | S1 |
| C | | | 2.447 | 1.224 | 0.000 | |
| D | | | -2.379 | -1.190 | 0.000 | |
| E | | | -1.144 | -0.572 | 0.001 | |
| F | | | 0.065 | 0.032 | 0.845 | S1 |
| G | | | -0.063 | -0.031 | 0.849 | S1 |
| H | | | 1.992 | 0.996 | 0.000 | |
| BH | | | -0.963 | -0.482 | 0.005 | |
| CD | FG | | 1.859 | 0.929 | 0.000 | S4 |
| DE | | | 0.846 | 0.423 | 0.012 | |
| DH | | | 0.780 | 0.390 | 0.020 | |
| Ct Pt | | | | 4.736 | 0.000 | |

R-Sq. = 91.67%   R-Sq. (adj.) = 90.12%

Notes:
S1 Red Shading - Main effects retained to preserve hierarchy
S4 Yellow Shading – Statistically significant aliased (confounded) interactions

There are forty-four degrees of freedom (DOF) available for estimating the Mean Squared Error (MSE). The three main effects which have a lack of significance are labeled "S1" in Table 24.  The statistically significant aliased two-way interactions are shaded and labeled "S4" in Table 24.   The aliased two-way interactions, CD and FG can be compared for significance using the hierarchy principle.  The CD confounded two-way interaction would be selected to be retained since the other aliased interaction contains the main effects F and G, both of which had a lack of significance.

The p-value for the center point in Table 24 provides a test for quadratic curvature.  A p-value less than the selected alpha value of 0.05 for the test indicates there is quadratic curvature.  Since the p-value for the center point was zero, quadratic curvature is indicated for the response surface region.

The experimental results of DOE3a and the four main residual plots are shown in Appendix 1.3.

7.4.9 SA3 - Steepest Ascent

The method of steepest ascent (SA3) based on following a path in the gradient direction was used to determine if a move toward a better response could be found using the DOE3a model.   The steepest ascent setup along with the coded coefficients are given below.

Path of Steepest Ascent Overview

Total # of Runs                        7
Total # of Factors                     8
Base Factor Name                 Factor A
Step Size Base Factor by         0.150

The step size was selected to be 0.15 which was the smallest possible for incrementing the independent variables at a measureable difference.  Table 25 shows the coded steepest ascent.

Table 25: Steepest Ascent SA3

|        | Factor A | Factor B | Factor C | Factor D | Factor E | Factor F | Factor G | Factor H | Eff% |
|--------|----------|----------|----------|----------|----------|----------|----------|----------|--------|
| Step 0 | 0.000 | 0.000 | 0.000 | 0.000 | 0.000 | 0.000 | 0.000 | 0.000 | 54.213 |
| Step 1 | 0.133 | 0.042 | 0.183 | -0.187 | -0.093 | 0.000 | 0.000 | 0.200 | 51.556 |
| Step 2 | 0.333 | 0.084 | 0.373 | -0.373 | -0.187 | 0.000 | -0.005 | 0.400 | 51.510 |
| Step 3 | 0.467 | 0.126 | 0.556 | -0.560 | -0.267 | 0.005 | -0.005 | 0.550 | 51.356 |
| Step 4 | 0.600 | 0.167 | 0.745 | -0.747 | -0.360 | 0.005 | -0.010 | 0.750 | 51.140 |
| Step 5 | 0.733 | 0.209 | 0.928 | -0.933 | -0.453 | 0.005 | -0.010 | 0.950 | 50.755 |
| Step 6 | 0.933 | 0.251 | 1.118 | -1.120 | -0.547 | 0.005 | -0.015 | 1.150 | 50.293 |
| Step 7 | 1.067 | 0.293 | 1.301 | -1.320 | -0.627 | 0.005 | -0.015 | 1.350 | 50.031 |

Step 5 of the steepest ascent represents the boundary of the DOE3a cube in the design space.  The predicted responses shown in Table 25 decrease as points on the path are moved away from the center point, which indicates that a maximum response point may lie inside the DOE3a cube.

Thus, the next step of the RSM/DOE approach was to generate a second-order model using a Central Composite experimental design to better evaluate the response surface within the region of experimentation.

## 7.4.10 DOE3b Central Composite Model

The DOE3a effects model indicated a potential maximum located inside the DOE3a experimental region.   A second-order Central Composite design was established around the center point of the DOE3a experimental cube.  The following independent variable setting values were used as the high, low, star and center point values.

Table 26: DOE3b High, Low, Star, and Center Point Values

|        | Factor A | Factor B | Factor C | Factor D | Factor E | Factor F | Factor G | Factor H |
|--------|----------|----------|----------|----------|----------|----------|----------|----------|
| L-Star | 10.24 | 37.50 | 75.24 | 29.13 | 5.20 | 35.33 | 27.50 | 40.00 |
| Low    | 16.67 | 53.13 | 81.67 | 38.27 | 12.05 | 59.33 | 46.00 | 56.00 |
| Center | 20.24 | 60.94 | 85.24 | 43.27 | 15.80 | 72.67 | 56.00 | 64.00 |
| High   | 23.81 | 68.75 | 88.81 | 48.27 | 19.55 | 86.00 | 66.00 | 72.00 |
| H-Star | 30.24 | 84.38 | 95.48 | 57.40 | 26.40 | 110.67 | 84.00 | 84.00 |

The following table shows the coverage of the feasible ranges provided by the high and low point values.

Table 27: DOE3b - Feasibility Variable Range

|                     | Factor A | Factor B | Factor C | Factor D | Factor E | Factor F | Factor G | Factor H |
|---------------------|----------|----------|----------|----------|----------|----------|----------|----------|
| % of Range          | 11% | 19% | 10% | 14% | 12% | 29% | 28% | 6% |
| % to Min (Center pt) | 23% | 75% | 65% | 48% | 22% | 65% | 66% | 95% |
| % to Max (Center Pt) | 78% | 25% | 35% | 52% | 78% | 36% | 34% | 5% |

The Central Composite Design included two replicates and twenty center points. A quarter fraction CCD was chosen to reduce the cost of the experimental trials.  The following Central Composite Design shows the design parameters selected.

Central Composite Design

Factors:    8    Replicates:    2
Base runs:   90    Total runs:    180
Base blocks:   1    Total blocks:    1

Two-level factorial: Quarter fraction

Cube points:            128
Center points in cube:   20
Axial points:            32
Center points in axial:    0

The following aliased (confounding) structure represents the quarter fraction

Central Composite Design up to three-way interaction terms.

Alias Structure (up to order 3)

| | |
|---|---|
| AB + CDG + EFH | AC + BDG |
| AD + BCG | AE + BFH |
| AF + BEH | AG + BCD |
| AH + BEF | BC + ADG |
| BD + ACG | BE + AFH |
| BF + AEH | BG + ACD |
| BH + AEF | CD + ABG |
| CG + ABD | DG + ABC |
| EF + ABH | EH + ABF |
| FH + ABE | |

The coded DOE3b Central Composite effects model results are shown in Table 28.

Table 28: Estimated Regression Coefficients for DOE3b (coded units)

| Term | Coef | T | P | S |
|---|---|---|---|---|
| Constant | 55.0169 | 145.486 | 0.000 | |
| A | 1.0458 | 7.822 | 0.000 | |
| B | -0.0972 | -0.727 | 0.468 | S1 |
| C | 0.8634 | 6.457 | 0.000 | |
| D | -1.1222 | -8.393 | 0.000 | |
| E | -0.3574 | -2.673 | 0.008 | |
| F | 0.0894 | 0.668 | 0.505 | S1 |
| G | 0.0836 | 0.625 | 0.533 | S1 |
| H | 0.9518 | 7.119 | 0.000 | |
| AA | -1.8864 | -17.017 | 0.000 | |
| BB | -0.8338 | -7.522 | 0.000 | S2 |
| CC | -0.9506 | -8.575 | 0.000 | |
| DD | -0.4441 | -4.006 | 0.000 | S2 |
| EE | -1.4796 | -13.346 | 0.000 | |
| FF | -0.7965 | -7.185 | 0.000 | S2 |
| GG | -0.8083 | -7.291 | 0.000 | S2 |
| HH | -0.7051 | -6.36 | 0.000 | S2 |
| AB | -0.0197 | -0.132 | 0.895 | S2 |
| AC | -0.0132 | -0.088 | 0.930 | S2 |
| AD | -0.0077 | -0.052 | 0.959 | S2 |
| AE | -0.0031 | -0.021 | 0.983 | S2 |
| AF | 0.1483 | 0.992 | 0.323 | S2 |
| AG | 0.4460 | 2.984 | 0.003 | |
| AH | 0.0171 | 0.114 | 0.909 | S2 |
| BC | 0.2074 | 1.387 | 0.168 | S2 |
| BD | 0.0023 | 0.015 | 0.988 | S2 |
| BE | 0.0471 | 0.315 | 0.753 | S2 |
| BF | 0.0318 | 0.213 | 0.832 | S2 |
| BG | 0.0058 | 0.039 | 0.969 | S2 |
| BH | 0.1092 | 0.731 | 0.466 | S2 |
| CD | 0.7967 | 5.330 | 0.000 | |
| CE | 0.2003 | 1.34 | 0.183 | S2 |
| CF | -0.0001 | -0.001 | 1.000 | S2 |
| CG | -0.0044 | -0.029 | 0.977 | S2 |
| CH | 0.0386 | 0.258 | 0.797 | S2 |
| DE | 0.3035 | 2.031 | 0.044 | S2 |
| DF | -0.0302 | -0.202 | 0.840 | S2 |
| DG | 0.0012 | 0.008 | 0.994 | S2 |
| DH | 0.5004 | 3.347 | 0.001 | |
| EF | 0.0309 | 0.207 | 0.837 | S2 |
| EG | -0.0267 | -0.179 | 0.859 | S2 |
| EH | -0.2281 | -1.526 | 0.129 | S2 |
| FG | 0.2025 | 1.354 | 0.178 | S2 |
| FH | 0.0136 | 0.091 | 0.928 | S2 |
| GH | -0.0012 | -0.008 | 0.994 | S2 |

R-Sq. = 85.85% R-Sq. (adj.) = 81.24%

Notes:

Main and Interaction Effects - 2 x Coefficient

S1 Red Shading - Main effects having a lack of statistical significance

S2 Blue Shading – Other effects eliminated due to a lack of statistical significance

A level of significance of $\alpha > 0.05$ was used to compare with the p-values in Table 28 to determine which of the main effects and interactions in the model were statistically significant. The main effects having a lack of significance are B, F, and G which are shaded and labeled "S1" in Table 28. The two-way interactions having a lack of significance which can be eliminated from the DOE3b effects model are shaded and labeled "S2" in Table 28. Based on the alias or confounded structure, there were no significant confounded interaction terms to consider. The DOE3b experimental results and the four residual plots are shown in Appendix 1.4.

7.4.11 Reduced DOE3b Central Composite Model

A reduced effects model was generated based on eliminating the main effects and interactions having a lack of statistical significance. . The main effects having a lack of significance from DOE3b were kept to preserve hierarchy. The results of the coded estimated effects and coefficients are shown below in Table 29.

Table 29: Estimated Regression Coefficients (coded units)

| Term | Coef | T | P | S |
|---|---|---|---|---|
| Constant | 55.0169 | 145.466 | 0.000 | |
| A | 1.0458 | 7.821 | 0.000 | |
| B | -0.0972 | -0.727 | 0.468 | S1 |
| C | 0.8634 | 6.457 | 0.000 | |
| D | -1.1222 | -8.392 | 0.000 | |
| E | -0.3574 | -2.672 | 0.008 | |
| F | 0.0894 | 0.668 | 0.505 | S1 |
| G | 0.0836 | 0.625 | 0.533 | S1 |
| H | 0.9518 | 7.118 | 0.000 | |
| AA | -1.8864 | -17.014 | 0.000 | |
| BB | -0.8338 | -7.521 | 0.000 | |
| CC | -0.9506 | -8.573 | 0.000 | |
| DD | -0.4441 | -4.005 | 0.000 | |
| EE | -1.4796 | -13.345 | 0.000 | |
| FF | -0.7965 | -7.184 | 0.000 | |
| GG | -0.8083 | -7.29 | 0.000 | |
| HH | -0.7051 | -6.359 | 0.000 | |
| AG | 0.4460 | 2.983 | 0.003 | |
| CD | 0.7967 | 5.329 | 0.000 | |

R-Sq. = 83.23% R-Sq. (adj.) = 81.24%

The main effects B, F and G having a lack of significance, but kept to preserve hierarchy are labeled "S1" in Table 29.  By eliminating the effects having a lack of significance, the change in the R squared and the adjusted R squared were evaluated below. (See section 3.2.3)

DOE3b – Full:          R-Sq. = 85.85% R-Sq. (adj.) = 81.24%
DOE3b – Reduced:       R-Sq. = 83.23% R-Sq. (adj.) = 81.24%

R squared decreased in value, but was considered reasonable since terms were eliminated.  The adjusted R squared value remained the same so the improvement in the model variability by eliminating the effects having a lack of significance was considered valid.

Contour plots were created from the DOE3b model.  The following two figures show the contour plots of the reduced DOE3b model.  The darkest (green) contour circles in Figure 25 and Figure 26  shows an area of maximum response.  The contour plots indicate there may be a maximum response in or very near the experimental region.
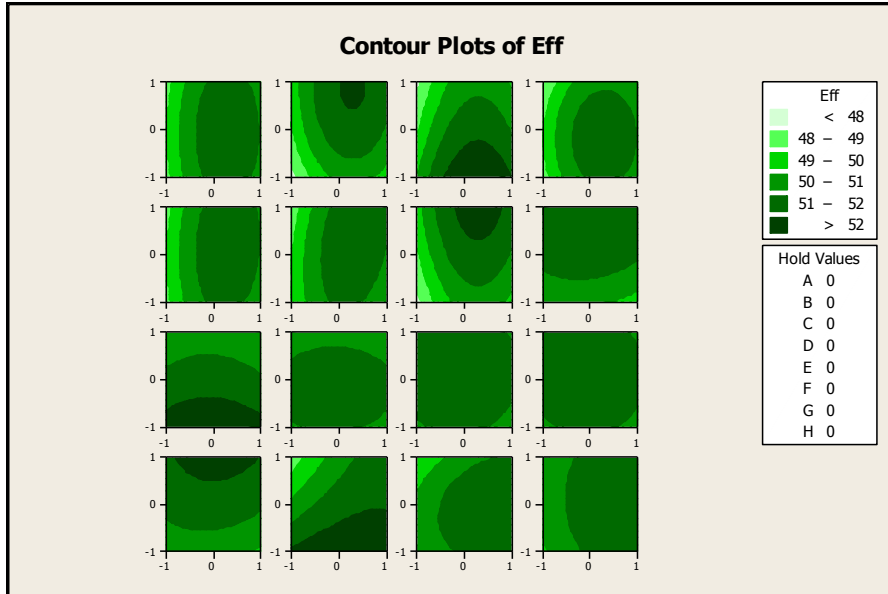
Figure 25: DOE3b Contour Plot 1 of 2
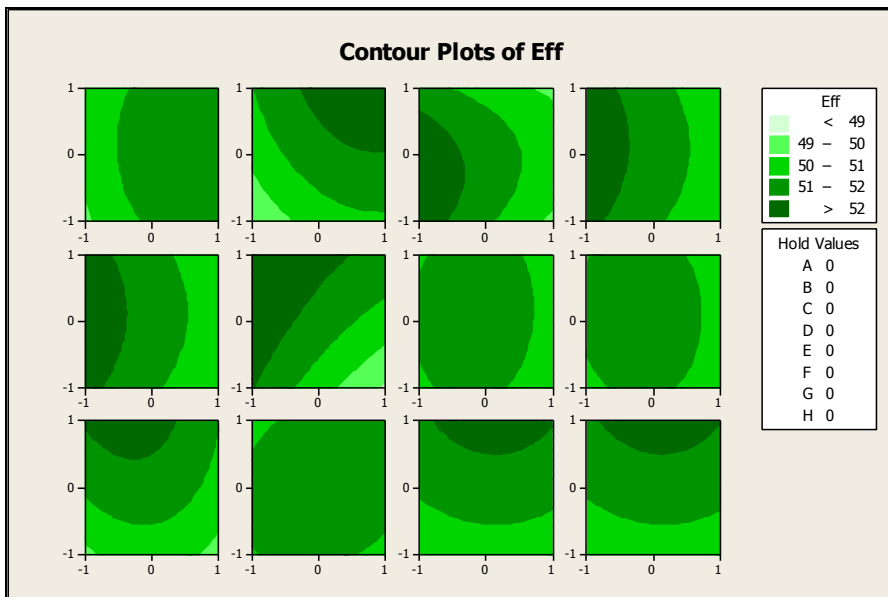

Figure 26: DOE3b Contour Plot 2 of 2

7.4.12 DOE3b Optimum Response

The reduced coded DOE3b quadratic coefficients from Table 29 were used to generate the following quadratic objective function.

MAX = 55.016 + 1.046 * A - 0.097*B + 0.086*C - 1.12*D - 0.357*E + 0.0894*F +
    0.084*G + 0.952*H – 1.886*A*A – 0.834*B*B – 0.951*C*C – 0.444*D*D –
    1.48*E*E – 0.797*F*F – 0.808*G*G – 0.705*H*H + 0.446*A*G + 0.796*C*D

The boundary of the DOE3b cube face was used to create the following constraint set.

Variable Constraints Set
-1.00 ≤ A ≤ 1.00
-1.00 ≤ B ≤ 1.00
-1.00 ≤ C ≤ 1.00
-1.00 ≤ D ≤ 1.00
-1.00 ≤ E ≤ 1.00
-1.00 ≤ F ≤ 1.00
-1.00 ≤ G ≤ 1.00
-1.00 ≤ H ≤ 1.00

The maximum found using Quadratic Programming with the quadratic objective function and the constraint set was 55.927.  The following table shows the settings corresponding to the results of the optimization.

Table 30: DOE3b Optima Response Settings

| Factor | Value |
|--------|-------|
| A | 20.0 |
| B | 68.8 |
| C | 63.3 |
| D | 48.3 |
| E | 17.6 |
| F | 59.6 |
| G | 66.0 |
| H | 95.1 |

Twenty experimental trials were conducted at the setting for the Quadratic Program maximum point.   The following table shows the variance analysis and the

ninety-five percent confidence intervals of the experimental trials at the DOE3b

maximizing point.  A sample size of two was used to create the confidence intervals

shown in Table 31.  The confidence intervals were based on a pooled standard

deviation derived from twelve experimental populations.  The development of the pooled

standard deviation is shown in Appendix 1.12.

Table 31: Experimental Trial Variance Analysis

| DOE3b Maximizer Validation | Mean | 55.222 |
|---|---|---|
| | Stdev | 0.9446 |
| | n | 20 |
| 95% Confidence Interval Formula $\bar{x} \pm Z * \dfrac{\sigma}{\sqrt{n}}$ | Z | 1.96 |
| | CI +/- | 1.309 |
| | CI Min | 53.913 |
| | CI Max | 56.531 |
| | Prediction | 55.927 |

The value found from the Quadratic Program was well inside the defined

confidence interval shown in Table 31.

The RSM approach could have been continued to find a point closer to the

optimum, but the progression so far indicated that the maximum response point

determined by the Quadratic Program was close to an optimum.   With additional cost

and time for conducting more trials, the estimate of the response surface optimum could

be improved.  However, based on the local analysis of the response surface, it was

decided that the estimate of the found point was sufficiently close for the purposes of

the study and that further investment of cost and effort was not warranted. The

experimental trial results can be found at Appendix 1.5.

7.4.13 RSM/DOE  Experimental Summary

A summary of the RSM/DOE analysis steps were as follows:



| DOE/RSM Steps: | |
| --- | --- |
| 1) DOE1a $1^{st}$-order model | |
| 2) SA1 steepest ascent | |
| 3) DOE2a $1^{st}$-order model | |
| 4) SA2 steepest ascent | |
| 5) DOE3a $1^{st}$-order model | |
| 6) DOE3b $2^{nd}$-order model | |
| 7) SA3 steepest ascent | |
| 8) Contour Plots | |
| 9) Quadratic Programming | |
| 10) Validation Trials | |
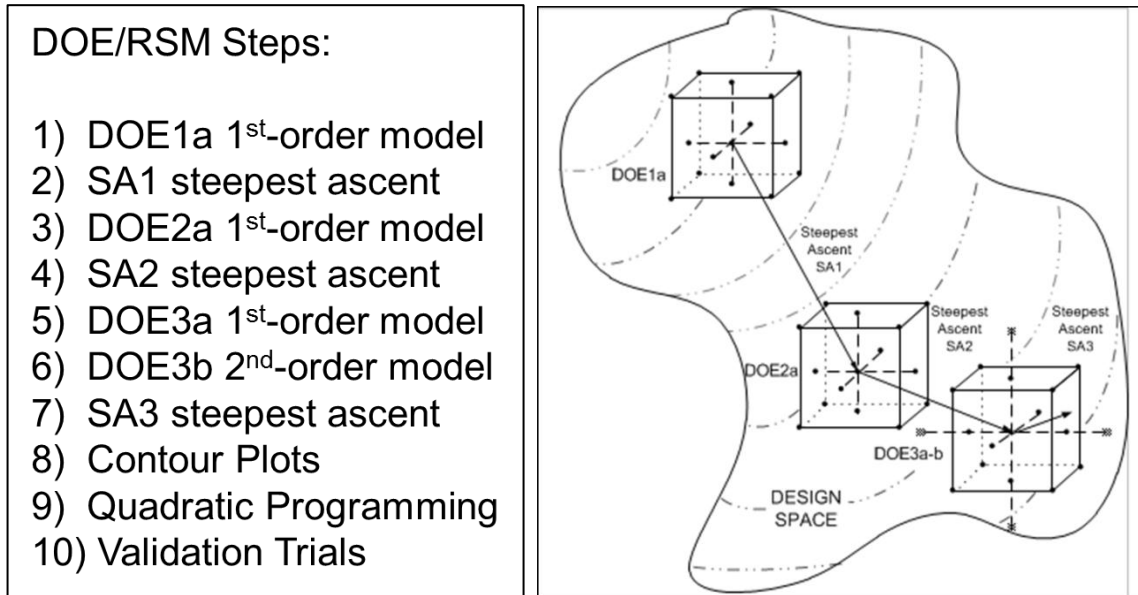
Figure 27: RSM/DOE Analysis Overview

A summary of the generated DOE models and the steepest ascents for the

RSM/DOE approach is shown in Table 32.

Table 32: RSM/DOE Approach Summary

| | Factor A | Factor B | Factor C | Factor D | Factor E | Factor F | Factor G | Factor H | Eff% |
| --- | --- | --- | --- | --- | --- | --- | --- | --- | --- |
| DOE1a | | | | | | | | | |
| Low | 70.95 | 45.31 | 23.81 | 30.00 | 66.00 | 40.00 | 61.00 | 32.00 | 30.827 |
| Center | 73.81 | 53.13 | 28.57 | 33.33 | 67.00 | 46.67 | 60.00 | 40.00 | 32.534 |
| High | 76.90 | 60.94 | 33.33 | 36.67 | 68.00 | 53.33 | 59.00 | 48.00 | 34.524 |
| SA1 | | | | | | | | | |
| Step 0 | 73.81 | 53.13 | 28.57 | 33.33 | 67.00 | 63.33 | 60.00 | 40.00 | 32.534 |
| Step 1 | 61.90 | 54.69 | 40.24 | 35.20 | 56.40 | 65.20 | 59.20 | 45.60 | 30.892 |
| Step 2 | 50.00 | 56.25 | 51.90 | 37.07 | 45.80 | 67.07 | 58.40 | 51.20 | 36.225 |
| Step 3 | 38.10 | 57.81 | 63.33 | 38.93 | 35.20 | 68.93 | 57.60 | 56.80 | 40.518 |
| Step 4 | 26.19 | 59.38 | 75.00 | 40.80 | 24.60 | 70.80 | 56.80 | 62.40 | 42.336 |
| Step 5 | 14.29 | 60.94 | 86.90 | 42.67 | 14.00 | 72.67 | 56.00 | 68.00 | 44.573 |
| Step 6 | 2.38 | 62.50 | 98.57 | 44.53 | 3.40 | 74.53 | 55.20 | 73.60 | 37.465 |
| DOE2a | | | | | | | | | |
| Low | 11.43 | 53.13 | 82.14 | 39.33 | 11.00 | 69.33 | 53.50 | 60.00 | 39.731 |
| Center | 14.29 | 60.94 | 86.90 | 42.67 | 14.00 | 72.67 | 56.00 | 68.00 | 44.573 |
| High | 17.38 | 68.75 | 91.67 | 46.00 | 16.00 | 76.00 | 58.50 | 80.00 | 42.111 |
| SA2 | | | | | | | | | |
| Step 0 | 14.29 | 60.94 | 86.90 | 42.67 | 14.00 | 72.67 | 56.00 | 68.00 | 44.573 |
| Step 1 | 15.71 | 60.94 | 86.43 | 42.80 | 14.50 | 72.67 | 56.50 | 68.00 | 45.926 |
| Step 2 | 17.38 | 60.94 | 85.95 | 43.00 | 15.00 | 72.67 | 56.50 | 68.00 | 46.575 |

| | | | | | | | | | |
|---|---|---|---|---|---|---|---|---|---|
| Step 3 | 18.81 | 60.94 | 85.71 | 43.13 | 15.50 | 72.67 | 56.50 | 68.00 | 47.886 |
| Step 4 | 20.24 | 60.94 | 85.24 | 43.27 | 16.00 | 72.67 | 57.00 | 64.00 | 49.197 |
| Step 5 | 21.67 | 60.94 | 84.76 | 43.40 | 16.50 | 72.67 | 57.00 | 64.00 | 48.780 |
| Step 6 | 23.33 | 60.94 | 84.29 | 43.53 | 17.00 | 72.67 | 57.00 | 64.00 | 48.363 |
| Step 7 | 25.00 | 60.94 | 83.81 | 43.67 | 17.50 | 72.67 | 57.50 | 64.00 | 47.947 |
| DOE3a | | | | | | | | | |
| Low | 16.67 | 53.13 | 81.67 | 38.00 | 12.00 | 59.33 | 46.00 | 56.00 | 49.321 |
| Center | 20.24 | 60.94 | 85.24 | 43.33 | 16.00 | 72.67 | 56.00 | 64.00 | 54.213 |
| High | 23.81 | 68.75 | 88.81 | 48.00 | 19.50 | 86.00 | 66.00 | 72.00 | 46.286 |
| DOE3b | | | | | | | | | |
| L-Low | 10.00 | 37.50 | 75.24 | 29.33 | 5.00 | 35.33 | 27.50 | 40.00 | 50.111 |
| Low | 16.67 | 53.13 | 81.67 | 38.00 | 12.00 | 59.33 | 46.00 | 56.00 | 49.321 |
| Center | 20.24 | 60.94 | 85.24 | 43.33 | 16.00 | 72.67 | 56.00 | 64.00 | 54.213 |
| High | 23.81 | 68.75 | 88.81 | 48.00 | 19.50 | 86.00 | 66.00 | 72.00 | 46.286 |
| H-High | 30.24 | 84.38 | 95.48 | 57.33 | 26.50 | 110.67 | 84.00 | 84.00 | 45.569 |
| SA3 | | | | | | | | | |
| Step 0 | 20.24 | 60.94 | 85.24 | 43.27 | 15.80 | 72.67 | 56.00 | 64.00 | 54.213 |
| Step 1 | 20.71 | 61.25 | 85.95 | 42.33 | 15.45 | 72.73 | 55.95 | 65.20 | 51.556 |
| Step 2 | 21.43 | 61.56 | 86.67 | 41.40 | 15.10 | 72.80 | 55.90 | 66.80 | 51.510 |
| Step 3 | 21.90 | 61.88 | 87.38 | 40.47 | 14.80 | 72.87 | 55.85 | 68.00 | 51.356 |
| Step 4 | 22.38 | 62.19 | 88.10 | 39.53 | 14.45 | 72.87 | 55.80 | 69.20 | 51.140 |
| Step 5 | 22.86 | 62.50 | 88.57 | 38.60 | 14.10 | 72.93 | 55.80 | 70.40 | 50.755 |
| Step 6 | 23.57 | 62.81 | 89.29 | 37.67 | 13.75 | 73.00 | 55.75 | 72.00 | 50.293 |
| Step 7 | 24.05 | 63.13 | 90.00 | 36.67 | 13.45 | 73.07 | 55.70 | 73.20 | 50.031 |

The normed distance from the center point of each DOE to the DOE3b maximizer was calculated and the results are shown in Table 33. An example of the normed distance calculation is shown on Appendix 1.11.

Table 33: Normed Distance from DOE3b Maximizer to the DOE Cube Center Points

| RSM/DOE Step | Normed Distance |
|---|---|
| DOE1 | 1.657 |
| DOE2 | 0.398 |
| DOE3 | 0.404 |
| DOE3b Maximizer | 0.000 |

Confidence Intervals were calculated at each DOE center point. The confidence intervals were based on a pooled standard deviation derived from twelve experimental populations. The calculations for the pooled standard deviation are shown in Appendix 1.12.

Table 34: RSM/DOE Center Point Confidence Intervals

| 95% Confidence Interval Formula $\bar{x} \pm Z * \dfrac{\sigma}{\sqrt{n}}$ | DOE1a | DOE2a | DOE3a | DOE3b |
|---|---|---|---|---|
| Mean | 32.534 | 44.573 | 54.694 | 55.017 |
| Stdev (Pooled) | 0.945 | 0.945 | 0.945 | 0.945 |
| n | 69 | 67 | 67 | 180 |
| Z | 1.96 | 1.96 | 1.96 | 1.96 |
| CI +/- | 0.223 | 0.226 | 0.226 | 0.138 |
| CI Min | 32.311 | 44.346 | 54.468 | 54.879 |
| CI Max | 32.757 | 44.799 | 54.921 | 55.155 |

The following figure shows a graphical representation of the response vs. normed distance from tables 32, 33 and 34.
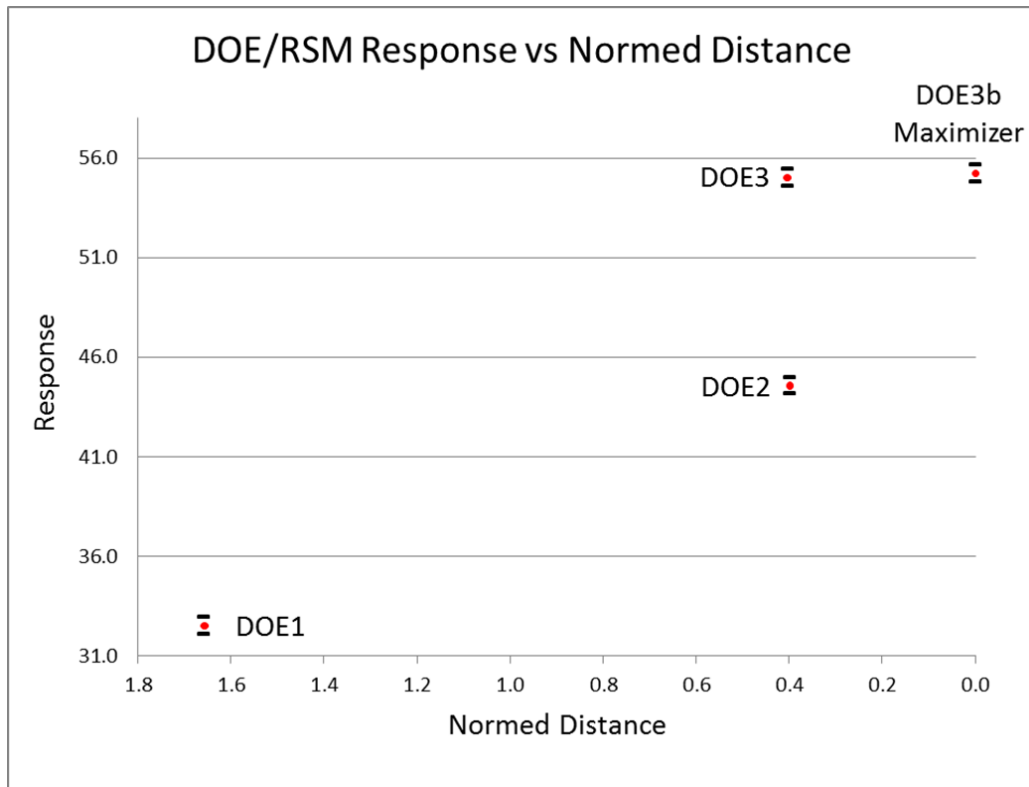
Figure 28: Response/Normed Distance

As shown in Figure 28, the progressive steps associated with the RSM/DOE optimization process were able to move toward an increased response.

7.5 Fiber Morphology Evaluation

There were a number of different defects noted in the various fiber analyses conducted in the experimental trials.  The primary defects were holes and beads.   The beads are formed by small polymer droplets.  The beads are more pronounced as the concentration level of the polymer solution is decreased.  By decreasing the polymer solution concentration, the viscosity and surface tension decrease also.

The holes are formed by large drops of polymer solution.  These larger drops are not dry when they reach the substrate and the non-vaporized solvent basically melts the already formed fibers. These defects are shown in Figure 29.

87
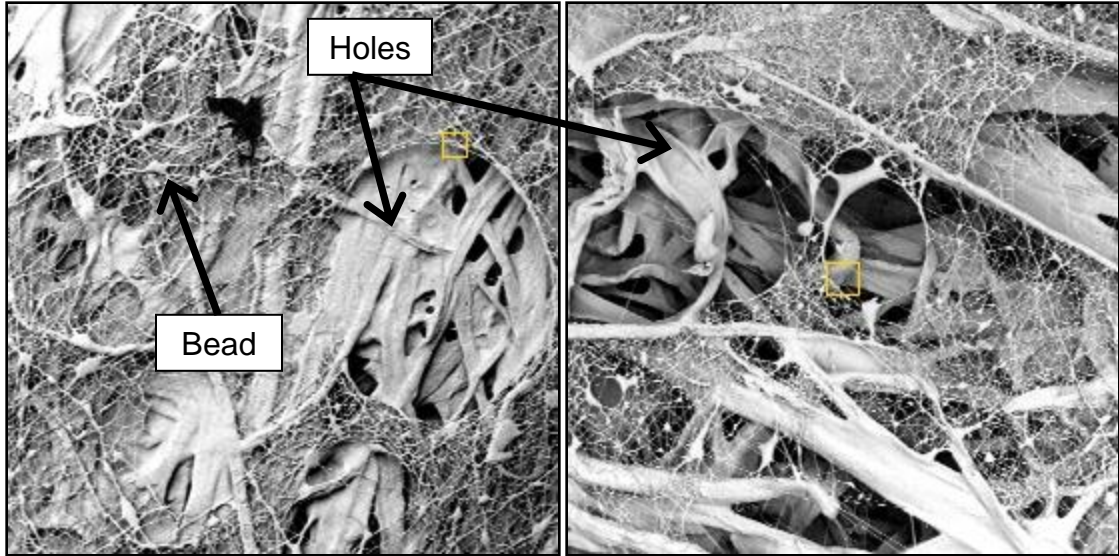
Figure 29: Fiber Morphology - Holes and Beads Examples

# CHAPTER 8 BUILDING AN ANN

## 8.1 Overview

The purpose of this part of the research is to build a Feed Forward (FF) ANN that accurately predicts response surface values. A database for building the ANN is constructed by identifying a set of points on the response surface that both span the feasible region and cover its interior. The success of the ANN in predicting response surface values is evaluated.

## 8.2 ANN Neural Networks

The Feed Forward (FF) neural networks was selected as the ANN architecture for this research. This neural network model was chosen based on the neural network models used in similar processes found in the electrospinning research.[3,9,20,21,153] The Feed Forward ANN is a popular supervised learning architecture used in neural network analysis.[130] The Neural Network Toolbox in the MATLAB software described in Appendix 1.9 was used to design and train the network models. A set of experimental data was collected over the experimental region for the neural network model analysis. Section 8.3 explains the approach used to generate the experimental data set.

Each neural network architecture was trained to highest quality performance using the experimental data set. The three primary analysis plots used to evaluate the ANN model training performance were the performance plot, the residual plot, and the error histogram plot. The two specific measures used to evaluate the goodness of fit of an ANN model were the mean square error (MSE) and the coefficient of determination

(R squared).  Once the Feed Forward network was properly trained, the MSE and R

squared value were calculated.  Also, three validated experimental points in the

experimental region were used to compare the output prediction of the trained ANN

neural network.


8.3 Experimental Data

Because of the time and the expense required for each experimental trial, it was

necessary to determine an efficient experimental data collection approach to minimize

the number of experimental trials and still provide a reasonable sampling of data points

over the entire experimental region.  Since ANN models typically are not proficient at

extrapolating, it was necessary to have several experimental data points near the

boundary of the experimental region.  The minimum and maximum variable values

which established the experimental region are shown in Table 35.

Table 35: ANN Experimental Variable Boundary

|  | Factor A | Factor B | Factor C | Factor D | Factor E | Factor F | Factor G | Factor H |
|---|---|---|---|---|---|---|---|---|
| Min | 2.38 | 45.31 | 64.29 | 6.67 | 7.50 | 46.67 | 45.00 | 33.33 |
| Max | 73.81 | 92.19 | 100.00 | 86.67 | 52.50 | 86.67 | 75.00 | 73.33 |

Utilizing a randomized number generating process, forty-nine experimental data

points were selected within the defined experimental region.  Figure 30 shows a

graphical representation of the selected data points using this approach.  The figure

shows a comparison of factor A to the other seven factors.
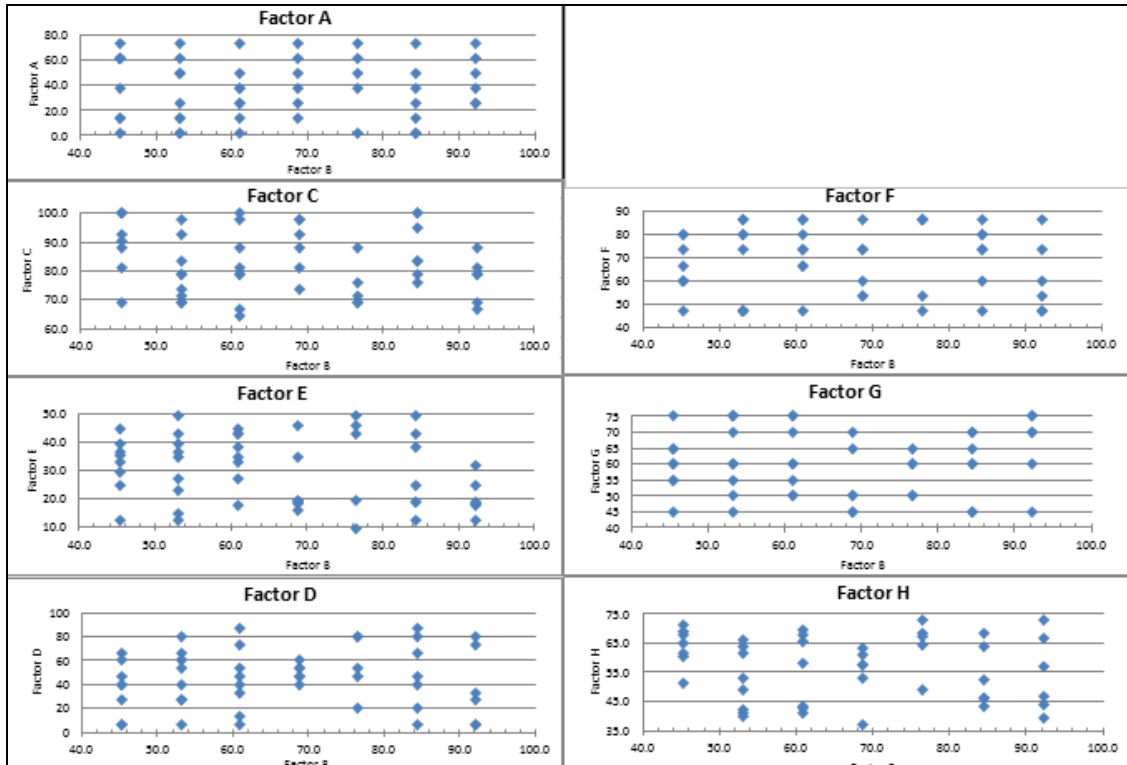
Figure 30: ANN Randomized Experimental Data Collection Approach

Two replicates were conducted at each of the forty-nine experimental points.

The experimental trial data set along with experimental responses can be found in

Appendix 1.6.


8.4 ANN Model – Feed Forward Architecture


The Feed Forward (FF) neural network was one of the two neural network

architectures selected.   In this type of neural network architecture, the information

moves in only one direction, forward, from the input nodes, through the hidden nodes

and to the output nodes. [30] There are no cycles or loops in the network.

There are several algorithms that could be used with a Feed Forward neural

network. [137]  The Levenberg-Marquardt training algorithm was selected to be used in

the Feed Forward neural network.   This widely used algorithm is a gradient descent approach based on minimizing the error between the actual output of the training population and the projected output of the neural network. [70]   The gradient descent approach is also called stochastic gradient descent which is a gradient descent optimization method for minimizing an objective function that is written as a sum of differentiable functions. [70]

Since the process under study was a prototype and there was limited knowledge of the significance that each selected variable had, there was no weighting applied to the inputs.  For the same reason, there was no initial bias used in the ANN model design.  The data was separated into three sample groups.  Seventy percent of the data was used for training the network, fifteen percent of the data was used for testing the network, and fifteen percent of the data was used for validating the network.  The use of the training, validation, and test samples for the ANN model training process are described in Chapter 3.

The ANN model was retrained three times using the same number of hidden neurons to see if the model performance could be improved.  Six different hidden neuron values were evaluated to determine which number of hidden neurons provided the highest-quality ANN model performance.  The following table shows the results of the Feed Forward model training.

Table 36: Feed Forward Trained Model Evaluation

| Feed Forward Neural Network Architecture | | | | | | |
|---|---|---|---|---|---|---|
| Hidden Neurons | Training | | Validation | | Testing | |
| | MSE | R^2 | MSE | R^2 | MSE | R^2 |
| 5 | 2.5 | 0.967 | 14.6 | 0.724 | 83.2 | 0.468 |
| 10 | 3.4 | 0.946 | 9.2 | 0.869 | 61.29 | 0.633 |
| 15 | 9.8 | 0.998 | 28.4 | 0.802 | 130.5 | 0.357 |
| 20 | 1.6 | 0.975 | 68.8 | 0.405 | 95.3 | 0.412 |
| 25 | 1.3 | 0.988 | 68.9 | 0.328 | 116.7 | 0.674 |
| 30 | 1.0 | 0.987 | 41.8 | 0.331 | 114.5 | 0.356 |

Based on the MSE and the R squared value for both the trained data set and the validation data set from Table 36, the hidden neuron value which equaled ten was selected to provide the best possible ANN model performance.  The following figure shows the Feed Forward neural network design.
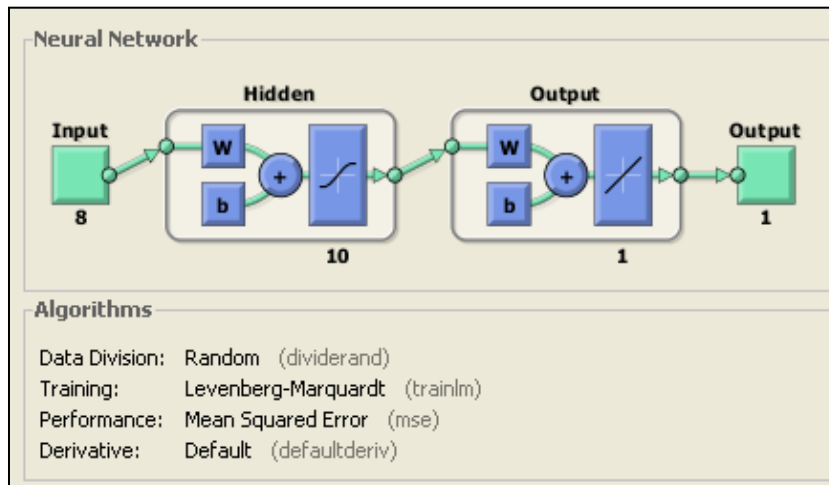


Figure 31: Feed Forward Neural Network

The performance plot was used to evaluate the neural network model performance.[137] If the test curve in the plot increases significantly before the validation curve, then it is possible some overfitting had occurred.[137] For a proper performance fit, the training, testing, and validation performance should remain parallel

as they converge to the point where the gradient changes sign.[137]  Figure 32 shows the performance plot.



**Best Validation Performance is 12.1022 at epoch 6**
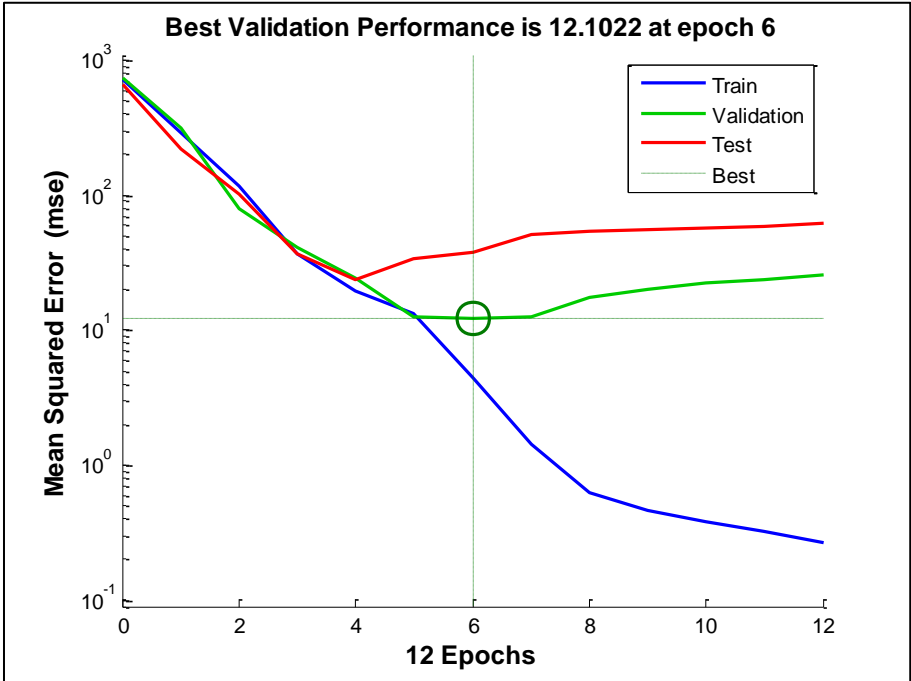
Figure 32: Feed Forward Performance Plot

All three curves in Figure 32 converge through epoch 5 and the training is stopped at epoch 6 when the MSE stops improving.

For the ANN model residual plot, the coefficient of determination measure is evaluated for the training, validation, and testing data set. The following figure shows the residual plots for training, validating, and testing.
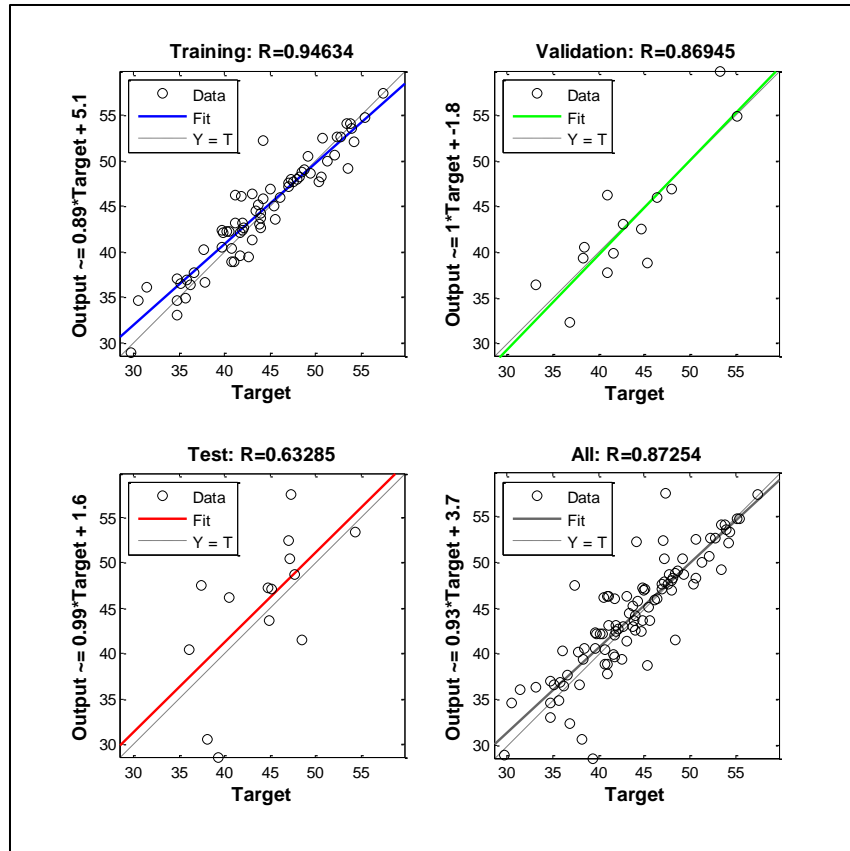
Figure 33: Feed Forward Residual Plots

From Figure 33, the trained ANN model had a coefficient of determination of
0.946 for training and 0.869 for validation.

The next plot to evaluate the ANN model performance was the Error Histogram
plot. [137]  Figure 34 shows the Error Histogram Plot.
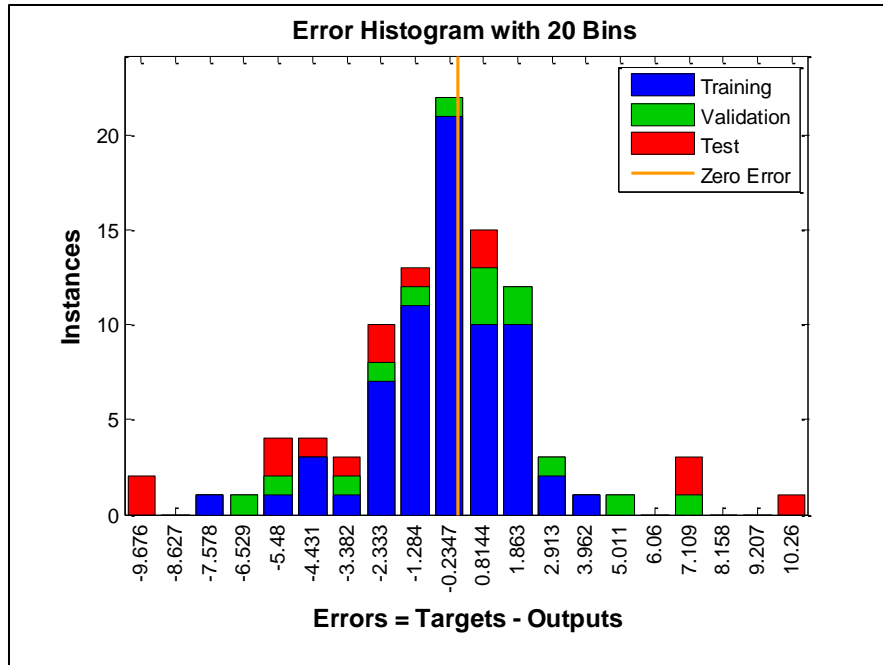
Figure 34: Feed Forward Error Histogram Plot

From Figure 34, the Error Histogram has a reasonable distribution around zero, but there are outliers.  The overall model performance results indicate the Feed Forward ANN model would demonstrate a quality ANN model of the experimental region. [137]


8.5 ANN Model Performance Evaluation

The MSE and two coefficient of determination measures were used to evaluate the two trained ANN models for both the trained and validation data set.  The following table shows the evaluation using the three comparison measures.

Table 37: Neural Network Performance Evaluation

| Neural Network Type | Trained R-Sq. | Validated R-Sq. | MSE |
|---|---|---|---|
| Feed Forward | 0.946 | 0.869 | 3.4 |

The Feed Forward Neural Network had trained R squared values greater than 0.93, which according to *MATLAB* [137] would indicate satisfactory performance and

goodness of fit. The Feed Forward Neural Network had validated R square values that were representative of the best possible values during the ANN model training process, which according to *MATLAB* [137] would indicate satisfactory performance and goodness of fit. The Feed Forward Neural Network had a MSE value less than 10, which according to *MATLAB* [137] would indicate a satisfactory value for ANN modeling. Based on the three performance measures, the FF trained ANN model architecture was satisfactory for model performance and goodness of fit to the experimental data. A satisfactory performance measure of the ANN models does not mean the ANN models will make accurate predictions over the entire experimental region in which the ANN models were trained, but it indicates how well the trained models will fit the experimental points which it was trained on.

To compare how well the trained FF ANN model would predict response values within the experiment region, five different points validated by twenty experimental trials on the prototype were used. The five points were the maximum experimental trial response point from the ANN experimental data set (ANN-Max), the center point of the Chapter 7 DOE3b experimental design (DOE3bCP), the maximum point determined from the Quadratic Program from Chapter 7 of the DOE3b experiment (DOE3bMax), and two arbitrary points (PT4 and PT5) in the experimental region showing good performance. Using the Chapter 7 DOE3b Quadratic Program Maximizer point as a reference point, the normed distance to the other four points was calculated to evaluate the effect the distances from the reference point may have on the accuracy of the ANN model predictions. The experimental point information and the normed distance to the DOE3b Quadratic Program Maximizer is shown in Table 38.

Table 38: ANN Model Comparison Points

| Test Point | Factor A | Factor B | Factor C | Factor D | Factor E | Factor F | Factor G | Factor H | Norm Distance to DOE3b Maximizer | Validation Average Response |
|---|---|---|---|---|---|---|---|---|---|---|
| ANN Database Maximum | 14.29 | 84.38 | 95.24 | 20.00 | 13.00 | 60.00 | 60.00 | 43.33 | 0.808 | 52.311 |
| DOE3b Center Point | 20.24 | 60.94 | 85.24 | 43.33 | 16.00 | 72.67 | 56.00 | 53.33 | 0.419 | 54.214 |
| DOE3b Quadratic Program Maximizer | 21.43 | 64.06 | 88.81 | 48.27 | 20.80 | 69.33 | 66.00 | 60.00 | 0.000 | 55.222 |
| PT4 | 25.24 | 50.00 | 95.48 | 23.33 | 14.00 | 66.67 | 66.50 | 66.67 | 0.529 | 51.339 |
| PT5 | 30.95 | 50.00 | 97.14 | 23.33 | 14.00 | 69.33 | 73.50 | 73.33 | 0.675 | 48.538 |

An ANOVA of the validation points was conducted to compare predictions with the maximizing values obtained in Chapter 7.   Figure 35 shows the ANOVA analysis using the experimental responses of the five data points.

```
                    Individual 95% CIs For Mean Based on Pooled StDev
Level               +---------+---------+---------+---------
ANN MAX                                        (-*-)
DOE3b Center Pt                                    (-*-)
DOE3b QP                                              (-*-)
PT4                                     (-*-)
PT5                       (-*-)
                    +---------+---------+---------+---------
                   48.0      50.0      52.0      54.0
```
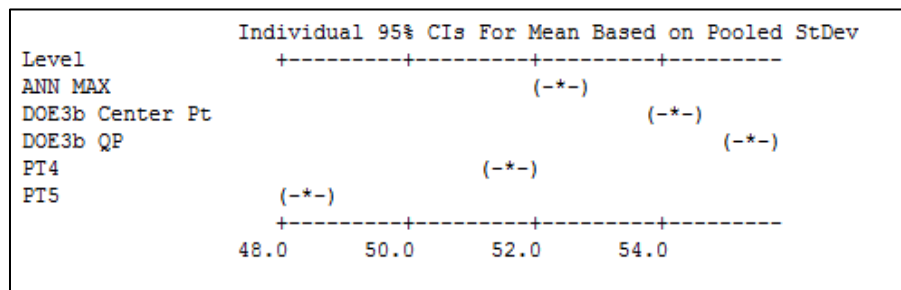
Figure 35: ANOVA Analysis

A sample size of twenty was used to calculate confidence intervals for each of the five validation points using the pooled standard deviation shown in Appendix 1.12. The confidence intervals for each validation point are shown in Table 39.   The trained ANN model was then used to predict the response at each of the five validation points. The ANN response predictions were then compared to the confidence intervals to determine if the ANN model predictions were within the confidence interval of each validation point. These results are shown in Table 39.

Table 39: ANN Model Point Fit Comparison

| Test Point | Norm Distance to DOE3b Maximizer | Validation Average Response | 95% Confidence Interval (Pooled Std Dev 0.9446) | | FF ANN %Eff | |
|---|---|---|---|---|---|---|
| | | % Eff | Min | Max | % Eff | Location |
| ANN Database Maximum | 0.808 | 52.311 | 51.002 | 53.620 | 52.521 | Within CI |
| DOE3b Center Point | 0.419 | 54.214 | 54.076 | 54.352 | 52.175 | Not Within CI |
| DOE3b Quadratic Program Maximizer | 0.000 | 55.222 | 53.913 | 56.531 | 54.038 | Within CI |
| PT4 | 0.529 | 51.339 | 50.030 | 52.648 | 53.128 | Not Within CI |
| PT5 | 0.675 | 48.538 | 47.229 | 49.847 | 50.625 | Not Within CI |

As shown in Table 39, the trained ANN model response predictions for the ANN database maximum were within the confidence interval.

The next four experimental points used as a comparison were not part of the ANN experimental data set.  These four points were chosen to evaluate how well the ANN model would predict a response value that was not part of the ANN training process.   Based on the ANOVA confidence intervals shown in Table 39, one of the four FF ANN model predictions was within the confidence intervals.   The trained Feed Forward ANN model will be used in Chapter 9 for the ANN prediction process.

CHAPTER 9 OPTIMIZING USING ALTERNATIVE APPROACHES

9.1 Overview

The purpose of this part of the research is to evaluate the effectiveness of the

Feed Forward ANN model as a replacement for experimentation on the prototype in the

RSM/DOE optimization process. The steps in the RSM/DOE optimization process as

presented in Figure 14 in Chapter 7 are followed and the various potential RMS/DOE

procedure termination points are validated by experiments on the prototype.

9.2 Step 0: Direct Use of the ANN Database

As a simple approach and to provide the basis for subsequent comparisons that

use the ANN model, the maximizing point in the ANN database described in section 8.2

was selected to be validated by experiments on the prototype.  Twenty experimental

replications were used.  The experimental data can be found in Appendix 1.7.

The comparison between the maximizing response from the ANN data and the

validation results is shown in Table 39.  Note that the ANN database average value of

52.459 was within the confidence interval of (51.095, 53.626) shown in Table 39.

9.3 Utilizing ANN Model in Place of Experiments on the Prototype

Figure 14 from Chapter 7, repeated below as Figure 36, shows the procedure for

conducting a RSM/DOE optimization. In the subsequent sections of this chapter running

the ANN model will be used in place of experiments on the prototype.  This approach

will add experimentation effort to build the ANN model and some validation

experimentation effort, but will eliminate the experimentation effort required to build

models for the DOE and SA approaches.  The following table, basically the same as in

Table 5 in Chapter 7, lists the reference terminology used in the RSM/DOE.

Table 40: RSM/DOE with ANN Terminology Reference

| DOE | Design of Experiments |
|---|---|
| DOEna | Two level factorial experimental design for the $n^{th}$ iteration of the analysis used for building $1^{st}$ order models |
| DOEnb | Experimental design with addition of FCCD points to DOEn used for building 2nd order models |
| SA | Steepest Ascent |
| RSM | Response Surface Method |
| SAn | SA optimization search from the DOEna center point in the gradient direction |
| Quadratic Programming | Optimization of a quadratic equation subject to a linear set of inequalities |
| Validation | Testing of a point found by the various investigative processes by experimentation on the prototype |

Figure 36: RSM/DOE Flow Diagram

9.4 Step 1: One DOE and One SA

The following sequence constitutes step 1.

1) Construct a two-level design (DOE1a)

2) Using the trained ANN model, determine the predicted responses

3) Develop a first-order model from the DOE1a design

4) If the steps in Figure 36 so indicate, perform the SA1 process using the ANN model

5) Determine the maximum response step from the SA1

6) Conduct experimental validation trials on the prototype at the point determined
in step 5

9.4.1 DOE1a Experimental Design

A one-half fractional factorial experimental design DOE1a was developed using
the maximum response point from the ANN database as the center point of the
experimental design.

Fractional Factorial Design

Factors:   8   Base Design:        8, 129   Resolution:  VIII
Runs:    129   Replicates:          1   Fraction:    1/2
Blocks:   1    Center pts. (total):    1

Since the predicted responses from the ANN model would produce the same
response value, only one center point and one replicate were used in the experimental
design.  The DOE1a variable values are shown in Table 41. The corner point values of
the DOE1a design were determined by using a cube size similar to the Chapter 7
DOE3a design.

Table 41: DOE1a High, Low, and Center Point Values

|        | Factor A | Factor B | Factor C | Factor D | Factor E | Factor F | Factor G | Factor H |
|--------|----------|----------|----------|----------|----------|----------|----------|----------|
| Low    | 10.71    | 76.56    | 94.05    | 15.00    | 9.25     | 53.33    | 55.00    | 36.67    |
| Center | 14.29    | 84.38    | 95.24    | 20.00    | 13.00    | 60.00    | 60.00    | 43.33    |
| High   | 17.86    | 92.19    | 96.43    | 25.00    | 16.75    | 66.67    | 65.00    | 50.00    |

The following table shows the coverage of the feasible ranges provided by the
initial high and low point values.

Table 42: DOE1a – Feasibility Variable Range

| Feasible Variable Range | Factor A | Factor B | Factor C | Factor D | Factor E | Factor F | Factor G | Factor H |
|---|---|---|---|---|---|---|---|---|
| % of Range | 3.8% | 8.3% | 1.2% | 5.0% | 4.2% | 5.0% | 5.0% | 2.4% |
| % to Min (Center pt.) | 16% | 92% | 73% | 25% | 19% | 50% | 65% | 91% |

The response values for the half fractional factorial design were determined from the trained FF ANN model discussed in Chapter 8. The results of the coded estimates effects and coefficients analysis are shown in Table 43.

Table 43: First-Order Model Effects & Coefficients

| Term | Effect | Coef | Term | Effect | Coef | Term | Effect | Coef |
|---|---|---|---|---|---|---|---|---|
| Constant | | 52.970 | | | | | | |
| A | 7.147 | 3.574 | A*C*E | 0.014 | 0.007 | D*F*H | 0.141 | 0.070 |
| B | -3.958 | -1.979 | A*C*F | 0.006 | 0.003 | D*G*H | -0.063 | -0.032 |
| C | -0.009 | -0.005 | A*C*G | 0.082 | 0.041 | E*F*G | 0.170 | 0.085 |
| D | -0.521 | -0.260 | A*C*H | -0.016 | -0.008 | E*F*H | -0.252 | -0.126 |
| E | 0.095 | 0.048 | A*D*E | -0.015 | -0.008 | E*G*H | -0.054 | -0.027 |
| F | -8.449 | -4.224 | A*D*F | 0.000 | 0.000 | F*G*H | 2.030 | 1.015 |
| G | 6.300 | 3.150 | A*D*G | -0.066 | -0.033 | A*B*C*D | -0.055 | -0.027 |
| H | 2.431 | 1.216 | A*D*H | -0.047 | -0.023 | A*B*C*E | -0.042 | -0.021 |
| A*B | 0.094 | 0.047 | A*E*F | -0.112 | -0.056 | A*B*C*F | -0.005 | -0.003 |
| A*C | 0.056 | 0.028 | A*E*G | 0.169 | 0.084 | A*B*C*G | -0.015 | -0.007 |
| A*D | -0.019 | -0.009 | A*E*H | -0.017 | -0.009 | A*B*C*H | -0.007 | -0.004 |
| A*E | 0.353 | 0.177 | A*F*G | 0.391 | 0.195 | A*B*D*E | 0.006 | 0.003 |
| A*F | 1.827 | 0.913 | A*F*H | 0.361 | 0.180 | A*B*D*F | 0.019 | 0.010 |
| A*G | -0.067 | -0.033 | A*G*H | 0.011 | 0.006 | A*B*D*G | 0.019 | 0.009 |
| A*H | -0.235 | -0.118 | B*C*D | 0.030 | 0.015 | A*B*D*H | -0.015 | -0.008 |
| B*C | 0.115 | 0.057 | B*C*E | 0.021 | 0.011 | A*B*E*F | 0.077 | 0.038 |
| B*D | -0.620 | -0.310 | B*C*F | 0.055 | 0.027 | A*B*E*G | -0.030 | -0.015 |
| B*E | -0.552 | -0.276 | B*C*G | -0.001 | -0.001 | A*B*E*H | 0.021 | 0.011 |
| B*F | -2.627 | -1.313 | B*C*H | -0.015 | -0.008 | A*B*F*G | -0.061 | -0.031 |
| B*G | 1.263 | 0.632 | B*D*E | -0.016 | -0.008 | A*B*F*H | 0.230 | 0.115 |
| B*H | -0.053 | -0.027 | B*D*F | -0.072 | -0.036 | A*B*G*H | 0.001 | 0.001 |
| C*D | 0.007 | 0.003 | B*D*G | -0.097 | -0.048 | A*C*D*E | 0.266 | 0.133 |
| C*E | -0.000 | -0.000 | B*D*H | -0.048 | -0.024 | A*C*D*F | 0.015 | 0.007 |
| C*F | 0.057 | 0.028 | B*E*F | 0.094 | 0.047 | A*C*D*G | 0.244 | 0.122 |
| C*G | 0.208 | 0.104 | B*E*G | 0.294 | 0.147 | A*C*D*H | 0.028 | 0.014 |
| C*H | -0.016 | -0.008 | B*E*H | 0.074 | 0.037 | A*C*E*F | -0.014 | -0.007 |
| D*E | -0.118 | -0.059 | B*F*G | 1.445 | 0.722 | A*C*E*G | 0.020 | 0.010 |
| D*F | -0.823 | -0.412 | B*F*H | -0.505 | -0.252 | A*C*E*H | 0.002 | 0.001 |
| D*G | 0.670 | 0.335 | B*G*H | -0.036 | -0.018 | A*C*F*G | -0.017 | -0.008 |
| D*H | -0.072 | -0.036 | C*D*E | 0.033 | 0.017 | A*C*F*H | 0.010 | 0.005 |
| E*F | 0.326 | 0.163 | C*D*F | -0.002 | -0.001 | A*C*G*H | 0.004 | 0.002 |
| E*G | 0.458 | 0.229 | C*D*G | -0.014 | -0.007 | A*D*E*F | 0.003 | 0.001 |
| E*H | 0.403 | 0.201 | C*D*H | -0.012 | -0.006 | A*D*E*G | 0.007 | 0.003 |
| F*G | -1.836 | -0.918 | C*E*F | -0.001 | -0.000 | A*D*E*H | -0.042 | -0.021 |
| F*H | 4.820 | 2.410 | C*E*G | -0.013 | -0.006 | A*D*F*G | -0.000 | -0.000 |
| G*H | -0.363 | -0.182 | C*E*H | 0.024 | 0.012 | A*D*F*H | -0.010 | -0.005 |
| A*B*C | -0.029 | -0.014 | C*F*G | 0.001 | 0.000 | A*D*G*H | -0.025 | -0.012 |
| A*B*D | -0.032 | -0.016 | C*F*H | -0.020 | -0.010 | A*E*F*G | -0.050 | -0.025 |
| A*B*E | -0.024 | -0.012 | C*G*H | -0.028 | -0.014 | A*E*F*H | -0.097 | -0.048 |
| A*B*F | -0.173 | -0.087 | D*E*F | 0.009 | 0.005 | A*E*G*H | 0.017 | 0.008 |
| A*B*G | 0.448 | 0.224 | D*E*G | -0.027 | -0.014 | A*F*G*H | -0.082 | -0.041 |
| A*B*H | 0.170 | 0.085 | D*E*H | 0.000 | 0.000 | Ct Pt | | -0.449 |
| A*C*D | -0.001 | -0.001 | D*F*G | -0.094 | -0.047 | | | |

The MSE for the first-order model was undefined since the ANN based model was deterministic.

The contour plots in Figure 37 and Figure 38 show the properties of the response surface as depicted by the first-order model fitted to the DOE1a.
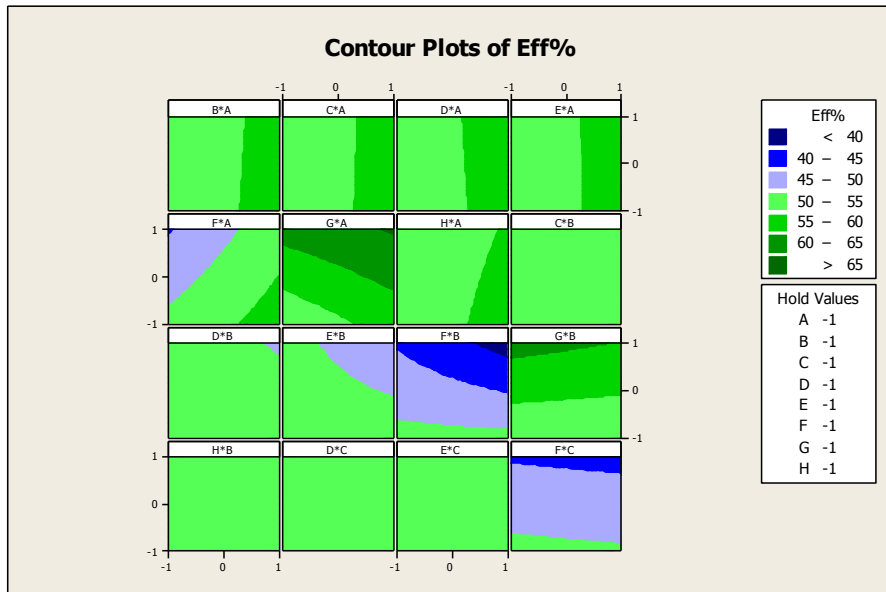
Figure 37: DOE1a Contour Plot 1 of 2
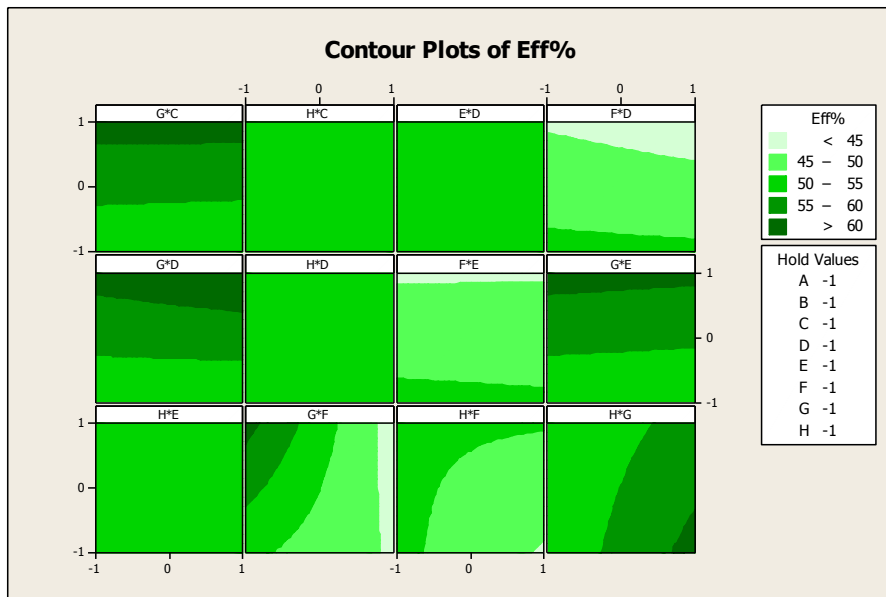

Figure 38: DOE1a Contour Plot 2 of 2

To further explore for a maximum response, a steepest ascent was conducted.

9.4.2 SA1 Steepest Ascent

The method of steepest ascent (SA1) based on following a path in the gradient direction was used to move toward a better response. The step size was selected to be 0.15. The steepest ascent design characteristics are given below.

Path of Steepest Ascent Overview

Total # of Runs                    25
Total # of Factors                  8
Base Factor Name             Factor A
Step Size Base Factor by        0.15
Coded Coefficient of Base Factor     3.5736

9.4.3 SA1 Response Predictions

Table 44 shows the uncoded steepest ascent along with the predicted response from using the trained FF neural network model.

Table 44: SA1 Steepest Ascent

| Step | Factor A | Factor B | Factor C | Factor D | Factor E | Factor F | Factor G | Factor H | ANN Prediction |
|------|----------|----------|----------|----------|----------|----------|----------|----------|----------------|
| 1 | 14.29 | 64.84 | 95.26 | 20.00 | 13.00 | 60.00 | 60.00 | 43.33 | 53.567 |
| 2 | 14.76 | 63.33 | 95.29 | 19.93 | 13.00 | 59.20 | 60.45 | 43.67 | 53.620 |
| 3 | 15.00 | 61.82 | 95.31 | 19.93 | 13.00 | 58.40 | 60.90 | 43.67 | 53.680 |
| 4 | 15.48 | 60.31 | 95.33 | 19.87 | 13.00 | 57.67 | 61.30 | 44.00 | 53.719 |
| 5 | 15.71 | 58.80 | 95.36 | 19.87 | 13.00 | 56.87 | 61.75 | 44.33 | 53.751 |
| 6 | 15.95 | 57.29 | 95.38 | 19.80 | 13.00 | 56.07 | 62.20 | 44.33 | 53.790 |
| 7 | 16.43 | 55.78 | 95.40 | 19.80 | 13.05 | 55.27 | 62.65 | 44.67 | 53.825 |
| 8 | 16.90 | 54.27 | 95.43 | 19.73 | 13.05 | 54.47 | 63.10 | 45.00 | 53.856 |
| 9 | 17.14 | 52.76 | 95.45 | 19.73 | 13.05 | 53.67 | 63.55 | 45.00 | 53.888 |
| 10 | 17.62 | 51.25 | 95.48 | 19.67 | 13.05 | 52.93 | 63.95 | 45.33 | 53.917 |
| 11 | 17.86 | 49.74 | 95.52 | 19.67 | 13.05 | 52.13 | 64.40 | 45.67 | 53.960 |
| 12 | 18.33 | 48.23 | 95.55 | 19.60 | 13.05 | 51.33 | 64.85 | 45.67 | 53.988 |
| 13 | 18.57 | 46.72 | 95.57 | 19.53 | 13.05 | 50.53 | 65.30 | 46.00 | 54.014 |
| 14 | 19.05 | 45.21 | 95.60 | 19.53 | 13.05 | 49.73 | 65.75 | 46.33 | 54.029 |
| 15 | 19.29 | 43.70 | 95.62 | 19.47 | 13.05 | 49.00 | 66.15 | 46.67 | 54.052 |
| 16 | 19.76 | 42.19 | 95.64 | 19.47 | 13.05 | 48.20 | 66.60 | 46.67 | 54.053 |
| 17 | 20.00 | 40.68 | 95.67 | 19.40 | 13.10 | 47.40 | 67.05 | 47.00 | 54.038 |
| 18 | 20.48 | 39.17 | 95.69 | 19.40 | 13.10 | 46.60 | 67.50 | 47.33 | 54.032 |
| 19 | 20.71 | 37.66 | 95.71 | 19.33 | 13.10 | 45.80 | 67.95 | 47.33 | 53.992 |
| 20 | 21.19 | 36.15 | 95.74 | 19.33 | 13.10 | 45.00 | 68.35 | 47.67 | 53.953 |
| 21 | 21.43 | 34.64 | 95.79 | 19.27 | 13.10 | 44.27 | 68.80 | 48.00 | 53.913 |
| 22 | 21.90 | 33.13 | 95.81 | 19.27 | 13.10 | 43.47 | 69.25 | 48.00 | 53.858 |

| 23 | 22.14 | 31.62 | 95.83 | 19.20 | 13.10 | 42.67 | 69.70 | 48.33 | 53.790 |
| 24 | 22.62 | 30.11 | 95.86 | 19.13 | 13.10 | 41.87 | 70.15 | 48.67 | 53.743 |
| 25 | 22.86 | 28.60 | 95.88 | 19.13 | 13.10 | 41.07 | 70.60 | 48.67 | 53.567 |

At step 16 of SA1, the response stopped increasing.  The following figure shows the steepest ascent responses with the progression to the DOE1a cube boundary at step 11.
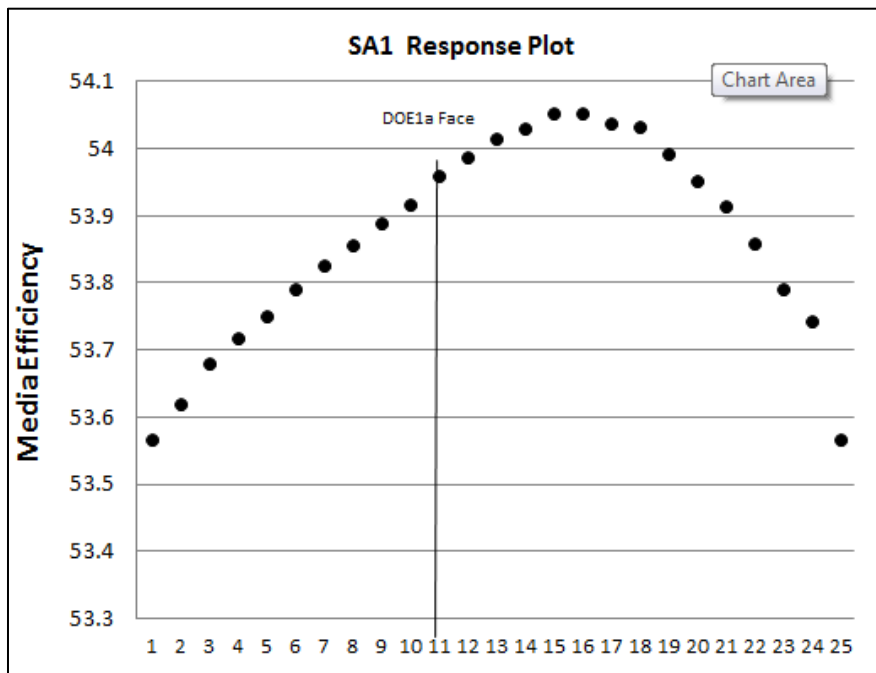


Figure 39: SA1 Response Plot

## 9.4.4 Compare SA1 Predicted vs. Experimental Response

The following table shows a comparison of the average experimental response on the prototype to the response prediction from the trained ANN at step 16 of the steepest ascent.

Table 45: SA1 Trial Results

| Factor A | Factor B | Factor C | Factor D | Factor E | Factor F | Factor G | Factor H | FF Prediction | Trial Average |
|----------|----------|----------|----------|----------|----------|----------|----------|---------------|---------------|
| 19.76 | 45.31 | 95.64 | 19.47 | 13.05 | 48.20 | 66.60 | 46.67 | 54.053 | 53.220 |

The following table shows the statistical results for the SA1 experimental trials along with the ANN model prediction. The confidence intervals were based on a pooled standard deviation derived from twelve experimental populations. The pooled standard deviation is based on the assumption that the population was normal and independently distributed. The calculations for the pooled standard deviation are shown in Appendix 1.12. The confidence interval in Table 46 was based on a sample size of two (n=2) to be comparable to the ANN database which had a sample size of two, also.

Table 46: SA1 Mean and Confidence Interval

| | | |
|---|---|---|
| SA1 Maximizer Validation | Mean | 53.220 |
| | Stdev | 0.9446 |
| | n | 20 |
| 95% Confidence Interval Formula $\bar{x} \pm Z * \dfrac{\sigma}{\sqrt{n}}$ | Z | 1.96 |
| | CI +/- | 1.309 |
| | CI Min | 51.911 |
| | CI Max | 54.529 |
| | Prediction | 54.053 |

The response prediction from step 16 of the SA1 path was within the ANN database based experiment ninety-five percent confidence interval. The experimental trials results can be found at Appendix 1.10.

9.5 Step 2: Addition of a Second DOE and SA

A continuation of the RSM/DOE analysis as shown in Figure 36 was conducted using the trained FF ANN model to predict the response values. The step 1 sequence

plus the following sequence constitutes the RSM/DOE optimization process through step 2.

1) Develop a first-order design (DOE2a) using the maximum response from the SA1
2) Develop a first-order model from the DOE2a design
3) If the approach in Figure 36 so indicates: Perform the SA2 process using the ANN model
4) If the approach in Figure 36 so indicates, develop a second-order model DOE2b
5) If the approach in Figure 36 so indicates, using a Quadratic Programming locate a maximum with the DOE2b cube
6) Conduct experimental validation trials on the prototype at the maximum response point determined from the Quadratic Programming results

9.5.1 DOE2a Experimental Design

A one-half fractional factorial experimental design DOE2a was developed using the maximum response point from SA1 as the center point of the experimental design. The following fractional factorial design was used for the DOE2a experimental design.

Fractional Factorial Design

Factors:   8   Base Design:      8, 129   Resolution:  VIII
Runs:    129   Replicates:            1   Fraction:    1/2
Blocks:    1   Center pts. (total):    1

Since the predicted responses from the ANN model would produce the same response value, only one center point and one replicate were used in the experimental design.  The DOE2a variable values are shown in Table 47.  The corner point values of

110

the DOE2a design were determined by using a cube size similar to the Chapter 7

DOE3a experimental design.

Table 47: DOE2a High, Low, and Center Point Values

| | Factor A | Factor B | Factor C | Factor D | Factor E | Factor F | Factor G | Factor H |
|---|---|---|---|---|---|---|---|---|
| Low | 16.19 | 37.50 | 95.00 | 17.33 | 12.00 | 41.33 | 61.50 | 33.33 |
| Center | 19.76 | 45.31 | 95.71 | 19.33 | 13.00 | 48.00 | 66.50 | 46.67 |
| High | 23.33 | 53.13 | 96.43 | 21.33 | 14.00 | 54.67 | 71.50 | 60.00 |

The following table shows the coverage of the feasible ranges provided by the

initial high and low point values.

Table 48: DOE2a – Feasibility Variable Range

| Feasible Variable Range | Factor A | Factor B | Factor C | Factor D | Factor E | Factor F | Factor G | Factor H |
|---|---|---|---|---|---|---|---|---|
| % of Range | 3.8% | 8.3% | 0.7% | 2.0% | 1.1% | 5.0% | 5.0% | 4.9% |
| % to Min (Center pt.) | 22% | 50% | 73% | 21% | 16% | 41% | 72% | 95% |

The response values for the half fractional factorial design were determined from

the trained FF ANN model discussed in Chapter 8.  The results of the coded estimates

effects and coefficients analysis are shown in Table 49.

Table 49: DOE2a Effects & Coefficients

| Term | Effect | Coef | Term | Effect | Coef | Term | Effect | Coef |
|---|---|---|---|---|---|---|---|---|
| Constant | 52.97 | | | | | | | |
| A | 7.147 | 3.574 | A*C*D | -0.001 | -0.001 | D*E*H | 0.000 | 0.000 |
| B | -3.958 | -1.979 | A*C*E | 0.014 | 0.007 | D*F*G | -0.094 | -0.047 |
| C | -0.009 | -0.005 | A*C*F | 0.006 | 0.003 | D*F*H | 0.141 | 0.070 |
| D | -0.521 | -0.260 | A*C*G | 0.082 | 0.041 | D*G*H | -0.063 | -0.032 |
| E | 0.095 | 0.048 | A*C*H | -0.016 | -0.008 | E*F*G | 0.170 | 0.085 |
| F | -8.449 | -4.224 | A*D*E | -0.015 | -0.008 | E*F*H | -0.252 | -0.126 |
| G | 6.300 | 3.150 | A*D*F | 0.000 | 0.000 | E*G*H | -0.054 | -0.027 |
| H | 2.431 | 1.216 | A*D*G | -0.066 | -0.033 | F*G*H | 2.030 | 1.015 |
| A*B | 0.094 | 0.047 | A*D*H | -0.047 | -0.023 | A*B*C*D | -0.055 | -0.027 |
| A*C | 0.056 | 0.028 | A*E*F | -0.112 | -0.056 | A*B*C*E | -0.042 | -0.021 |
| A*D | -0.019 | -0.009 | A*E*G | 0.169 | 0.084 | A*B*C*F | -0.005 | -0.003 |
| A*E | 0.353 | 0.177 | A*E*H | -0.017 | -0.009 | A*BS*C*G | -0.015 | -0.007 |
| A*F | 1.827 | 0.913 | A*F*G | 0.391 | 0.195 | A*B*C*H | -0.007 | -0.004 |
| A*G | -0.067 | -0.033 | A*F*H | 0.361 | 0.180 | A*B*D*E | 0.006 | 0.003 |
| A*H | -0.235 | -0.118 | A*G*H | 0.011 | 0.006 | A*B*D*F | 0.019 | 0.010 |
| B*C | 0.115 | 0.057 | B*C*D | 0.030 | 0.015 | A*B*D*G | 0.019 | 0.009 |
| B*D | -0.620 | -0.310 | B*C*E | 0.021 | 0.011 | A*B*D*H | -0.015 | -0.008 |
| B*E | -0.552 | -0.276 | B*C*F | 0.055 | 0.027 | A*B*E*F | 0.077 | 0.038 |
| B*F | -2.627 | -1.313 | B*C*G | -0.001 | -0.001 | A*B*E*G | -0.030 | -0.015 |

| | | | | | | | | |
|---|---|---|---|---|---|---|---|---|
| B*G | 1.263 | 0.632 | B*C*H | -0.015 | -0.008 | A*B*E*H | 0.021 | 0.011 |
| B*H | -0.053 | -0.027 | B*D*E | -0.016 | -0.008 | A*B*F*G | -0.061 | -0.031 |
| C*D | 0.007 | 0.003 | B*D*F | -0.072 | -0.036 | A*B*F*H | 0.230 | 0.115 |
| C*E | 0.000 | 0.000 | B*D*G | -0.097 | -0.048 | A*B*G*H | 0.001 | 0.001 |
| C*F | 0.057 | 0.028 | B*D*H | -0.048 | -0.024 | A*C*D*E | 0.266 | 0.133 |
| C*G | 0.208 | 0.104 | B*E*F | 0.094 | 0.047 | A*C*D*F | 0.015 | 0.007 |
| C*H | -0.016 | -0.008 | B*E*G | 0.294 | 0.147 | A*C*D*G | 0.244 | 0.122 |
| D*E | -0.118 | -0.059 | B*E*H | 0.074 | 0.037 | A*C*D*H | 0.028 | 0.014 |
| D*F | -0.823 | -0.412 | B*F*G | 1.445 | 0.722 | A*C*E*F | -0.014 | -0.007 |
| D*G | 0.670 | 0.335 | B*F*H | -0.505 | -0.252 | A*C*E*G | 0.020 | 0.010 |
| D*H | -0.072 | -0.036 | B*G*H | -0.036 | -0.018 | A*C*E*H | 0.002 | 0.001 |
| E*F | 0.326 | 0.163 | C*D*E | 0.033 | 0.017 | A*C*F*G | -0.017 | -0.008 |
| E*G | 0.458 | 0.229 | C*D*F | -0.002 | -0.001 | A*C*F*H | 0.010 | 0.005 |
| E*H | 0.403 | 0.201 | C*D*G | -0.014 | -0.007 | A*C*G*H | 0.004 | 0.002 |
| F*G | -1.836 | -0.918 | C*D*H | -0.012 | -0.006 | A*D*E*F | 0.003 | 0.001 |
| F*H | 4.820 | 2.410 | C*E*F | -0.001 | 0.000 | A*D*E*G | 0.007 | 0.003 |
| G*H | -0.363 | -0.182 | C*E*G | -0.013 | -0.006 | A*D*E*H | -0.042 | -0.021 |
| A*B*C | -0.029 | -0.014 | C*E*H | 0.024 | 0.012 | A*D*F*G | 0.000 | 0.000 |
| A*B*D | -0.032 | -0.016 | C*F*G | 0.001 | 0.000 | A*D*F*H | -0.010 | -0.005 |
| A*B*E | -0.024 | -0.012 | C*F*H | -0.020 | -0.010 | A*D*G*H | -0.025 | -0.012 |
| A*B*F | -0.173 | -0.087 | C*G*H | -0.028 | -0.014 | A*E*F*G | -0.050 | -0.025 |
| A*B*G | 0.448 | 0.224 | D*E*F | 0.009 | 0.005 | A*E*F*H | -0.097 | -0.048 |
| A*B*H | 0.170 | 0.085 | D*E*G | -0.027 | -0.014 | A*E*G*H | 0.017 | 0.008 |
| | | | | | | A*F*G*H | -0.082 | -0.041 |

The MSE for the DOE2a model was undefined since the ANN based model was deterministic.

The contour plots in Figure 40 and Figure 41 show the properties of the response surface as depicted by the first-order model.
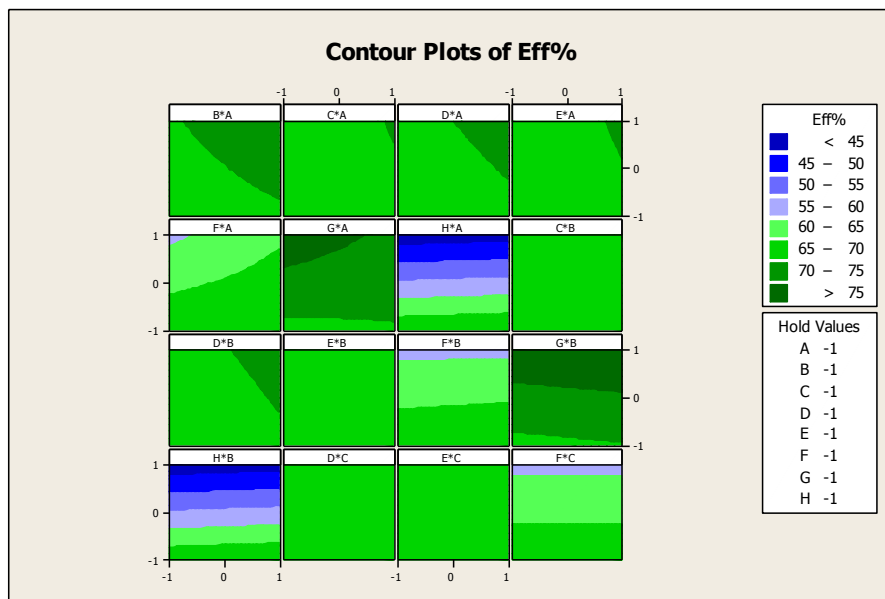


Figure 40: DOE2a Contour Plot 1 of 2
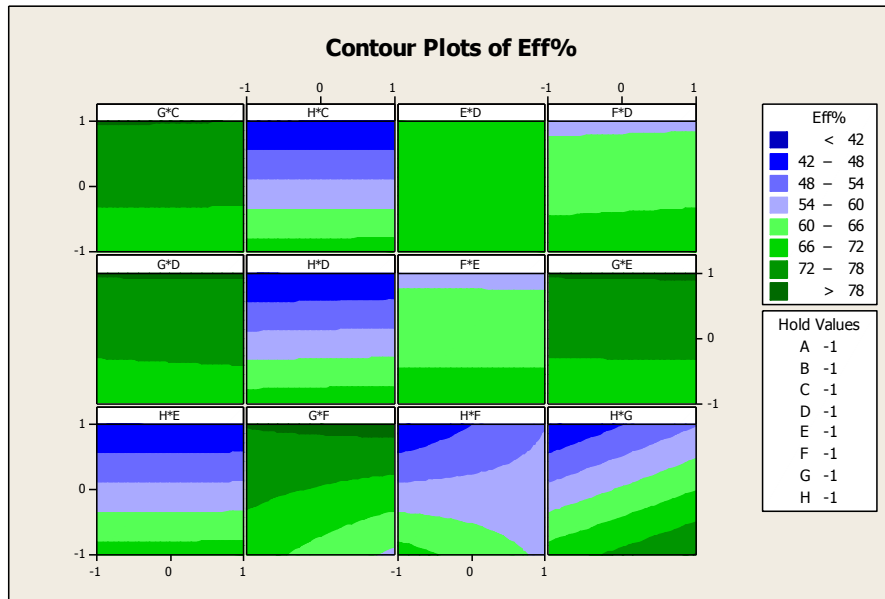
Figure 41: DOE2a Contour Plot 2 of 2

To determine if a maximum response might be in the interior of the DOE2a cube, a steepest ascent was conducted.

9.5.2 SA2 Steepest Ascent

The method of steepest ascent (SA2) based on following a path in the gradient direction was used to move toward a better response. The step size was selected to be 0.15. The characteristics of the steepest ascent design are given below.

Path of Steepest Ascent Overview

Total # of Runs              20
Total # of Factors            8
Base Factor Name          Factor A
Step Size Base Factor by      0.15
Coded Coefficient of Base Factor    3.5736

9.5.3 SA2 Response Predictions

Table 50 shows the uncoded steepest ascent along with the predicted response using the trained FF neural network model.

113

Table 50: SA2 Steepest Ascent

| Step | Factor A | Factor B | Factor C | Factor D | Factor E | Factor F | Factor G | Factor H | ANN Prediction |
|------|----------|----------|----------|----------|----------|----------|----------|----------|----------------|
| 1 | 19.76 | 45.31 | 95.64 | 19.47 | 13.05 | 48.20 | 66.60 | 46.67 | 54.053 |
| 2 | 20.12 | 45.98 | 95.67 | 19.43 | 13.07 | 48.60 | 67.05 | 48.00 | 54.290 |
| 3 | 20.48 | 46.64 | 95.69 | 19.40 | 13.08 | 49.00 | 67.50 | 49.00 | 54.517 |
| 4 | 20.83 | 47.30 | 95.71 | 19.37 | 13.10 | 49.40 | 67.95 | 50.33 | 54.762 |
| 5 | 21.19 | 47.96 | 95.74 | 19.33 | 13.11 | 49.80 | 68.40 | 51.33 | 54.989 |
| 6 | 21.55 | 48.63 | 95.76 | 19.30 | 13.13 | 50.20 | 68.85 | 52.67 | 55.241 |
| 7 | 21.90 | 49.29 | 95.79 | 19.27 | 13.14 | 50.60 | 69.30 | 53.67 | 55.412 |
| 8 | 22.26 | 49.95 | 95.81 | 19.23 | 13.16 | 51.00 | 69.75 | 55.00 | 55.631 |
| 9 | 22.62 | 50.61 | 95.83 | 19.20 | 13.17 | 51.40 | 70.20 | 56.00 | 55.901 |
| 10 | 22.98 | 51.28 | 95.86 | 19.17 | 13.19 | 51.80 | 70.65 | 57.33 | 56.114 |
| 11 | 23.33 | 51.94 | 95.88 | 19.13 | 13.20 | 52.20 | 71.10 | 58.33 | 56.371 |
| 12 | 23.69 | 52.60 | 95.90 | 19.10 | 13.22 | 52.60 | 71.55 | 59.67 | 56.258 |
| 13 | 24.05 | 53.26 | 95.93 | 19.07 | 13.23 | 53.00 | 72.00 | 60.67 | 56.142 |
| 14 | 24.40 | 53.93 | 95.95 | 19.03 | 13.25 | 53.40 | 72.45 | 62.00 | 55.875 |
| 15 | 24.76 | 54.59 | 95.98 | 19.00 | 13.26 | 53.80 | 72.90 | 63.00 | 55.537 |
| 16 | 25.12 | 55.25 | 96.00 | 18.97 | 13.28 | 54.20 | 73.35 | 64.33 | 55.282 |
| 17 | 25.48 | 55.91 | 96.02 | 18.93 | 13.29 | 54.60 | 73.80 | 65.33 | 54.934 |
| 18 | 25.83 | 56.58 | 96.05 | 18.90 | 13.31 | 55.00 | 74.25 | 66.67 | 54.792 |
| 19 | 26.19 | 57.24 | 96.07 | 18.87 | 13.32 | 55.40 | 74.70 | 67.67 | 54.535 |
| 20 | 26.55 | 57.90 | 96.10 | 18.83 | 13.34 | 55.80 | 75.15 | 69.00 | 54.134 |

At step 11 of SA2, the response stopped increasing. The following figure shows the steepest responses with the progression to the DOE2a cube boundary at step 10.
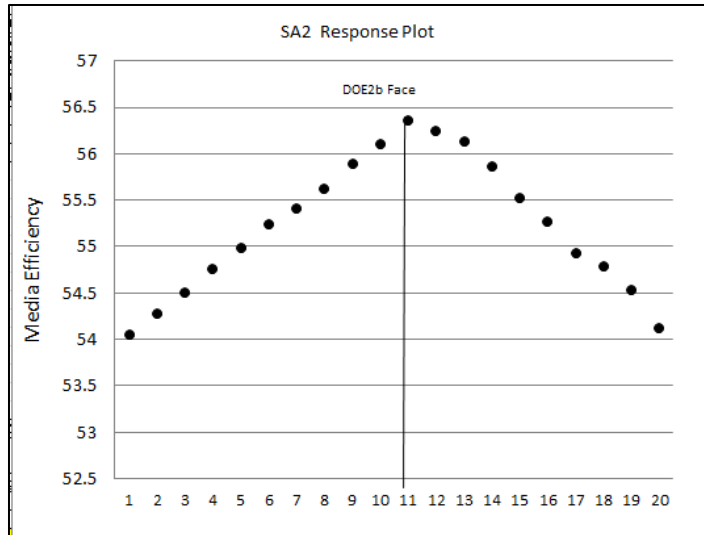
Figure 42: SA2 Response Plot

The predicted responses continued to increase within the DOE2a cube and started to decrease at the edge of the DOE2a cube. This would suggest that a saddle point or a point of maximum response is near the boundary of the DOE2a cube.

The next step of the RSM/DOE approach according to Figure 42 would be to generate a DOE3a using the maximum point from the SA2. However, it will be useful to generate a second-order model using a Central Composite experimental design based on a DOE2b. This reflects what was done in Chapter 7 when, in the interest of minimizing the cost of experimentation, the sequential process of Figure 42 was shortened prematurely when it was realized that an optimum appeared to be nearby.

9.5.4 DOE2b Experimental Design

A Central Composite experimental design was generated. As described previously, it was more useful to use the DOE2a center point than the maximum point of SA2. This experimental design was designated DOE2b. The DOE2b model variable values are shown in Table 51. The corner and star point values of the DOE2b effects

model were determined by using experimental dimensions similar to the DOE3b design in Chapter 7. The following independent variable settings were established for the DOE2b Central Composite Design.

Table 51: DOE2b High, Low, and Center Point Values

| DOE2b | Factor A | Factor B | Factor C | Factor D | Factor E | Factor F | Factor G | Factor H |
|---|---|---|---|---|---|---|---|---|
| L-Low | 7.86 | 60.94 | 93.33 | 12.60 | 9.65 | 25.33 | 49.50 | 3.33 |
| Low | 16.19 | 37.50 | 95.00 | 17.33 | 12.00 | 41.33 | 61.50 | 33.33 |
| Center | 19.76 | 45.31 | 95.71 | 19.33 | 13.00 | 48.00 | 66.50 | 46.67 |
| High | 23.33 | 53.13 | 96.43 | 21.33 | 14.00 | 54.67 | 71.50 | 60.00 |
| H-High | 31.67 | 107.81 | 98.10 | 26.07 | 16.35 | 70.67 | 83.50 | 90.00 |

The following Central Composite Design was used for DOE2b.

Central Composite Design

Factors:  8          Replicates:     1
Base runs:    145  Total runs:    145
Base blocks:    1     Total blocks:  1

Two-level factorial: Half fraction

Cube points:   128
Center points in cube:    1
Axial points:    16
Center points in axial:    0

Since the predicted responses from the ANN model would produce the same response value, only one center point and one replicate were used in the experimental design.

9.5.5 DOE2b Response Predictions

The trained Feed Forward neural network from section 8.3 was used to determine the predicted responses for the DOE2b experimental design.  Using the trained Feed Forward ANN model, the predicted responses for each data point including star points of the DOE2b experimental design were determined.

9.5.6 DOE2b Effects Analysis

The second-order model that was created from the DOE2b experiment is shown

below in Table 52.

Table 52: Estimated Regression Coefficients for second order model

| Term | Coef | P | S |
|---|---|---|---|
| Constant | 54.053 | 0.000 | |
| A | 0.324 | 0.000 | |
| B | -1.089 | 0.000 | |
| C | 0.154 | 0.021 | |
| D | -1.397 | 0.000 | |
| E | 0.271 | 0.000 | |
| F | -0.440 | 0.000 | |
| G | 1.613 | 0.000 | |
| H | 2.141 | 0.000 | |
| AA | -0.131 | 0.071 | S2 |
| BB | -0.088 | 0.235 | S2 |
| CC | 0.031 | 0.675 | S2 |
| DD | 0.000 | 0.991 | S2 |
| EE | -0.034 | 0.632 | S2 |
| FF | -0.601 | 0.681 | S2 |
| GG | -0.575 | 0.000 | |
| HH | -0.491 | 0.000 | |
| AB | 0.179 | 0.013 | |
| AC | 0.015 | 0.835 | S2 |
| AD | -0.071 | 0.331 | S2 |
| AE | 0.036 | 0.621 | S2 |
| AF | 0.461 | 0.000 | |
| AG | 0.119 | 0.102 | S2 |
| AH | 0.240 | 0.001 | |
| BC | -0.018 | 0.802 | S2 |
| BD | 0.079 | 0.284 | S2 |
| BE | 0.033 | 0.656 | S2 |
| BF | -0.584 | 0.000 | |
| BG | -0.736 | 0.000 | |
| BH | -0.225 | 0.002 | |
| CD | -0.014 | 0.843 | S2 |
| CE | 0.013 | 0.851 | S2 |
| CF | 0.007 | 0.923 | S2 |
| CG | -0.056 | 0.442 | S2 |
| CH | -0.035 | 0.622 | S2 |
| DE | 0.194 | 0.009 | |
| DF | -0.165 | 0.056 | S2 |
| DG | -0.345 | 0.091 | S2 |
| DH | 0.176 | 0.087 | S2 |
| EF | 0.101 | 0.167 | S2 |
| EG | 0.236 | 0.002 | |
| EH | -0.258 | 0.001 | |
| FG | -0.688 | 0.361 | S2 |
| FH | 0.170 | 0.071 | S2 |

| | | | |
|---|---|---|---|
| GH | -0.057 | 0.435 | S2 |

R-Sq. = 92.48% R-Sq. (adj.) = 94.32%

Notes:
S2 Blue Shading - Effects eliminated due to lack of statistical significance

A level of significance of $\alpha > 0.05$ was used to compare with the p-values in Table 52 to determine which of the effects in the model were statistically significant. The effects having a lack of significance which can be eliminated from the DOE2b effects model are shaded and labeled "S2" in Table 52. The reduced DOE2b effects analysis results are presented in Table 53.

Table 53: Regression Coefficients for the second-order reduced model (coded units)

| Term | Coef | P |
|---|---|---|
| Constant | 54.051 | 0.000 |
| A | 0.332 | 0.000 |
| B | -1.088 | 0.000 |
| C | 0.159 | 0.018 |
| D | -1.393 | 0.000 |
| E | 0.276 | 0.000 |
| F | -0.438 | 0.000 |
| G | 1.622 | 0.000 |
| H | 2.144 | 0.000 |
| GG | -0.572 | 0.000 |
| HH | -0.470 | 0.000 |
| AB | 0.184 | 0.011 |
| AF | 0.469 | 0.000 |
| AH | 0.246 | 0.001 |
| BF | -0.576 | 0.000 |
| BG | -0.731 | 0.000 |
| BH | -0.221 | 0.002 |
| DE | 0.197 | 0.007 |
| EG | 0.244 | 0.001 |
| EH | -0.258 | 0.000 |

R-Sq. = 89.56% R-Sq. (adj.) = 90.72%

Contour plots were created from the DOE2b model. The following two figures show the contour plots of the DOE2b model. The darkest (green) contour circles in Figure 43 and Figure 44 show a peak in the quadratic function when vary two variables.

118

The contour plots suggest there might be a maximum response or saddle point near the boundary of the experimental region.
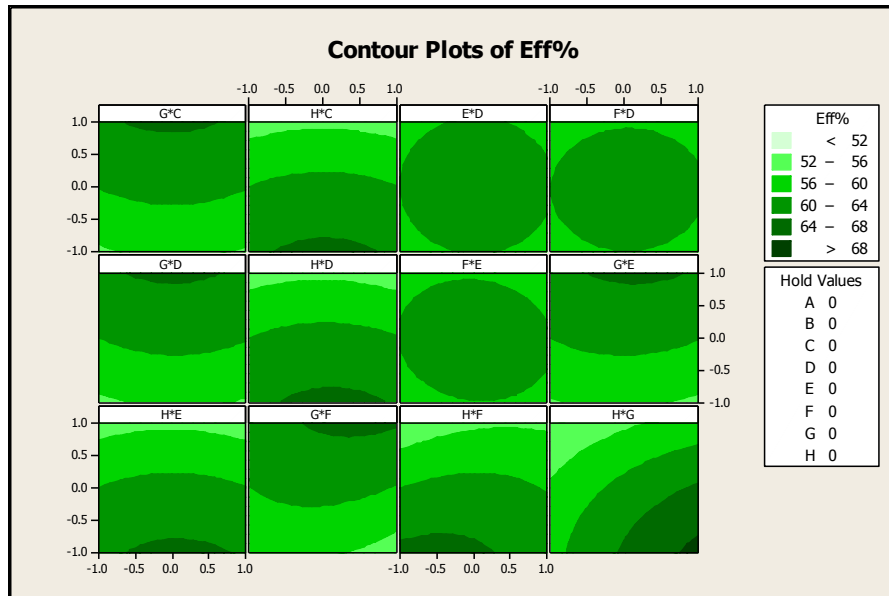


Figure 43: DOE2b Contour Plot 1 of 2
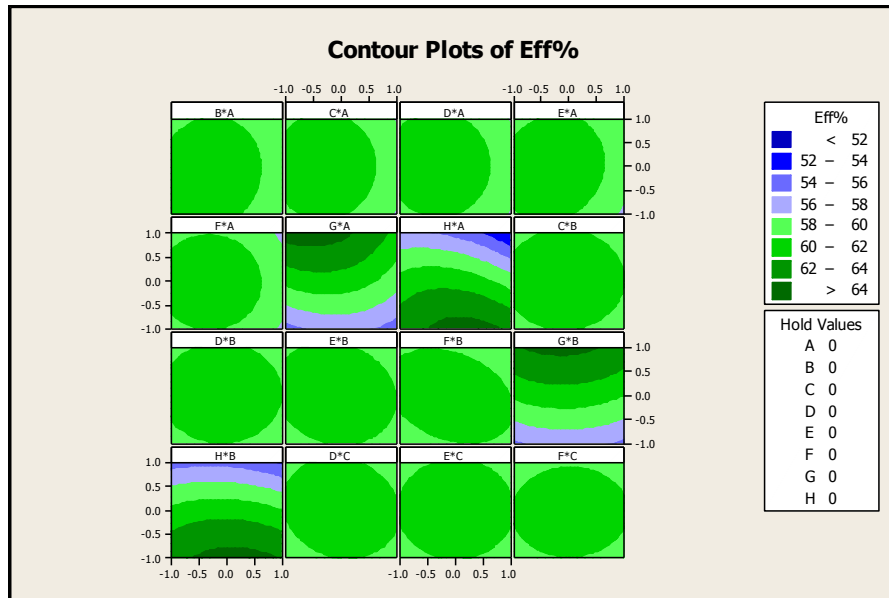


Figure 44: DOE2b Contour Plot 2 of 2

9.5.7 DOE2b Quadratic Objective Function

The reduced coded DOE2b coefficients from Table 53 can be written as the

quadratic objective function shown below.

$$MAX = 54.051 + .33A - 1.09B + 0.16C - 1.39D + 0.27E - 0.44F +$$
$$1.62G + 2.14H - 0.57GG - 0.47HH + 0.18AB + 0.47AF + 0.25AH -$$
$$- 0.58BF - 0.73BG - 0.22BH + 0.19DE + 0.24EG - .26EH$$

The quadratic objective function and the constraint set determined by the DOE

variable cube design points constitute a Quadratic Program.

Variable Constraints Set One
$$-1.00 \le A \le 1.00$$
$$-1.00 \le B \le 1.00$$
$$-1.00 \le C \le 1.00$$
$$-1.00 \le D \le 1.00$$
$$-1.00 \le E \le 1.00$$
$$-1.00 \le F \le 1.00$$
$$-1.00 \le G \le 1.00$$
$$-1.00 \le H \le 1.00$$

The Quadratic Program was used to determine the maximum response and the

associated factor values.  The results are shown in Table 54.

Table 54: Maximum Response and Factor Values

| Factor | Coded |
|---|---|
| A | 23.33 |
| B | 53.13 |
| C | 96.43 |
| D | 19.33 |
| E | 13.00 |
| F | 48.00 |
| G | 71.50 |
| H | 56.67 |
| Prediction Response | 56.143 |

9.5.8 DOE2b Quadratic Programming Maximum Response Experimental Validation

Twenty experimental trials were conducted at the Quadratic Programming maximum point to evaluate the current prediction of the ANN model. The experimental trial results can be found at Appendix 1.10. The following table shows the statistical analysis results of the experimental trials at the DOE2b Quadratic Programming maximum point along with the ANN predictions. The confidence intervals were based on a pooled standard deviation derived from twelve experimental populations. The pooled standard deviation is based on the assumption that the population was normal and independently distributed. The calculations for the pooled standard deviation are shown in Appendix 1.12. The confidence interval in Table 55 was based on a sample size of two to be comparable to the ANN database development which used a sample size of two (n=2) as well.

Table 55: Maximum Response Trial Variance Analysis

| DOE2b Maximizer Validation | Mean | 54.743 |
|---|---|---|
| | Stdev | 0.9446 |
| | n | 20 |
| 95% Confidence Interval Formula $\bar{x} \pm Z * \dfrac{\sigma}{\sqrt{n}}$ | Z | 1.96 |
| | CI +/- | 1.309 |
| | CI Min | 53.434 |
| | CI Max | 56.052 |
| | Prediction | 56.143 |

As shown in Table 55, the predicted response of 56.143 was outside of the ANN database based ninety-five percent confidence interval. Since optimum response was determined to be outside the DOE2a experimental region, a DOE3a was conducted in step 3 using the maximum response point of SA2.

9.6 Step 3: Addition of a Third DOE and SA

A continuation of the RSM/DOE analysis as shown in Figure 36 needs to be conducted using the trained FF ANN model to predict the response values.  The step 2 sequence plus the following sequence constitutes the RSM/DOE optimization process through step 3.


1) Develop a first-order design (DOE3a) using the maximum response from the SA2 (PT3) as the center point
2) Develop a first-order model from the DOE3a design
3) If the approach in Figure 36 so indicates: Perform the SA3 process using the ANN model
4) If the approach in Figure 36 so indicates, develop a second-order model DOE3b
5) If the approach in Figure 36 so indicates, using Quadratic Programming, locate a maximum within the DOE3b cube
6) Conduct experimental validation trials on the prototype at the maximum response point determined from the Quadratic Programming results


9.6.1 DOE3a Experimental Design

A one-half fractional factorial experimental design DOE3a was developed using PT3 the maximum response point from SA2 as the center point of the experimental design.  The following fractional factorial design was used for the DOE3a experimental design.

Fractional Factorial Design

Factors:   8    Base Design:   8, 129   Resolution:  VIII
Runs:     129   Replicates:          1     Fraction:    1/2
Blocks:    1     Center pts. (total):  1

Since the predicted responses from the ANN model would produce the same response value, only one center point and a single replicate were used in the experimental design. The DOE3a variable values are shown in Table 56. The corner point values of the DOE3a design were determined by using a cube size similar to the Chapter 7 DOE3a design.

Table 56: DOE3a High, Low, and Center Point Values

|  | Factor A | Factor B | Factor C | Factor D | Factor E | Factor F | Factor G | Factor H |
|---|---|---|---|---|---|---|---|---|
| Low | 19.76 | 37.50 | 95.17 | 17.13 | 12.20 | 45.53 | 66.10 | 45.00 |
| Center | 23.33 | 53.13 | 95.88 | 19.13 | 13.20 | 52.20 | 71.10 | 58.33 |
| High | 26.90 | 68.75 | 96.60 | 21.13 | 14.20 | 58.87 | 76.10 | 71.67 |

The following table shows the coverage of the feasible ranges provided by the initial high and low point values.

Table 57: DOE3a – Feasibility Variable Range

| Feasible Variable Range | Factor A | Factor B | Factor C | Factor D | Factor E | Factor F | Factor G | Factor H |
|---|---|---|---|---|---|---|---|---|
| % of Range | 3.7% | 16.7% | 0.7% | 2.0% | 1.1% | 5.0% | 5.0% | 4.9% |
| % to Min (Center pt.) | 25.8% | 66.7% | 72.8% | 21.1% | 15.8% | 44.2% | 76.1% | 99.4% |

The results of the coded estimates effects and coefficients analysis are shown in Table 58.

Table 58: DOE3a Effects & Coefficients

| Term | Effect | Coef | Term | Effect | Coef | Term | Effect | Coef |
|---|---|---|---|---|---|---|---|---|
| Constant | 55.933 |  | A*C*D | -0.282 | -0.141 | D*F*G | -0.285 | -0.143 |
| A | 4.721 | 2.361 | A*C*E | -0.295 | -0.147 | D*F*H | 0.619 | 0.309 |
| B | -3.057 | -1.529 | A*C*F | -0.656 | -0.328 | D*G*H | -0.37 | -0.185 |
| C | 0.241 | 0.12 | A*C*G | 0.551 | 0.275 | E*F*G | 0.557 | 0.279 |
| D | -0.316 | -0.158 | A*C*H | -0.397 | -0.199 | E*F*H | -0.049 | -0.025 |
| E | -0.373 | -0.187 | A*D*E | 0.695 | 0.347 | E*G*H | -0.347 | -0.174 |
| F | -7.79 | -3.895 | A*D*F | -0.308 | -0.154 | F*G*H | 0.882 | 0.441 |
| G | 4.474 | 2.237 | A*D*G | 0.276 | 0.138 | A*B*C*D | 0.237 | 0.118 |
| H | 2.498 | 1.249 | A*D*H | -0.428 | -0.214 | A*B*C*E | 0.275 | 0.138 |
| A*B | 0.598 | 0.299 | A*E*F | 0.167 | 0.083 | A*B*C*F | -0.383 | -0.191 |
| A*C | 0.609 | 0.304 | A*E*G | -0.171 | -0.085 | A*B*C*G | 0.126 | 0.063 |
| A*D | 0.337 | 0.168 | A*E*H | -0.542 | -0.271 | A*B*C*H | -0.214 | -0.107 |
| A*E | -0.063 | -0.032 | A*F*G | 0.698 | 0.349 | A*B*D*E | -0.168 | -0.084 |
| A*F | 1.918 | 0.959 | A*F*H | -0.326 | -0.163 | A*B*D*F | 0.327 | 0.163 |
| A*G | -1.373 | -0.686 | A*G*H | -0.352 | -0.176 | A*B*D*G | -0.37 | -0.185 |
| A*H | -0.716 | -0.358 | B*C*D | 0.404 | 0.202 | A*B*D*H | 0.142 | 0.071 |
| B*C | 0.778 | 0.389 | B*C*E | 0.399 | 0.199 | A*B*E*F | -0.252 | -0.126 |
| B*D | -1.202 | -0.601 | B*C*F | -0.896 | -0.448 | A*B*E*G | 0.295 | 0.148 |
| B*E | -0.347 | -0.173 | B*C*G | 0.768 | 0.384 | A*B*E*H | 0.199 | 0.1 |

| | | | | | | | | |
|---|---|---|---|---|---|---|---|---|
| B*F | -2.449 | -1.225 | B*C*H | -0.833 | -0.417 | A*B*F*G | 0.223 | 0.112 |
| B*G | 1.958 | 0.979 | B*D*E | 0.214 | 0.107 | A*B*F*H | 0.366 | 0.183 |
| B*H | 0.384 | 0.192 | B*D*F | 0.443 | 0.221 | A*B*G*H | 0.73 | 0.365 |
| C*D | -0.206 | -0.103 | B*D*G | -0.624 | -0.312 | A*C*D*E | 0.575 | 0.287 |
| C*E | -0.243 | -0.122 | B*D*H | 0.285 | 0.142 | A*C*D*F | 0.257 | 0.128 |
| C*F | -0.233 | -0.116 | B*E*F | -0.132 | -0.066 | A*C*D*G | 0.101 | 0.051 |
| C*G | 0.342 | 0.171 | B*E*G | 0.384 | 0.192 | A*C*D*H | -0.1 | -0.05 |
| C*H | -0.149 | -0.074 | B*E*H | 0.267 | 0.133 | A*C*E*F | 0.298 | 0.149 |
| D*E | -0.016 | -0.008 | B*F*G | 1.426 | 0.713 | A*C*E*G | -0.279 | -0.139 |
| D*F | -1.052 | -0.526 | B*F*H | -0.042 | -0.021 | A*C*E*H | 0.624 | 0.312 |
| D*G | 0.904 | 0.452 | B*G*H | 0.277 | 0.139 | A*C*F*G | -0.77 | -0.385 |
| D*H | -0.351 | -0.175 | C*D*E | -0.051 | -0.025 | A*C*F*H | 0.373 | 0.187 |
| E*F | 0.708 | 0.354 | C*D*F | 0.143 | 0.072 | A*C*G*H | -0.606 | -0.303 |
| E*G | 0.012 | 0.006 | C*D*G | -0.137 | -0.069 | A*D*E*F | -0.655 | -0.327 |
| E*H | 0.101 | 0.05 | C*D*H | -0.362 | -0.181 | A*D*E*G | 0.476 | 0.238 |
| F*G | -0.964 | -0.482 | C*E*F | 0.186 | 0.093 | A*D*E*H | -0.771 | -0.385 |
| F*H | 3.546 | 1.773 | C*E*G | -0.194 | -0.097 | A*D*F*G | -0.326 | -0.163 |
| G*H | -0.286 | -0.143 | C*E*H | 0.372 | 0.186 | A*D*F*H | 0.413 | 0.206 |
| A*B*C | -0.005 | -0.002 | C*F*G | -0.46 | -0.23 | A*D*G*H | -0.454 | -0.227 |
| A*B*D | -0.553 | -0.277 | C*F*H | 0.029 | 0.015 | A*E*F*G | 0.256 | 0.128 |
| A*B*E | 0.311 | 0.155 | C*G*H | -0.153 | -0.077 | A*E*F*H | 0.286 | 0.143 |
| A*B*F | 0.393 | 0.196 | D*E*F | 0.023 | 0.012 | A*E*G*H | -0.417 | -0.209 |
| A*B*G | 0.683 | 0.341 | D*E*G | -0.128 | -0.064 | A*F*G*H | -0.541 | -0.271 |
| A*B*H | 1.041 | 0.521 | D*E*H | -0.1 | -0.05 | Ct | Pt | 4.438 |

The MSE for the DOE3a model was undefined since the ANN based model was deterministic. The contour plots in Figure 45 and Figure 46 show the properties of the response surface as depicted by the first-order model.
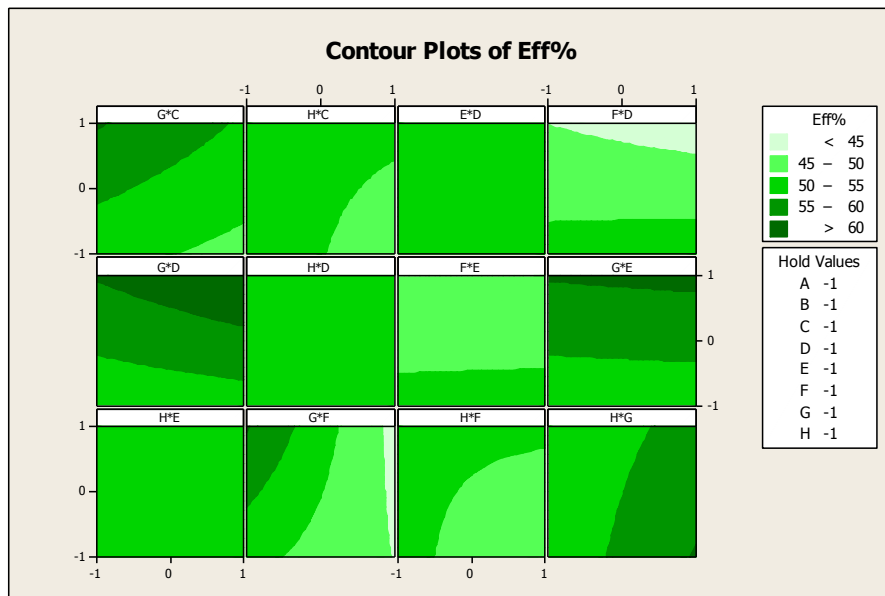


Figure 45: DOE3a Contour Plot 1 of 2
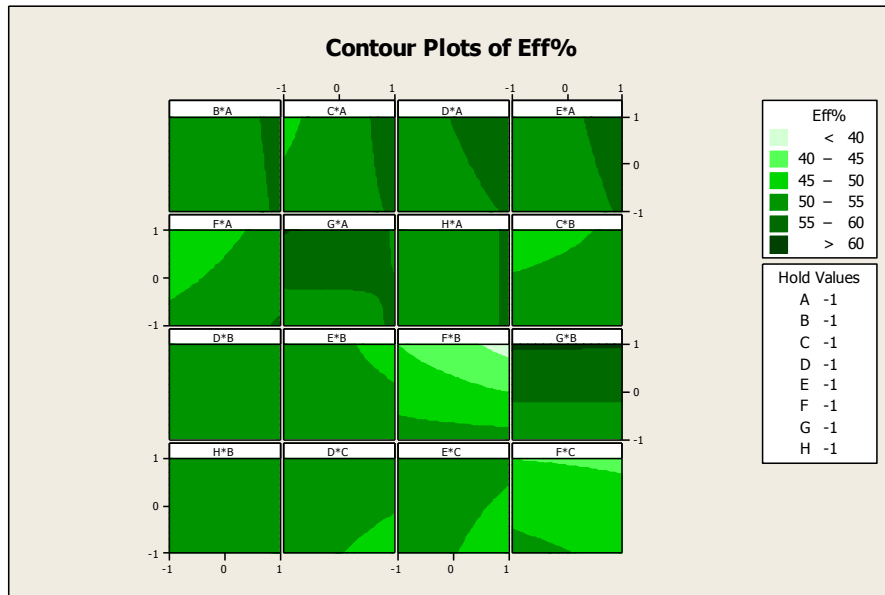
Figure 46: DOE3a Contour Plot 2 of 2

The response values for the half fractional factorial design were determined from the trained FF ANN model discussed in Chapter 8.   A steepest ascent was then conducted.


9.6.2 SA3 Steepest Ascent

The method of steepest ascent (SA3) based on following a path in the gradient direction was used.   The step size was selected to be 0.15. The characteristics of the steepest ascent design are given below.


Path of Steepest Ascent Overview

Total # of Runs                        20
Total # of Factors                      8
Base Factor Name                    Factor A
Step Size Base Factor by           0.15
Coded Coefficient of Base Factor    4.306

| Step | Factor A | Factor B | Factor C | Factor D | Factor E | Factor F | Factor G | Factor H | ANN Prediction |
|------|----------|----------|----------|----------|----------|----------|----------|----------|----------------|
| 1 | 23.33 | 53.13 | 95.88 | 19.13 | 13.20 | 52.20 | 71.10 | 58.33 | 56.371 |
| 2 | 23.81 | 52.11 | 95.88 | 19.13 | 13.20 | 51.13 | 71.55 | 59.00 | 56.248 |
| 3 | 24.05 | 51.10 | 95.88 | 19.13 | 13.20 | 50.00 | 72.05 | 59.67 | 55.878 |
| 4 | 24.29 | 50.09 | 95.88 | 19.07 | 13.20 | 48.93 | 72.50 | 60.33 | 55.813 |
| 5 | 24.76 | 49.08 | 95.90 | 19.07 | 13.15 | 47.80 | 73.00 | 61.00 | 55.444 |
| 6 | 25.00 | 48.07 | 95.90 | 19.07 | 13.15 | 46.73 | 73.45 | 62.00 | 55.158 |
| 7 | 25.48 | 47.06 | 95.90 | 19.07 | 13.15 | 45.60 | 73.95 | 62.67 | 55.005 |
| 8 | 25.95 | 46.04 | 95.90 | 19.07 | 13.15 | 44.53 | 74.40 | 63.33 | 54.676 |
| 9 | 26.19 | 45.03 | 95.90 | 19.00 | 13.15 | 43.40 | 74.90 | 64.00 | 54.461 |
| 10 | 26.43 | 44.02 | 95.90 | 19.00 | 13.15 | 42.33 | 75.35 | 64.67 | 54.367 |
| 11 | 26.90 | 43.01 | 95.93 | 19.00 | 13.10 | 41.20 | 75.85 | 65.33 | 54.233 |
| 12 | 27.14 | 42.00 | 95.93 | 19.00 | 13.10 | 40.13 | 76.30 | 66.00 | 54.196 |
| 13 | 27.62 | 40.98 | 95.93 | 19.00 | 13.10 | 39.00 | 76.80 | 66.67 | 53.931 |
| 14 | 27.86 | 39.97 | 95.93 | 18.93 | 13.10 | 37.93 | 77.25 | 67.67 | 53.838 |
| 15 | 28.33 | 38.96 | 95.93 | 18.93 | 13.10 | 36.80 | 77.75 | 68.33 | 53.699 |
| 16 | 28.57 | 37.95 | 95.93 | 18.93 | 13.10 | 35.73 | 78.20 | 69.00 | 53.533 |
| 17 | 29.05 | 36.94 | 95.93 | 18.93 | 13.05 | 34.60 | 78.70 | 69.67 | 53.526 |
| 18 | 29.29 | 35.93 | 95.95 | 18.93 | 13.05 | 33.53 | 79.15 | 70.33 | 53.243 |
| 19 | 29.76 | 34.91 | 95.95 | 18.87 | 13.05 | 32.40 | 79.65 | 71.00 | 52.911 |
| 20 | 30.00 | 33.90 | 95.95 | 18.87 | 13.05 | 31.33 | 80.10 | 71.67 | 52.813 |

9.6.3 SA3 Response Predictions

Table 59 shows the uncoded progression along the gradient path with the

predicted response using the trained FF neural network model.

Table 59: SA3 Steepest Ascent

The following figure shows the responses along the gradient path with the

progression to the DOE3a cube boundary at step 11.
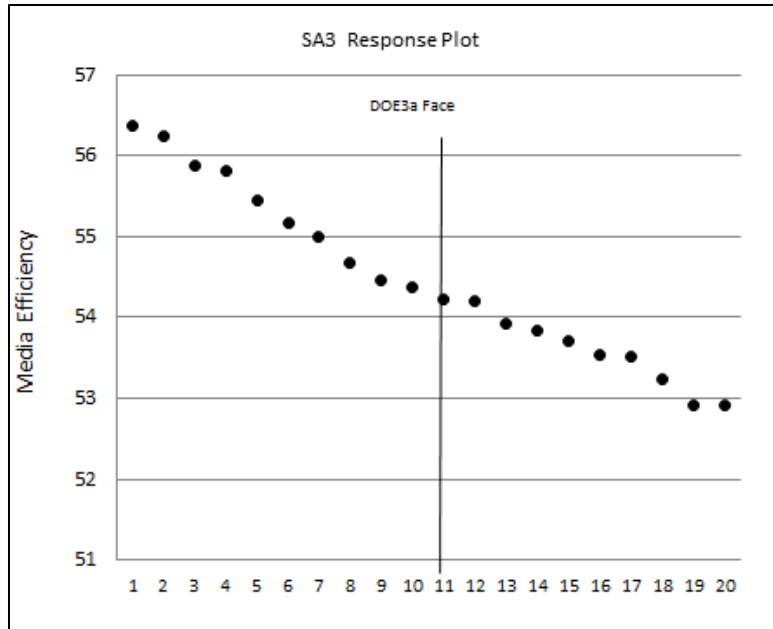
Figure 47: SA3 Response Plot

The predicted responses did not increase within the DOE3b cube.  The next step of the RSM/DOE approach would be to generate a Central Composite experimental design using the same center point as DOE3a.

9.6.4 DOE3b Experimental Design

A Star Point Central Composite experimental design using the same center point as DOE3a was conducted and is designated as DOE3b.  The DOE3b model variable values are shown in Table 60. The corner and star point values of the DOE3b effects model were determined by using a cube size similar to the DOE3b design in Chapter 7. The following independent variable settings were established for the DOE3b Central Composite Design.

Table 60: DOE3b High, Low, and Center Point Values

| | Factor A | Factor B | Factor C | Factor D | Factor E | Factor F | Factor G | Factor H |
|---|---|---|---|---|---|---|---|---|
| L-Low | 11.43 | 60.94 | 93.57 | 12.40 | 9.85 | 30.00 | 54.50 | 13.33 |
| Low | 19.76 | 37.50 | 95.17 | 17.13 | 12.20 | 45.53 | 66.10 | 45.00 |
| Center | 23.33 | 53.13 | 95.88 | 19.13 | 13.20 | 52.20 | 71.10 | 58.33 |
| High | 26.90 | 68.75 | 96.60 | 21.13 | 14.20 | 58.87 | 76.10 | 71.67 |
| H-High | 35.24 | 107.81 | 98.33 | 25.87 | 16.55 | 74.67 | 88.00 | 103.33 |

The following Central Composite Design was used for DOE3b.

Central Composite Design

Factors:     8     Replicates:     1
Base runs:     145     Total runs:     145
Base blocks:     1     Total blocks:     1

Two-level factorial: Half fraction

Cube points:               128
Center points in cube:     1
Axial points:               16
Center points in axial:     0

Since the predicted responses from the ANN model would produce the same response value, only one center point and one replicate were used in the experimental design.

9.6.5 DOE3b Response Predictions

The trained Feed Forward neural network from section 8.3 was used to determine the predicted responses for the DOE3b experimental design.  Using the trained Feed Forward ANN model, the predicted responses for each data point of the DOE3b experimental design were determined.

9.6.6 DOE3b Effects Analysis

The second-order model that was created from the DOE3b experiment is shown below in Table 61.

Table 61: Estimated Regression Coefficients for second order model

| Term | Coef | P | S |
|---|---|---|---|
| Constant | 56.3645 | 0.000 | |
| A | -0.9152 | 0.002 | |
| B | -0.2295 | 0.423 | S1 |
| C | -0.078 | 0.785 | S1 |
| D | 0.1031 | 0.719 | S1 |
| E | 0.1503 | 0.599 | S1 |
| F | -0.0841 | 0.769 | S1 |
| G | 2.4941 | 0.000 | |
| H | -2.3702 | 0.000 | |
| AA | -0.2247 | 0.470 | S2 |
| BB | 0.6958 | 0.027 | |
| CC | 0.7079 | 0.025 | |
| DD | 0.6914 | 0.028 | |
| EE | 0.7072 | 0.025 | |
| FF | 0.7218 | 0.022 | |
| GG | 0.7173 | 0.023 | |
| HH | 0.7436 | 0.018 | |
| AB | 0.1686 | 0.587 | S2 |
| AC | -0.1215 | 0.695 | S2 |
| AD | 0.0334 | 0.914 | S2 |
| AE | 0.2712 | 0.383 | S2 |
| AF | -0.1374 | 0.658 | S2 |
| AG | -0.6234 | 0.047 | |
| AH | -1.2602 | 0.000 | |
| BC | -0.1851 | 0.551 | S2 |
| BD | 0.1632 | 0.599 | S2 |
| BE | -0.2043 | 0.511 | S2 |
| BF | -0.4435 | 0.155 | S2 |
| BG | -0.0052 | 0.987 | S2 |
| BH | -0.45 | 0.149 | S2 |
| CD | -0.4949 | 0.113 | S2 |
| CE | -0.1211 | 0.696 | S2 |
| CF | 0.124 | 0.690 | S2 |
| CG | -0.1735 | 0.576 | S2 |
| CH | 0.1029 | 0.740 | S2 |
| DE | 0.1453 | 0.640 | S2 |
| DF | -0.0897 | 0.773 | S2 |
| DG | -0.012 | 0.969 | S2 |
| DH | -0.1923 | 0.536 | S2 |
| EF | -0.1329 | 0.668 | S2 |
| EG | 0.4257 | 0.172 | S2 |
| EH | -0.3112 | 0.317 | S2 |
| FG | 0.7256 | 0.021 | |
| FH | 1.529 | 0.000 | |
| GH | 0.3688 | 0.236 | S2 |

R-Sq. = 71.04% R-Sq. (adj) = 58.30%

Notes:
S1 Red Shading – Main effects retained to preserve hierarchy
S2 Blue Shading - Effects eliminated due to lack of statistical significance

A level of significance of $\alpha > 0.05$ was used to compare to the p-values in

Table 61 to determine which of the effects in the model were statistically significant.

The effects having a lack of significance which can be eliminated from the DOE3b

effects model are shaded and labeled "S2" in Table 61. The main effects having a lack

of significance were retained to preserve hierarchy.  The reduced DOE2b effects

analysis results are presented in Table 62.

Table 62: Estimated Regression Coefficients for the second-order reduced model (coded units)

| Term | Coef | P |
|---|---|---|
| Constant | 56.3102 | 0.000 |
| A | -0.9152 | 0.001 |
| B | -0.2295 | 0.405 |
| C | -0.078 | 0.777 |
| D | 0.1031 | 0.708 |
| E | 0.1503 | 0.585 |
| F | -0.0841 | 0.760 |
| G | 2.4941 | 0.000 |
| H | -2.3702 | 0.000 |
| BB | 0.8086 | 0.002 |
| CC | 0.8208 | 0.002 |
| DD | 0.8042 | 0.002 |
| EE | 0.8201 | 0.002 |
| FF | 0.8347 | 0.002 |
| GG | 0.8302 | 0.002 |
| HH | 0.8565 | 0.001 |
| AG | -0.6234 | 0.038 |
| AH | -1.2602 | 0.000 |
| FG | 0.7256 | 0.016 |
| FH | 1.529 | 0.000 |

R-Sq. = 66.49% R-Sq. (adj.) = 61.40%

Contour plots were created from the DOE3b model.  The following two figures

show the contour plots of the DOE3b model.  The darkest (green) contour circles in

Figure 48 and Figure 49 show an area of maximum response.
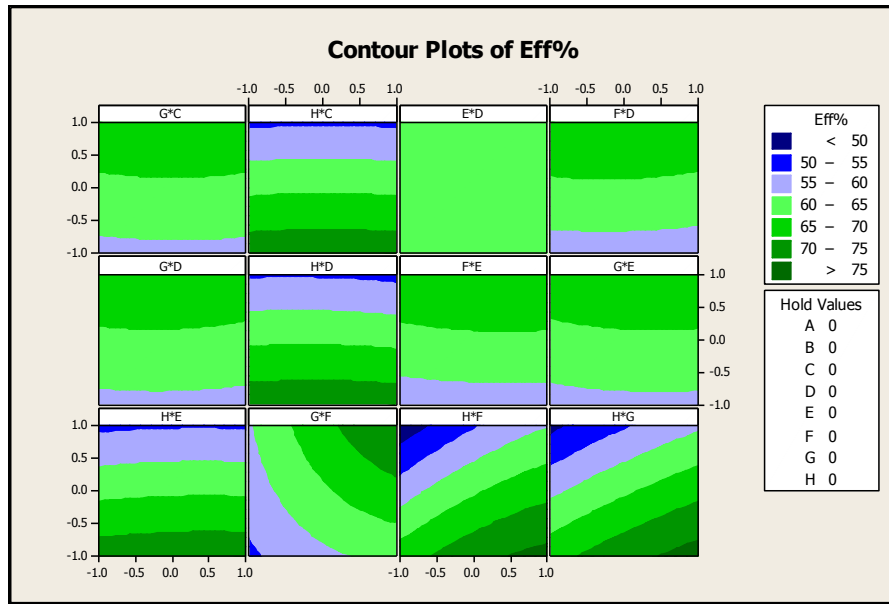
Figure 48: DOE3b Contour Plot 1 of 2
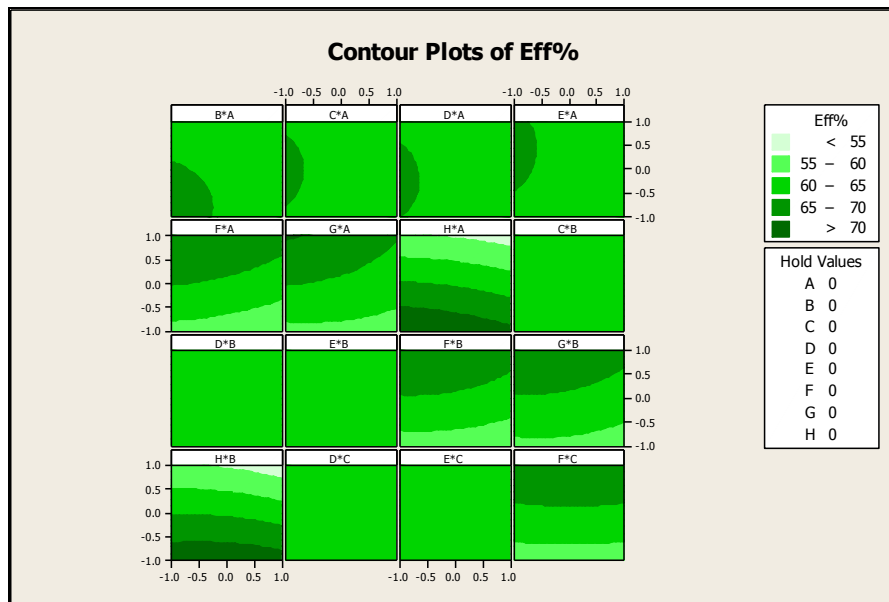

Figure 49: DOE3b Contour Plot 2 of 2

9.6.7 DOE3b Quadratic Objective Function

The reduced coded DOE3b coefficients from Table 62 were used to produce the quadratic objective function shown below.

131

$$MAX = 56.3102 - 0.915A - 0.230B - 0.078C + 0.103D + 0.15E - 0.084F +$$
$$2.494G - 2.37H + 0.809BB + 0.821CC + 0.804DD + 0.82EE + 0.838FF +$$
$$0.83GG + 0.857HH - 0.623AG - 1.26AH + 0.725FG + 1.529FH$$

The quadratic objective function and the constraint set determined by the DOE

cube variable design points constitute a Quadratic Program.

Variable Constraints
$-1.00 \leq A \leq 1.00$
$-1.00 \leq B \leq 1.00$
$-1.00 \leq C \leq 1.00$
$-1.00 \leq D \leq 1.00$
$-1.00 \leq E \leq 1.00$
$-1.00 \leq F \leq 1.00$
$-1.00 \leq G \leq 1.00$
$-1.00 \leq H \leq 1.00$

The Quadratic Program was used to determine the optima response and

associated optimal factor settings.  The results are shown in Table 63.

Table 63: Maximum Response and Settings

| Factor | Coded |
|---|---|
| A | 23.33 |
| B | 53.13 |
| C | 95.95 |
| D | 19.33 |
| E | 13.00 |
| F | 52.00 |
| G | 72.00 |
| H | 66.67 |
| Prediction Response | 56.846 |

### 9.6.8 DOE3b Maximum Response Experimental Validation

Twenty experimental trials were conducted at the maximum point to evaluate the prediction of the ANN model at this point in the experimental region.    The following table shows the statistical analysis results of the experimental trials at the DOE3b maximum point along with the ANN model prediction.  The confidence intervals were based on a pooled standard deviation derived from twelve experimental populations. The calculations for the pooled standard deviation are shown in Appendix 1.12.  The confidence interval in Table 64 was based on a sample size of two (n=2) to be comparable to the ANN database which was built up from individual points that had two replications.

Table 64: Maximum Response Trial Variance Analysis

| DOE3b Maximizer Validation | Mean | 54.335 |
|---|---|---|
| | Stdev | 0.9446 |
| | n | 20 |
| 95% Confidence Interval Formula $\bar{x} \pm Z * \dfrac{\sigma}{\sqrt{n}}$ | Z | 1.96 |
| | CI +/- | 1.309 |
| | CI Min | 53.026 |
| | CI Max | 55.645 |
| | Prediction | 56.846 |

As shown in Table 64, the predicted response of 56.846 was outside of the confidence interval.  The experimental trial results can be found at Appendix 1.10.

9.7 Chapter Summary

The steps formulated using a combination of RSM/DOE and ANN were designed to eliminate the experimentation effort required to build models for the DOE and SA approaches.

The number of trials associated with the different steps was used to compare the experimentation effort.   The following table shows the number of trials, polymer batches, and setups required for the RSM/DOE approach conducted in Chapter 7 and the four alternative steps conducted in Chapter 9.

Table 65: Experiment Trial Summary Overview

| Trial Notation | # of Runs | Polymer Batches | Setups | Comments | RSM/DOE | | Step 0 | | Step 1 | | Step 2 | | Step 3 | |
|---|---|---|---|---|---|---|---|---|---|---|---|---|---|---|
| | | | | | | Trials | | Trials | | Trials | | Trials | | Trials |
| DOE 1a | 69 | 3 | 1 | 5 center points | X | 69 | | | | | | | | |
| SA1 | 18 | 6 | 1 | 6 steps w\ 3 replicates | X | 18 | | | | | | | | |
| DOE2a | 67 | 3 | 1 | 3 center points | X | 67 | | | | | | | | |
| SA2 | 21 | 7 | 1 | 7 steps w\ 3 replicates | X | 21 | | | | | | | | |
| DOE3a | 67 | 3 | 1 | 3 center points | X | 67 | | | | | | | | |
| DOE3b | 180 | 3 | 1 | Required 180, but used 3 center pints from DOE3a | X | 180 | | | | | | | | |
| SA3 | 21 | 7 | 1 | 7 steps w\ 3 replicates | X | 21 | | | | | | | | |
| DOE3bMax | 20 | 1 | 1 | Validation trial for DOE3b Maximum | X | 20 | | | | | | | | |
| ANN-Random | 98 | 7 | 1 | Randomized trials over design space | | | X | 98 | X | 98 | X | 98 | X | 98 |
| ANN - Max | 20 | 1 | 1 | Validation trial for DOE3b Maximum | | | X | 20 | | | | | | |
| SA1 Max | 20 | 1 | 1 | Validation trial at ANN SA1 - Maximum | | | | | X | 20 | | | | |
| DOE2bMax | 20 | 1 | 1 | Validation trial at DOE2b Max | | | | | | | X | 20 | | |
| DOE3bMax | 20 | 1 | 1 | Validation trial at DOE3b Max | | | | | | | | | X | 20 |
| | | | | Total | | 463 | | 118 | | 118 | | 118 | | 118 |

As seen from Table 65, the experimentation effort based on the number of trials for the RSM/DOE approach was higher than the alternative ANN based steps used in chapter 9.

Along with experimentation effort, the effectiveness of the alternative steps in reaching a maximum response was analyzed.  Utilizing the maximum response point from Chapter 7 as a reference point, the normed distance to the alternative responses was calculated for the alternative steps.  An example of the normed distance calculation can be found in Appendix 1.11.  The following table shows the calculated normed distance of the maximum response points determined by each of the alternative steps to the DOE3a maximizer point from Chapter 7.

Table 66: Normed Distance Comparison

| Step Notation | Normed Distance |
|---|---|
| Step 0 | 1.278 |
| Step 1 | 0.883 |
| Step 2 | 0.801 |
| Step 3 | 0.740 |
| DOE3b Chapter 7 Maximizer | 0.000 |

A comparison of the performance of each step, along with the ninety-five percent confidence intervals and the normed distance, was evaluated.  The following figure shows this comparison along with the DOE3b maximum response from Chapter 7.
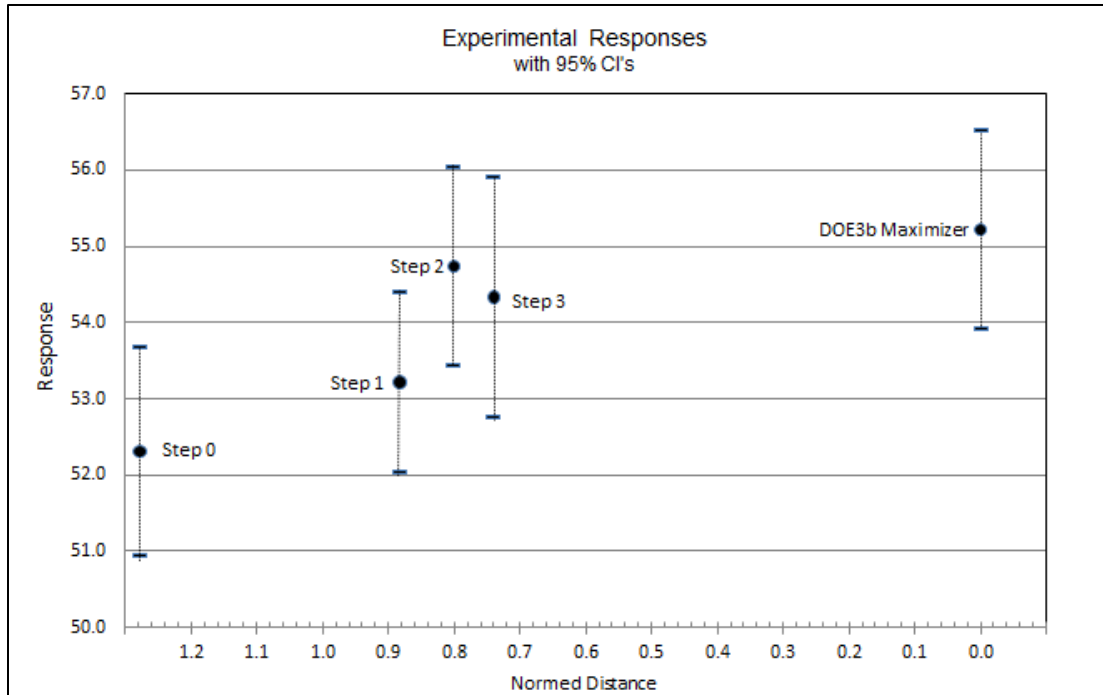
Figure 50: Response vs. Normed Distance

As shown in Figure 50, step 2 has the closest maximum response value to the average DOE3b maximum response as compared to the other three steps, but step 3 has a closer normed distance to the DOE3b maximizer point.

The use of the ANN model in the RSM/DOE optimization process in place of experiments was able to improve the maximum response on the prototype in the ANN model formulated database and produce a response close to the maximum response found in chapter 7.

CHAPTER 10 RESULTS AND ANALYSIS

10.1 Summary

The first objective of this research was to review and compare the known centrifugal electrospinning designs and select the most promising design concept(s) for producing a functional centrifugal electrospinning test apparatus.  Five specific designs were selected from the research to provide conceptual alternatives for developing a function prototype.  Attributes of several designs were integrated to develop a functional electrospinning test apparatus.  These designs are reviewed in Chapter 5.  A successful prototype of the centrifugal electrospinning process was developed and patent application is currently pending on the centrifugal electrospinning applicator.

The second objective of the research was to create an experimental test plan which identified the fixed process variables, their feasible ranges, the independent process variables, the resolution of the recorded independent process variables, and the test equipment setup.  A robust experimental test plan was developed which included identification of the fixed process variables, the independent variables and their range limitations, the resolution of the equipment settings, the test equipment, test methods, and the selection of response variables.

The third objective of the research was to execute a RSM/DOE analysis.   The RSM/DOE approach along with the algebraic models was used to search for optimum response.  First-order models with interactions and second-order models were used in the RSM/DOE analysis.  When the proximity of a potential optimum was found, a

second-degree polynomial analysis was conducted.   Additional experimental trials were used to validate the resulting maximum response.

The RSM approach could have been continued to find a point closer to the optimum, but the progression so far indicated that the maximum response point determined by the Quadratic Program is close to an optimum.   With additional cost and time for conducting more trials, the estimate of the response surface optimum might be improved.  However, based on the local analysis of the response surface, it was decided that the estimate of the found point was sufficiently close to an optimum for the purposes of the study and that further investment of cost and effort was not warranted.

The fourth objective of the research was to develop a Feed Forward (FF) Artificial Neural Network (ANN) using a structured ANN experimental data set for training.  The trained FF ANN model had satisfactory performance based on the performance measures used for evaluation.  The trained FF ANN model was then used to provide the predicted responses for the RSM/DOE alternative approach in Chapter 9.

The fifth objective of the research was to evaluate the effectiveness of the ANN model as a replacement for experimentation on the prototype in the RSM/DOE optimization process.  Though the use of the ANN model in the RSM/DOE optimization process in place of experiments on the prototype was able to improve the maximum response settings for the prototype beyond those of the ANN model formulation database and produce a response value close to the optimum found in chapter 7, though response surface predictions did not precisely match actual response surface values.

There were no journal articles found in the research that discussed using a limited amount of controlled data points over a structured experimental region for training an ANN model.   The data set used to train the ANN model for this research was controlled and purposely designed to have a structured set of data points within the appropriate experimental region.  The data points were randomly scattered throughout the experimental region while also being structured to ensure a reasonable number of data points were near the boundary of the experimental region.   This provided a training data set sample that prevented the ANN model from needing to extrapolate beyond the experimental region and still provided a satisfactory training performance and predicted accuracy.

Based on the research findings in Chapters 7, 8 and 9, there were three notable conclusions

1) The number of experimental trials required for the RSM/DOE optimization approach could be reduced while retaining the capability to improve the experimental settings by using the trained ANN model to predict the RSM/DOE responses.

2) The estimate of the optimal settings could be improved beyond the best point in the ANN database by using the trained ANN model to predict the RSM/DOE responses.

3) The settings found for operating the prototype produced a response surface value close to the response surface value of the maximum point found in Chapter 7.

For this study, the additional experimentation effort to build an ANN model reduced the overall experimentation effort required for the RSM/DOE approach. This research also provides additional insights into the effectiveness of the RSM/DOE approach in the context of prototype development and provides an alternative approach into how different combinations of RSM/DOE and ANN may be applied to complex processes.

REFERENCES

1.      Montgomery, D.C., *Design and Analysis of Experiments*. 2001: John Wiley.
2.      Picciani, P.H.S., et al., *Advances in Electroactive Electrospun Nanofibers.* European Cells and Materials.
3.      Bourquin, J., et al., *Advantages of Artificial Neural Networks (ANNs) as alternative modelling technique for data sets showing non-linear relationships using data from a galenical study on a solid dosage form.* European Journal of Pharmaceutical Sciences, 1998. 7(1): p. 5-16.
4.      Carnell, L.S., et al., *Aligned mats from electrospun single fibers.* Macromolecules, 2008. 41(14): p. 5345-5349.
5.      Thompson, C., *An analysis of variable effects on a theoretical model of the electrospin process for making nanofibers*, 2007, The University of Akron.
6.      Sarkar, K., *Application of Dimensional Analysis to Predict Poly Ethylene Oxide (PEO) Fiber Diameters from Electrospinning Process.* Textile Research Journal.
7.      Lu, P. and B. Ding, *Applications of electrospun fibers.* Recent patents on nanotechnology, 2008. 2(3): p. 169-182.
8.      Schreuder-Gibson, H.L. and P. Gibson, *Applications of electrospun nanofibers in current and future materials.* US Army Research, Development & Engineering Command Natick Soldier Center, Kansas Street, Natick, MA, 2006.
9.      Propst, M.D., *Applying Linear Regression and Neural Network Meta-Models for Evolutionary Algorithm Based Simulation Optimization.* 2009.
10.     Amani, A., D. Mohammadyani, and C. Hui, *Artificial Neural Networks: Applications in Nanotechnology.* Artificial neural networks− application. Rijeka: INTECH, 2011.
11.     Tomczak, N., N.F. van Hulst, and G.J. Vancso, *Beaded electrospun fibers for photonic applications.* Macromolecules, 2005. 38(18): p. 7863-7866.
12.     Yarin, A., S. Koombhongse, and D. Reneker, *Bending instability in electrospinning of nanofibers.* Journal of Applied Physics, 2001. 89: p. 3018.
13.     Koláčná, L., et al., *Biochemical and biophysical aspects of collagen nanostructure in the extracellular matrix.* Physiol Res, 2007. 56(Suppl 1): p. 51-60.
14.     Mironov, V., et al., *Biofabrication: a 21st century manufacturing paradigm.* Biofabrication, 2009. 1: p. 022001.
15.     Ford, E., R.E. Popil, and S. Kumar, *BREATHABLE WATER-RESISTANT LINERBOARD COATINGS BY ELECTROSPRAYING APPLICATION.* BioResources, 2009. 4(2).
16.     Engström, J. and B. Hagström, *Centrifugal spinning of nanofiber webs-A parameter study of a novel spinning process.* Textile Research Journal, 2009.
17.     Cooper, A., *Chitosan-Based Nanofibers for Biomedical Applications*, 2011, University of Washington: United States -- Washington.
18.     SA, M. and G. CE, *The coming era of nanotechnology and the production of polymer fibers: A brief review on nanotechnology.* ChemClass Journal, 2007. 2(0).
19.     Göktepe, F., *Comparative Analysis of Various Electrospinning Methods of Nanofibre Formation.*

20. Bourquin, J., et al., *Comparison of artificial neural networks (ANN) with classical modelling techniques using different experimental designs and data from a galenical study on a solid dosage form.* European Journal of Pharmaceutical Sciences, 1998. 6(4): p. 287-300.

21. Oznergiz, E., et al., *Comparison of empirical and neural network hot-rolling process models.* Proceedings of the Institution of Mechanical Engineers Part B-Journal of Engineering Manufacture, 2009. 223(3): p. 305-312.

22. Krupke, R., et al., *Contacting single bundles of carbon nanotubes with alternating electric fields.* Applied Physics A: Materials Science & Processing, 2003. 76(3): p. 397-400.

23. Chang, C., K. Limkrailassiri, and L. Lin, *Continuous near-field electrospinning for large area deposition of orderly nanofiber patterns.* Applied Physics Letters, 2008. 93: p. 123111.

24. Latifi, M., et al., *Continuous twisted yarn from well-aligned nanofibers by a water vortex.* Physical Review E.

25. Wu, Y., L.A. Carnell, and R.L. Clark, *Control of electrospun mat width through the use of parallel auxiliary electrodes.* Polymer, 2007. 48(19): p. 5653-5661.

26. Bisht, G.S., et al., *Controlled continuous patterning of polymeric nanofibers on three-dimensional substrates using low-voltage near-field electrospinning.* Nano Lett, 2011. 11(4): p. 1831-7.

27. Deitzel, J., et al., *Controlled deposition of electrospun poly (ethylene oxide) fibers.* Polymer, 2001. 42(19): p. 8163-8170.

28. Fridrikh, S., et al., *Controlling the Fiber Diameter during Electrospinning.* Physical Review Letters, 2003. 90(14).

29. Kim, S.J., et al., *Design of Selective Gas Sensors Using Additive-Loaded In2O3 Hollow Spheres Prepared by Combinatorial Hydrothermal Reactions.* Sensors, 2011. 11(11): p. 10603-10614.

30. Raissi, S., *Developing new processes and optimizing performance using response surface methodology.* World Academy of Science, Engineering and Technology, 2009. 49: p. 1039-1042.

31. Thoppey Muthuraman, N., *Development and Optimization of an Alternative Electrospinning Process for High Throughput.*

32. Goethals, P.L. and B.R. Cho, *The development of a robust design methodology for time-oriented dynamic quality characteristics with a target profile.* Quality and Reliability Engineering International, 2011. 27(4): p. 403-414.

33. Laudenslager, M.J. and W.M. Sigmund, *Developments in electrohydrodynamic forming: Fabricating.* American Ceramic Society Bulletin. 90(2).

34. Darcovich, K., K. Jonasson, and C. Capes, *Developments in the control of fine particulate air emissions.* Advanced Powder Technology, 1997. 8(3).

35. Dalton, P.D., et al., *Direct in vitro electrospinning with polymer melts.* Biomacromolecules, 2006. 7(3): p. 686-690.

36. Desai, K. and C. Sung. *DOE optimization and phase morphology of electrospun nanofibers of PANI/PMMA blends.* 2004.

37. Lembach, A.N., et al., *Drop Impact, Spreading, Splashing, and Penetration into Electrospun Nanofiber Mats.* Langmuir, 2010. 26(12): p. 9516-9523.

38. Anh Tuan, D. and O. JIRSAK, *EFFECT OF CROSS-LINKING AGENT ON ELECTROSPINNING OF POLY (VINYL) ALCOHOL.* Textile Research Journal.

39. Tsai, P.P. and H. Schreuder-Gibson. *Effect of electrospinning material and conditions upon residual electrostatic charge of polymer nanofibers.* 2001.

40. Chowdhury, M. and G. Stylios, *Effect of experimental parameters on the morphology of electrospun Nylon 6 fibres.* International Journal of Basic & Applied Sciences, 2010. 10(06).

41. Evcin, A. and D.A. Kaya, *Effect of production parameters on the structure and morphology of aluminum titanate nanofibers produced using electrospinning technique.* Scientific Research and Essays, 2010. 5(23): p. 3682-3686.

42. Shendokar, S., et al. *Effect of Sintering Temperature on Mechanical Properties of Electrospun Silica Nanofibers.* 2008. ASME.

43. Lin, Y.J., et al., *Effect of solvent on surface wettability of electrospun polyphosphazene nanofibers.* Journal of applied polymer science, 2010. 115(6): p. 3393-3400.

44. Liu, X., *Effective control of cell behavior on conducting polymers*, 2009, Department of Chemistry-Faculty of Science, University of Wollongong.

45. Kilic, A., F. Oruc, and A. Demir, *Effects of polarity on electrospinning process.* Textile Research Journal, 2008. 78(6): p. 532.

46. Sun, H., *Efficiency Improvement of Evolutionary Multiobjective Optimization Methods for CFD-Based Shape Optimization*, 2010, TU Darmstadt.

47. Soa, D.S., et al., *Electrical impedance properties of a nanoweb electrode embedded carbon nanotube for a bio-chemical sensor.* Journal of Ceramic Processing Research, 2011. 12(3): p. 343-347.

48. Kongkhlang, T., et al., *Electrospinning as a new technique to control the crystal morphology and molecular orientation of polyoxymethylene nanofibers.* Journal of the American Chemical Society, 2008. 130(46): p. 15460-15466.

49. Yeo, L.Y. and J.R. Friend, *Electrospinning carbon nanotube polymer composite nanofibers.* Journal of Experimental Nanoscience, 2006. 1(2): p. 177-209.

50. Meli, L., et al., *Electrospinning from room temperature ionic liquids for biopolymer fiber formation.* Green Chem., 2010. 12(11): p. 1883-1892.

51. Li, D., Y. Wang, and Y. Xia, *Electrospinning of polymeric and ceramic nanofibers as uniaxially aligned arrays.* Nano Lett, 2003. 3(8): p. 1167-1171.

52. Ali, A.A. and M. El-Hamid, *Electro-spinning optimization for precursor carbon nanofibers.* Composites Part A: Applied Science and Manufacturing, 2006. 37(10): p. 1681-1687.

53. Sarkar, K., et al., *Electrospinning to Forcespinning™.* Materials Today, 2010. 13(11): p. 12-14.

54. Dalton, P.D., D. Klee, and M. Möller, *Electrospinning with dual collection rings.* Polymer, 2005. 46(3): p. 611-614.

55. Liu, W., Y. Wang, and J. Su, *ELECTROSPINNING: SHAPE AND ALIGNMENT CONTROL.* Ieee Sensors Journal.

56. Bock, N., et al., *Electrospraying, a Reproducible Method for Production of Polymeric Microspheres for Biomedical Applications.* Polymers, 2011. 3(1): p. 131-149.

57.   Gibson, P., H. Schreuder-Gibson, and D. Rivin, *Electrospun fiber mats: transport properties.* AIChE journal, 1999. 45(1): p. 190-195.

58.   Bretcanu, O., et al., *Electrospun nanofibrous biodegradable polyester coatings on Bioglass®-based glass-ceramics for tissue engineering.* Materials Chemistry and Physics, 2009. 118(2-3): p. 420-426.

59.   Dotti, F., et al., *Electrospun porous mats for high efficiency filtration.* Journal of Industrial Textiles, 2007. 37(2): p. 151-162.

60.   Theron, A., E. Zussman, and A. Yarin, *Electrostatic field-assisted alignment of electrospun nanofibres.* Nanotechnology, 2001. 12: p. 384.

61.   McNenly, M.J., M.A. Gallis, and I.D. Boyd, *Empirical slip and viscosity model performance for microscale gas flow.* International journal for numerical methods in fluids, 2005. 49(11): p. 1169-1191.

62.   Chang, C.C., et al., *Enhancement of light scattering and photoluminescence in electrospun polymer nanofibers.* Optics Express, 2010. 18(S2): p. A174-A187.

63.   Shin, Y., et al., *Experimental characterization of electrospinning: the electrically forced jet and instabilities.* Polymer, 2001. 42(25): p. 09955-09967.

64.   Yang, D., et al., *Fabrication of aligned fibrous arrays by magnetic electrospinning.* Advanced Materials, 2007. 19(21): p. 3702-3706.

65.   Li, M., et al., *Fabrication of one dimensional superfine polymer fibers by double-spinning.* Journal of Materials Chemistry, 2011. 21(35): p. 13159-13162.

66.   Qin, X.H. and S.Y. Wang, *Filtration properties of electrospinning nanofibers.* Journal of applied polymer science, 2006. 102(2): p. 1285-1290.

67.   Mohan, A., *Formation and characterization of electrospun nonwoven webs.* Fibres & Textiles in Eastern Europe, 2003.

68.   Zussman, E., A. Theron, and A. Yarin, *Formation of nanofiber crossbars in electrospinning.* Applied Physics Letters, 2003. 82: p. 973.

69.   Matsumoto, H. and A. Tanioka, *Functionality in Electrospun Nanofibrous Membranes Based on Fiber's Size, Surface Area, and Molecular Orientation.* Membranes, 2011. 1(3): p. 249-264.

70.   Tsoukalas, L.H. and R.E. Uhrig, *Fuzzy and neural approaches in engineering.* 1997: Wiley.

71.   Ding, B., et al., *Gas Sensors Based on Electrospun Nanofibers.* Sensors, 2009. 9(3): p. 1609-1624.

72.   Wu, D., et al., *High Throughput Tip-Less Electrospinning via a Circular Cylindrical Electrode.* Journal of Nanoscience and Nanotechnology, 2010. 10(7): p. 4221-4226.

73.   Peterson, C.T., *Hybrid Nanomanufacturing Process for High-Rate Polymer Nanofiber Production.* Dissertation - UON, 2010.

74.   Petrík, S., *Industrial Production Technology for Nanofibers.* European Cells and Materials.

75.   Chen, L.J., *Integrated robust design using response surface methodology and constrained optimization.* 2008.

76.   Tran, S.B.Q., et al., *Liquid meniscus oscillation and drop ejection by ac voltage, pulsed dc voltage, and superimposing dc to ac voltages.* Physical Review E, 2009. 80(2): p. 026318.

77. Raghavan, B. and G. Chase, *Loading of fibrous Filter Media with Solid Aerosol Particles–Modeling Study.*

78. POKORNÝ, P. and O. JIRSÁK, *Measurement of electric current during electrospinning.* Textile Research Journal, 2010.

79. Kurokawa, T., et al., *METHOD AND APPARATUS FOR PRODUCING NANOFIBERS*, 2009, Google Patents.

80. Chronakis, I.S., *Micro-/Nano-Fibers by Electrospinning Technology: Processing, Properties and Applications.* Micromanufacturing Engineering and Technology, 2010: p. 264.

81. Megelski, S., et al., *Micro-and nanostructured surface morphology on electrospun polymer fibers.* Macromolecules, 2002. 35(22): p. 8456-8466.

82. Spivak, A., Y. Dzenis, and D. Reneker, *A model of steady state jet in the electrospinning process.* Mechanics research communications, 2000. 27: p. 37-42.

83. Kowalewski, T.A., S. Barral, and T. Kowalczyk. *Modeling Electrospinning of Nanofibers.* 2009. Springer.

84. Srivastava, Y., M. Marquez, and T. Thorsen, *Multijet electrospinning of conducting nanofibers from microfluidic manifolds.* Journal of applied polymer science, 2007. 106(5): p. 3171-3178.

85. Theron, S.A., et al., *Multiple jets in electrospinning: experiment and modeling.* Polymer, 2005. 46(9): p. 2889-2899.

86. Soliman, S., et al., *Multiscale three-dimensional scaffolds for soft tissue engineering via multimodal electrospinning.* Acta Biomater, 2010. 6(4): p. 1227-37.

87. Hardick, O., B. Stevens, and D.G. Bracewell, *Nanofiber fabrication in a temperature and humidity controlled environment for improved fibre consistency.* Nature Proceedings, 2010.

88. Grafe, T.H. and K.M. Graham. *Nanofiber webs from electrospinning.* 2003.

89. Engström, J., et al., *Nanofibers–small fibers with big potential.* Textile Research Journal, 2009.

90. Schaefer, K., et al., *Nano-Fibres for Filter Materials.* Multifunctional Barriers for Flexible Structure, 2007: p. 125-138.

91. Bognitzki, M., et al., *Nanostructured fibers via electrospinning.* Advanced Materials, 2001. 13(1): p. 70-72.

92. Kubinova, S. and E. Sykova, *Nanotechnologies in regenerative medicine.* Minim Invasive Ther Allied Technol, 2010. 19(3): p. 144-56.

93. Gerke, D., *NASA 2009 Body of Knowledge (BoK) carbon nanotube technology.* NASA, 2009.

94. Sun, D., et al., *Near-field electrospinning.* Nano Lett, 2006. 6(4): p. 839-842.

95. Wang, X., et al., *Needleless Electrospinning of nanofibers with a conical wire coil.* Polymer Engineering & Science, 2009. 49(8): p. 1582-1586.

96. Niu, H., T. Lin, and X. Wang, *Needleless electrospinning. I. A comparison of cylinder and disk nozzles.* Journal of applied polymer science, 2009. 114(6): p. 3524-3530.

97. JIRSAK, O. and S. PETRIK, *NEEDLELESS ELECTROSPINNING–HISTORY, PRESENT AND FUTURE.* Textile Research Journal.

98.    Sarkar, K., et al., *A neural network model for the numerical prediction of the diameter of electro-spun polyethylene oxide nanofibers.* Journal of Materials Processing Technology, 2009. 209(7): p. 3156-3165.

99.    Chase, G.G., J.S. Varabhas, and D.H. Reneker, *New Methods to Electrospin Nanofibers.* UOA.

100.   Schauer, C. and M. Austero, *A new platform for creating versatile nonwoven mats.* Society of Plastics Engineers–Plastics Research Online.

101.   Zeng, Y., Z. Pei, and X. Wang. *Numerical Simulation of Whipping Process in Electrospinning.* 2009. World Scientific and Engineering Academy and Society.

102.   Padron, S., D.I. Caruntu, and K. Lozano, *ON 2D FORCESPINNING™ MODELING.* Ieee Sensors Journal.

103.   Gadallah, M.H. *Optimization Formulation Based on Limited Data and RSM: An Approximation.* 2009.

104.   Maleki, M., M. Latifi, and M. Amani-Tehran, *Optimizing Electrospinning Parameters for Finest diameter of Nano Fibers.* Textile Research Journal.

105.   Shendokar, S., et al. *PARAMETRIC INVESTIGATIONS ON THE EFFECT OF ELECTROSPINNING PROCESS VERIABLES ON THE MACROSCOPIC PROPERTIES OF HYBRID COMPOSITES.* 2009. ASME.

106.   Gibson, P. and H. Schreuder-Gibson, *Patterned electrospray fiber structures*, 2005.

107.   Sbiaa, R. and S.N. Piramanayagam, *Patterned media towards nano-bit magnetic recording: Fabrication and challenges.* Recent patents on nanotechnology, 2007. 1(1): p. 29-40.

108.   Bourquin, J., et al., *Pitfalls of artificial neural networks (ANN) modelling technique for data sets containing outlier measurements using a study on mixture properties of a direct compressed dosage form.* European Journal of Pharmaceutical Sciences, 1998. 7(1): p. 17-28.

109.   Jirsak, O., et al., *Polyamic Acid Nanofibers Produced by Needleless Electrospinning.* Journal of Nanomaterials, 2010. 2010: p. 1-6.

110.   Frenot, A. and I.S. Chronakis, *Polymer nanofibers assembled by electrospinning.* Current opinion in colloid & interface science, 2003. 8(1): p. 64-75.

111.   Weitz, R., et al., *Polymer nanofibers via nozzle-free centrifugal spinning.* Nano Lett, 2008. 8(4): p. 1187-1191.

112.   Grafe, T. and K. Graham, *Polymeric nanofibers and nanofiber webs: a new class of nonwovens.* Nonwoven Technol Rev, 2003: p. 51-5.

113.   Graham, K., et al. *Polymeric nanofibers in air filtration applications.* in *Fithteenth Annual Technical Conference & Expo of the American Filtration & Separations Society.* 2002.

114.   Kalayci, V., M. Ouyang, and K. Graham, *Polymeric nanofibres in high efficiency filtration applications.* FILTRATION-COALVILLE-, 2006. 6(4): p. 286.

115.   Ding, B., et al., *Preparation and characterization of a nanoscale poly(vinyl alcohol) fiber aggregate produced by an electrospinning method.* Journal of Polymer Science Part B: Polymer Physics, 2002. 40(13): p. 1261-1268.

116.   Jin-Shan, T., L. Yun-Ze, and L. Meng-Meng, *Preparation of Aligned Polymer Micro/Nanofibres by Electrospinning.* Chinese Physics Letters, 2008. 25: p. 3067.

117. Bognitzki, M., et al., *Preparation of fibers with nanoscaled morphologies: Electrospinning of polymer blends.* Polymer Engineering & Science, 2001. 41(6): p. 982-989.

118. Hakala, T. and P. Heikkilä, *Press Felts Coated with Electrospun Nanofibres.* Fibres & Textiles in Eastern Europe, 2011. 19(1): p. 84.

119. Sigmund, W., et al., *Processing and Structure Relationships in Electrospinning of Ceramic Fiber Systems.* Journal of the American Ceramic Society, 2006. 89(2): p. 395-407.

120. Uecker, J.C., *The Production and Filtration Efficiency Testing of Nonwoven Electrospun Fiber Mats*, 2009, Virginia Commonwealth University Richmond, VA.

121. Dabirian, F. and S. Ravandi, *Production and Some Characteristics of Bulk Nanofibers Layers by Manipulation of Electrospinning System.* Iranian Journal of Polymer Science and Technology, 2008. 21(4): p. 1.

122. Petrik, S. and M. Maly. *Production nozzle-less electrospinning nanofiber technology.* 2009. Elmarco s.r.p.

123. Maly, M. and S. Petrik, *Production Technology for Nanofiber Filtration Media.* NSTI - Nanotech 2010.

124. Jirsák, O. and T. Dao, *Production, Properties and End-Uses of Nanofibres.* Nanotechnology in Construction 3, 2009: p. 95-99.

125. Luzhansky, D.M. *Quality control in manufacturing of electrospun nanofiber composites.* 2002.

126. Stephens, J., et al., *" Real Time" Raman Studies of Electrospun Fibers.* Applied Spectroscopy, 2001. 55(10): p. 1287-1290.

127. Vashist, S.K. and P. Vashist, *Recent Advances in Quartz Crystal Microbalance-Based Sensors.* Journal of Sensors, 2011. 2011.

128. Jaroszczyk, T., S. Petrik, and K. Donahue, *Recent development in heavy duty engine air filtration and the role of nanofiber filter media.* Journal of KONES, 2009. 16(4): p. 207-216.

129. Kleijnen, J.P.C., *Response surface methodology for constrained simulation optimization: An overview.* Simulation Modelling Practice and Theory, 2008. 16(1): p. 50-64.

130. Myers, R.H., D.C. Montgomery, and C.M. Anderson-Cook, *Response surface methodology: process and product optimization using designed experiments*. Vol. 705. 2009: John Wiley & Sons Inc.

131. Teo, W. and S. Ramakrishna, *A review on electrospinning design and nanofibre assemblies.* Nanotechnology, 2006. 17: p. R89.

132. Tsai, P., H.L. Schreuder-Gibson, and N.S. Center, *The Role of Fiber Charging on Co-electrospinning and the Resident Life of the Residual Charges from the Electrospinning Process.* 2003.

133. Senthilram, T., et al., *Self crimped and aligned fibers.* Materials Today, 2011. 14(5): p. 226-229.

134. Medeiros, E.S., et al., *Solution blow spinning: A new method to produce micro- and nanofibers from polymer solutions.* Journal of applied polymer science, 2009. 113(4): p. 2322-2330.

135. Marshall, L.R., et al., *SOLUTION SPUN FIBER PROCESS*, 2008, EP Patent 1,999,304.

136. Marshall, L.R., et al., *SOLUTION SPUN FIBER PROCESS*, 2009, Google Patents.
137. *MATLAB* version R2012a [computer software]; The MathWorks Inc.: Natick, Massachusetts, 2003.
138. Raissi, S. and R.E. Farsani, *Statistical process optimization through multi-response surface methodology.* World Academy of Science, Engineering and Technology, 2009. 51(46): p. 267-271.
139. Cheng, Y.W., et al., *Syndiotactic polystyrene nanofibers obtained from high-temperature solution electrospinning process.* Macromolecules, 2010. 43(5): p. 2371-2376.
140. Wu, Y., et al., *Template-assisted assembly of electrospun fibers.* Polymer, 2010. 51(14): p. 3244-3248.
141. Wan, Y.Q., Q. Guo, and N. Pan, *Thermo-electro-hydrodynamic model for electrospinning process.* International Journal of Nonlinear Sciences and Numerical Simulation, 2004. 5(1): p. 5-8.
142. Lan, X., W. Liang, and F. Naeem, *A thermo-electro-hydrodynamic model for vibration-electrospinning process.* Thermal Science, 2011. 15(suppl. 1): p. 131-135.
143. Xu, L., L. Wang, and N. Faraz, *A thermo-electro-hydrodynamic model for vibration-electrospinning process.* Thermal Science, 2011. 15(suppl. 1): p. 131-135.
144. Tong, H.W. and M. Wang, *Tissue engineering scaffolds formed by pseudo-negative voltage electrospinning.* Society of Plastics Engineers–Plastics Research Online, 2011.
145. Salata, O.V., *Tools of nanotechnology: Electrospray.* Current nanoscience, 2005. 1(1): p. 25-33.
146. Baede, T., *Towards a new position-controlled electrospinning setup.*
147. Reznik, S.N., et al., *Transient and steady shapes of droplets attached to a surface in a strong electric field.* Journal of Fluid Mechanics, 2004. 516: p. 349-377.
148. Schreuder-Gibson, H.L., P. Gibson, and A.R.S.S. Center, *Transport properties of electrospun nonwoven membranes.* Int Nonwoven J, 2002. 11(2): p. 21-6.
149. Milleret, V., et al., *Tuning electrospinning parameters for production of 3D-fiber-fleeces with increased porosity for soft tissue engineering applications.* European Cells and Materials, 2011. 21: p. 286-303.
150. Supaphol, P., C. Mit-uppatham, and M. Nithitanakul, *Ultrafine Electrospun Polyamide-6 Fibers: Effects of Solvent System and Emitting Electrode Polarity on Morphology and Average Fiber Diameter.* Macromolecular Materials and Engineering, 2005. 290(9): p. 933-942.
151. Yarin, A.L. and E. Zussman, *Upward needleless electrospinning of multiple nanofibers.* Polymer, 2004. 45(9): p. 2977-2980.
152. Schreder-Gibson, H. and P. Gibson, *Use of electrospun nanofiber for aerosol filtration in textile structures.* US Army Soldier Systems Cent AMSSB-RSS-MS (N) Natick, MA http://www. asc2004. com/23rdASC/oral_summaries/L/LO-05. PDF, 2004.

153. Wei, C., et al., *Integration of design of experiments and artificial neural networks for achieving affordable concurrent design*, in *38th Structures, Structural Dynamics, and Materials Conference*. 1997, American Institute of Aeronautics and Astronautics.

# APPENDICES

## 1.1 DOE1a - Four Main Residual Plots and Experimental Data Results
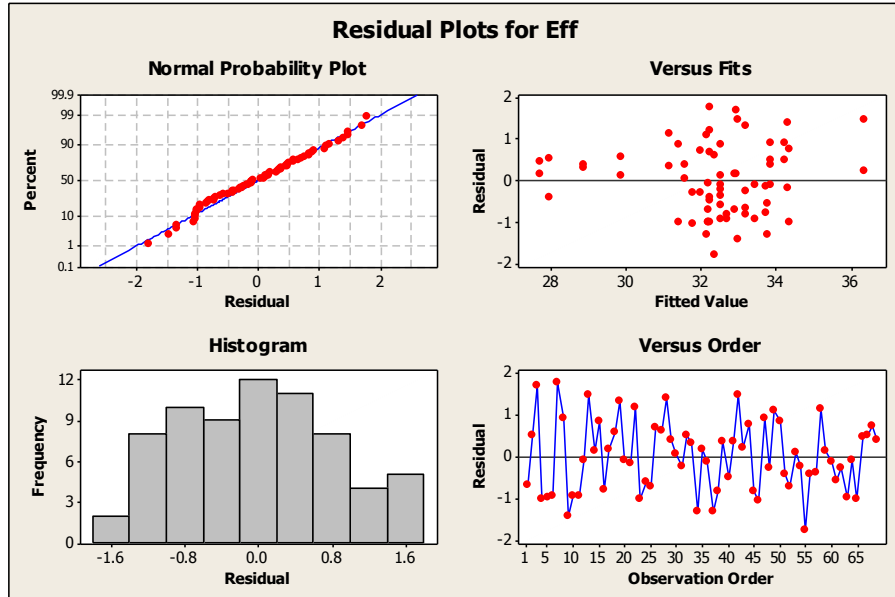


Residual Plots for Eff

| Std Order (i) | Run Order (i) | Basic Design | | | | | Factor F=ABC | Factor G=ABD | Factor H=BCDE | Eff % |
|---|---|---|---|---|---|---|---|---|---|---|
| | | Factor A | Factor B | Factor C | Factor D | Factor E | | | | |
| 1 | 34 | 82.29 | 12.50 | 20.00 | 30.00 | 73.33 | 40.00 | 61.00 | 48.00 | 30.827 |
| 2 | 5 | 89.29 | 12.50 | 20.00 | 30.00 | 73.33 | 53.33 | 59.00 | 48.00 | 31.191 |
| 3 | 40 | 82.29 | 37.50 | 20.00 | 30.00 | 73.33 | 53.33 | 59.00 | 32.00 | 31.736 |
| 4 | 7 | 89.29 | 37.50 | 20.00 | 30.00 | 73.33 | 40.00 | 61.00 | 32.00 | 34.016 |
| 5 | 61 | 82.29 | 12.50 | 30.00 | 30.00 | 73.33 | 53.33 | 61.00 | 32.00 | 33.197 |
| 6 | 47 | 89.29 | 12.50 | 30.00 | 30.00 | 73.33 | 40.00 | 59.00 | 32.00 | 35.156 |
| 7 | 11 | 82.29 | 37.50 | 30.00 | 30.00 | 73.33 | 40.00 | 59.00 | 48.00 | 32.510 |
| 8 | 8 | 89.29 | 37.50 | 30.00 | 30.00 | 73.33 | 53.33 | 61.00 | 48.00 | 34.785 |
| 9 | 14 | 82.29 | 12.50 | 20.00 | 36.67 | 73.33 | 40.00 | 59.00 | 32.00 | 30.000 |
| 10 | 55 | 89.29 | 12.50 | 20.00 | 36.67 | 73.33 | 53.33 | 61.00 | 32.00 | 30.570 |
| 11 | 3 | 82.29 | 37.50 | 20.00 | 36.67 | 73.33 | 53.33 | 61.00 | 48.00 | 34.645 |
| 12 | 38 | 89.29 | 37.50 | 20.00 | 36.67 | 73.33 | 40.00 | 59.00 | 48.00 | 32.353 |
| 13 | 48 | 82.29 | 12.50 | 30.00 | 36.67 | 73.33 | 53.33 | 59.00 | 48.00 | 31.695 |
| 14 | 52 | 89.29 | 12.50 | 30.00 | 36.67 | 73.33 | 40.00 | 61.00 | 48.00 | 31.461 |
| 15 | 43 | 82.29 | 37.50 | 30.00 | 36.67 | 73.33 | 40.00 | 61.00 | 32.00 | 36.604 |
| 16 | 44 | 89.29 | 37.50 | 30.00 | 36.67 | 73.33 | 53.33 | 59.00 | 32.00 | 35.125 |
| 17 | 26 | 82.29 | 12.50 | 20.00 | 30.00 | 75.56 | 40.00 | 61.00 | 32.00 | 32.915 |
| 18 | 29 | 89.29 | 12.50 | 20.00 | 30.00 | 75.56 | 53.33 | 59.00 | 32.00 | 34.230 |
| 19 | 58 | 82.29 | 37.50 | 20.00 | 30.00 | 75.56 | 53.33 | 59.00 | 48.00 | 32.282 |
| 20 | 45 | 89.29 | 37.50 | 20.00 | 30.00 | 75.56 | 40.00 | 61.00 | 48.00 | 31.881 |
| 21 | 66 | 82.29 | 12.50 | 30.00 | 30.00 | 75.56 | 53.33 | 61.00 | 48.00 | 28.122 |
| 22 | 41 | 89.29 | 12.50 | 30.00 | 30.00 | 75.56 | 40.00 | 59.00 | 48.00 | 29.228 |
| 23 | 15 | 82.29 | 37.50 | 30.00 | 30.00 | 75.56 | 40.00 | 59.00 | 32.00 | 32.236 |
| 24 | 57 | 89.29 | 37.50 | 30.00 | 30.00 | 75.56 | 53.33 | 61.00 | 32.00 | 32.140 |
| 25 | 9 | 82.29 | 12.50 | 20.00 | 36.67 | 75.56 | 40.00 | 59.00 | 48.00 | 31.539 |
| 26 | 28 | 89.29 | 12.50 | 20.00 | 36.67 | 75.56 | 53.33 | 61.00 | 48.00 | 35.735 |
| 27 | 16 | 82.29 | 37.50 | 20.00 | 36.67 | 75.56 | 53.33 | 61.00 | 32.00 | 32.963 |
| 28 | 25 | 89.29 | 37.50 | 20.00 | 36.67 | 75.56 | 40.00 | 59.00 | 32.00 | 32.158 |
| 29 | 67 | 82.29 | 12.50 | 30.00 | 36.67 | 75.56 | 53.33 | 59.00 | 32.00 | 28.457 |
| 30 | 30 | 89.29 | 12.50 | 30.00 | 36.67 | 75.56 | 40.00 | 61.00 | 32.00 | 31.609 |
| 31 | 46 | 82.29 | 37.50 | 30.00 | 36.67 | 75.56 | 40.00 | 61.00 | 48.00 | 30.723 |
| 32 | 19 | 89.29 | 37.50 | 30.00 | 36.67 | 75.56 | 53.33 | 59.00 | 48.00 | 34.524 |

| | | | | | | | | | | |
|---|---|---|---|---|---|---|---|---|---|---|
| 33 | 49 | 82.29 | 12.50 | 20.00 | 30.00 | 73.33 | 40.00 | 61.00 | 48.00 | 33.248 |
| 34 | 12 | 89.29 | 12.50 | 20.00 | 30.00 | 73.33 | 53.33 | 59.00 | 48.00 | 32.114 |
| 35 | 23 | 82.29 | 37.50 | 20.00 | 30.00 | 73.33 | 53.33 | 59.00 | 32.00 | 31.201 |
| 36 | 22 | 89.29 | 37.50 | 20.00 | 30.00 | 73.33 | 40.00 | 61.00 | 32.00 | 33.418 |
| 37 | 37 | 82.29 | 12.50 | 30.00 | 30.00 | 73.33 | 53.33 | 61.00 | 32.00 | 32.441 |
| 38 | 2 | 89.29 | 12.50 | 30.00 | 30.00 | 73.33 | 40.00 | 59.00 | 32.00 | 34.734 |
| 39 | 64 | 82.29 | 37.50 | 30.00 | 30.00 | 73.33 | 40.00 | 59.00 | 48.00 | 33.361 |
| 40 | 32 | 89.29 | 37.50 | 30.00 | 30.00 | 73.33 | 53.33 | 61.00 | 48.00 | 34.369 |
| 41 | 18 | 82.29 | 12.50 | 20.00 | 36.67 | 73.33 | 40.00 | 59.00 | 32.00 | 30.460 |
| 42 | 27 | 89.29 | 12.50 | 20.00 | 36.67 | 73.33 | 53.33 | 61.00 | 32.00 | 32.961 |
| 43 | 35 | 82.29 | 37.50 | 20.00 | 36.67 | 73.33 | 53.33 | 61.00 | 48.00 | 33.102 |
| 44 | 1 | 89.29 | 37.50 | 20.00 | 36.67 | 73.33 | 40.00 | 59.00 | 48.00 | 32.509 |
| 45 | 68 | 82.29 | 12.50 | 30.00 | 36.67 | 73.33 | 53.33 | 59.00 | 48.00 | 32.706 |
| 46 | 4 | 89.29 | 12.50 | 30.00 | 36.67 | 73.33 | 40.00 | 61.00 | 48.00 | 31.152 |
| 47 | 42 | 82.29 | 37.50 | 30.00 | 36.67 | 73.33 | 40.00 | 61.00 | 32.00 | 37.865 |
| 48 | 63 | 89.29 | 37.50 | 30.00 | 36.67 | 73.33 | 53.33 | 59.00 | 32.00 | 33.364 |
| 49 | 56 | 82.29 | 12.50 | 20.00 | 30.00 | 75.56 | 40.00 | 61.00 | 32.00 | 31.829 |
| 50 | 20 | 89.29 | 12.50 | 20.00 | 30.00 | 75.56 | 53.33 | 59.00 | 32.00 | 33.752 |
| 51 | 39 | 82.29 | 37.50 | 20.00 | 30.00 | 75.56 | 53.33 | 59.00 | 48.00 | 31.485 |
| 52 | 10 | 89.29 | 37.50 | 20.00 | 30.00 | 75.56 | 40.00 | 61.00 | 48.00 | 31.758 |
| 53 | 59 | 82.29 | 12.50 | 30.00 | 30.00 | 75.56 | 53.33 | 61.00 | 48.00 | 27.809 |
| 54 | 33 | 89.29 | 12.50 | 30.00 | 30.00 | 75.56 | 40.00 | 59.00 | 48.00 | 29.166 |
| 55 | 65 | 82.29 | 37.50 | 30.00 | 30.00 | 75.56 | 40.00 | 59.00 | 32.00 | 30.370 |
| 56 | 6 | 89.29 | 37.50 | 30.00 | 30.00 | 75.56 | 53.33 | 61.00 | 32.00 | 31.593 |
| 57 | 13 | 82.29 | 12.50 | 20.00 | 36.67 | 75.56 | 40.00 | 59.00 | 48.00 | 34.464 |
| 58 | 21 | 89.29 | 12.50 | 20.00 | 36.67 | 75.56 | 53.33 | 61.00 | 48.00 | 34.153 |
| 59 | 36 | 82.29 | 37.50 | 20.00 | 36.67 | 75.56 | 53.33 | 61.00 | 32.00 | 33.613 |
| 60 | 17 | 89.29 | 37.50 | 20.00 | 36.67 | 75.56 | 40.00 | 59.00 | 32.00 | 33.057 |
| 61 | 51 | 82.29 | 12.50 | 30.00 | 36.67 | 75.56 | 53.33 | 59.00 | 32.00 | 27.516 |
| 62 | 69 | 89.29 | 12.50 | 30.00 | 36.67 | 75.56 | 40.00 | 61.00 | 32.00 | 31.959 |
| 63 | 62 | 82.29 | 37.50 | 30.00 | 36.67 | 75.56 | 40.00 | 61.00 | 48.00 | 31.489 |
| 64 | 31 | 89.29 | 37.50 | 30.00 | 36.67 | 75.56 | 53.33 | 59.00 | 48.00 | 32.938 |
| CP1 | 53 | 85.71 | 25.00 | 25.00 | 33.33 | 74.44 | 46.67 | 60.00 | 40.00 | 32.629 |
| CP2 | 50 | 85.71 | 25.00 | 25.00 | 33.33 | 74.44 | 46.67 | 60.00 | 40.00 | 33.386 |
| CP3 | 54 | 85.71 | 25.00 | 25.00 | 33.33 | 74.44 | 46.67 | 60.00 | 40.00 | 32.305 |
| CP4 | 24 | 85.71 | 25.00 | 25.00 | 33.33 | 74.44 | 46.67 | 60.00 | 40.00 | 31.930 |
| CP5 | 60 | 85.71 | 25.00 | 25.00 | 33.33 | 74.44 | 46.67 | 60.00 | 40.00 | 32.421 |

## 1.2 DOE2a - Four Main Residual Plots and Experimental Data Results
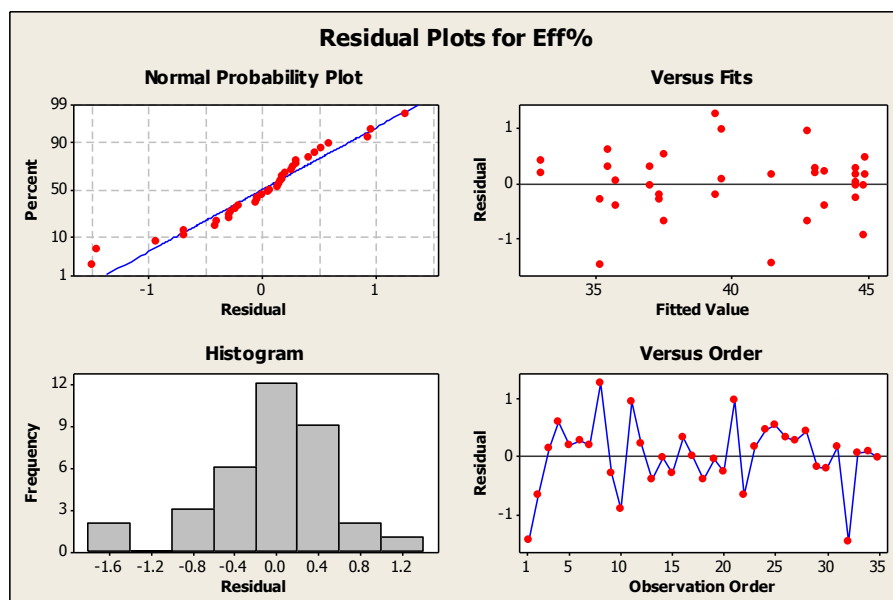


Residual Plots for Eff%

| Std Order (i) | Run Order (i) | Basic Design | | | | | Factor F=ABC | Factor G=ABD | Factor H=BCDE | Eff % |
|---|---|---|---|---|---|---|---|---|---|---|
| | | Factor A | Factor B | Factor C | Factor D | Factor E | | | | |
| 1 | 26 | 10.86 | 25.00 | 76.25 | 36.00 | 15.56 | 66.00 | 51.00 | 68.00 | 39.731 |
| 2 | 43 | 18.00 | 25.00 | 76.25 | 36.00 | 15.56 | 76.00 | 56.00 | 68.00 | 43.033 |
| 3 | 55 | 10.86 | 50.00 | 76.25 | 36.00 | 15.56 | 76.00 | 56.00 | 48.00 | 35.776 |
| 4 | 18 | 18.00 | 50.00 | 76.25 | 36.00 | 15.56 | 66.00 | 51.00 | 48.00 | 41.627 |
| 5 | 27 | 10.86 | 25.00 | 86.25 | 36.00 | 15.56 | 76.00 | 51.00 | 48.00 | 36.822 |
| 6 | 29 | 18.00 | 25.00 | 86.25 | 36.00 | 15.56 | 66.00 | 56.00 | 48.00 | 40.662 |
| 7 | 56 | 10.86 | 50.00 | 86.25 | 36.00 | 15.56 | 66.00 | 56.00 | 68.00 | 33.702 |
| 8 | 42 | 18.00 | 50.00 | 86.25 | 36.00 | 15.56 | 76.00 | 51.00 | 68.00 | 43.254 |
| 9 | 35 | 10.86 | 25.00 | 76.25 | 42.67 | 15.56 | 66.00 | 56.00 | 48.00 | 35.332 |
| 10 | 48 | 18.00 | 25.00 | 76.25 | 42.67 | 15.56 | 76.00 | 51.00 | 48.00 | 44.801 |
| 11 | 53 | 10.86 | 50.00 | 76.25 | 42.67 | 15.56 | 76.00 | 51.00 | 68.00 | 36.971 |
| 12 | 10 | 18.00 | 50.00 | 76.25 | 42.67 | 15.56 | 66.00 | 56.00 | 68.00 | 45.408 |
| 13 | 66 | 10.86 | 25.00 | 86.25 | 42.67 | 15.56 | 76.00 | 56.00 | 68.00 | 37.044 |
| 14 | 57 | 18.00 | 25.00 | 86.25 | 42.67 | 15.56 | 76.00 | 56.00 | 68.00 | 44.719 |
| 15 | 36 | 10.86 | 50.00 | 86.25 | 42.67 | 15.56 | 76.00 | 56.00 | 48.00 | 33.392 |
| 16 | 6 | 18.00 | 50.00 | 86.25 | 42.67 | 15.56 | 76.00 | 56.00 | 48.00 | 43.727 |
| 17 | 34 | 10.86 | 25.00 | 76.25 | 36.00 | 22.62 | 66.00 | 51.00 | 48.00 | 40.615 |
| 18 | 39 | 18.00 | 25.00 | 76.25 | 36.00 | 22.62 | 66.00 | 51.00 | 48.00 | 43.641 |
| 19 | 17 | 10.86 | 50.00 | 76.25 | 36.00 | 22.62 | 66.00 | 51.00 | 68.00 | 36.065 |
| 20 | 13 | 18.00 | 50.00 | 76.25 | 36.00 | 22.62 | 66.00 | 51.00 | 68.00 | 40.036 |
| 21 | 52 | 10.86 | 25.00 | 86.25 | 36.00 | 22.62 | 76.00 | 51.00 | 68.00 | 38.035 |
| 22 | 23 | 18.00 | 25.00 | 86.25 | 36.00 | 22.62 | 76.00 | 51.00 | 68.00 | 39.206 |
| 23 | 45 | 10.86 | 50.00 | 86.25 | 36.00 | 22.62 | 76.00 | 51.00 | 48.00 | 34.897 |
| 24 | 54 | 18.00 | 50.00 | 86.25 | 36.00 | 22.62 | 76.00 | 51.00 | 48.00 | 43.341 |
| 25 | 51 | 10.86 | 25.00 | 76.25 | 42.67 | 22.62 | 66.00 | 56.00 | 68.00 | 35.791 |
| 26 | 32 | 18.00 | 25.00 | 76.25 | 42.67 | 22.62 | 66.00 | 56.00 | 68.00 | 43.922 |
| 27 | 3 | 10.86 | 50.00 | 76.25 | 42.67 | 22.62 | 66.00 | 56.00 | 48.00 | 37.311 |
| 28 | 21 | 18.00 | 50.00 | 76.25 | 42.67 | 22.62 | 66.00 | 56.00 | 48.00 | 45.106 |
| 29 | 1 | 10.86 | 25.00 | 86.25 | 42.67 | 22.62 | 76.00 | 56.00 | 48.00 | 37.112 |
| 30 | 58 | 18.00 | 25.00 | 86.25 | 42.67 | 22.62 | 76.00 | 56.00 | 48.00 | 44.529 |
| 31 | 44 | 10.86 | 50.00 | 86.25 | 42.67 | 22.62 | 76.00 | 56.00 | 68.00 | 33.162 |
| 32 | 50 | 18.00 | 50.00 | 86.25 | 42.67 | 22.62 | 76.00 | 56.00 | 68.00 | 42.111 |

| | | | | | | | | | |
|---|---|---|---|---|---|---|---|---|---|
| 33 | 40 | 10.86 | 25.00 | 76.25 | 36.00 | 15.56 | 66.00 | 51.00 | 68.00 | 39.677 |
| 34 | 7 | 18.00 | 25.00 | 76.25 | 36.00 | 15.56 | 76.00 | 56.00 | 68.00 | 43.482 |
| 35 | 12 | 10.86 | 50.00 | 76.25 | 36.00 | 15.56 | 76.00 | 56.00 | 48.00 | 34.633 |
| 36 | 5 | 18.00 | 50.00 | 76.25 | 36.00 | 15.56 | 66.00 | 51.00 | 48.00 | 42.505 |
| 37 | 37 | 10.86 | 25.00 | 86.25 | 36.00 | 15.56 | 76.00 | 51.00 | 48.00 | 35.485 |
| 38 | 47 | 18.00 | 25.00 | 86.25 | 36.00 | 15.56 | 66.00 | 56.00 | 48.00 | 40.960 |
| 39 | 41 | 10.86 | 50.00 | 86.25 | 36.00 | 15.56 | 66.00 | 56.00 | 68.00 | 33.740 |
| 40 | 65 | 18.00 | 50.00 | 86.25 | 36.00 | 15.56 | 76.00 | 51.00 | 68.00 | 42.672 |
| 41 | 8 | 10.86 | 25.00 | 76.25 | 42.67 | 15.56 | 66.00 | 56.00 | 48.00 | 35.864 |
| 42 | 60 | 18.00 | 25.00 | 76.25 | 42.67 | 15.56 | 76.00 | 51.00 | 48.00 | 43.829 |
| 43 | 38 | 10.86 | 50.00 | 76.25 | 42.67 | 15.56 | 76.00 | 51.00 | 68.00 | 36.518 |
| 44 | 61 | 18.00 | 50.00 | 76.25 | 42.67 | 15.56 | 66.00 | 56.00 | 68.00 | 46.266 |
| 45 | 46 | 10.86 | 25.00 | 86.25 | 42.67 | 15.56 | 76.00 | 56.00 | 68.00 | 35.967 |
| 46 | 14 | 18.00 | 25.00 | 86.25 | 42.67 | 15.56 | 76.00 | 56.00 | 68.00 | 44.397 |
| 47 | 9 | 10.86 | 50.00 | 86.25 | 42.67 | 15.56 | 76.00 | 56.00 | 48.00 | 33.438 |
| 48 | 49 | 18.00 | 50.00 | 86.25 | 42.67 | 15.56 | 76.00 | 56.00 | 48.00 | 44.275 |
| 49 | 62 | 10.86 | 25.00 | 76.25 | 36.00 | 22.62 | 66.00 | 51.00 | 48.00 | 41.536 |
| 50 | 28 | 18.00 | 25.00 | 76.25 | 36.00 | 22.62 | 66.00 | 51.00 | 48.00 | 42.821 |
| 51 | 20 | 10.86 | 50.00 | 76.25 | 36.00 | 22.62 | 66.00 | 51.00 | 68.00 | 37.458 |
| 52 | 15 | 18.00 | 50.00 | 76.25 | 36.00 | 22.62 | 66.00 | 51.00 | 68.00 | 39.297 |
| 53 | 11 | 10.86 | 25.00 | 86.25 | 36.00 | 22.62 | 76.00 | 51.00 | 68.00 | 37.295 |
| 54 | 63 | 18.00 | 25.00 | 86.25 | 36.00 | 22.62 | 76.00 | 51.00 | 68.00 | 39.007 |
| 55 | 4 | 10.86 | 50.00 | 86.25 | 36.00 | 22.62 | 76.00 | 51.00 | 48.00 | 35.581 |
| 56 | 31 | 18.00 | 50.00 | 86.25 | 36.00 | 22.62 | 76.00 | 51.00 | 48.00 | 44.691 |
| 57 | 59 | 10.86 | 25.00 | 76.25 | 42.67 | 22.62 | 66.00 | 56.00 | 68.00 | 35.094 |
| 58 | 64 | 18.00 | 25.00 | 76.25 | 42.67 | 22.62 | 66.00 | 56.00 | 68.00 | 43.902 |
| 59 | 22 | 10.86 | 50.00 | 76.25 | 42.67 | 22.62 | 66.00 | 56.00 | 48.00 | 37.313 |
| 60 | 25 | 18.00 | 50.00 | 76.25 | 42.67 | 22.62 | 66.00 | 56.00 | 48.00 | 45.705 |
| 61 | 2 | 10.86 | 25.00 | 86.25 | 42.67 | 22.62 | 76.00 | 56.00 | 48.00 | 35.912 |
| 62 | 24 | 18.00 | 25.00 | 86.25 | 42.67 | 22.62 | 76.00 | 56.00 | 48.00 | 45.397 |
| 63 | 33 | 10.86 | 50.00 | 86.25 | 42.67 | 22.62 | 76.00 | 56.00 | 68.00 | 31.769 |
| 64 | 16 | 18.00 | 50.00 | 86.25 | 42.67 | 22.62 | 76.00 | 56.00 | 68.00 | 43.472 |
| CP-1 | 30 | 14.29 | 37.50 | 81.25 | 39.33 | 19.09 | 69.33 | 53.50 | 60.00 | 44.846 |
| CP-2 | 19 | 14.29 | 37.50 | 81.25 | 39.33 | 19.09 | 69.33 | 53.50 | 60.00 | 44.295 |
| CP-3 | 67 | 14.29 | 37.50 | 81.25 | 39.33 | 19.09 | 69.33 | 53.50 | 60.00 | 44.577 |

## 1.3 DOE3a - Four Main Residual Plots and Experimental Data Results
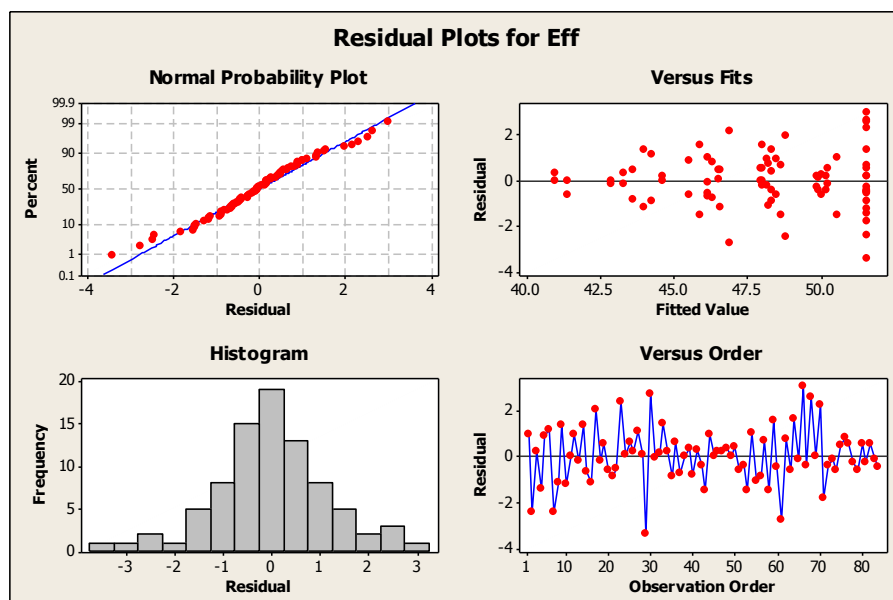


Residual Plots for Eff

| Std Order (i) | Run Order (i) | Basic Design | | | | | Factor F=ABC | Factor G=ABD | Factor H=BCDE | Response |
|---|---|---|---|---|---|---|---|---|---|---|
| | | Factor A | Factor B | Factor C | Factor D | Factor E | | | | Eff % |
| 1 | 62 | 17.14 | 25.00 | 80.75 | 38.27 | 13.39 | 59.33 | 46.00 | 72.00 | 47.585 |
| 2 | 53 | 25.71 | 25.00 | 80.75 | 38.27 | 13.39 | 86.00 | 66.00 | 72.00 | 48.559 |
| 3 | 42 | 17.14 | 50.00 | 80.75 | 38.27 | 13.39 | 86.00 | 66.00 | 56.00 | 47.822 |
| 4 | 82 | 25.71 | 50.00 | 80.75 | 38.27 | 13.39 | 59.33 | 46.00 | 56.00 | 47.186 |
| 5 | 75 | 17.14 | 25.00 | 88.25 | 38.27 | 13.39 | 86.00 | 46.00 | 56.00 | 48.821 |
| 6 | 63 | 25.71 | 25.00 | 88.25 | 38.27 | 13.39 | 59.33 | 66.00 | 56.00 | 49.992 |
| 7 | 49 | 17.14 | 50.00 | 88.25 | 38.27 | 13.39 | 59.33 | 66.00 | 72.00 | 49.670 |
| 8 | 3 | 25.71 | 50.00 | 88.25 | 38.27 | 13.39 | 86.00 | 46.00 | 72.00 | 49.917 |
| 9 | 79 | 17.14 | 25.00 | 80.75 | 48.27 | 13.39 | 59.33 | 66.00 | 56.00 | 41.845 |
| 10 | 39 | 25.71 | 25.00 | 80.75 | 48.27 | 13.39 | 86.00 | 46.00 | 56.00 | 45.249 |
| 11 | 56 | 17.14 | 50.00 | 80.75 | 48.27 | 13.39 | 86.00 | 46.00 | 72.00 | 43.919 |
| 12 | 54 | 25.71 | 50.00 | 80.75 | 48.27 | 13.39 | 59.33 | 66.00 | 72.00 | 47.792 |
| 13 | 13 | 17.14 | 25.00 | 88.25 | 48.27 | 13.39 | 86.00 | 66.00 | 72.00 | 45.859 |
| 14 | 41 | 25.71 | 25.00 | 88.25 | 48.27 | 13.39 | 59.33 | 46.00 | 72.00 | 50.833 |
| 15 | 5 | 17.14 | 50.00 | 88.25 | 48.27 | 13.39 | 59.33 | 46.00 | 56.00 | 43.614 |
| 16 | 55 | 25.71 | 50.00 | 88.25 | 48.27 | 13.39 | 86.00 | 66.00 | 56.00 | 47.504 |
| 17 | 16 | 17.14 | 25.00 | 80.75 | 38.27 | 21.72 | 59.33 | 46.00 | 56.00 | 47.298 |
| 18 | 64 | 25.71 | 25.00 | 80.75 | 38.27 | 21.72 | 86.00 | 66.00 | 56.00 | 47.471 |
| 19 | 20 | 17.14 | 50.00 | 80.75 | 38.27 | 21.72 | 86.00 | 66.00 | 72.00 | 48.529 |
| 20 | 80 | 25.71 | 50.00 | 80.75 | 38.27 | 21.72 | 59.33 | 46.00 | 72.00 | 48.417 |
| 21 | 59 | 17.14 | 25.00 | 88.25 | 38.27 | 21.72 | 86.00 | 46.00 | 72.00 | 49.106 |
| 22 | 67 | 25.71 | 25.00 | 88.25 | 38.27 | 21.72 | 59.33 | 66.00 | 72.00 | 49.525 |
| 23 | 70 | 17.14 | 50.00 | 88.25 | 38.27 | 21.72 | 59.33 | 66.00 | 56.00 | 48.017 |
| 24 | 2 | 25.71 | 50.00 | 88.25 | 38.27 | 21.72 | 86.00 | 46.00 | 56.00 | 48.998 |
| 25 | 77 | 17.14 | 25.00 | 80.75 | 48.27 | 21.72 | 59.33 | 66.00 | 72.00 | 45.925 |
| 26 | 74 | 25.71 | 25.00 | 80.75 | 48.27 | 21.72 | 86.00 | 46.00 | 72.00 | 48.396 |
| 27 | 48 | 17.14 | 50.00 | 80.75 | 48.27 | 21.72 | 86.00 | 46.00 | 56.00 | 42.290 |
| 28 | 65 | 25.71 | 50.00 | 80.75 | 48.27 | 21.72 | 59.33 | 66.00 | 56.00 | 46.762 |
| 29 | 34 | 17.14 | 25.00 | 88.25 | 48.27 | 21.72 | 86.00 | 66.00 | 56.00 | 43.747 |
| 30 | 24 | 25.71 | 25.00 | 88.25 | 48.27 | 21.72 | 59.33 | 46.00 | 56.00 | 48.041 |
| 31 | 21 | 17.14 | 50.00 | 88.25 | 48.27 | 21.72 | 59.33 | 46.00 | 72.00 | 46.326 |
| 32 | 46 | 25.71 | 50.00 | 88.25 | 48.27 | 21.72 | 86.00 | 66.00 | 72.00 | 51.314 |

154

| 33 | 43 | 17.14 | 25.00 | 80.75 | 38.27 | 13.39 | 59.33 | 46.00 | 72.00 | 49.068 |
|----|----|-------|-------|-------|-------|-------|-------|-------|-------|--------|
| 34 | 27 | 25.71 | 25.00 | 80.75 | 38.27 | 13.39 | 86.00 | 66.00 | 72.00 | 49.794 |
| 35 | 14 | 17.14 | 50.00 | 80.75 | 38.27 | 13.39 | 86.00 | 66.00 | 56.00 | 47.691 |
| 36 | 83 | 25.71 | 50.00 | 80.75 | 38.27 | 13.39 | 59.33 | 46.00 | 56.00 | 47.665 |
| 37 | 8 | 17.14 | 25.00 | 88.25 | 38.27 | 13.39 | 86.00 | 46.00 | 56.00 | 49.649 |
| 38 | 12 | 25.71 | 25.00 | 88.25 | 38.27 | 13.39 | 59.33 | 66.00 | 56.00 | 48.985 |
| 39 | 25 | 17.14 | 50.00 | 88.25 | 38.27 | 13.39 | 59.33 | 66.00 | 72.00 | 50.856 |
| 40 | 81 | 25.71 | 50.00 | 88.25 | 38.27 | 13.39 | 86.00 | 46.00 | 72.00 | 51.464 |
| 41 | 45 | 17.14 | 25.00 | 80.75 | 48.27 | 13.39 | 59.33 | 66.00 | 56.00 | 41.494 |
| 42 | 73 | 25.71 | 25.00 | 80.75 | 48.27 | 13.39 | 86.00 | 46.00 | 56.00 | 45.872 |
| 43 | 6 | 17.14 | 50.00 | 80.75 | 48.27 | 13.39 | 86.00 | 46.00 | 72.00 | 45.562 |
| 44 | 15 | 25.71 | 50.00 | 80.75 | 48.27 | 13.39 | 59.33 | 66.00 | 72.00 | 47.583 |
| 45 | 44 | 17.14 | 25.00 | 88.25 | 48.27 | 13.39 | 86.00 | 66.00 | 72.00 | 45.712 |
| 46 | 51 | 25.71 | 25.00 | 88.25 | 48.27 | 13.39 | 59.33 | 46.00 | 72.00 | 50.779 |
| 47 | 37 | 17.14 | 50.00 | 88.25 | 48.27 | 13.39 | 59.33 | 46.00 | 56.00 | 43.929 |
| 48 | 76 | 25.71 | 50.00 | 88.25 | 48.27 | 13.39 | 86.00 | 66.00 | 56.00 | 47.418 |
| 49 | 9 | 17.14 | 25.00 | 80.75 | 38.27 | 21.72 | 59.33 | 46.00 | 56.00 | 47.250 |
| 50 | 58 | 25.71 | 25.00 | 80.75 | 38.27 | 21.72 | 86.00 | 66.00 | 56.00 | 47.671 |
| 51 | 31 | 17.14 | 50.00 | 80.75 | 38.27 | 21.72 | 86.00 | 66.00 | 72.00 | 46.769 |
| 52 | 38 | 25.71 | 50.00 | 80.75 | 38.27 | 21.72 | 59.33 | 46.00 | 72.00 | 47.316 |
| 53 | 18 | 17.14 | 25.00 | 88.25 | 38.27 | 21.72 | 86.00 | 46.00 | 72.00 | 50.565 |
| 54 | 32 | 25.71 | 25.00 | 88.25 | 38.27 | 21.72 | 59.33 | 66.00 | 72.00 | 49.535 |
| 55 | 61 | 17.14 | 50.00 | 88.25 | 38.27 | 21.72 | 59.33 | 66.00 | 56.00 | 49.342 |
| 56 | 17 | 25.71 | 50.00 | 88.25 | 38.27 | 21.72 | 86.00 | 46.00 | 56.00 | 49.227 |
| 57 | 40 | 17.14 | 25.00 | 80.75 | 48.27 | 21.72 | 59.33 | 66.00 | 72.00 | 45.099 |
| 58 | 1 | 25.71 | 25.00 | 80.75 | 48.27 | 21.72 | 86.00 | 46.00 | 72.00 | 49.591 |
| 59 | 11 | 17.14 | 50.00 | 80.75 | 48.27 | 21.72 | 86.00 | 46.00 | 56.00 | 42.689 |
| 60 | 69 | 25.71 | 50.00 | 80.75 | 48.27 | 21.72 | 59.33 | 66.00 | 56.00 | 46.449 |
| 61 | 28 | 17.14 | 25.00 | 88.25 | 48.27 | 21.72 | 86.00 | 66.00 | 56.00 | 43.564 |
| 62 | 19 | 25.71 | 25.00 | 88.25 | 48.27 | 21.72 | 59.33 | 46.00 | 56.00 | 48.876 |
| 63 | 50 | 17.14 | 50.00 | 88.25 | 48.27 | 21.72 | 59.33 | 46.00 | 72.00 | 46.386 |
| 64 | 72 | 25.71 | 50.00 | 88.25 | 48.27 | 21.72 | 86.00 | 66.00 | 72.00 | 50.535 |
| CP-1 | 30 | 21.43 | 37.50 | 84.43 | 43.27 | 17.56 | 72.33 | 56.15 | 65.60 | 54.695 |
| CP-2 | 84 | 21.43 | 37.50 | 84.43 | 43.27 | 17.56 | 72.33 | 56.15 | 65.60 | 54.223 |
| CP-3 | 36 | 21.43 | 37.50 | 84.43 | 43.27 | 17.56 | 72.33 | 56.15 | 65.60 | 55.165 |

## 1.4 DOE3b - Experimental Data Results



Residual Plots for Eff
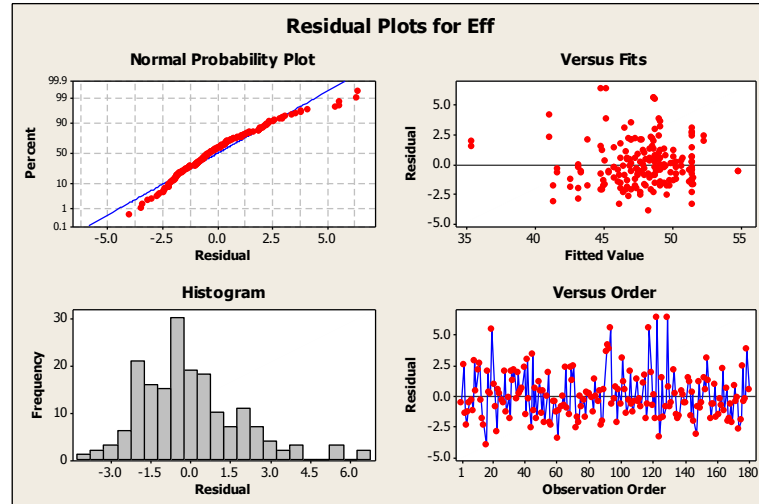
| Std Order (i) | Run Order (i) | Basic Design | | | | | Factor F=ABC | Factor G=ABD | Factor H=BCDE | Response y |
|---|---|---|---|---|---|---|---|---|---|---|
| | | Factor A | Factor B | Factor C | Factor D | Factor E | | | | Eff % |
| 1 | 99 | 17.14 | 25.00 | 80.75 | 38.27 | 13.39 | 59.33 | 66.00 | 72.00 | 49.321 |
| 2 | 82 | 25.71 | 25.00 | 80.75 | 38.27 | 13.39 | 59.33 | 46.00 | 56.00 | 49.118 |
| 3 | 37 | 17.14 | 50.00 | 80.75 | 38.27 | 13.39 | 59.33 | 46.00 | 56.00 | 47.908 |
| 4 | 95 | 25.71 | 50.00 | 80.75 | 38.27 | 13.39 | 59.33 | 66.00 | 72.00 | 50.124 |
| 5 | 135 | 17.14 | 25.00 | 88.25 | 38.27 | 13.39 | 59.33 | 46.00 | 72.00 | 47.700 |
| 6 | 41 | 25.71 | 25.00 | 88.25 | 38.27 | 13.39 | 59.33 | 66.00 | 56.00 | 47.871 |
| 7 | 87 | 17.14 | 50.00 | 88.25 | 38.27 | 13.39 | 59.33 | 66.00 | 56.00 | 47.363 |
| 8 | 7 | 25.71 | 50.00 | 88.25 | 38.27 | 13.39 | 59.33 | 46.00 | 72.00 | 50.031 |
| 9 | 57 | 17.14 | 25.00 | 80.75 | 48.27 | 13.39 | 59.33 | 46.00 | 72.00 | 44.091 |
| 10 | 3 | 25.71 | 25.00 | 80.75 | 48.27 | 13.39 | 59.33 | 66.00 | 56.00 | 43.566 |
| 11 | 147 | 17.14 | 50.00 | 80.75 | 48.27 | 13.39 | 59.33 | 66.00 | 56.00 | 38.261 |
| 12 | 38 | 25.71 | 50.00 | 80.75 | 48.27 | 13.39 | 59.33 | 46.00 | 72.00 | 47.166 |
| 13 | 64 | 17.14 | 25.00 | 88.25 | 48.27 | 13.39 | 59.33 | 66.00 | 72.00 | 47.908 |
| 14 | 53 | 25.71 | 25.00 | 88.25 | 48.27 | 13.39 | 59.33 | 46.00 | 56.00 | 44.484 |
| 15 | 110 | 17.14 | 50.00 | 88.25 | 48.27 | 13.39 | 59.33 | 46.00 | 56.00 | 47.151 |
| 16 | 79 | 25.71 | 50.00 | 88.25 | 48.27 | 13.39 | 59.33 | 66.00 | 72.00 | 51.997 |
| 17 | 61 | 17.14 | 25.00 | 80.75 | 38.27 | 21.72 | 59.33 | 66.00 | 56.00 | 42.827 |
| 18 | 10 | 25.71 | 25.00 | 80.75 | 38.27 | 21.72 | 59.33 | 46.00 | 72.00 | 48.857 |
| 19 | 156 | 17.14 | 50.00 | 80.75 | 38.27 | 21.72 | 59.33 | 46.00 | 72.00 | 45.536 |
| 20 | 50 | 25.71 | 50.00 | 80.75 | 38.27 | 21.72 | 59.33 | 66.00 | 56.00 | 48.469 |
| 21 | 171 | 17.14 | 25.00 | 88.25 | 38.27 | 21.72 | 59.33 | 46.00 | 56.00 | 48.369 |
| 22 | 138 | 25.71 | 25.00 | 88.25 | 38.27 | 21.72 | 59.33 | 66.00 | 72.00 | 49.506 |
| 23 | 17 | 17.14 | 50.00 | 88.25 | 38.27 | 21.72 | 59.33 | 66.00 | 72.00 | 49.084 |
| 24 | 170 | 25.71 | 50.00 | 88.25 | 38.27 | 21.72 | 59.33 | 46.00 | 56.00 | 46.354 |
| 25 | 54 | 17.14 | 25.00 | 80.75 | 48.27 | 21.72 | 59.33 | 46.00 | 56.00 | 43.227 |
| 26 | 74 | 25.71 | 25.00 | 80.75 | 48.27 | 21.72 | 59.33 | 66.00 | 72.00 | 44.866 |
| 27 | 14 | 17.14 | 50.00 | 80.75 | 48.27 | 21.72 | 59.33 | 66.00 | 72.00 | 42.008 |
| 28 | 107 | 25.71 | 50.00 | 80.75 | 48.27 | 21.72 | 59.33 | 46.00 | 56.00 | 42.694 |
| 29 | 27 | 17.14 | 25.00 | 88.25 | 48.27 | 21.72 | 59.33 | 66.00 | 56.00 | 44.776 |
| 30 | 122 | 25.71 | 25.00 | 88.25 | 48.27 | 21.72 | 59.33 | 46.00 | 72.00 | 47.770 |
| 31 | 125 | 17.14 | 50.00 | 88.25 | 48.27 | 21.72 | 59.33 | 46.00 | 72.00 | 47.425 |
| 32 | 160 | 25.71 | 50.00 | 88.25 | 48.27 | 21.72 | 59.33 | 66.00 | 56.00 | 46.286 |
| 33 | 28 | 17.14 | 25.00 | 80.75 | 38.27 | 13.39 | 86.00 | 66.00 | 56.00 | 49.871 |
| 34 | 60 | 25.71 | 25.00 | 80.75 | 38.27 | 13.39 | 86.00 | 46.00 | 72.00 | 49.037 |
| 35 | 103 | 17.14 | 50.00 | 80.75 | 38.27 | 13.39 | 86.00 | 46.00 | 72.00 | 49.364 |
| 36 | 166 | 25.71 | 50.00 | 80.75 | 38.27 | 13.39 | 86.00 | 66.00 | 56.00 | 51.779 |
| 37 | 111 | 17.14 | 25.00 | 88.25 | 38.27 | 13.39 | 86.00 | 46.00 | 56.00 | 47.062 |
| 38 | 140 | 25.71 | 25.00 | 88.25 | 38.27 | 13.39 | 86.00 | 66.00 | 72.00 | 51.792 |
| 39 | 148 | 17.14 | 50.00 | 88.25 | 38.27 | 13.39 | 86.00 | 66.00 | 72.00 | 47.910 |

156

| 40 | 25 | 25.71 | 50.00 | 88.25 | 38.27 | 13.39 | 86.00 | 46.00 | 56.00 | 49.063 |
|----|-----|-------|-------|-------|-------|-------|--------|-------|-------|--------|
| 41 | 168 | 17.14 | 25.00 | 80.75 | 48.27 | 13.39 | 86.00 | 46.00 | 56.00 | 40.719 |
| 42 | 150 | 25.71 | 25.00 | 80.75 | 48.27 | 13.39 | 86.00 | 66.00 | 72.00 | 47.772 |
| 43 | 78 | 17.14 | 50.00 | 80.75 | 48.27 | 13.39 | 86.00 | 66.00 | 72.00 | 43.385 |
| 44 | 89 | 25.71 | 50.00 | 80.75 | 48.27 | 13.39 | 86.00 | 46.00 | 56.00 | 41.156 |
| 45 | 102 | 17.14 | 25.00 | 88.25 | 48.27 | 13.39 | 86.00 | 66.00 | 56.00 | 46.169 |
| 46 | 130 | 25.71 | 25.00 | 88.25 | 48.27 | 13.39 | 86.00 | 46.00 | 72.00 | 51.328 |
| 47 | 105 | 17.14 | 50.00 | 88.25 | 48.27 | 13.39 | 86.00 | 46.00 | 72.00 | 48.438 |
| 48 | 128 | 25.71 | 50.00 | 88.25 | 48.27 | 13.39 | 86.00 | 66.00 | 56.00 | 47.089 |
| 49 | 175 | 17.14 | 25.00 | 80.75 | 38.27 | 21.72 | 86.00 | 66.00 | 72.00 | 44.810 |
| 50 | 22 | 25.71 | 25.00 | 80.75 | 38.27 | 21.72 | 86.00 | 46.00 | 56.00 | 47.449 |
| 51 | 144 | 17.14 | 50.00 | 80.75 | 38.27 | 21.72 | 86.00 | 46.00 | 56.00 | 44.606 |
| 52 | 29 | 25.71 | 50.00 | 80.75 | 38.27 | 21.72 | 86.00 | 66.00 | 72.00 | 48.534 |
| 53 | 133 | 17.14 | 25.00 | 88.25 | 38.27 | 21.72 | 86.00 | 46.00 | 72.00 | 49.529 |
| 54 | 100 | 25.71 | 25.00 | 88.25 | 38.27 | 21.72 | 86.00 | 66.00 | 56.00 | 49.203 |
| 55 | 164 | 17.14 | 50.00 | 88.25 | 38.27 | 21.72 | 86.00 | 66.00 | 56.00 | 49.087 |
| 56 | 35 | 25.71 | 50.00 | 88.25 | 38.27 | 21.72 | 86.00 | 46.00 | 72.00 | 49.240 |
| 57 | 163 | 17.14 | 25.00 | 80.75 | 48.27 | 21.72 | 86.00 | 46.00 | 72.00 | 44.083 |
| 58 | 46 | 25.71 | 25.00 | 80.75 | 48.27 | 21.72 | 86.00 | 66.00 | 56.00 | 44.603 |
| 59 | 109 | 17.14 | 50.00 | 80.75 | 48.27 | 21.72 | 86.00 | 66.00 | 56.00 | 41.242 |
| 60 | 115 | 25.71 | 50.00 | 80.75 | 48.27 | 21.72 | 86.00 | 46.00 | 72.00 | 47.964 |
| 61 | 72 | 17.14 | 25.00 | 88.25 | 48.27 | 21.72 | 86.00 | 66.00 | 72.00 | 45.074 |
| 62 | 63 | 25.71 | 25.00 | 88.25 | 48.27 | 21.72 | 86.00 | 46.00 | 56.00 | 46.579 |
| 63 | 86 | 17.14 | 50.00 | 88.25 | 48.27 | 21.72 | 86.00 | 46.00 | 56.00 | 45.683 |
| 64 | 8 | 25.71 | 50.00 | 88.25 | 48.27 | 21.72 | 86.00 | 66.00 | 72.00 | 50.384 |
| 65 | 126 | 9.43 | 37.50 | 84.43 | 43.27 | 17.56 | 72.33 | 56.15 | 65.60 | 36.935 |
| 66 | 92 | 33.43 | 37.50 | 84.43 | 43.27 | 17.56 | 72.33 | 56.15 | 65.60 | 45.216 |
| 67 | 20 | 21.43 | 0.00 | 84.43 | 43.27 | 17.56 | 72.33 | 56.15 | 65.60 | 52.306 |
| 68 | 145 | 21.43 | 75.00 | 84.43 | 43.27 | 17.56 | 72.33 | 56.15 | 65.60 | 46.727 |
| 69 | 93 | 21.43 | 37.50 | 74.03 | 43.27 | 17.56 | 72.33 | 56.15 | 65.60 | 47.115 |
| 70 | 149 | 21.43 | 37.50 | 95.25 | 43.27 | 17.56 | 72.33 | 56.15 | 65.60 | 49.302 |
| 71 | 141 | 21.43 | 37.50 | 84.43 | 29.13 | 17.56 | 72.33 | 56.15 | 65.60 | 52.272 |
| 72 | 94 | 21.43 | 37.50 | 84.43 | 57.40 | 17.56 | 72.33 | 56.15 | 65.60 | 52.258 |
| 73 | 67 | 21.43 | 37.50 | 84.43 | 43.27 | 5.78 | 72.33 | 56.15 | 65.60 | 43.610 |
| 74 | 152 | 21.43 | 37.50 | 84.43 | 43.27 | 29.33 | 72.33 | 56.15 | 65.60 | 44.338 |
| 75 | 33 | 21.43 | 37.50 | 84.43 | 43.27 | 17.56 | 35.53 | 56.15 | 65.60 | 47.934 |
| 76 | 154 | 21.43 | 37.50 | 84.43 | 43.27 | 17.56 | 111.00 | 56.15 | 65.60 | 50.342 |
| 77 | 142 | 21.43 | 37.50 | 84.43 | 43.27 | 17.56 | 72.33 | 27.45 | 65.60 | 48.109 |
| 78 | 176 | 21.43 | 37.50 | 84.43 | 43.27 | 17.56 | 72.33 | 84.00 | 65.60 | 49.495 |
| 79 | 11 | 21.43 | 37.50 | 84.43 | 43.27 | 17.56 | 72.33 | 56.15 | 38.40 | 47.114 |
| 80 | 119 | 21.43 | 37.50 | 84.43 | 43.27 | 17.56 | 72.33 | 56.15 | 83.60 | 52.275 |
| 81 | 15 | 21.43 | 37.50 | 84.43 | 43.27 | 17.56 | 72.33 | 56.15 | 65.60 | 53.343 |
| 82 | 178 | 21.43 | 37.50 | 84.43 | 43.27 | 17.56 | 72.33 | 56.15 | 65.60 | 56.665 |
| 83 | 124 | 21.43 | 37.50 | 84.43 | 43.27 | 17.56 | 72.33 | 56.15 | 65.60 | 54.803 |
| 84 | 151 | 21.43 | 37.50 | 84.43 | 43.27 | 17.56 | 72.33 | 56.15 | 65.60 | 55.409 |
| 85 | 62 | 21.43 | 37.50 | 84.43 | 43.27 | 17.56 | 72.33 | 56.15 | 65.60 | 54.348 |
| 86 | 84 | 21.43 | 37.50 | 84.43 | 43.27 | 17.56 | 72.33 | 56.15 | 65.60 | 54.958 |
| 87 | 51 | 21.43 | 37.50 | 84.43 | 43.27 | 17.56 | 72.33 | 56.15 | 65.60 | 54.481 |
| 88 | 2 | 21.43 | 37.50 | 84.43 | 43.27 | 17.56 | 72.33 | 56.15 | 65.60 | 54.141 |
| 89 | 19 | 21.43 | 37.50 | 84.43 | 43.27 | 17.56 | 72.33 | 56.15 | 65.60 | 54.844 |
| 90 | 13 | 21.43 | 37.50 | 84.43 | 43.27 | 17.56 | 72.33 | 56.15 | 65.60 | 55.886 |
| 91 | 137 | 17.14 | 25.00 | 80.75 | 38.27 | 13.39 | 59.33 | 66.00 | 72.00 | 47.140 |
| 92 | 49 | 25.71 | 25.00 | 80.75 | 38.27 | 13.39 | 59.33 | 46.00 | 56.00 | 52.352 |
| 93 | 106 | 17.14 | 50.00 | 80.75 | 38.27 | 13.39 | 59.33 | 46.00 | 56.00 | 49.708 |
| 94 | 153 | 25.71 | 50.00 | 80.75 | 38.27 | 13.39 | 59.33 | 66.00 | 72.00 | 51.320 |
| 95 | 90 | 17.14 | 25.00 | 88.25 | 38.27 | 13.39 | 59.33 | 46.00 | 72.00 | 49.708 |
| 96 | 75 | 25.71 | 25.00 | 88.25 | 38.27 | 13.39 | 59.33 | 66.00 | 56.00 | 49.424 |
| 97 | 43 | 17.14 | 50.00 | 88.25 | 38.27 | 13.39 | 59.33 | 66.00 | 56.00 | 46.731 |
| 98 | 120 | 25.71 | 50.00 | 88.25 | 38.27 | 13.39 | 59.33 | 46.00 | 72.00 | 49.578 |
| 99 | 162 | 17.14 | 25.00 | 80.75 | 48.27 | 13.39 | 59.33 | 46.00 | 72.00 | 46.268 |
| 100 | 136 | 25.71 | 25.00 | 80.75 | 48.27 | 13.39 | 59.33 | 66.00 | 56.00 | 43.118 |
| 101 | 31 | 17.14 | 50.00 | 80.75 | 48.27 | 13.39 | 59.33 | 66.00 | 56.00 | 39.514 |
| 102 | 108 | 25.71 | 50.00 | 80.75 | 48.27 | 13.39 | 59.33 | 46.00 | 72.00 | 45.445 |
| 103 | 143 | 17.14 | 25.00 | 88.25 | 48.27 | 13.39 | 59.33 | 66.00 | 72.00 | 49.072 |
| 104 | 114 | 25.71 | 25.00 | 88.25 | 48.27 | 13.39 | 59.33 | 46.00 | 56.00 | 47.741 |
| 105 | 112 | 17.14 | 50.00 | 88.25 | 48.27 | 13.39 | 59.33 | 46.00 | 56.00 | 45.530 |

| | | | | | | | | | | |
|---|---|---|---|---|---|---|---|---|---|---|
| 106 | 173 | 25.71 | 50.00 | 88.25 | 48.27 | 13.39 | 59.33 | 66.00 | 72.00 | 50.591 |
| 107 | 113 | 17.14 | 25.00 | 80.75 | 38.27 | 21.72 | 59.33 | 66.00 | 56.00 | 45.320 |
| 108 | 165 | 25.71 | 25.00 | 80.75 | 38.27 | 21.72 | 59.33 | 46.00 | 72.00 | 47.224 |
| 109 | 83 | 17.14 | 50.00 | 80.75 | 38.27 | 21.72 | 59.33 | 46.00 | 72.00 | 46.061 |
| 110 | 116 | 25.71 | 50.00 | 80.75 | 38.27 | 21.72 | 59.33 | 66.00 | 56.00 | 46.281 |
| 111 | 76 | 17.14 | 25.00 | 88.25 | 38.27 | 21.72 | 59.33 | 46.00 | 56.00 | 46.734 |
| 112 | 21 | 25.71 | 25.00 | 88.25 | 38.27 | 21.72 | 59.33 | 66.00 | 72.00 | 51.038 |
| 113 | 121 | 17.14 | 50.00 | 88.25 | 38.27 | 21.72 | 59.33 | 66.00 | 72.00 | 47.058 |
| 114 | 40 | 25.71 | 50.00 | 88.25 | 38.27 | 21.72 | 59.33 | 46.00 | 56.00 | 50.819 |
| 115 | 96 | 17.14 | 25.00 | 80.75 | 48.27 | 21.72 | 59.33 | 46.00 | 56.00 | 43.020 |
| 116 | 169 | 25.71 | 25.00 | 80.75 | 48.27 | 21.72 | 59.33 | 66.00 | 72.00 | 46.398 |
| 117 | 32 | 17.14 | 50.00 | 80.75 | 48.27 | 21.72 | 59.33 | 66.00 | 72.00 | 45.889 |
| 118 | 132 | 25.71 | 50.00 | 80.75 | 48.27 | 21.72 | 59.33 | 46.00 | 56.00 | 42.825 |
| 119 | 65 | 17.14 | 25.00 | 88.25 | 48.27 | 21.72 | 59.33 | 66.00 | 56.00 | 44.621 |
| 120 | 44 | 25.71 | 25.00 | 88.25 | 48.27 | 21.72 | 59.33 | 46.00 | 72.00 | 47.055 |
| 121 | 1 | 17.14 | 50.00 | 88.25 | 48.27 | 21.72 | 59.33 | 46.00 | 72.00 | 48.700 |
| 122 | 58 | 25.71 | 50.00 | 88.25 | 48.27 | 21.72 | 59.33 | 66.00 | 56.00 | 47.574 |
| 123 | 117 | 17.14 | 25.00 | 80.75 | 38.27 | 13.39 | 86.00 | 66.00 | 56.00 | 47.241 |
| 124 | 134 | 25.71 | 25.00 | 80.75 | 38.27 | 13.39 | 86.00 | 46.00 | 72.00 | 51.566 |
| 125 | 6 | 17.14 | 50.00 | 80.75 | 38.27 | 13.39 | 86.00 | 46.00 | 72.00 | 48.281 |
| 126 | 85 | 25.71 | 50.00 | 80.75 | 38.27 | 13.39 | 86.00 | 66.00 | 56.00 | 50.137 |
| 127 | 146 | 17.14 | 25.00 | 88.25 | 38.27 | 13.39 | 86.00 | 46.00 | 56.00 | 45.444 |
| 128 | 161 | 25.71 | 25.00 | 88.25 | 38.27 | 13.39 | 86.00 | 66.00 | 72.00 | 49.822 |
| 129 | 77 | 17.14 | 50.00 | 88.25 | 38.27 | 13.39 | 86.00 | 66.00 | 72.00 | 48.506 |
| 130 | 80 | 25.71 | 50.00 | 88.25 | 38.27 | 13.39 | 86.00 | 46.00 | 56.00 | 49.010 |
| 131 | 5 | 17.14 | 25.00 | 80.75 | 48.27 | 13.39 | 86.00 | 46.00 | 56.00 | 41.330 |
| 132 | 4 | 25.71 | 25.00 | 80.75 | 48.27 | 13.39 | 86.00 | 66.00 | 72.00 | 46.322 |
| 133 | 18 | 17.14 | 50.00 | 80.75 | 48.27 | 13.39 | 86.00 | 66.00 | 72.00 | 45.385 |
| 134 | 23 | 25.71 | 50.00 | 80.75 | 48.27 | 13.39 | 86.00 | 46.00 | 56.00 | 40.238 |
| 135 | 56 | 17.14 | 25.00 | 88.25 | 48.27 | 13.39 | 86.00 | 66.00 | 56.00 | 42.846 |
| 136 | 30 | 25.71 | 25.00 | 88.25 | 48.27 | 13.39 | 86.00 | 46.00 | 72.00 | 49.443 |
| 137 | 97 | 17.14 | 50.00 | 88.25 | 48.27 | 13.39 | 86.00 | 46.00 | 72.00 | 49.527 |
| 138 | 159 | 25.71 | 50.00 | 88.25 | 48.27 | 13.39 | 86.00 | 66.00 | 56.00 | 48.976 |
| 139 | 180 | 17.14 | 25.00 | 80.75 | 38.27 | 21.72 | 86.00 | 66.00 | 72.00 | 47.302 |
| 140 | 16 | 25.71 | 25.00 | 80.75 | 38.27 | 21.72 | 86.00 | 46.00 | 56.00 | 44.365 |
| 141 | 24 | 17.14 | 50.00 | 80.75 | 38.27 | 21.72 | 86.00 | 46.00 | 56.00 | 46.763 |
| 142 | 48 | 25.71 | 50.00 | 80.75 | 38.27 | 21.72 | 86.00 | 66.00 | 72.00 | 48.006 |
| 143 | 52 | 17.14 | 25.00 | 88.25 | 38.27 | 21.72 | 86.00 | 46.00 | 72.00 | 47.802 |
| 144 | 139 | 25.71 | 25.00 | 88.25 | 38.27 | 21.72 | 86.00 | 66.00 | 56.00 | 49.996 |
| 145 | 174 | 17.14 | 50.00 | 88.25 | 38.27 | 21.72 | 86.00 | 66.00 | 56.00 | 44.146 |
| 146 | 155 | 25.71 | 50.00 | 88.25 | 38.27 | 21.72 | 86.00 | 46.00 | 72.00 | 50.827 |
| 147 | 98 | 17.14 | 25.00 | 80.75 | 48.27 | 21.72 | 86.00 | 46.00 | 72.00 | 42.728 |
| 148 | 26 | 25.71 | 25.00 | 80.75 | 48.27 | 21.72 | 86.00 | 66.00 | 56.00 | 45.478 |
| 149 | 157 | 17.14 | 50.00 | 80.75 | 48.27 | 21.72 | 86.00 | 66.00 | 56.00 | 40.933 |
| 150 | 167 | 25.71 | 50.00 | 80.75 | 48.27 | 21.72 | 86.00 | 46.00 | 72.00 | 44.163 |
| 151 | 88 | 17.14 | 25.00 | 88.25 | 48.27 | 21.72 | 86.00 | 66.00 | 72.00 | 45.369 |
| 152 | 59 | 25.71 | 25.00 | 88.25 | 48.27 | 21.72 | 86.00 | 46.00 | 56.00 | 47.002 |
| 153 | 68 | 17.14 | 50.00 | 88.25 | 48.27 | 21.72 | 86.00 | 46.00 | 56.00 | 44.587 |
| 154 | 73 | 25.71 | 50.00 | 88.25 | 48.27 | 21.72 | 86.00 | 66.00 | 72.00 | 49.794 |
| 155 | 55 | 9.43 | 37.50 | 84.43 | 43.27 | 17.56 | 72.33 | 56.15 | 65.60 | 37.321 |
| 156 | 69 | 33.43 | 37.50 | 84.43 | 43.27 | 17.56 | 72.33 | 56.15 | 65.60 | 43.368 |
| 157 | 9 | 21.43 | 0.00 | 84.43 | 43.27 | 17.56 | 72.33 | 56.15 | 65.60 | 49.777 |
| 158 | 70 | 21.43 | 75.00 | 84.43 | 43.27 | 17.56 | 72.33 | 56.15 | 65.60 | 47.713 |
| 159 | 123 | 21.43 | 37.50 | 74.03 | 43.27 | 17.56 | 72.33 | 56.15 | 65.60 | 49.651 |
| 160 | 104 | 21.43 | 37.50 | 95.25 | 43.27 | 17.56 | 72.33 | 56.15 | 65.60 | 46.720 |
| 161 | 158 | 21.43 | 37.50 | 84.43 | 29.13 | 17.56 | 72.33 | 56.15 | 65.60 | 52.207 |
| 162 | 118 | 21.43 | 37.50 | 84.43 | 57.40 | 17.56 | 72.33 | 56.15 | 65.60 | 52.258 |
| 163 | 42 | 21.43 | 37.50 | 84.43 | 43.27 | 5.78 | 72.33 | 56.15 | 65.60 | 43.590 |
| 164 | 129 | 21.43 | 37.50 | 84.43 | 43.27 | 29.33 | 72.33 | 56.15 | 65.60 | 44.322 |
| 165 | 36 | 21.43 | 37.50 | 84.43 | 43.27 | 17.56 | 35.53 | 56.15 | 65.60 | 48.639 |
| 166 | 91 | 21.43 | 37.50 | 84.43 | 43.27 | 17.56 | 111.00 | 56.15 | 65.60 | 50.803 |
| 167 | 34 | 21.43 | 37.50 | 84.43 | 43.27 | 17.56 | 72.33 | 27.45 | 65.60 | 48.774 |
| 168 | 179 | 21.43 | 37.50 | 84.43 | 43.27 | 17.56 | 72.33 | 84.00 | 65.60 | 50.963 |
| 169 | 45 | 21.43 | 37.50 | 84.43 | 43.27 | 17.56 | 72.33 | 56.15 | 38.40 | 48.478 |
| 170 | 71 | 21.43 | 37.50 | 84.43 | 43.27 | 17.56 | 72.33 | 56.15 | 83.60 | 52.776 |
| 171 | 101 | 21.43 | 37.50 | 84.43 | 43.27 | 17.56 | 72.33 | 56.15 | 65.60 | 54.967 |

| 172 | 66 | 21.43 | 37.50 | 84.43 | 43.27 | 17.56 | 72.33 | 56.15 | 65.60 | 53.514 |
|-----|-----|-------|-------|-------|-------|-------|-------|-------|-------|--------|
| 173 | 177 | 21.43 | 37.50 | 84.43 | 43.27 | 17.56 | 72.33 | 56.15 | 65.60 | 53.880 |
| 174 | 131 | 21.43 | 37.50 | 84.43 | 43.27 | 17.56 | 72.33 | 56.15 | 65.60 | 56.133 |
| 175 | 127 | 21.43 | 37.50 | 84.43 | 43.27 | 17.56 | 72.33 | 56.15 | 65.60 | 54.954 |
| 176 | 47 | 21.43 | 37.50 | 84.43 | 43.27 | 17.56 | 72.33 | 56.15 | 65.60 | 54.399 |
| 177 | 81 | 21.43 | 37.50 | 84.43 | 43.27 | 17.56 | 72.33 | 56.15 | 65.60 | 56.531 |
| 178 | 12 | 21.43 | 37.50 | 84.43 | 43.27 | 17.56 | 72.33 | 56.15 | 65.60 | 55.695 |
| 179 | 172 | 21.43 | 37.50 | 84.43 | 43.27 | 17.56 | 72.33 | 56.15 | 65.60 | 56.223 |
| 180 | 39 | 21.43 | 37.50 | 84.43 | 43.27 | 17.56 | 72.33 | 56.15 | 65.60 | 55.165 |

## 1.5 DOE3b Maximizer Experimental Validation Trial

| Run # | Response |
|-------|----------|
| 1 | 56.693 |
| 2 | 55.876 |
| 3 | 54.467 |
| 4 | 54.120 |
| 5 | 56.804 |
| 6 | 54.592 |
| 7 | 55.223 |
| 8 | 54.939 |
| 9 | 56.005 |
| 10 | 55.289 |
| 11 | 55.241 |
| 12 | 54.172 |
| 13 | 55.747 |
| 14 | 54.072 |
| 15 | 56.407 |
| 16 | 55.102 |
| 17 | 55.055 |
| 18 | 54.570 |
| 19 | 56.483 |
| 20 | 53.578 |

## 1.6 ANN Experimental Data Set

| Std Order | Run Order | Factor A | Factor B | Factor C | Factor D | Factor E | Factor F | Factor G | Factor H | Eff % Rep 1 | Eff % Rep 2 |
|---|---|---|---|---|---|---|---|---|---|---|---|
| 1 | 17 | 2.78 | 62.50 | 70.00 | 46.67 | 55.56 | 86.67 | 50.00 | 80.00 | 25.485 | 24.295 |
| 2 | 25 | 2.78 | 75.00 | 82.50 | 6.67 | 27.78 | 80.00 | 70.00 | 56.00 | 32.420 | 31.793 |
| 3 | 32 | 2.78 | 25.00 | 77.50 | 66.67 | 44.44 | 80.00 | 75.00 | 64.00 | 34.650 | 36.035 |
| 4 | 14 | 2.78 | 25.00 | 82.50 | 6.67 | 16.67 | 46.67 | 55.00 | 52.00 | 39.190 | 39.937 |
| 5 | 22 | 2.78 | 12.50 | 87.50 | 46.67 | 44.44 | 80.00 | 75.00 | 72.00 | 36.620 | 38.083 |
| 6 | 44 | 2.78 | 37.50 | 77.50 | 86.67 | 38.89 | 80.00 | 75.00 | 40.00 | 33.540 | 32.874 |
| 7 | 47 | 2.78 | 75.00 | 100.00 | 80.00 | 55.56 | 46.67 | 45.00 | 76.00 | 30.795 | 31.948 |
| 8 | 34 | 16.67 | 37.50 | 100.00 | 33.33 | 50.00 | 73.33 | 70.00 | 84.00 | 44.173 | 43.736 |
| 9 | 38 | 16.67 | 12.50 | 100.00 | 66.67 | 14.44 | 73.33 | 65.00 | 40.00 | 44.834 | 44.873 |
| 10 | 36 | 16.67 | 50.00 | 97.50 | 60.00 | 20.56 | 53.33 | 65.00 | 76.00 | 39.754 | 39.211 |
| 11 | 35 | 16.67 | 75.00 | 95.00 | 20.00 | 14.44 | 60.00 | 60.00 | 52.00 | 53.890 | 54.676 |
| 12 | 10 | 16.67 | 25.00 | 77.50 | 53.33 | 47.78 | 46.67 | 60.00 | 48.00 | 48.946 | 48.176 |
| 13 | 8 | 16.67 | 12.50 | 92.50 | 60.00 | 41.11 | 60.00 | 55.00 | 80.00 | 52.768 | 52.189 |
| 14 | 31 | 16.67 | 25.00 | 67.50 | 40.00 | 41.11 | 73.33 | 70.00 | 76.00 | 50.484 | 51.654 |
| 15 | 9 | 30.56 | 87.50 | 80.00 | 73.33 | 20.00 | 46.67 | 70.00 | 80.00 | 41.511 | 40.649 |
| 16 | 13 | 30.56 | 75.00 | 100.00 | 40.00 | 47.78 | 86.67 | 60.00 | 40.00 | 50.870 | 50.401 |
| 17 | 16 | 30.56 | 37.50 | 77.50 | 46.67 | 47.78 | 66.67 | 60.00 | 68.00 | 49.419 | 49.164 |
| 18 | 26 | 30.56 | 87.50 | 65.00 | 26.67 | 14.44 | 73.33 | 75.00 | 88.00 | 46.376 | 45.185 |
| 19 | 29 | 30.56 | 25.00 | 67.50 | 26.67 | 14.44 | 46.67 | 75.00 | 72.00 | 47.116 | 48.354 |
| 20 | 15 | 30.56 | 50.00 | 97.50 | 46.67 | 22.22 | 53.33 | 45.00 | 68.00 | 48.130 | 47.891 |
| 21 | 49 | 30.56 | 37.50 | 65.00 | 6.67 | 20.00 | 73.33 | 60.00 | 48.00 | 48.290 | 49.214 |
| 22 | 40 | 44.44 | 50.00 | 92.50 | 53.33 | 17.78 | 73.33 | 50.00 | 68.00 | 35.569 | 36.437 |
| 23 | 28 | 44.44 | 12.50 | 90.00 | 40.00 | 37.22 | 60.00 | 45.00 | 80.00 | 42.617 | 44.067 |
| 24 | 12 | 44.44 | 75.00 | 77.50 | 46.67 | 42.78 | 73.33 | 45.00 | 56.00 | 43.451 | 43.862 |
| 25 | 23 | 44.44 | 62.50 | 75.00 | 20.00 | 11.11 | 53.33 | 50.00 | 80.00 | 34.702 | 35.924 |
| 26 | 41 | 44.44 | 37.50 | 97.50 | 13.33 | 42.78 | 66.67 | 50.00 | 80.00 | 48.400 | 47.169 |
| 27 | 11 | 44.44 | 37.50 | 87.50 | 73.33 | 37.22 | 46.67 | 55.00 | 52.00 | 40.476 | 39.275 |
| 28 | 48 | 44.44 | 87.50 | 67.50 | 80.00 | 20.56 | 60.00 | 45.00 | 68.00 | 34.344 | 35.320 |
| 29 | 3 | 58.33 | 25.00 | 92.50 | 80.00 | 26.11 | 86.67 | 75.00 | 80.00 | 37.630 | 36.908 |
| 30 | 46 | 58.33 | 62.50 | 67.50 | 80.00 | 47.78 | 46.67 | 60.00 | 88.00 | 36.039 | 34.883 |
| 31 | 30 | 58.33 | 25.00 | 72.50 | 60.00 | 55.56 | 80.00 | 50.00 | 60.00 | 41.980 | 41.536 |
| 32 | 33 | 58.33 | 50.00 | 87.50 | 53.33 | 21.67 | 86.67 | 45.00 | 72.00 | 35.730 | 34.807 |
| 33 | 5 | 58.33 | 87.50 | 77.50 | 6.67 | 35.56 | 53.33 | 70.00 | 56.00 | 40.650 | 40.900 |
| 34 | 43 | 58.33 | 75.00 | 75.00 | 86.67 | 21.67 | 80.00 | 70.00 | 84.00 | 31.931 | 31.772 |
| 35 | 39 | 58.33 | 37.50 | 80.00 | 53.33 | 47.78 | 86.67 | 75.00 | 52.00 | 42.983 | 42.011 |
| 36 | 24 | 72.22 | 12.50 | 67.50 | 40.00 | 33.33 | 60.00 | 60.00 | 72.00 | 30.180 | 30.006 |
| 37 | 6 | 72.22 | 50.00 | 72.50 | 46.67 | 38.89 | 60.00 | 50.00 | 44.00 | 28.190 | 27.286 |
| 38 | 27 | 72.22 | 12.50 | 100.00 | 26.67 | 27.78 | 80.00 | 60.00 | 60.00 | 38.010 | 38.028 |
| 39 | 20 | 72.22 | 25.00 | 97.50 | 60.00 | 38.89 | 86.67 | 45.00 | 40.00 | 36.760 | 37.807 |
| 40 | 19 | 72.22 | 87.50 | 77.50 | 33.33 | 27.78 | 86.67 | 75.00 | 52.00 | 31.630 | 30.641 |
| 41 | 2 | 72.22 | 62.50 | 87.50 | 53.33 | 22.22 | 86.67 | 60.00 | 76.00 | 33.501 | 34.372 |
| 42 | 1 | 72.22 | 12.50 | 80.00 | 6.67 | 50.00 | 46.67 | 65.00 | 84.00 | 40.560 | 41.429 |
| 43 | 45 | 86.11 | 37.50 | 62.50 | 40.00 | 30.56 | 86.67 | 50.00 | 80.00 | 31.084 | 32.053 |
| 44 | 42 | 86.11 | 25.00 | 70.00 | 26.67 | 30.56 | 46.67 | 60.00 | 48.00 | 32.886 | 34.196 |
| 45 | 4 | 86.11 | 62.50 | 67.50 | 80.00 | 51.67 | 86.67 | 65.00 | 60.00 | 29.764 | 29.264 |
| 46 | 21 | 86.11 | 50.00 | 80.00 | 40.00 | 51.67 | 73.33 | 70.00 | 64.00 | 33.166 | 33.568 |
| 47 | 7 | 86.11 | 12.50 | 100.00 | 6.67 | 40.00 | 66.67 | 55.00 | 84.00 | 39.016 | 39.167 |
| 48 | 18 | 86.11 | 87.50 | 87.50 | 6.67 | 21.67 | 46.67 | 60.00 | 48.00 | 39.036 | 39.773 |
| 49 | 37 | 86.11 | 75.00 | 82.50 | 66.67 | 21.67 | 73.33 | 65.00 | 64.00 | 26.388 | 26.054 |

## 1.7 ANN Maximum Database Validation Trial

| Run # | Response |
|-------|----------|
|       | Eff% |
| 1 | 51.154 |
| 2 | 51.950 |
| 3 | 53.340 |
| 4 | 53.105 |
| 5 | 51.615 |
| 6 | 51.789 |
| 7 | 53.391 |
| 8 | 53.611 |
| 9 | 51.974 |
| 10 | 50.924 |
| 11 | 53.459 |
| 12 | 52.571 |
| 13 | 53.085 |
| 14 | 52.906 |
| 15 | 50.828 |
| 16 | 52.238 |
| 17 | 52.575 |
| 18 | 51.100 |
| 19 | 53.600 |
| 20 | 51.007 |

## 1.8 PT4 and PT5 Experimental Trial Results

| Run # | PT4 Trials | PT5 Trials |
|---|---|---|
| 1 | 52.081 | 50.489 |
| 2 | 52.084 | 49.408 |
| 3 | 51.380 | 48.410 |
| 4 | 52.896 | 46.809 |
| 5 | 52.430 | 47.085 |
| 6 | 51.006 | 47.496 |
| 7 | 50.244 | 50.936 |
| 8 | 52.827 | 48.890 |
| 9 | 50.560 | 48.698 |
| 10 | 51.108 | 48.531 |
| 11 | 49.472 | 47.563 |
| 12 | 52.458 | 47.113 |
| 13 | 51.572 | 48.509 |
| 14 | 52.663 | 49.188 |
| 15 | 49.975 | 49.038 |
| 16 | 51.656 | 49.039 |
| 17 | 49.502 | 49.528 |
| 18 | 51.368 | 48.061 |
| 19 | 50.034 | 48.880 |
| 20 | 51.463 | 47.085 |

1.9 Research Software

1) *MATLAB* version R2012a [computer software]; The MathWorks Inc.: Natick, Massachusetts, 2003 with Neural Network Toolbox

MATLAB$^{®}$ is a high-level language and interactive environment for numerical computation, visualization, and programming.[138]   MATLAB software was used in this research to develop and train neural network models.

2) LINGO 14.0 - Optimization Modeling Software for Linear, Nonlinear, and Integer Programming

LINGO is a comprehensive tool designed to make building and solving Linear, Nonlinear, Quadratic, Quadratically Constrained, Second Order Cone, Stochastic**,** and Integer optimization models faster, easier and more efficient.  For this research the Lingo software was used to solve quadratic models.

## 1.10   SA1, DOE2b, and DOE3b Maximum Response Trial Results

| Trial # | SA1 | DOE2b | DOE3b |
|---|---|---|---|
| 1 | 54.053 | 56.143 | 56.143 |
| 2 | 53.942 | 56.427 | 56.065 |
| 3 | 54.054 | 55.843 | 55.614 |
| 4 | 54.644 | 55.358 | 54.946 |
| 5 | 53.949 | 54.423 | 54.447 |
| 6 | 54.041 | 54.731 | 54.206 |
| 7 | 53.556 | 55.183 | 53.438 |
| 8 | 52.678 | 54.774 | 52.576 |
| 9 | 51.886 | 55.446 | 52.963 |
| 10 | 51.816 | 54.894 | 52.951 |
| 11 | 52.655 | 54.995 | 53.684 |
| 12 | 53.270 | 54.949 | 52.705 |
| 13 | 52.381 | 54.277 | 53.433 |
| 14 | 52.519 | 53.487 | 54.395 |
| 15 | 52.555 | 52.897 | 55.304 |
| 16 | 52.903 | 52.912 | 55.229 |
| 17 | 53.825 | 53.899 | 55.602 |
| 18 | 53.149 | 54.419 | 54.363 |
| 19 | 54.313 | 54.685 | 55.206 |
| 20 | 52.216 | 55.122 | 53.438 |

## 1.11 Normed Distance Calculation Example

Table 67 shows the ranges of the experimental region variable values and two points within the experimental region. The variable values are normalized based on the variable ranges. The normalized calculations are shown in the table.

Table 67: Normed Distance Calculation

| Experimental Region | | | | DOE3b Maximizer | | ANN Max Point | |
|---|---|---|---|---|---|---|---|
| Uncoded | | Normed | | Uncoded | Normed | Uncoded | Normed |
| Min Datum | Max Value | Min Datum | Max Value | Value | Value | Value | Value |
| 2.38 | 73.81 | 0 | 1 | 21.43 | 0.267 | 14.29 | 0.167 |
| 46.88 | 93.75 | 0 | 1 | 64.06 | 0.4 | 84.38 | 0.833 |
| 28.57 | 100 | 0 | 1 | 88.81 | 0.843 | 95.24 | 0.933 |
| 6.67 | 86.67 | 0 | 1 | 48.27 | 0.52 | 20 | 0.167 |
| 7.5 | 67 | 0 | 1 | 20.8 | 0.224 | 13 | 0.092 |
| 46.67 | 86.67 | 0 | 1 | 69.33 | 0.567 | 60 | 0.333 |
| 45 | 75 | 0 | 1 | 66 | 0.7 | 60 | 0.5 |
| 33.33 | 73.33 | 0 | 1 | 60 | 0.667 | 43.33 | 0.25 |

The normed distance from the DOE3b Maximizer to the ANN Maximum point was calculated using the following distance formula.

$$d(\mathbf{q}, \mathbf{p}) = \sqrt{(q_1 - p_1)^2 + (q_2 - p_2)^2 + \cdots + (q_n - p_n)^2} = \sqrt{\sum_{i=1}^{n} (q_i - p_i)^2}.$$

The normed distance equation from the DOE3b Maximizer to the ANN Maximum point would be as follows:

$$d1 = \sqrt{(.267 - .167)^2 + (.4 - .833)^2 + (.843 - .933)^2 + (.52 - .167)^2 + (.224 - .092)^2 + (.567 - .333)^2 + (.7 - .5)^2 + (.667 - .25)^2}$$

$$d1 = 0.785$$

## 1.12 Standard Deviation Equality Hypothesis Test

A paired comparison using the standard deviations of twelve different populations was evaluated to determine if the pooled standard deviation could be used to improve the precision or estimate of variability.   Eight of the twelve populations are shown in Table 68 and four of the twelve populations are shown in Table 69.  The significant outliers were evaluated from the data sets by using the Grubbs' Test (Grubbs 1969 and Stefansky 1972) or Extreme Studentized Deviate (ESD).  The Grubbs' test is used to detect outliers in a data set. It is based on the assumption of normality.  Grubbs' test detects one outlier at a time. This outlier is removed from the dataset and the test is iterated until no outliers are detected.  The following figure shows the definition of the Grubbs' Test.

| | Grubbs' test is also known as the maximum normed residual test. |
|---|---|
| *Definition* | Grubbs' test is defined for the hypothesis: |
| | $H_0$:  There are no outliers in the data set |
| | $H_a$:  There is exactly one outlier in the data set |
| | Test Statistic: The Grubbs' test statistic is defined as: |
| | $$G = \frac{\max |Y_i - \bar{Y}|}{s}$$ |
| | with $\bar{Y}$ and $s$ denoting the sample mean and standard deviation, respectively. The Grubbs' test statistic is the largest absolute deviation from the sample mean in units of the sample standard deviation. |

Figure 51: Grubbs' Test Hypothesis (Quoted from the Engineering and Statistics Handbook, paragraph 1.3.5.17)

An alpha value of 0.05 was used as the significant outlier criteria for the Grubb's test.  Based on the Grubbs' Test, none of the values were eliminated from the eight data sets in Table 68.

Table 68: Experimental Trial Response Data

| Trial # | DOE3b Center Pt | DOE3b Maximizer | ANN DB Maximum | SA1 Maximizer | DOE2b Maximizer | DOE3b Maximizer | PT4 | PT5 |
|---|---|---|---|---|---|---|---|---|
| 1 | 54.967 | 56.693 | 51.154 | 54.053 | 56.143 | 56.143 | 52.081 | 50.489 |
| 2 | 53.514 | 55.876 | 51.950 | 53.942 | 56.427 | 56.065 | 52.084 | 49.408 |
| 3 | 53.880 | 54.467 | 53.340 | 54.054 | 55.843 | 55.614 | 51.380 | 48.410 |
| 4 | 56.133 | 54.120 | 53.105 | 54.644 | 55.358 | 54.946 | 52.896 | 46.809 |
| 5 | 54.954 | 56.804 | 51.615 | 53.949 | 54.423 | 54.447 | 52.430 | 47.085 |
| 6 | 54.399 | 54.592 | 51.789 | 54.041 | 54.731 | 54.206 | 51.006 | 47.496 |
| 7 | 56.531 | 55.223 | 53.391 | 53.556 | 55.183 | 53.438 | 50.244 | 50.936 |
| 8 | 55.695 | 54.939 | 53.611 | 52.678 | 54.774 | 52.576 | 52.827 | 48.890 |
| 9 | 56.223 | 56.005 | 51.974 | 51.886 | 55.446 | 52.963 | 50.560 | 48.698 |
| 10 | 55.165 | 55.289 | 50.924 | 51.816 | 54.894 | 52.951 | 51.108 | 48.531 |
| 11 | 53.343 | 55.241 | 53.459 | 52.655 | 54.995 | 53.684 | 49.472 | 47.563 |
| 12 | 56.665 | 54.172 | 52.571 | 53.270 | 54.949 | 52.705 | 52.458 | 47.113 |
| 13 | 54.803 | 55.747 | 53.085 | 52.381 | 54.277 | 53.433 | 51.572 | 48.509 |
| 14 | 55.409 | 54.072 | 52.906 | 52.519 | 53.487 | 54.395 | 52.663 | 49.188 |
| 15 | 54.348 | 56.407 | 50.828 | 52.555 | 52.897 | 55.304 | 49.975 | 49.038 |
| 16 | 54.958 | 55.102 | 52.238 | 52.903 | 52.912 | 55.229 | 51.656 | 49.039 |
| 17 | 54.481 | 55.055 | 52.575 | 53.825 | 53.899 | 55.602 | 49.502 | 49.528 |
| 18 | 54.141 | 54.570 | 51.100 | 53.149 | 54.419 | 54.363 | 51.368 | 48.061 |
| 19 | 54.844 | 56.483 | 53.600 | 54.313 | 54.685 | 55.206 | 50.034 | 48.880 |
| 20 | 55.886 | 53.578 | 51.007 | 52.216 | 55.122 | 53.438 | 51.463 | 47.085 |
| Average | 55.017 | 55.222 | 52.311 | 53.220 | 54.743 | 54.335 | 51.339 | 48.538 |
| N | 20 | 20 | 20 | 20 | 20 | 20 | 20 | 20 |
| Std Dev | $\sigma_1$ | $\sigma_2$ | $\sigma_3$ | $\sigma_4$ | $\sigma_5$ | $\sigma_6$ | $\sigma_7$ | $\sigma_8$ |
| Std Dev | 0.9576 | 0.9414 | 0.9801 | 0.8564 | 0.9410 | 1.1425 | 1.0884 | 1.1241 |

Table 69: Design of Experimental Data

|  | DOE1a | DOE2a | DOE3a | DOE3b |
|---|---|---|---|---|
| Average | 32.534 | 44.573 | 54.694 | 55.016 |
| Std Dev | $\sigma_9$ | $\sigma_{10}$ | $\sigma_{11}$ | $\sigma_{12}$ |
| Std Dev (RMSE) | 0.815 | 0.761 | 0.72 | 1.04 |
| N | 69 | 67 | 67 | 180 |

Although there are different types of paired comparison test that could be used to test if the standard deviations of the eight populations from Table 68 and the four populations from Table 69 were equal, the paired F-test was selected as an adequate choice for this study. The F-test (Snedecor and Cochran, 1983) was used to test if the

variances of two populations are equal. This test can be a two-tailed test or a one-tailed

test. The two-tailed pairwise F-test was selected in this case to accept or reject the

following hypothesis test.

$$H_o: \sigma_1 = \sigma_2 = \sigma_3 = \sigma_4 = \sigma_5 = \sigma_6 = \sigma_7 = \sigma_8 = \sigma_9 = \sigma_{10} = \sigma_{11} = \sigma_{12}$$
$$H_a: \sigma_1 \neq \sigma_2 \neq \sigma_3 \neq \sigma_4 \neq \sigma_5 \neq \sigma_6 \neq \sigma_7 \neq \sigma_8 \neq \sigma_9 \neq \sigma_{10} \neq \sigma_{11} \neq \sigma_{12}$$

Test Statistic: $\qquad F = \dfrac{\sigma_i^2}{\sigma_j^2}$

where i and j represent the sixty-six pairwise combinations for the twelve

standard deviations.

The two-tailed hypothesis is rejected if

$$F < F_{(1-\alpha/2,N_1-1,N_2-1)}$$

or

$$F > F_{(\alpha/2,N_1-1,N_2-1)}$$

where $F_{(\alpha,N_1-1,N_2-1)}$ is the critical value of the F distribution with

$N_1 - 1$ and $N_2 - 1$ equal to the degrees of freedom and $\alpha$ equal to the

significance level.

The following example shows the calculations used for one pair of standard

deviation combinations from Table 69.

Example (1): Test Statistic is $F_{1/9} = \dfrac{\sigma_1^2}{\sigma_9^2} = \dfrac{0.9576^2}{0.815^2} = 1.381$

Given (from Table 69): $N_1 = 20, N_9 = 37, df_1 = N_1 - 1 = 19, df_2 = N_2 - 1 = 36, \alpha = 0.05$

The critical value of

$$F_{(1-\alpha/2,N_1-1,N_2-1)} = F_{(.975,19,36)} = 0.40$$

$$F_{(\alpha/2,N_1-1,N_2-1)} = F_{(.025,19,36)} = 2.53$$

Rejection Region:  Reject $H_o$ if F < 2.53 or F > 0.40

The F test indicates there is insufficient statistical evidence to reject the null hypothesis that the two standard deviations are equal at the 0.05 significance level.

The following second example shows the inverse calculations used for the first pair of standard deviation combinations in from Table 69.

Example (2):  Test Statistic is $F_{9/1} = \dfrac{\sigma_9^2}{\sigma_1^2} = \dfrac{0.8150^2}{0.9576^2} = 0.724$

Given (from Table 69): $N_1 = 37, N_2 = 20, df_1 = N_1 - 1 = 36, df_2 = N_2 - 1 = 19, \alpha = 0.05$

The critical value of

$$F_{(1-\alpha/2,N_1-1,N_2-1)} = F_{(.975,36,19)} = 0.47$$

$$F_{(\alpha/2,N_1-1,N_2-1)} = F_{(.025,36,19)} = 2.35$$

Rejection Region:  Reject $H_o$ if F < 2.35 or F > 0.47

The F test indicates there is not enough evidence to reject the null hypothesis that the two standard deviations are equal at the 0.05 significance level.

Using the standard deviations from Table 68 and Table 69, sixty-six pairwise combinations along with the inverse of the pairwise combination were evaluated for the F-test hypothesis.  The results of this evaluation are shown in the following table.

## Table 70: Paired Combination Hypothesis Test

| Pair # | StdDev (1) | StdDev (2) | DOF (1) | DOF (2) | Ratio (1/2) | F Statistic | F – Value (0.025,1,2) | F – Value (0.975,1,2) | Ratio (2) | F Statistic | F – Value (0.025,2,1) | F – Value (0.975,2,1) | Hypothesis Test |
|---|---|---|---|---|---|---|---|---|---|---|---|---|---|
| 1 | σ1 | σ2 | 19 | 19 | σ1/σ2 | 1.035 | 0.4 | 2.53 | σ2/σ1 | 0.967 | 0.40 | 2.53 | Fail To Reject Ho |
| 2 | σ1 | σ3 | 19 | 19 | σ1/σ3 | 0.955 | 0.4 | 2.53 | σ3/σ1 | 1.048 | 0.40 | 2.53 | Fail To Reject Ho |
| 3 | σ1 | σ4 | 19 | 19 | σ1/σ4 | 1.25 | 0.4 | 2.53 | σ4/σ1 | 0.800 | 0.40 | 2.53 | Fail To Reject Ho |
| 4 | σ1 | σ5 | 19 | 19 | σ1/σ5 | 1.036 | 0.4 | 2.53 | σ5/σ1 | 0.966 | 0.40 | 2.53 | Fail To Reject Ho |
| 5 | σ1 | σ6 | 19 | 19 | σ1/σ6 | 0.702 | 0.4 | 2.53 | σ6/σ1 | 1.424 | 0.40 | 2.53 | Fail To Reject Ho |
| 6 | σ1 | σ7 | 19 | 19 | σ1/σ7 | 0.774 | 0.4 | 2.53 | σ7/σ1 | 1.292 | 0.40 | 2.53 | Fail To Reject Ho |
| 7 | σ1 | σ8 | 19 | 19 | σ1/σ8 | 0.726 | 0.4 | 2.53 | σ8/σ1 | 1.378 | 0.40 | 2.53 | Fail To Reject Ho |
| 8 | σ1 | σ9 | 19 | 36 | σ1/σ9 | 1.381 | 0.42 | 2.13 | σ9/σ1 | 0.724 | 0.47 | 2.35 | Fail To Reject Ho |
| 9 | σ1 | σ10 | 19 | 36 | σ1/σ10 | 1.583 | 0.42 | 2.13 | σ10/σ1 | 0.632 | 0.47 | 2.35 | Fail To Reject Ho |
| 10 | σ1 | σ11 | 19 | 32 | σ1/σ11 | 1.769 | 0.42 | 2.13 | σ11/σ1 | 0.565 | 0.46 | 2.38 | Fail To Reject Ho |
| 11 | σ1 | σ12 | 19 | 99 | σ1/σ12 | 0.848 | 0.45 | 1.87 | σ12/σ1 | 1.180 | 0.53 | 2.22 | Fail To Reject Ho |
| 12 | σ2 | σ3 | 19 | 19 | σ2/σ3 | 0.923 | 0.4 | 2.53 | σ3/σ2 | 1.084 | 0.40 | 2.53 | Fail To Reject Ho |
| 13 | σ2 | σ4 | 19 | 19 | σ2/σ4 | 1.208 | 0.4 | 2.53 | σ4/σ2 | 0.828 | 0.40 | 2.53 | Fail To Reject Ho |
| 14 | σ2 | σ5 | 19 | 19 | σ2/σ5 | 1.001 | 0.4 | 2.53 | σ5/σ2 | 0.999 | 0.40 | 2.53 | Fail To Reject Ho |
| 15 | σ2 | σ6 | 19 | 19 | σ2/σ6 | 0.679 | 0.4 | 2.53 | σ6/σ2 | 1.473 | 0.40 | 2.53 | Fail To Reject Ho |
| 16 | σ2 | σ7 | 19 | 19 | σ2/σ7 | 0.748 | 0.4 | 2.53 | σ7/σ2 | 1.337 | 0.40 | 2.53 | Fail To Reject Ho |
| 17 | σ2 | σ8 | 19 | 19 | σ2/σ8 | 0.701 | 0.4 | 2.53 | σ8/σ2 | 1.426 | 0.40 | 2.53 | Fail To Reject Ho |
| 18 | σ2 | σ9 | 19 | 36 | σ2/σ9 | 1.334 | 0.42 | 2.13 | σ9/σ2 | 0.749 | 0.47 | 2.35 | Fail To Reject Ho |
| 19 | σ2 | σ10 | 19 | 36 | σ2/σ10 | 1.53 | 0.42 | 2.13 | σ10/σ2 | 0.653 | 0.47 | 2.35 | Fail To Reject Ho |
| 20 | σ2 | σ11 | 19 | 32 | σ2/σ11 | 1.71 | 0.42 | 2.13 | σ11/σ2 | 0.585 | 0.46 | 2.38 | Fail To Reject Ho |
| 21 | σ2 | σ12 | 19 | 99 | σ2/σ12 | 0.819 | 0.45 | 1.87 | σ12/σ2 | 1.220 | 0.53 | 2.22 | Fail To Reject Ho |
| 22 | σ3 | σ4 | 19 | 19 | σ3/σ4 | 1.31 | 0.4 | 2.53 | σ4/σ3 | 0.764 | 0.40 | 2.53 | Fail To Reject Ho |
| 23 | σ3 | σ5 | 19 | 19 | σ3/σ5 | 1.085 | 0.4 | 2.53 | σ5/σ3 | 0.922 | 0.40 | 2.53 | Fail To Reject Ho |
| 24 | σ3 | σ6 | 19 | 19 | σ3/σ6 | 0.736 | 0.4 | 2.53 | σ6/σ3 | 1.359 | 0.40 | 2.53 | Fail To Reject Ho |
| 25 | σ3 | σ7 | 19 | 19 | σ3/σ7 | 0.811 | 0.4 | 2.53 | σ7/σ3 | 1.233 | 0.40 | 2.53 | Fail To Reject Ho |
| 26 | σ3 | σ8 | 19 | 19 | σ3/σ8 | 0.76 | 0.4 | 2.53 | σ8/σ3 | 1.315 | 0.40 | 2.53 | Fail To Reject Ho |
| 27 | σ3 | σ9 | 19 | 36 | σ3/σ9 | 1.446 | 0.42 | 2.13 | σ9/σ3 | 0.692 | 0.47 | 2.35 | Fail To Reject Ho |
| 28 | σ3 | σ10 | 19 | 36 | σ3/σ10 | 1.659 | 0.42 | 2.13 | σ10/σ3 | 0.603 | 0.47 | 2.35 | Fail To Reject Ho |
| 29 | σ3 | σ11 | 19 | 32 | σ3/σ11 | 1.853 | 0.42 | 2.13 | σ11/σ3 | 0.540 | 0.46 | 2.38 | Fail To Reject Ho |
| 30 | σ3 | σ12 | 19 | 99 | σ3/σ12 | 0.888 | 0.45 | 1.87 | σ12/σ3 | 1.126 | 0.53 | 2.22 | Fail To Reject Ho |
| 31 | σ4 | σ5 | 19 | 19 | σ4/σ5 | 0.828 | 0.4 | 2.53 | σ5/σ4 | 1.207 | 0.40 | 2.53 | Fail To Reject Ho |
| 32 | σ4 | σ6 | 19 | 19 | σ4/σ6 | 0.562 | 0.4 | 2.53 | σ6/σ4 | 1.780 | 0.40 | 2.53 | Fail To Reject Ho |
| 33 | σ4 | σ7 | 19 | 19 | σ4/σ7 | 0.619 | 0.4 | 2.53 | σ7/σ4 | 1.615 | 0.40 | 2.53 | Fail To Reject Ho |
| 34 | σ4 | σ8 | 19 | 19 | σ4/σ8 | 0.58 | 0.4 | 2.53 | σ8/σ4 | 1.723 | 0.40 | 2.53 | Fail To Reject Ho |
| 35 | σ4 | σ9 | 19 | 36 | σ4/σ9 | 1.104 | 0.42 | 2.13 | σ9/σ4 | 0.906 | 0.47 | 2.35 | Fail To Reject Ho |
| 36 | σ4 | σ10 | 19 | 36 | σ4/σ10 | 1.266 | 0.42 | 2.13 | σ10/σ4 | 0.790 | 0.47 | 2.35 | Fail To Reject Ho |
| 37 | σ4 | σ11 | 19 | 32 | σ4/σ11 | 1.415 | 0.42 | 2.13 | σ11/σ4 | 0.707 | 0.46 | 2.38 | Fail To Reject Ho |
| 38 | σ4 | σ12 | 19 | 99 | σ4/σ12 | 0.678 | 0.45 | 1.87 | σ12/σ4 | 1.475 | 0.53 | 2.22 | Fail To Reject Ho |
| 39 | σ5 | σ6 | 19 | 19 | σ5/σ6 | 0.678 | 0.4 | 2.53 | σ6/σ5 | 1.474 | 0.40 | 2.53 | Fail To Reject Ho |
| 40 | σ5 | σ7 | 19 | 19 | σ5/σ7 | 0.748 | 0.4 | 2.53 | σ7/σ5 | 1.338 | 0.40 | 2.53 | Fail To Reject Ho |
| 41 | σ5 | σ8 | 19 | 19 | σ5/σ8 | 0.701 | 0.4 | 2.53 | σ8/σ5 | 1.427 | 0.40 | 2.53 | Fail To Reject Ho |
| 42 | σ5 | σ9 | 19 | 36 | σ5/σ9 | 1.333 | 0.42 | 2.13 | σ9/σ5 | 0.750 | 0.47 | 2.35 | Fail To Reject Ho |
| 43 | σ5 | σ10 | 19 | 36 | σ5/σ10 | 1.529 | 0.42 | 2.13 | σ10/σ5 | 0.654 | 0.47 | 2.35 | Fail To Reject Ho |
| 44 | σ5 | σ11 | 19 | 32 | σ5/σ11 | 1.708 | 0.42 | 2.13 | σ11/σ5 | 0.585 | 0.46 | 2.38 | Fail To Reject Ho |
| 45 | σ5 | σ12 | 19 | 99 | σ5/σ12 | 0.819 | 0.45 | 1.87 | σ12/σ5 | 1.222 | 0.53 | 2.22 | Fail To Reject Ho |
| 46 | σ6 | σ7 | 19 | 19 | σ6/σ7 | 1.102 | 0.4 | 2.53 | σ7/σ6 | 0.907 | 0.40 | 2.53 | Fail To Reject Ho |
| 47 | σ6 | σ8 | 19 | 19 | σ6/σ8 | 1.033 | 0.4 | 2.53 | σ8/σ6 | 0.968 | 0.40 | 2.53 | Fail To Reject Ho |
| 48 | σ6 | σ9 | 19 | 36 | σ6/σ9 | 1.965 | 0.42 | 2.13 | σ9/σ6 | 0.509 | 0.47 | 2.35 | Fail To Reject Ho |
| 49 | σ6 | σ10 | 19 | 36 | σ6/σ10 | 2.254 | 0.42 | 2.13 | σ10/σ6 | 0.444 | 0.47 | 2.35 | Reject Ho |
| 50 | σ6 | σ11 | 19 | 32 | σ6/σ11 | 2.518 | 0.42 | 2.13 | σ11/σ6 | 0.397 | 0.46 | 2.38 | Reject Ho |
| 51 | σ6 | σ12 | 19 | 99 | σ6/σ12 | 1.207 | 0.45 | 1.87 | σ12/σ6 | 0.829 | 0.53 | 2.22 | Fail To Reject Ho |
| 52 | σ7 | σ8 | 19 | 19 | σ7/σ8 | 0.937 | 0.4 | 2.53 | σ8/σ7 | 1.067 | 0.40 | 2.53 | Fail To Reject Ho |
| 53 | σ7 | σ9 | 19 | 36 | σ7/σ9 | 1.783 | 0.42 | 2.13 | σ9/σ7 | 0.561 | 0.47 | 2.35 | Fail To Reject Ho |
| 54 | σ7 | σ10 | 19 | 36 | σ7/σ10 | 2.045 | 0.42 | 2.13 | σ10/σ7 | 0.489 | 0.47 | 2.35 | Fail To Reject Ho |
| 55 | σ7 | σ11 | 19 | 32 | σ7/σ11 | 2.285 | 0.42 | 2.13 | σ11/σ7 | 0.438 | 0.46 | 2.38 | Reject Ho |
| 56 | σ7 | σ12 | 19 | 99 | σ7/σ12 | 1.095 | 0.45 | 1.87 | σ12/σ7 | 0.913 | 0.53 | 2.22 | Fail To Reject Ho |
| 57 | σ8 | σ9 | 19 | 36 | σ8/σ9 | 1.902 | 0.42 | 2.13 | σ9/σ8 | 0.526 | 0.47 | 2.35 | Fail To Reject Ho |
| 58 | σ8 | σ10 | 19 | 36 | σ8/σ10 | 2.182 | 0.42 | 2.13 | σ10/σ8 | 0.458 | 0.47 | 2.35 | Reject Ho |
| 59 | σ8 | σ11 | 19 | 32 | σ8/σ11 | 2.437 | 0.42 | 2.13 | σ11/σ8 | 0.410 | 0.46 | 2.38 | Reject Ho |
| 60 | σ8 | σ12 | 19 | 99 | σ8/σ12 | 1.168 | 0.45 | 1.87 | σ12/σ8 | 0.856 | 0.53 | 2.22 | Fail To Reject Ho |
| 61 | σ9 | σ10 | 36 | 36 | σ9/σ10 | 1.147 | 0.51 | 1.94 | σ10/σ9 | 0.872 | 0.51 | 1.94 | Fail To Reject Ho |
| 62 | σ9 | σ11 | 36 | 32 | σ9/σ11 | 1.281 | 0.51 | 2.00 | σ11/σ9 | 0.780 | 0.50 | 1.97 | Fail To Reject Ho |
| 63 | σ9 | σ12 | 36 | 99 | σ9/σ12 | 0.614 | 0.56 | 1.67 | σ12/σ9 | 1.628 | 0.60 | 1.79 | Fail To Reject Ho |
| 64 | σ10 | σ11 | 36 | 32 | σ10/σ11 | 1.117 | 0.51 | 2.00 | σ11/σ10 | 0.895 | 0.50 | 1.97 | Fail To Reject Ho |
| 65 | σ10 | σ12 | 36 | 99 | σ10/σ12 | 0.535 | 0.56 | 1.67 | σ12/σ10 | 1.868 | 0.60 | 1.79 | Reject Ho |
| 66 | σ11 | σ12 | 32 | 99 | σ11/σ12 | 0.479 | 0.56 | 1.70 | σ12/σ11 | 2.086 | 0.59 | 1.85 | Reject Ho |

From Table 70, fifty-nine of the sixty-six pairwise combinations fail to reject $H_o$.

The seven combinations that rejected the null hypothesis shown in Table 70 were not

related to a specific sample set. One would have expected 3 or 4 rejections due to the inherent variability of the data. However, the fact that efficiency test equipment itself had a certain level of accuracy could have contributed to some additional pairwise combinations of the null hypothesis being rejected. Based on the overall F-test results using the significance level of 0.05, it was reasonably concluded that there is still insufficient statistical evidence to conclude the standard deviations across the experimental region are not equal. This would imply that a pooled standard deviation could be used for an estimate of the standard deviation throughout the experimental region, with the benefit of a more accurate estimate of variability.

Using the following pooled standard deviation formula and the data from the hypothesis tests, the pooled standard deviation was calculated.

### Pooled Standard Deviation Formula

$$S_p^2 = \frac{(19)0.957^2+(19)0.941^2+(19)0.980^2+(19)0.856^2+(19)0.941^2+(19)1.142^2+(19)1.088^2+(19)1.124^2+(36)0.815^2+(36)0.761^2+(32)0.720^2+(99)1.040^2}{19+19+19+19+19+19+19+36+36+32+99}$$

$$S_p^2 = \frac{335.33}{355} = 0.9446$$

## 1.13   Composite Objective Function

The following responses were tracked during the SA1 steepest ascent to determine if there was any significant correlation with the primary response. The following secondary and alternate responses were recorded.

Response Variable (Secondary):

- $y_1$ - Minimum fiber diameter (nm)

172

Response Variable (Alternate):

- $y_2$ - Mean fiber diameter (nm)

- $y_3$ - Maximum fiber diameter (nm)

- $y_4$ - Range of fiber diameter (nm)

A Scatter Plot of the secondary and alternate responses from DOE1a was generated to observe any potential relationships between these responses and the primary efficiency response. The results of this comparison can be seen in Figure 52.
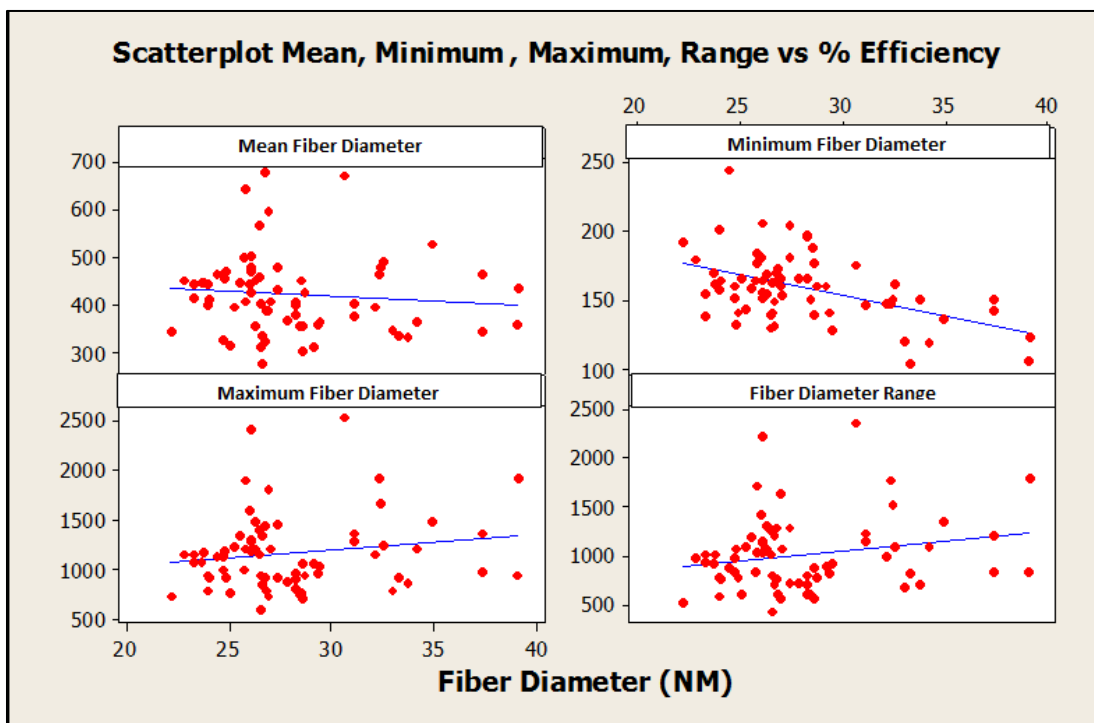


Figure 52: Scatter Plot of Secondary/Alternate Responses

The filtration theory discussed earlier in the research references the importance of fiber diameter for increasing the media efficiency. Fiber diameters under 500nm are the largest factor for producing high efficiency filtration media while minimizing the negative pressure drop. From Figure 52, the most significant relationship observed

173

was the relationship between the smallest fiber diameter (Min_1) and the efficiency response which supports the filtration theory.

Although there is not a compelling relationship represented between the maximum fiber diameter and the media efficiency shown in Figure 52, the filtration theory supports the idea that fiber diameters greater than one micron increase negative pressure drop when additional fibers are applied.

Based on the response information collected during the SA1 experiment and the theories behind air filtration, a composite objective function was composed as a comparison to the efficiency response.  The following composite objective function used for this comparison.

Composite Objective Function: $\qquad y_C = y_0 - .9 \, y_1 - .2 y_2$

$\qquad y_0$ = Primary Response - Media Efficiency
$\qquad y_1$ = Percent of Fiber Diameters < 500 nm
$\qquad y_2$ = Percent of Fiber Diameters > 1000nm

The comparison of the responses for each step of SA1 is shown in the table below.

Table 71: SA1 - Uncoded Composite Objective Function Comparison

|  | Eff | Comp | DOE1a Predict Response |
|---|---|---|---|
| Step 0 | 23.857 | 23.159 | 28.340 |
| Step 1 | 30.892 | 30.209 | 31.824 |
| Step 2 | 36.225 | 35.518 | 36.461 |
| Step 3 | 40.518 | 39.800 | 42.286 |
| Step 4 | 42.336 | 41.674 | 48.666 |
| Step 5 | 44.573 | 43.888 | 55.534 |
| Step 6 | 37.465 | 36.834 | 63.353 |

The following figure shows a graphical illustration of the response comparison.

## SA1 Response Plot

| | Step 0 | Step 1 | Step 2 | Step 3 | Step 4 | Step 5 | Step 6 |
|---|---|---|---|---|---|---|---|
| — Trial Eff% | 23.857 | 30.892 | 36.225 | 40.518 | 42.336 | 44.573 | 37.465 |
| ■ Composite Eff% | 23.159 | 30.209 | 35.518 | 39.800 | 41.674 | 43.888 | 36.834 |
| △ DOE1 Eff% | 28.340 | 31.824 | 36.461 | 42.286 | 48.666 | 55.534 | 63.353 |
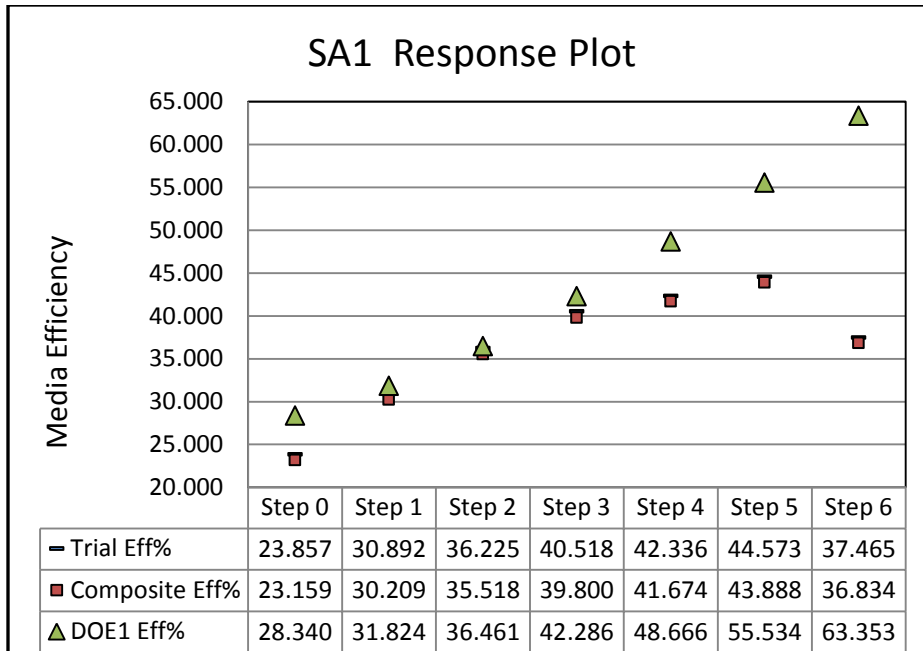
Figure 53: SA1 Response Comparison

The composite objective function response values were very close to the efficiency response values.  This would present an strong argument that there may be credible extensibility and robustness of the composite objective function.

175